ADVANCES IN APPLIED MICROBIOLOGY

VOLUME 71

Academic Press is an imprint of Elsevier
525 B Street, Suite 1900, San Diego, CA 92101-4495, USA
30 Corporate Drive, Suite 400, Burlington, MA 01803, USA
32 Jamestown Road, London NW1 7BY, UK

First edition 2010

ISBN: 978-0-12-380993-3
ISSN: 0065-2164

Printed and bound in the USA
10 11 12 13 10 9 8 7 6 5 4 3 2 1

CONTRIBUTORS

Amruta Bedekar
Department of Chemical and Biological Engineering, University at Buffalo, SUNY, Buffalo, New York, USA

José M. Bruno-Bárcena
Department of Microbiology; Golden Leaf Bio-manufacturing Training and Education Center, North Carolina State University, Raleigh, North Carolina, USA

Suzanne F. Dagher
Department of Microbiology, North Carolina State University, Raleigh, North Carolina, USA

R. Giebel
Department of Biology and Microbiology, University of Wisconsin Oshkosh, Halsey Science Center, Oshkosh, Wisconsin, USA

Alexander R. Horswill
Department of Microbiology, Roy J. and Lucille A. Carver College of Medicine, University of Iowa, Iowa City, Iowa, USA

G. T. Kleinheinz
Department of Biology and Microbiology, University of Wisconsin Oshkosh, Halsey Science Center, Oshkosh, Wisconsin, USA

Mattheos Koffas
Department of Chemical and Biological Engineering, University at Buffalo, SUNY, Buffalo, New York, USA

Ronan O'Toole
School of Biological Sciences, Victoria University of Wellington, Wellington, New Zealand

Fumiko Obata
Department of Microbiology and Immunology, University of Maryland School of Medicine, HSF I suite 380, Baltimore, Maryland, USA

Alicia L. Ragout
PROIMI, Universidad Nacional de Tucumán, Belgrano y Pje, Caseros, SM Tucumán, Argentina

M. Robbins
Department of Chemistry, The University of Tennessee, Knoxville, Tennessee, USA

S. M. Rust
Division of Mathematical and Natural Sciences, Arizona State University, Phoenix, Arizona, USA

T. R. Sandrin
Division of Mathematical and Natural Sciences, Arizona State University, Phoenix, Arizona, USA

Karan Shah
Department of Chemical and Biological Engineering, University at Buffalo, SUNY, Buffalo, New York, USA

Faustino Siñeriz
PROIMI; Cátedra de Microbiología Superior, Fac. Bioq. Qca. y Fcia, Universidad Nacional de Tucumán, Belgrano y Pje, Caseros, SM Tucumán, Argentina

Matthew Thoendel
Department of Microbiology, Roy J. and Lucille A. Carver College of Medicine, University of Iowa, Iowa City, Iowa, USA

C. Worden
Department of Biology and Microbiology, University of Wisconsin Oshkosh, Halsey Science Center, Oshkosh, Wisconsin, USA

CHAPTER 1

Influence of *Escherichia coli* Shiga Toxin on the Mammalian Central Nervous System

Fumiko Obata

Contents

Department of Microbiology and Immunology, University of Maryland School of Medicine, HSF I suite 380, Baltimore, Maryland, USA

Advances in Applied Microbiology, Volume 71
ISSN 0065-2164, DOI: 10.1016/S0065-2164(10)71001-7

Abstract

In severe cases of the infectious disease by Shiga toxin-producing *Escherichia coli* (STEC), patients display renal dysfunction known as hemolytic uremic syndrome (HUS) and central nervous system (CNS) failure. Among those severe symptoms, patients with CNS dysfunction with HUS have a greater chance of getting severe sequelae and mortality than with HUS alone. Autopsy of the CNS shows mostly edema and hypoxic-ischemic changes, often with microhemorrhages. Magnetic resonance imaging (MRI) of brains of patients confirms hemorrhagic component involvement. This suggests the weakening of the blood–brain barrier (BBB) during the disease. Also, cerebrospinal fluid (CSF) analysis shows the weakening of the blood–CSF barrier. Although evidence of vascular involvement in CNS exists, the typical observation of microthrombosis in renal pathology is often absent in CNS. Importantly, there are people who develop CNS symptoms before the onset of HUS. This suggests direct involvement of Shiga toxin (Stx) in CNS disease which is in addition to renal involvement.

The advantages of animal models are that Stx receptor expression in normal CNS tissue can be determined, and changes in histopathology, hematology, and serum and CSF contents can be analyzed at several different time points, which allow investigation of the nature of the disease. Importantly, in animal models with either STEC oral inoculation or purified Stx injection, paralysis of extremities is commonly observed. This shows the central role of Stx in CNS dysfunction in this disease. It is anticipated that precise mechanisms of Stx influence in the CNS will be delineated, and this information will lead to effective therapeutics in the near future.

I. INTRODUCTION

Shiga toxin-producing *Escherichia coli* (STEC) is a food- and waterborne pathogen. STEC outbreaks as well as sporadic cases have been reported worldwide. The Centers for Disease Control and Prevention (CDC) reported 29 and 43 outbreaks in 2006 and 2007, respectively (http://www.cdc.gov/foodborneoutbreaks/outbreak_data.htm). Over the years, the incidence of STEC infection has gradually increased, and remains a significant problem in public health.

STEC infection causes diarrhea and bloody diarrhea, and in severe cases patients develop hemolytic uremic syndrome (HUS) and central

nervous system (CNS) impairment. STEC-induced neuronal disabilities include a broad spectrum of symptoms such as cortical blindness, poor fine-motor coordination, seizures, and changes in consciousness, including coma. Importantly, CNS manifestations often associated with mortality or severe sequelae. STEC produces Shiga toxins 1 and 2 (Stx1 and Stx2); among them Stx2 is more potent as a cause of severe HUS and CNS impairment. However, precise mechanisms of Shiga toxin-induced CNS impairment are not yet clear.

To define the nature of the diseases in humans, animal models have been established and analyzed. The animal models must resemble the human disease, in this case STEC infection-induced CNS dysfunction. In this chapter, the nature of STEC disease in humans, with special emphasis on CNS, and characteristics of animal models, including those that resemble the human disease will be described. Because an animal model usually does not reconstruct the full features of human disease, the challenges and problems of those animal models will also be discussed.

II. STEC INFECTION IN HUMAN PATIENTS

A. Symptoms

STEC causes diarrhea and bloody diarrhea, and in severe cases HUS and CNS dysfunction occurs in humans (Cleary, 1988; Karmali *et al.*, 1985; Lopez *et al.*, 1989). CNS symptoms in STEC disease vary from decerebrate posture, hemipaesis, ataxia, cranial nerve palsy, and ophthalmological dysfunctions such as hallucinations to seizures (focal and generalized) and changes in consciousness ranging from lethargy to coma (Bale *et al.*, 1980; Brasher and Siegler, 1981; Cimolai *et al.*, 1992; Gianantonio *et al.*, 1973; Hamano *et al.*, 1993; Karmali *et al.*, 1985; Rooney *et al.*, 1971; Sheth *et al.*, 1986; Siegler *et al.*, 1994; Tapper *et al.*, 1995; Taylor *et al.*, 1986; Upadhyaya *et al.*, 1980; Verweyen *et al.*, 1999). Among these, seizures and coma are related to poor outcomes such as increased mortality and severe sequelae (Garg *et al.*, 2003). The central mechanism of the STEC disease is thought be due to the action of Shiga toxin (Stx). Among the two types of Stx, Stx1 and Stx2, Stx2 is more related to severe disease in HUS and CNS dysfunction (Cimolai and Carter, 1998; Ostroff *et al.*, 1989).

B. Relation between D + HUS and CNS occurrences

The severe renal failure symptom such as HUS which occurs after diarrhea is called diarrhea-associated HUS or D + HUS (Robson *et al.*, 1993). D + HUS is associated with STEC infections as opposed to atypical HUS

which is of noninfectious origin. D + HUS is a clinical triad that includes hemolytic anemia, thrombocytopenia, and renal failure. As generally explained, STEC infection causes a coagulation cascade with reduced platelet numbers in blood (thrombocytopenia), and the cascade induces fibrin thrombi in vessels. As red blood cells pass through occluded vessels, cells are shredded, thereby causing hemolytic anemia. As the thrombosis progresses in glomeruli of kidneys, dysfunction of the ultrafiltration apparatus contributes to acute renal failure. Approximately, 35% of patients with D + HUS progress to CNS dysfunction (Bale *et al.*, 1980; Brasher and Siegler, 1981; Cimolai *et al.*, 1992; Gerber *et al.*, 2002; Gianantonio *et al.*, 1973; Karmali *et al.*, 1985; Rooney *et al.*, 1971; Sheth *et al.*, 1986; Siegler *et al.*, 1994; Taylor *et al.*, 1986; Upadhyaya *et al.*, 1980; Verweyen *et al.*, 1999). However, it is noteworthy that before onset of HUS, 9–15% of patients display CNS dysfunction, suggesting that changes in the CNS can occur prior to or during other elements of systemic disease (Bale *et al.*, 1980; Brasher and Siegler, 1981; Siegler *et al.*, 1994; Taylor *et al.*, 1986; Upadhyaya *et al.*, 1980). Mortality rate of patients with CNS dysfunction within D + HUS is approximately two- to threefold higher than that with D + HUS alone (Bale *et al.*, 1980; Cimolai *et al.*, 1992; Sheth *et al.*, 1986; Siegler *et al.*, 1994; Taylor *et al.*, 1986; Upadhyaya *et al.*, 1980).

C. CNS histopathology from autopsy

Predominant histopathological lesions of CNS from autopsies are gross changes, such as edema, which can be determined by the weight of the brain as compared to normal weight (Sheth *et al.*, 1986) and hypoxic/anoxic/ischemic changes that are focal infarcts with focal edema and necrosis (Upadhyaya *et al.*, 1980). Microhemorrhages (leaking of blood cells from small vessels) are often found, though both hypoxic-ischemic changes and microhemorrhages appear nonspecifically throughout the brain (Gianantonio *et al.*, 1973; Rooney *et al.*, 1971; Upadhyaya *et al.*, 1980). Most of the autopsy cases are without microthrombosis (small vessels clogged by some deposits like fibrin) in CNS (Gianantonio *et al.*, 1973; Upadhyaya *et al.*, 1980). These findings suggest that endothelial damage is involved, but in the absence of significant platelet and coagulation activation in CNS. In addition to intraparenchymal hemorrhage, extraparenchymal hemorrhage such as subarachnoid hemorrhages have been reported (Sheth *et al.*, 1986) suggesting the occurrence of blood–brain barrier (BBB) breakage or weakening (parenchymal microhemorrhages) as well as neuronal barrier weakening (subarachnoid hemorrhages) other than BBB.

D. CNS pathology from MRI

Basal ganglia with a hemorrhagic component is predominant in the CNS of the patient (DiMario *et al.*, 1987; Jeong *et al.*, 1994; Signorini *et al.*, 2000; Steinborn *et al.*, 2004). This indicates the presence of vascular damage. Some patients exhibit thalamus, cerebellum, and brain stem findings in addition to the basal ganglia (Steinborn *et al.*, 2004).

E. CSF contents

At the choroid plexus, fluid from serum leaks out to the ventricle to make cerebrospinal fluid (CSF). In normal CSF, the protein concentration is low compared to serum, because the blood–CSF barrier at the choroid plexus prevents the protein leaking into CSF. However, 10–30% of CNS patients had an elevated protein concentration in CSF (Bale *et al.*, 1980; Hamano *et al.*, 1993; Sheth *et al.*, 1986). This indicates that the blood–CSF barrier is dysfunctional during the course of disease.

F. Serum proteins and electrolytes

One of the three criteria of HUS is acute renal failure. To assess renal failure, increase in serum creatinine and blood urea nitrogen (BUN) levels are often used as markers. Renal dysfunction also causes electrolyte imbalance including Ca^{2+}, Na^{+}, K^{+}, Mg^{2+}, Cl^{-}, PO_4^{3-} (phosphate), and HCO_3^{-} (bicarbonate). The relation between the occurrences of CNS symptoms and renal failures is still controversial (Bale *et al.*, 1980; Brasher and Siegler, 1981; Cimolai *et al.*, 1992; Gianantonio *et al.*, 1973; Sheth *et al.*, 1986). Siegler *et al.* (1994) noted that a reduction of CNS symptoms within D + HUS reported over the years might be the result of earlier diagnosis and better fluid and electrolyte management, thus suggesting renal involvement in CNS symptoms within D + HUS. On the other hand, Hamano *et al.* (1993) reported that in three patients with CNS symptoms which occurred prior to renal failure, electrolyte imbalance was not sufficiently severe to cause dysfunction in the CNS, suggesting a more direct influence of Shiga toxin on the CNS, without renal involvement.

III. ANIMAL MODELS

A. Types of animal models

STEC oral and gastrointestinal inoculation models and Stx injection models (i.p., intraperitoneal; i.v., intravascular; i.t., intrathecal (via cisterna magna); i.c.v., intracerebroventricular) have been reported by different

researchers. Because Stx is thought to be the main cause of the disease, Stx alone injection models are the established ones of the STEC infectious disease. However, from several reports, the lipopolysaccharide (LPS) component on the outer membrane of Gram-negative bacteria has separate effects *in vivo* as evidenced by the comparison of Stx alone and Stx+LPS injection models which have different histopathology, biochemistry, and outcomes.

B. Stx purification and LPS removal

Because Stx preparations are derived by expression in the Gram-negative bacterium *E. coli*, and then purified, researchers should always be conscious about LPS contamination in the Stx end product. LPS removal should be performed and the amount of LPS in purified Stx solutions should be quantified by Limulus Amebocyte Lysate assay and specified in Endotoxin Unit (EU)/mL. The concentration of Stx should be analyzed by protein assay and the purity of Stx by sodium dodecyl sulfate-polyacrylamide gel electrophoresis (SDS–PAGE) with silver stain and with western blot using Stx-specific antibodies. Biological cytotoxic activity should be assessed by Stx-sensitive cell lines such as Vero cell.

C. CNS symptoms of animal models

In general, animal models develop CNS symptoms, whether they express kidney disease or not as described below.

1. Baboon

Purified Stx1 (0.1 μg/kg) i.v. caused full features of HUS and also caused seizures in 50% of animals, which progressed to coma and death (Siegler *et al.*, 2001).

2. Pig

Pigs are known to develop ''edema disease'' with Stx2e-producing STEC infection (Stx2e is a subtype of Stx2). The edema disease is characterized by CNS symptoms such as ataxia, incoordination, and recumbency with edema in various tissues (Matise *et al.*, 2000). However, it is shown that Stx2-producing STEC or its lysate (crude Stx2) can cause CNS symptoms similar to edema disease including muscular incoordination, staggering gait leading to complete ataxia with tremors and convulsions, head pressing, leg paddling, squealing, paralysis, and recumbency (Dean-Nystrom *et al.*, 2000; Donohue-Rolfe *et al.*, 2000; Tzipori *et al.*, 1988, 1995).

3. Rabbit

Stx1 (i.v.) injection models show extremityparalysis as well as trunk, head, and neck paralysis, motor incoordination, recumbency, tremors, and shallow, rapid respirations (Bast *et al.*, 1997; Richardson *et al.*, 1992; Zoja *et al.*, 1992). Stx2 (i.v.) injection models show similar CNS symptoms, including loss of activity, ataxic gait, convulsions, extremity paralysis, and recumbency (Fujii *et al.*, 1996; Mizuguchi *et al.*, 1996). These show that both Stx1 and Stx2 are able to induce CNS symptoms in rabbits.

4. Mouse

(a) Because experimental bacterial colonization of the gastrointestinal tract is difficult in mice after the normal flora is established, STEC bacterial infection models depend on methods to reduce the normal flora prior to infection or when animal without the establishment of normal intestinal flora, such as germ-free mouse, has been used. Among the different STEC infection models, such as pretreatment with mytomicin C/streptomycin (Fujii *et al.*, 1994), or prefasted model (Karpman *et al.*, 1997), or protein calorie malnutrition model (Kurioka *et al.*, 1998), or gnotobiotic model (Isogai *et al.*, 1998; Taguchi *et al.*, 2002), in all cases, the common CNS symptoms have been described as hindlimb paralysis and convulsions.

(b) Among Stx injection models, Sugatani *et al.* (2000) described hindlimb paralysis symptom with Stx2 i.v. injection, whereas Obata *et al.* (2008) described CNS symptoms induced by Stx2 i.p. injection as lethargy, shivering, abnormal gait, hindlimb paralysis, spasm-like seizures (hind limbs straightened and stiffened preventing an upright body position), and hindlimb paralysis with unilateral body mobility. In the latter case, it was noted that mice retained sensory neuron function in response testing in the presence of paralysis (Obata *et al.*, 2008).

D. CNS histopathology of animal models

1. Baboon

In the Stx1 2 μg/kg (i.v.) model, light microscopy showed no obvious lesions, while electron microscopy revealed disruption of compact myelin sheath, while glial elements appeared normal, and endothelial cells seemed normal with perivascular edema (Taylor *et al.*, 1999).

2. Pig

E. coli O157:H7, strain RCH/86, which is a human patient isolate and Stx1 and/or Stx2 producer, when inoculated orally caused hypoxic-ischemic changes in the cerebral cortex, thalamus, and hippocampus, and in

addition, microhemorrhages in the cerebellum (Tzipori *et al.*, 1988). When an Stx2-alone producing strain of STEC was inoculated orally, pigs developed similar histopathological lesions including multifocal hemorrhages in the cerebellum, with additional findings of necrosis in the granular layer, endothelial necrosis, and swelling with occluded arterioles (Dean-Nystrom *et al.*, 2000).

3. Rabbit

In Stx1 injection models, edema, hemorrhage, thrombosis/fibrin thrombi, and infarct were found in the CNS such as brain stem, cerebellum, and spinal cord (Bast *et al.*, 1997; Richardson *et al.*, 1992; Zoja *et al.*, 1992) by light microscopy. All of the lesions suggested endothelial damage.

In Stx2 injection models, light microscopic findings include degenerative changes in the myelin sheath, neuronal degeneration, gliosis, vascular changes (infarct, artery wall thickening and thrombotic occlusion, and necrotic change), and hemorrhage in a variety of CNS regions such as cerebral cortex, hippocampus, cerebellum, brain stem, hypothalamus, pons, and spinal cord (Fujii *et al.*, 1996; Mizuguchi *et al.*, 2001; Takahashi *et al.*, 2008). Ultrastructual study with electron microscopy showed vacuolated myelin sheath with normal appearances of axoplasm, similar to the baboon Stx1 model (Fujii *et al.*, 1996). Changes such as neuronal degeneration and gliosis suggest that there is either a direct influence of Stx2 on neurons and glial cells or a secondary effect due to inflammation.

4. Rat

In the rat model of intracerebral ventricular (i.c.v.) Stx2 injection, ultrastructual observation revealed that an apoptotic form of neuronal degeneration, demyelination, astrogliosis, and pathologic oligodendrocytes at the area of Stx2 injection (Boccoli *et al.*, 2008; Goldstein *et al.*, 2007). Since a 50% lethal dose of Stx2 in rat is 20 μg/kg i.p. (Zotta *et al.*, 2008), a total of 6 ng Stx2 i.c.v. seems to present a very small dose, yet it demonstrated a strong influence of Stx2 on the CNS.

5. Mouse

(a) In an Stx2c (a subtype of Stx2) producer STEC inoculation model, endothelial cells became edematous and a destroyed myelin sheath was evident (Fujii *et al.*, 1994). In STEC infections which produce both Stx1 and Stx2, hemorrhage, edematous changes, and microthrombi were observed as vascular damage and neurons were degenerative; however, myelin appeared intact in the cerebral cortex, hippocampus, and cerebellum (Isogai *et al.*, 1998; Kita *et al.*, 2000; Kurioka *et al.*, 1998;

Taguchi *et al.*, 2002; Watanabe *et al.*, 2004). In both cases, lesions related to endothelial damage were observed; however, neuronal degeneration and demyelination are controversial.

(b) In Stx2 injection models, hemorrhage, edema, congestion, and glial cell changes such as pyknosis of the oligodendrocytes and astrocyte nuclei were reported as light microscopic (Nishikawa *et al.*, 2002; Okuda *et al.*, 2006; Sugatani *et al.*, 2000). Electron microscopic observation revealed that lamellipodia-like processes, presumably of glial origin, appear between pre- and postsynaptic membranes (Obata *et al.*, 2008). Taken together, the light and electron microscopic observations suggest there are vascular changes as well as glial changes occurring in Stx2 injection models. The Stx+LPS injection model resulted in more severe hemorrhage in mouse brain compared to that caused by Stx2 alone (Sugatani *et al.*, 2000).

E. Pathologies by MRI (rabbit)

Magnetic resonance studies in Stx-injected rabbit models were conducted extensively by Fujii and colleagues. Following Stx2 5 μg/kg i.v. injection, all animals (12/12) showed high intensity in T2-weighted MRI image around the third ventricle involving hypothalamus after 24 h. In the area around the third ventricle, naturally leaky BBB areas called circumventricular organs (CVO) exist. They are organum vasculosum of the lamina terminalis (OVLT), the subfornical organ (SFO), subcommissured organ (SCO), and median eminence. This suggests that Stx2 is either leaking out from the CVO or crossing the blood–CSF barrier of choroid plexus at the ventricle. Less frequent findings of high intensity signals were observed at the brain stem (4/12) at 57 h, the medulla of the cerebral hemisphere (corpus callosum, external capsule, and lateral area of amygdale) in 4/12 animals at 57 h, the hippocampus (2/12) at 57 h, or the cerebellum vermis (4/12) at 80 h. Of these, moderate clinical features such as weakness, weight loss, and hemorrhagic diarrhea are seen in animals with MRI signals in cerebellar vermis, and severe features such as paralysis of extremities and convulsions were seen in animals with signals in brain stem, cerebrum, or hippocampus (Fujii *et al.*, 1996). The same dose of Stx2 (5 μg/kg) presented by an intrathecalroute (via cisterna magna) resulted in earlier high intense signal detection in the cerebellum at 48 h, compared to cerebellar signal at 80 h after i.v. injection of Stx2 (Fujii *et al.*, 1998). This suggests that Stx2 injected into subarachnoid space reached the cerebellum by crossing the glia limitans, which is formed by pia mater, basal lamina, and the end feet of astroyctes. In Gd-diethyltriaminepentaacetic acid (DTPA)-enhanced T1-weighted MRI images, hyperintensity was recognized in the area where intravenously

injected Gd-DTPA leaked, thus showing BBB impairment. In Stx2 (i.v.) pre-injected animal, Gd-DTPA-enhanced T1-weighted images showed hyperintense brain areas such as striatum, external capsules, and cerebellum (Fujii *et al.*, 2009). As these areas do not contain CVO, Stx2 pre-injection made the BBB leaky and allowed Gd-DTPA to cross the BBB of this area. Stx1 (i.v.) injected animals showed edema in the mid-brain, brain stem, and dorsal cervical spinal cord in T2-weighted images (Fujii *et al.*, 2001), which were similar to Stx2 MRI images. As rabbit expresses Gb_3 in endothelial cells and neurons (Ren *et al.*, 1999; Richardson *et al.*, 1992), it is likely that Stx2 damages endothelial cells of BBB or blood–CSF barriers to leak out directly from vessels to the CNS parenchyma or vessels to CNS parenchyma via ventricle, respectively, in rabbit CNS.

F. CSF contents of animal models

In rabbit models, CSF total protein concentration increases after Stx2 (i.v.) injection (Mizuguchi *et al.*, 1996). Moreover, intravenously administrated Stx2 increased in the CSF with a peak at 2 or 6 h after injection (Fujii *et al.*, 1998; Mizuguchi *et al.*, 1996). Similarly, i.v. injected Stx1 increased in CSF in a gradual manner up to 24 h (Fujii *et al.*, 2001). These data suggest that Stx caused blood–CSF barrier lesions and entry into CNS parenchyma through the ventricle/ependymal layer in the rabbit.

G. Hematology and serum of animal models

1. Baboon

In the dose of 2.0 μg/kg i.v. Stx1, a serum study showed increased creatinine and hyperkalemia, which are signs of renal failure, but the hematological study showed no sign of hemolytic anemia (normal hematocrit and no increase in schistocytes) or thrombocytopenia. Yet, in this dose, the animals had CNS lesions described as myelin separation and perivascular edema in electron microscopy ultrastructural study (Taylor *et al.*, 1999). In the dose of 0.1 μg/kg Stx1 (i.v.), animals developed complete HUS, and 50% of the animals had seizures; however, histopathology of CNS was not provided (Siegler *et al.*, 2001). Taken together, the occurrence of Stx1-induced CNS symptoms appears partially related to renal failure in the baboon.

2. Rabbit

Stx1-injected rabbits had no hemolytic anemia and no thrombocytopenia. Serum studies showed transient creatinine increase; however, it was caused by dehydration due to lack of water intake after hindleg paralysis (Richardson *et al.*, 1992). Overall, Stx1 did not cause renal dysfunction or

abnormal hematological status (Richardson *et al.*, 1992; Zoja *et al.*, 1992). Stx2 (i.v.) caused hemolytic anemia in rabbits, but not thrombocytopenia, and renal function was normal as assessed by BUN and creatinine values (Mizuguchi *et al.*, 1996). The above observations were done in New Zealand White and Japanese White rabbits, and Stx injection does not cause renal dysfunction or HUS in these rabbits. Recently, Garcia *et al.* (2002) reported that the Dutch Belted rabbit develops HUS after natural infection with STEC, and this was repeatable by experimental infection of STEC with strains that produced Stx1 alone or Stx1 plus Stx2 (Garcia *et al.*, 2006). In 2008, they showed that purified Stx2 alone (i.v.) caused histopathological lesions in kidneys and the brain stem, but hematological data and serum data were not provided (Garcia *et al.*, 2008). Therefore, the Dutch Belted rabbit might be a new type of rabbit model that develops renal disease.

3. Mouse

Keepers *et al.* (2006) reported that Stx2 alone (225 ng/kg, i.p.) did not cause thrombocytopenia, but caused hemolytic anemia (assessed by reticulocytosis) and increased serum creatinine and BUN. On the other hand, LPS alone (0.3 mg/kg, i.p.) induced thrombocytopenia, but not reticulocytosis or increased creatinine. A combination of Stx2 and LPS injection in above doses caused thrombocytopenia, reticulocytosis, and increased serum creatinine: thus a complete set of HUS criteria. Sugatani *et al.* (2000) also reported that Stx2 (5 ng/kg i.v.) + LPS (0.5 mg/kg i.v.) or Stx2 (50 ng/kg i.v.) + LPS (0.5 mg/kg i.v.) induce thrombocytopenia. However, Stx2 alone (i.v.) induced thrombocytopenia only at a dose of 50 ng/kg, but not at a lower dose of 5 ng/kg. An STEC infection mouse model which presumably received both Stx and LPS showed fragmentation of red blood cells, which is a sign of hemolytic anemia (Karpman *et al.*, 1997). Induction of thrombocytopenia by Stx2 alone is still controversial, but Stx2 alone is capable of causing renal failure (increase in serum creatinine and BUN), and Stx2 plus LPS makes the disease worse.

IV. SIMILARITIES BETWEEN HUMAN PATIENTS AND ANIMAL MODELS

The most common feature of all animal models is development of CNS symptoms such as paralysis, seizures, and in the end, a coma-like symptom in either STEC oral inoculation or purified Stx injection models. Histopathologically, the rabbit model more closely resembles a human in which it develops infarcts and microhemorrhages. Although

microthrombosis is often seen in rabbits, it is rare in human CNS. The pig also displays microhemorrhages, although it is restricted to the cerebellum. In contrast, microhemorrhages in humans spread throughout the whole brain. Microhemorrhages are detected in smaller amounts in the brain of the Stx2-injected mouse. Demyelination is observed in baboon, rabbit, rat, and mouse (Fujii *et al.*, 1994) models; however, it is not found in the human CNS. Whether this is due to a difference in Stx levels between the patient CNS and animal models is not clear.

MRI findings in the human brain are predominantly in the basal ganglia, whereas rabbit MRIs show the third ventricle area as predominant, and the brain stem signals were accompanied with severe symptoms such as paralysis and convulsion. A rabbit study measuring parameters representing autonomic dysfunction due to brain stem failure showed dysfunction of the baroreflex control system (homeostatic mechanisms for maintaining blood pressure), thus suggesting circulatory failure as the cause of death. This might suggest partial mechanism of CNS dysfunction due to Stx2, although the MRI findings of a human patient are not an exact match to those on a rabbit.

V. RELATION BETWEEN RENAL FAILURE AND CNS FAILURE

Serum analysis of rabbit injected (i.v.) with Stx1 or Stx2 showed that neither toxin causes renal impairment (Mizuguchi *et al.*, 1996; Richardson *et al.*, 1992; Zoja *et al.*, 1992). Measurements such as increased serum creatinine or BUN are signs of renal failure. None of these features was observed in New Zealand White or Japanese White rabbits. However, these rabbit models developed neuronal symptoms such as seizures, and presented histopathological CNS lesions such as edema, microhemorrhages, and thrombosis. This suggests that Stx1 or Stx2 has the potential to damage the CNS without renal influence. In mouse models, Keepers *et al.* (2006) reported that Stx2 (i.p.) alone induced only reticulocytosis (a sign of anemia) and increased serum creatinine, but not thrombocytopenia; thus it does not fulfill some characteristics of HUS, although Stx2 alone induces CNS symptoms such as hindlimb paralysis (Obata *et al.*, 2008; Sugatani *et al.*, 2000). These findings also suggest that Stx induces CNS impairment in the absence of renal dysfunction. In human STEC disease, a portion of patients are reported to have CNS dysfunction before the onset of HUS (Bale *et al.*, 1980; Brasher and Siegler, 1981; Siegler *et al.*, 1994; Taylor *et al.*, 1986; Upadhyaya *et al.*, 1980). These observations in human and animal models suggest that direct action of Stx in the CNS is involved in the STEC infectious disease.

VI. STX RECEPTOR, GLOBOTRIAOSYLCERAMIDE (GB_3) EXPRESSION IN THE NERVOUS SYSTEM

In the peripheral nervous system such as dorsal root ganglion (DRG), Ren *et al.* (1999) reported that rodent (rat and mouse) DRG neurons express Gb_3, whereas human and rabbit DRG endothelial cells express Gb_3 in addition to neurons. In the murine CNS, Obata *et al.* (2008) reported that the neuron is the only cell type to expresses Gb_3, whereas human cadaver CNS neurons and endothelial cells express Gb_3. In Gb_3 expressing mouse neurons, the Gb_3 is detected in the neuronal cell body, and within cell body, Gb_3 resides in membranous structures such as plasma membranes, vesicles, the Golgi apparatus, and endoplasmic reticulum. Also, in Stx2-injected mouse, Stx2 and Gb_3 are detected within neurons in the same membranous compartment associated with the Golgi apparatus. On the other hand, Okuda *et al.* (2006) reported that wild-type mice expressed Gb_3 in endothelial cells of the brain, and the anti-Gb_3 immunoreactivity was diminished in a Gb_3 synthase knockout mouse in which Gb_3 was not produced. However, Kolling *et al.* (2008) described that immersion fixation of tissues, instead of perfusion fixation, results in intravascular anti-Gb_3 staining of both renal and CNS, and this staining is a false positive compared to isotype-matched controls which also exhibit positive vascular stain.

VII. STX ROUTE FROM BLOOD TO CNS PARENCHYMA

Once Stx gets into blood stream, there are four ways for toxins to translocate to CNS parenchyma. The first is to pass through naturally leaky BBB (CVO) to reach the CNS directly. The second is to go through BBB by destroying the endothelial tight junction. The third and fourth involve crossing the blood–CSF barrier first, and once the toxin is in CSF (ventricle), it will either cross ependymal cells surrounding the ventricle or travel to subarachnoid space and enter the CNS by crossing glial limitans. In rabbit, it was shown that Stx injected i.v. translocated to the CSF, suggesting that the toxin can indeed cross the blood–CSF barrier (Fujii *et al.*, 1998; Mizuguchi *et al.*, 1996). Also, when Stx was injected into rabbit via intrathecal route into subarachnoid space, T2-weighted MRI images showed high intensity in the area of dorsal cerebellar region, which suggests that Stx translocated from subarachnoid space to CNS by crossing the glial limitans. In the mouse model, intraperitoneally injected Stx2 was detected in motoneurons of the spinal cords (Obata *et al.*, 2008). Between rabbit and mouse, there are certain differences in Gb_3 expressing cell types in CNS, indicating that rabbit expresses Gb_3 in

endothelial cells whereas mouse does not. This might suggest a different route taken by Stx to enter CNS from blood. That is, endothelial cells are altered by toxin in rabbit such that damaged endothelial tight junctions allow toxin to go through BBB and the blood–CSF barrier easily and efficiently, whereas mouse endothelial cells remain intact. The fact that Stx is detected in neurons after peripheral injection of the toxin suggests that there is an unknown mechanism(s) of Stx entry into the CNS parenchyma without breaking down endothelial cells.

Also, it should be noted that LPS is known to weaken the BBB by increasing permeability via cytokine induction in TLR4 (LPS receptor) expressing perivascular cells (Banks and Robinson, 2010; Glabinski and Ransohoff, 1999a; Glabinski and Ransohoff, 1999b; Mayhan, 2001), thus influencing Stx entry into CNS in the STEC oral infection model, in which both LPS and Stx are expected to enter the blood circulation.

VIII. FUTURE DIRECTIONS

HUS models of baboon using Stx1 (Siegler *et al.*, 2001) or Stx2 (Siegler *et al.*, 2003) have been published. As baboon is the closest species to humans among the animal models established for STEC disease, it will be quite useful information if the relationship between HUS and CNS symptoms is studied in this Stx-induced HUS model. New Zealand White and Japanese White rabbit models do not show renal failure, yet have CNS symptoms. As these rabbit models are likely to express Gb_3 in neurons of CNS in addition to vessels suggests that these are useful models to study Stx influence on vessels and neurons in CNS, which exhibit the same features as human CNS. Recent establishment of a Dutch Belted rabbit STEC infection model that presents with renal failure, which is also the feature of human patients, suggests that analysis of CNS symptoms in this model might complete all the features of human STEC disease, including gastrointestinal damage. An interesting rat model was established by Goldstein and coworkers in which Stx2 was injected directly into CNS parenchyma. Although detailed histopathologic features were described, the related CNS symptoms were not provided. CNS regions that are under the influence of the toxin might cause specific CNS dysfunction, so that the information will be insightful for future drug development for STEC CNS disease. In mouse CNS, neurons express Gb_3 but not other cell types, thus is quite different from human CNS, yet mice injected with purified Stx2 develop paralysis. This suggests that the mouse model might be suitable for studying direct action of Stx in CNS without endothelial damage. Also, this indicates the existence of unknown mechanisms of Stx2 entry into the CNS. Recently, the influence of Stx2 on neuronal function was shown by the examination of in vitro

mice brain slices in which Stx2-treated neurons increased the secretion of neurotransmitters (Obata *et al.*, 2008). Assay systems for evaluating neuronal dysfunction due to Stx2 need to be established.

ACKNOWLEDGMENTS

The author appreciates Dr. Tom G. Obrig (University of Maryland) for the expert advice on Shiga toxin animal models and also for a careful reading of the text. He also appreciates the expert advice of Dr. Koujiro Tohyama (Iwate Medical University) on the neuroanatomical aspects.

REFERENCES

Bale, J. F., Jr., Brasher, C., and Siegler, R. L. (1980). CNS manifestations of the hemolytic-uremic syndrome. Relationship to metabolic alterations and prognosis. *Am. J. Dis. Child.* **134,** 869–872.

Banks, W. A., and Robinson, S. M. (2010). Minimal penetration of lipopolysaccharide across the murine blood-brain barrier. *Brain Behav. Immun.* **24,** 102–109.

Bast, D. J., Brunton, J. L., Karmali, M. A., and Richardson, S. E. (1997). Toxicity and immunogenicity of a verotoxin 1 mutant with reduced globotriaosylceramide receptor binding in rabbits. *Infect. Immun.* **65,** 2019–2028.

Boccoli, J., Loidl, C. F., Lopez-Costa, J. J., Creydt, V. P., Ibarra, C., and Goldstein, J. (2008). Intracerebroventricular administration of Shiga toxin type 2 altered the expression levels of neuronal nitric oxide synthase and glial fibrillary acidic protein in rat brains. *Brain Res.* **1230,** 320–333.

Brasher, C., and Siegler, R. L. (1981). The hemolytic-uremic syndrome. *West. J. Med.* **134,** 193–197.

Cimolai, N., and Carter, J. E. (1998). Bacterial genotype and neurological complications of Escherichia coli O157:H7-associated haemolytic uraemic syndrome. *Acta Paediatr.* **87,** 593–594.

Cimolai, N., Morrison, B. J., and Carter, J. E. (1992). Risk factors for the central nervous system manifestations of gastroenteritis-associated hemolytic-uremic syndrome. *Pediatrics* **90,** 616–621.

Cleary, T. G. (1988). Cytotoxin-producing *Escherichia coli* and the hemolytic uremic syndrome. *Pediatr. Clin. North Am.* **35,** 485–501.

Dean-Nystrom, E. A., Pohlenz, J. F., Moon, H. W., and O'Brien, A. D. (2000). Escherichia coli O157:H7 causes more-severe systemic disease in suckling piglets than in colostrum-deprived neonatal piglets. *Infect. Immun.* **68,** 2356–2358.

DiMario, F. J., Jr., Bronte-Stewart, H., Sherbotie, J., and Turner, M. E. (1987). Lacunar infarction of the basal ganglia as a complication of hemolytic-uremic syndrome. MRI and clinical correlations. *Clin. Pediatr. (Phila.)* **26,** 586–590.

Donohue-Rolfe, A., Kondova, I., Oswald, S., Hutto, D., and Tzipori, S. (2000). Escherichia coli 0157:H7 strains that express Shiga toxin (Stx) 2 alone are more neurotropic for gnotobiotic piglets than are isotypes producing only Stx1 or both Stx1 and Stx2. *J. Infect. Dis.* **181,** 1825–1829.

Fujii, J., Kita, T., Yoshida, S., Takeda, T., Kobayashi, H., Tanaka, N., Ohsato, K., and Mizuguchi, Y. (1994). Direct evidence of neuron impairment by oral infection with verotoxin-producing *Escherichia coli* O157:H- in mitomycin-treated mice. *Infect. Immun.* **62,** 3447–3453.

Fujii, J., Kinoshita, Y., Kita, T., Higure, A., Takeda, T., Tanaka, N., and Yoshida, S. (1996). Magnetic resonance imaging and histopathological study of brain lesions in rabbits given intravenous verotoxin 2. *Infect. Immun.* **64,** 5053–5060.

Fujii, J., Kinoshita, Y., Yamada, Y., Yutsudo, T., Kita, T., Takeda, T., and Yoshida, S. (1998). Neurotoxicity of intrathecal Shiga toxin 2 and protection by intrathecal injection of anti-Shiga toxin 2 antiserum in rabbits. *Microb. Pathog.* **25,** 139–146.

Fujii, J., Kinoshita, Y., Yutsudo, T., Taniguchi, H., Obrig, T., and Yoshida, S. I. (2001). Toxicity of Shiga toxin 1 in the central nervous system of rabbits. *Infect. Immun.* **69,** 6545–6548.

Fujii, J., Kinoshita, Y., Matsukawa, A., Villanueva, S. Y., Yutsudo, T., and Yoshida, S. (2009). Successful steroid pulse therapy for brain lesion caused by Shiga toxin 2 in rabbits. *Microb. Pathog.* **46,** 179–184.

Garcia, A., Marini, R. P., Feng, Y., Vitsky, A., Knox, K. A., Taylor, N. S., Schauer, D. B., and Fox, J. G. (2002). A naturally occurring rabbit model of enterohemorrhagic Escherichia coli-induced disease. *J. Infect. Dis.* **186,** 1682–1686.

Garcia, A., Bosques, C. J., Wishnok, J. S., Feng, Y., Karalius, B. J., Butterton, J. R., Schauer, D. B., Rogers, A. B., and Fox, J. G. (2006). Renal injury is a consistent finding in Dutch Belted rabbits experimentally infected with enterohemorrhagic *Escherichia coli*. *J. Infect. Dis.* **193,** 1125–1134.

Garcia, A., Marini, R. P., Catalfamo, J. L., Knox, K. A., Schauer, D. B., Rogers, A. B., and Fox, J. G. (2008). Intravenous Shiga toxin 2 promotes enteritis and renal injury characterized by polymorphonuclear leukocyte infiltration and thrombosis in Dutch Belted rabbits. *Microbes Infect.* **10,** 650–656.

Garg, A. X., Suri, R. S., Barrowman, N., Rehman, F., Matsell, D., Rosas-Arellano, M. P., Salvadori, M., Haynes, R. B., and Clark, W. F. (2003). Long-term renal prognosis of diarrhea-associated hemolytic uremic syndrome: a systematic review, meta-analysis, and meta-regression. *JAMA* **290,** 1360–1370.

Gerber, A., Karch, H., Allerberger, F., Verweyen, H. M., and Zimmerhackl, L. B. (2002). Clinical course and the role of Shiga toxin-producing *Escherichia coli* infection in the hemolytic-uremic syndrome in pediatric patients, 1997-2000, in Germany and Austria: a prospective study. *J. Infect. Dis.* **186,** 493–500.

Gianantonio, C. A., Vitacco, M., Mendilaharzu, F., Gallo, G. E., and Sojo, E. T. (1973). The hemolytic-uremic syndrome. *Nephron* **11,** 174–192.

Glabinski, A. R., and Ransohoff, R. M. (1999a). Chemokines and chemokine receptors in CNS pathology. *J. Neurovirol.* **5,** 3–12.

Glabinski, A. R., and Ransohoff, R. M. (1999b). Sentries at the gate: Chemokines and the blood-brain barrier. *J. Neurovirol.* **5,** 623–634.

Goldstein, J., Loidl, C. F., Creydt, V. P., Boccoli, J., and Ibarra, C. (2007). Intracerebroventricular administration of Shiga toxin type 2 induces striatal neuronal death and glial alterations: An ultrastructural study. *Brain Res.* **1161,** 106–115.

Hamano, S., Nakanishi, Y., Nara, T., Seki, T., Ohtani, T., Oishi, T., Joh, K., Oikawa, T., Muramatsu, Y., Ogawa, Y., *et al.* (1993). Neurological manifestations of hemorrhagic colitis in the outbreak of *Escherichia coli* O157:H7 infection in Japan. *Acta Paediatr.* **82,** 454–458.

Isogai, E., Isogai, H., Kimura, K., Hayashi, S., Kubota, T., Fujii, N., and Takeshi, K. (1998). Role of tumor necrosis factor alpha in gnotobiotic mice infected with an *Escherichia coli* O157:H7 strain. *Infect. Immun.* **66,** 197–202.

Jeong, Y. K., Kim, I. O., Kim, W. S., Hwang, Y. S., Choi, Y., and Yeon, K. M. (1994). Hemolytic uremic syndrome: MR findings of CNS complications. *Pediatr. Radiol.* **24,** 585–586.

Karmali, M. A., Petric, M., Lim, C., Fleming, P. C., Arbus, G. S., and Lior, H. (1985). The association between idiopathic hemolytic uremic syndrome and infection by verotoxin-producing Escherichia coli. *J. Infect. Dis.* **151,** 775–782.

Karpman, D., Connell, H., Svensson, M., Scheutz, F., Alm, P., and Svanborg, C. (1997). The role of lipopolysaccharide and Shiga-like toxin in a mouse model of *Escherichia coli* O157: H7 infection. *J. Infect. Dis.* **175,** 611–620.

Keepers, T. R., Psotka, M. A., Gross, L. K., and Obrig, T. G. (2006). A murine model of HUS: Shiga toxin with lipopolysaccharide mimics the renal damage and physiologic response of human disease. *J. Am. Soc. Nephrol.* **17,** 3404–3414.

Kita, E., Yunou, Y., Kurioka, T., Harada, H., Yoshikawa, S., Mikasa, K., and Higashi, N. (2000). Pathogenic mechanism of mouse brain damage caused by oral infection with Shiga toxin-producing *Escherichia coli* O157:H7. *Infect. Immun.* **68,** 1207–1214.

Kolling, G. L., Obata, F., Gross, L. K., and Obrig, T. G. (2008). Immunohistologic techniques for detecting the glycolipid Gb(3) in the mouse kidney and nervous system. *Histochem. Cell Biol.* **130,** 157–164.

Kurioka, T., Yunou, Y., and Kita, E. (1998). Enhancement of susceptibility to Shiga toxin-producing *Escherichia coli* O157:H7 by protein calorie malnutrition in mice. *Infect. Immun.* **66,** 1726–1734.

Lopez, E. L., Diaz, M., Grinstein, S., Devoto, S., Mendilaharzu, F., Murray, B. E., Ashkenazi, S., Rubeglio, E., Woloj, M., Vasquez, M., *et al.* (1989). Hemolytic uremic syndrome and diarrhea in Argentine children: The role of Shiga-like toxins. *J. Infect. Dis.* **160,** 469–475.

Matise, I., Sirinarumitr, T., Bosworth, B. T., and Moon, H. W. (2000). Vascular ultrastructure and DNA fragmentation in swine infected with Shiga toxin-producing *Escherichia coli*. *Vet. Pathol.* **37,** 318–327.

Mayhan, W. G. (2001). Regulation of blood-brain barrier permeability. *Microcirculation* **8,** 89–104.

Mizuguchi, M., Tanaka, S., Fujii, I., Tanizawa, H., Suzuki, Y., Igarashi, T., Yamanaka, T., Takeda, T., and Miwa, M. (1996). Neuronal and vascular pathology produced by verocytotoxin 2 in the rabbit central nervous system. *Acta Neuropathol. (Berl.)* **91,** 254–262.

Mizuguchi, M., Sugatani, J., Maeda, T., Momoi, T., Arima, K., Takashima, S., Takeda, T., and Miwa, M. (2001). Cerebrovascular damage in young rabbits after intravenous administration of Shiga toxin 2. *Acta Neuropathol. (Berl.)* **102,** 306–312.

Nishikawa, K., Matsuoka, K., Kita, E., Okabe, N., Mizuguchi, M., Hino, K., Miyazawa, S., Yamasaki, C., Aoki, J., Takashima, S., Yamakawa, Y., Nishijima, M., *et al.* (2002). A therapeutic agent with oriented carbohydrates for treatment of infections by Shiga toxin-producing *Escherichia coli* O157:H7. *Proc. Natl. Acad. Sci. USA* **99,** 7669–7674.

Obata, F., Tohyama, K., Bonev, A. D., Kolling, G. L., Keepers, T. R., Gross, L. K., Nelson, M. T., Sato, S., and Obrig, T. G. (2008). Shiga toxin 2 affects the central nervous system through receptor globotriaosylceramide localized to neurons. *J. Infect. Dis.* **198,** 1398–1406.

Okuda, T., Tokuda, N., Numata, S., Ito, M., Ohta, M., Kawamura, K., Wiels, J., Urano, T., Tajima, O., and Furukawa, K. (2006). Targeted disruption of Gb3/CD77 synthase gene resulted in the complete deletion of globo-series glycosphingolipids and loss of sensitivity to verotoxins. *J. Biol. Chem.* **281,** 10230–10235.

Ostroff, S. M., Tarr, P. I., Neill, M. A., Lewis, J. H., Hargrett-Bean, N., and Kobayashi, J. M. (1989). Toxin genotypes and plasmid profiles as determinants of systemic sequelae in *Escherichia coli* O157:H7 infections. *J. Infect. Dis.* **160,** 994–998.

Ren, J., Utsunomiya, I., Taguchi, K., Ariga, T., Tai, T., Ihara, Y., and Miyatake, T. (1999). Localization of verotoxin receptors in nervous system. *Brain Res.* **825,** 183–188.

Richardson, S. E., Rotman, T. A., Jay, V., Smith, C. R., Becker, L. E., Petric, M., Olivieri, N. F., and Karmali, M. A. (1992). Experimental verocytotoxemia in rabbits. *Infect. Immun.* **60,** 4154–4167.

Robson, W. L., Leung, A. K., Trevenen, C. L., and Brant, R. (1993). Diarrhea-associated hemolytic uremic syndrome. *Can. Fam. Physician* **39,** 2139–2145.

Rooney, J. C., Anderson, R. M., and Hopkins, I. J. (1971). Clinical and pathologic aspects of central nervous system involvement in the haemolytic uraemic syndrome. *Proc. Aust. Assoc. Neurol.* **8,** 67–75.

Sheth, K. J., Swick, H. M., and Haworth, N. (1986). Neurological involvement in hemolytic-uremic syndrome. *Ann. Neurol.* **19,** 90–93.

Siegler, R. L., Pavia, A. T., Christofferson, R. D., and Milligan, M. K. (1994). A 20-year population-based study of postdiarrheal hemolytic uremic syndrome in Utah. *Pediatrics* **94,** 35–40.

Siegler, R. L., Pysher, T. J., Tesh, V. L., and Taylor, F. B., Jr. (2001). Response to single and divided doses of Shiga toxin-1 in a primate model of hemolytic uremic syndrome. *J. Am. Soc. Nephrol.* **12,** 1458–1467.

Siegler, R. L., Obrig, T. G., Pysher, T. J., Tesh, V. L., Denkers, N. D., and Taylor, F. B. (2003). Response to Shiga toxin 1 and 2 in a baboon model of hemolytic uremic syndrome. *Pediatr. Nephrol.* **18,** 92–96.

Signorini, E., Lucchi, S., Mastrangelo, M., Rapuzzi, S., Edefonti, A., and Fossali, E. (2000). Central nervous system involvement in a child with hemolytic uremic syndrome. *Pediatr. Nephrol.* **14,** 990–992.

Steinborn, M., Leiz, S., Rudisser, K., Griebel, M., Harder, T., and Hahn, H. (2004). CT and MRI in haemolytic uraemic syndrome with central nervous system involvement: distribution of lesions and prognostic value of imaging findings. *Pediatr. Radiol.* **34,** 805–810.

Sugatani, J., Igarashi, T., Munakata, M., Komiyama, Y., Takahashi, H., Komiyama, N., Maeda, T., Takeda, T., and Miwa, M. (2000). Activation of coagulation in C57BL/6 mice given verotoxin 2 (VT2) and the effect of co-administration of LPS with VT2. *Thromb. Res.* **100,** 61–72.

Taguchi, H., Takahashi, M., Yamaguchi, H., Osaki, T., Komatsu, A., Fujioka, Y., and Kamiya, S. (2002). Experimental infection of germ-free mice with hyper-toxigenic enterohaemorrhagic *Escherichia coli* O157:H7, strain 6. *J. Med. Microbiol.* **51,** 336–343.

Takahashi, K., Funata, N., Ikuta, F., and Sato, S. (2008). Neuronal apoptosis and inflammatory responses in the central nervous system of a rabbit treated with Shiga toxin-2. *J. Neuroinflammation* **5,** 11.

Tapper, D., Tarr, P., Avner, E., Brandt, J., and Waldhausen, J. (1995). Lessons learned in the management of hemolytic uremic syndrome in children. *J. Pediatr. Surg.* **30,** 158–163.

Taylor, C. M., White, R. H., Winterborn, M. H., and Rowe, B. (1986). Haemolytic-uraemic syndrome: clinical experience of an outbreak in the West Midlands. *Br. Med. J. (Clin. Res. Ed.)* **292,** 1513–1516.

Taylor, F. B., Jr., Tesh, V. L., DeBault, L., Li, A., Chang, A. C., Kosanke, S. D., Pysher, T. J., and Siegler, R. L. (1999). Characterization of the baboon responses to Shiga-like toxin: descriptive study of a new primate model of toxic responses to Stx-1. *Am. J. Pathol.* **154,** 1285–1299.

Tzipori, S., Chow, C. W., and Powell, H. R. (1988). Cerebral infection with *Escherichia coli* O157:H7 in humans and gnotobiotic piglets. *J. Clin. Pathol.* **41,** 1099–1103.

Tzipori, S., Gunzer, F., Donnenberg, M. S., de Montigny, L., Kaper, J. B., and Donohue-Rolfe, A. (1995). The role of the eaeA gene in diarrhea and neurological complications in a gnotobiotic piglet model of enterohemorrhagic *Escherichia coli* infection. *Infect. Immun.* **63,** 3621–3627.

Upadhyaya, K., Barwick, K., Fishaut, M., Kashgarian, M., and Siegel, N. J. (1980). The importance of nonrenal involvement in hemolytic-uremic syndrome. *Pediatrics* **65,** 115–120.

Verweyen, H. M., Karch, H., Allerberger, F., and Zimmerhackl, L. B. (1999). Enterohemorrhagic Escherichia coli (EHEC) in pediatric hemolytic-uremic syndrome: a prospective study in Germany and Austria. *Infection* **27,** 341–347.

Watanabe, M., Matsuoka, K., Kita, E., Igai, K., Higashi, N., Miyagawa, A., Watanabe, T., Yanoshita, R., Samejima, Y., Terunuma, D., Natori, Y., and Nishikawa, K. (2004). Oral therapeutic agents with highly clustered globotriose for treatment of Shiga toxigenic *Escherichia coli* infections. *J. Infect. Dis.* **189,** 360–368.

Zoja, C., Corna, D., Farina, C., Sacchi, G., Lingwood, C., Doyle, M. P., Padhye, V. V., Abbate, M., and Remuzzi, G. (1992). Verotoxin glycolipid receptors determine the localization of microangiopathic process in rabbits given verotoxin-1. *J. Lab. Clin. Med.* **120,** 229–238.

Zotta, E., Lago, N., Ochoa, F., Repetto, H. A., and Ibarra, C. (2008). Development of an experimental hemolytic uremic syndrome in rats. *Pediatr. Nephrol.* **23,** 559–567.

CHAPTER 2

Natural Products for Type II Diabetes Treatment

Amruta Bedekar, Karan Shah, and **Mattheos Koffas**[1]

Contents

Department of Chemical and Biological Engineering, University at Buffalo, SUNY, Buffalo, New York, USA
[1] Corresponding author: e-mail:mkoffas@eng.buffalo.edu

Advances in Applied Microbiology, Volume 71
ISSN 0065-2164, DOI: 10.1016/S0065-2164(10)71002-9

Abstract

Natural products such as plant extracts and complex microbial secondary metabolites have recently attracted the attention of scientific world for their potential use as drugs for treating chronic diseases such as Type II diabetes. Non-Insulin-Dependent Diabetes Mellitus (NIDDM) or Type II diabetes has complicated basis and has various treatment options, each targeting different mechanism of action. One such option relies on digestive enzyme inhibition. Almost all of the currently used clinically digestive enzyme inhibitors are bacterial secondary metabolites. However in most cases understanding of their complete biosynthetic pathways remains a challenge.

The currently used digestive enzyme inhibitors have significant side effects that have restricted their usage. Hence, many active plant metabolites are being investigated as more effective treatment with fewer side effects. Flavonoids, terpenoids, glycosides are few to name in that class. Many of these are proven inhibitors of digestive enzymes but their large scale production remains a technical conundrum. Their successful heterologous production in simple host bacteria in scalable quantities gives a new dimension to the continuously active research for better treatment for type II diabetes. Looking at existing and new methods of mass level production of digestive inhibitors and latest efforts to effectively discover new potential drugs is the subject of this book chapter.

I. INTRODUCTION

Diabetes mellitus is a heterogeneous endocrine disorder in which hyperglycemia is the unifying feature. The number of patients with diabetes is rising by 4–5% every year (Wagman and Nuss, 2001), and through its long-term effects it is a cause of highest morbidity rate around the globe. Type I diabetes is an autoimmune disorder that results in an absolute insulin deficiency. Type II diabetes, however, has a more complex pathophysiologic basis which is not yet completely understood. Type II diabetes characteristically comprises three abnormalities: relative insulin deficiency, insulin resistance involving myocytes and adipocytes, and hepatic insulin resistance (resulting in increased gluconeogenesis and impaired glycogen synthesis). It is considered as one of the pathological manifestations of the so-called ''metabolic syndrome.'' Biochemical abnormalities of Type II diabetes may include hyperinsulinemia and high levels of serum triglycerides (TG). Microvascular and macrovascular diseases account for most of the morbidity and mortality associated with

Type II diabetes. The increased prevalence of macrovascular diseases in patients with diabetes is the result of numerous factors, including but not limited to obesity, lipid abnormalities, hypertension, hyperglycemia, hypercoagulation, platelet dysfunction and endothelial dysfunction. Diabetic microvascular diseases are responsible for diabetic retinopathy and blindness, diabetic neuropathy (potentially resulting in lower-limb amputation), and diabetic nephropathy (leading to end-stage renal disease and the need for renal dialysis or transplantation) (Lebovitz, 1992).

The pathogenesis of diabetes mellitus and its management by the oral administration of hypoglycemic agents have stimulated great interest in recent years. Control over hyperglycemia can be potentially achieved by different mechanisms: (1) An increase in insulin secretion; (2) A decrease in nutrient ingestion; (3) An increase in peripheral glucose uptake; (4) A decrease in hepatic glucose production. Various groups of oral antidiabetic agents are available for clinical use such as sulfonylureas (increase insulin secretion), biguanides (increase in glucose uptake), and digestive enzyme inhibitors (delay in complex carbohydrate digestion and absorption) (Lebovitz, 1992). In addition to these, various plant extracts are being used mainly in folklore medicine worldwide as therapeutics for diabetes, and many of these have proven hypoglycemic activity along with antiobesity and antioxidant properties which make them an attractive substitution for traditional antidiabetic drugs (Aslan *et al.*, 2007; Yan *et al.*, 2008).

Among various classes of antidiabetic drugs, digestive enzyme inhibitors are natural products usually derived from microorganisms. There is substantial evidence that inhibitors, such as α-glucosidase inhibitors, could be an effective treatment for prevention or at least delay in the development of disease in patients with impaired glucose tolerance (IGT) (Scheen, 2007; Scheen, 2003). To date, extensive studies have been conducted to analyze the mechanism of action of digestive enzyme inhibitors as well as their effects on hyperglycemia. Almost all the drugs from this class inhibit various digestive enzymes, including α-glucosidases and α-amylases. However, their administration is limited by the wide range of gastrointestinal side effects they have on the patients receiving the treatment, such as abdominal discomfort, diarrhea, and flatulence (Krentz and Bailey, 2005; Lebovitz, 1992; Scheen, 2003). Among the advantages of digestive enzyme inhibitors, however, is their side effects are not too severe- for example, they do not cause hypoglycemia. In fact, there have been reports stating that they result in some significant health benefits such as substantial weight loss (Vichayanrat *et al.*, 2002). Because of the lack of severe negative side effect, some of these inhibitors are also considered a better therapy for elderly patients for diabetes treatment (Johnston *et al.*, 1997).

Digestive enzyme inhibitors chiefly include acarbose, miglitol, and voglibose, which are currently commercially available for the treatment of Type II diabetes (Fig. 2.1). Among these, acarbose is the inhibitor most

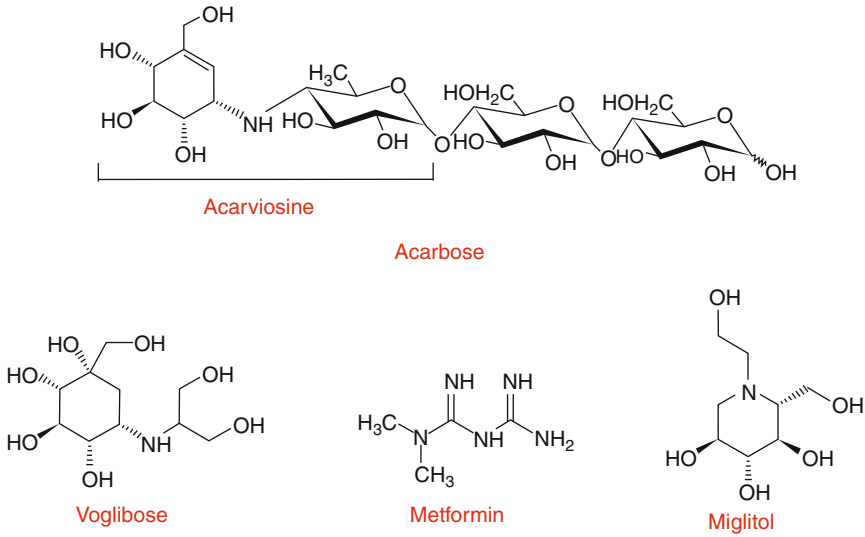

FIGURE 2.1 Structures of various digestive enzyme inhibitors and biguanides.

widely studied, but its complete biosynthetic route is not resolved; the biosynthetic routes of voglibose and miglitol are not fully understood either. Besides these three natural products, several other classes of compounds are currently of great interest as potential pharmacological agents for diabetes treatment: these are phytochemicals, with over 150 plant extracts currently being used in folklore medicine or currently under investigation for the treatment of diabetes. Some of their active compounds include flavonoids, tannins, alkaloids, glycosides, galactomannan gun, peptidoglycans, guanidine, terpenoids, inorganic ions, and glycopeptides. Most of the plant extracts that have the potential to treat Type II diabetes effectively have unfortunately not been studied in depth and very few have made it to the market as efficient drugs. In most cases, the biosynthetic pathways are not known completely while their chemical synthesis—if possible—tends to be cumbersome with low yields, which limits the potential progress to a successful drug. Considering the ongoing active research for novel solutions for the diabetes prevention and treatment, this large number of active compounds from plants can potentially provide better glycemic control with no or relatively fewer side effects. Here, an attempt has been made to summarize various natural compounds of either plant or microbial origin that possess proven or potential therapeutic properties for Type II diabetes treatment and their production methods.

II. ACARBOSE

Among the numerous antidiabetic drugs, acarbose is the most widely used digestive enzyme inhibitor for the treatment of Type-II diabetes. The story of acarbose begins with the screening by Bayer AG of various compounds isolated from a number of species of *Actinomycetes* as potent inhibitors of digestive enzymes such as α-amylase, sucrase, and maltase. It is now marketed by Bayer AG under the name Precose®. It is important to note that acarbose does not demonstrate any insulinotropic properties. This potent α-glucosidase inhibitor is a pseudotetrasacchride (Fig. 2.1) chemically known as *O*-4,6-dideoxy-4-[[(1*S*,4*R*,5*S*,6*S*)-4,5,6-trihydroxy-3-(hydroxymethyl)-2-cyclohexen-1-yl]amino]-α-D-glucopyranosyl-(1→4)-*O*-α-D-glcopyranosyl-(1 → 4)-D-glucose. It comprises acarviosine, which is made of a cyclitol moiety and an amino sugar with two glucose residues attached (Balfour and McTavish, 1993). Structural similarity of acarbose to oligosaccharides due to its glucose residues is considered to be responsible for the high-affinity binding to the sites of α-glucosidases. Acarbose inhibits various α-glucosidases in the following order: glucoamylase > sucrase > maltase > isomaltase (Tan, 1997); it also weakly inhibits α-amylases.

Acarbose is minimally absorbed (Scheen, 2007). Unlike other drugs for Type II diabetes treatment, acarbose does not have the risk of hypoglycemia (Donner, 2006), although it is important to note that acarbose and most other α-glucosidase inhibitors will be most effective when the diet is rich in starch and oligosaccharides. Because its action is directed against carbohydrate digestion, patients having diets rich in monosaccharides such as glucose will not see much help from acarbose therapy (Balfour and McTavish, 1993). Along with reducing blood glucose levels, acarbose also attenuates the levels of some other gastrointestinal and pancreatic hormones, such as decreasing plasma concentrations of gastrin and pacreozymin and increasing concentration of somatostatin (Tan, 1997). Glucagon-like peptide-1 secretion is increased by acarbose, but the release of gastric inhibitory polypeptide is reduced (Krentz and Bailey, 2005). Such a combination of decrease in blood glucose levels and rise in the glucagon-like peptide-1 levels is being considered as the new approach in the treatment of Type II diabetes (Goke *et al.*, 1994).

Acarbose is slightly less effective for fasting plasma glucose levels than sulfonylureas or biguanides, but performs additively when used in combination to sulfonylureas or metformin, since its mechanism of action is different from that of these drugs (Balfour and McTavish, 1993). It has various side effects such as diarrhea, abdominal pain, borborygmus and flatulence, due to its effect of causing delayed carbohydrate absorption. The side effects can be minimized by starting the treatment with a small dose and then gradually increasing it to higher amounts (Lebovitz, 2004).

A. Mechanism of action and pharmacokinetics

Acarbose inhibits α-glucosidases located in the brush border of the enterocytes lining of intestine (Fig. 2.2) and pancreatic α-amylases located in the lumen of the intestine competitively. Pancreatic α-amylases help digest complex starches to oligosaccharides, whereas sucrases, maltases, isomaltases hydrolyze oligosaccharides, trisacchrides and disaccharides into simple sugars, such as glucose. Its high binding affinity to these enzymes prevents them from binding to oligosaccharides and disaccharides, thus avoiding their cleavage into simple monosaccharides and deferring their complete digestion further away in jejunum. This affects the insulin secretion as delayed glucose absorption alters secretion of intestinal hormones (Krentz and Bailey, 2005; Tan, 1997). Inability of the digestive enzymes to hydrolyze acarbose is due to the presence of an imino bridge which cannot be hydrolyzed by the digestive enzymes; it is hence considered to be the key element in the inhibitory action of the molecule (Wehmeier, 2003).

Various studies have been conducted on the competitive behavior of acarbose on various digestive enzymes. The K_i for competitive inhibition of Baker's yeast α-glucosidase and rat intestine α-glucosidase are 80 and 0.006 μM, respectively. Acarbose's K_i value for inhibition of porcine pancreatic α-amylase is 100 times higher than that for rat intestine α-glucosidase (Kim *et al.*, 1999). Acarbose is absorbed negligibly into the system of the patient (Clissold and Edwards, 1988); as a result, it is generally accepted that its main mechanism of action is within the intestine. No accumulation of acarbose was noted during administration at a standard dosage of 300 mg, three times daily for 3 months (Putter *et al.*, 1982).

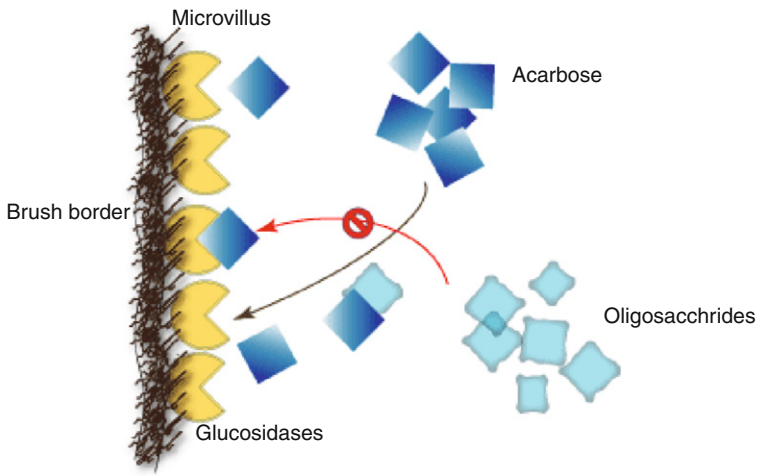

FIGURE 2.2 Mechanism of action of acarbose.

Acarbose degradation is observed to take place via two pathways: cleavage by intestinal digestive enzymes and biotransformation by intestinal microorganisms (Balfour and McTavish, 1993). Upon oral administration of the drug, 35% of acarbose and its metabolites are excreted by urinary and fecal routes whereas 94% is recovered in urinary form from an intravenous dose (Ahr *et al.*, 1989).

It is interesting to note the side effects acarbose has on patients, mainly due to its mechanism of action of delayed glucose absorption. The most common side effects are gastrointestinal symptoms that occurred to 83% of the subjects treated with acarbose versus only 60% treated with placebo in STOP-NIDDM study (Study To Prevent Non-Insulin-Dependent diabetes mellitus) (Chiasson *et al.*, 2002). Flatulence is the next most frequent side effect, with 68% of those treated with acarbose suffered from this as opposed to only 27% treated with placebo. Diarrhea, abdominal pain, nausea and constipation were observed in certain cases at comparable frequencies in both acarbose treated subjects as well as with placebo. It is remarkable that out of 714 subjects assigned for acarbose treatment for 3.3 years, 211 subjects withdrew from study within a year's time, mainly due to such side effects (Chiasson *et al.*, 2002). But as mentioned above, these effects can be alleviated by treating with small dosage initially and gradually increasing the dose strength.

B. Manufacturing of acarbose

As already mentioned, acarbose is manufactured by Bayer AG under various trade names in different countries, such as Precose® in North America, Prandose® in Canada, and originally Glucobay® in Europe. Acarbose is manufactured in a multistep batch fermentation process in its weakly basic form from *Actinoplanes* sp. SE50. Process volume is 30–100 m^3 in a medium supplemented mainly with starch and maltose (as maltose supplementation increases yields; (Frommer *et al.*, 1977a)) and essential salts. The resulting product is a mixture of acarbose and many compounds having high similarities to acarbose (Wehmeier and Piepersberg, 2004). The presence of starch in the culture gives rise mainly to amino sugars having 4–8 hexose units which are suitable for further breakdown into acarbose-like compounds. On the other hand, starch-free nutrients with addition of maltose produce mixtures dominated by di- and trisacchrides (Frommer *et al.*, 1977b). Its downsteam processing takes place in a stepwise manner (Rauenbusch and Schmidt, 1978), with various improvements incorporated over the years. The overall process is as follows:

I. A strong acidic cation exchanger and a basic anion exchanger are simultaneously added to the culture broth, preferably without mycelium. Weakly basic acarbose binds to the cation exchanger strongly and about 80–90% acarbose is thus separated from the culture at this step.

II. The resin mixture is separated from the broth along with mycelium (if any) via sieve screw centrifuge. After separation, washing by deionized water is carried out to free acarbose from adhering impurities.
III. Elution of acarbose is then carried out by using dilute (~0.1 M) basic salt solutions in kettles with nozzle sieves.
   a. Elution is pH and temperature sensitive. Having a pH in the 4.3–5.0 range is highly desirable. Also, low temperatures increase the adherance of acarbose to the column; hence room temperature or lower temperatures are maintained during the application of the substance, while for elution of acarbose raised temperatures of 40–70 °C are used. This results in rapid elution with good acarbose yields (Rauenbusch, 1987).
IV. The eluant is subjected to further purification by passing it through a series of three columns; cation/anion/cation exchangers (strongly acidic/basic/strongly acidic) for removal of basic cations, to raise the pH above 3, and to bind acarbose and its analogs strongly, respectively. Most of the acarbose and other compounds are bound in the topmost part of the third column.
V. This fraction is rinsed by deionized water and it is then eluted preferably by 0.025 N hydrochloric acid; the fractions containing acarbose are combined.
VI. The pH of the fraction containing acarbose is increased to 6.0–6.5 by addition of anion exchanger.
VII. The solution is then concentrated in vacuo, sterilized, and dried subsequently by lyophilization.

The schematic of the manufacturing process is given in Fig. 2.3. Various other improvements in the downstream processing and fermentation

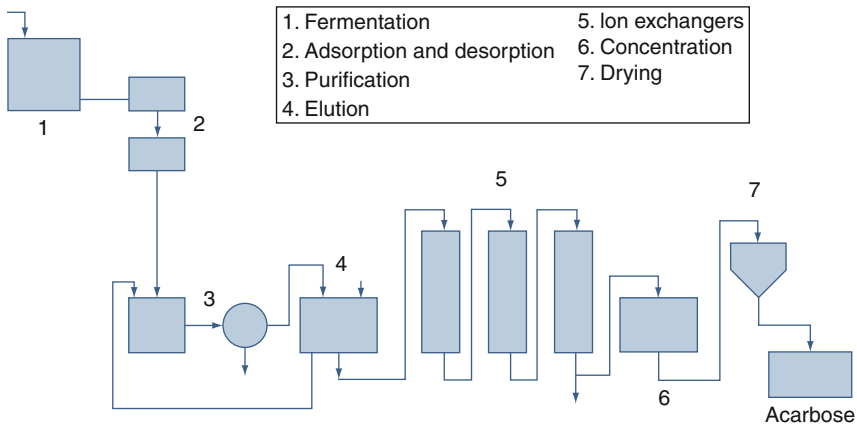

FIGURE 2.3 Manufacture of acarbose (Rauenbusch, 1987).

process have been published, such as use of special weakly acidic cation exchangers having carboxyl groups (Rauenbusch, 1987), controlling the osmolality of the culture at an optimum around 400 mosmol/kg (Beunink *et al.*, 1997), and the use of specifically developed cation exchangers made from macroporous, resistant polymers based on aromatic compounds (Lange and Rauenbusch, 1986). All these approaches have reported higher yields of acarbose and better separation.

The reported production of acarbose was 1 g/L for the *Actinoplanes* sp. SE50/110 under optimal culture conditions (Rauenbusch and Schmidt, 1978). The final concentration of acarbose is 98%.

C. Biosynthesis of acarbose in *Actinoplanes* sp. SE50/110

As already mentioned, acarbose is a secondary metabolite produced in bacterium species *Actinoplanes* sp. SE50. In the genome of *Actinoplanes* sp. SE50, 25 genes have been identified encoding various proteins necessary for biosynthesis of acarbose, its intra- and extracellular transport, and its metabolism (Wehmeier, 2003). A number of these genes have not been characterized and their function is speculated based on phylogenetic studies. A few crucial steps from the starting precursor 2-*epi*-5-*epi*-valiolone to acarviosine of acarbose are conjectural; in this chapter, the most recent developments in unraveling the acarbose biosynthetic pathway in *Actinoplanes* sp. SE50 are presented.

The entire *acb* gene cluster, consisting of 25 genes responsible for biosynthesis of the deoxyhexose and cyclitol moieties of acarbose, and its metabolism are shown in Fig. 2.4. The accession numbers of its genes are provided in Table 2.1.

Parallel to the formation of this cyclitol moiety of acarbose is the synthesis of the deoxysugar moiety, which starts with glucose-1-phosphate, activated by a nucleotidation step catalyzed by *acbA* (suggested dTDP-glucose synthase). The dTDP-D-glucose, thus formed, is further converted into dTDP-4-keto-6-deoxy-glucose by *acbB* (suggested dTDP-glucose-4-6-dehydratase) (Wehmeier and Piepersberg, 2004). The next reaction is catalyzed by *acbV*, an enzyme that belongs to the family of GabT-like aminotransferases, which is involved in primary metabolism (Piepersberg, 1997; Piepersberg and Distler, 1997; Piepersberg *et al.*, 2002). It is suggested that when *acbV* was heterologously expressed in *S. lividans 66*, it catalyzed the amination of dTDP-4-keto-6-deoxy-D-glucose probably resulting in dTDP-4-amino-4,6-dideoxy-D-glucose (Piepersberg *et al.*, 2002). This aminotransferase reaction is crucial in acarbose biosynthesis, as this amino group nitrogen bridges the valienamine moiety and the deoxysugar moiety. Another 12-step synthesis of dTDP-4-amino-4,6-dideoxy-D-glucose was suggested (Bowers *et al.*, 2002), wherein this

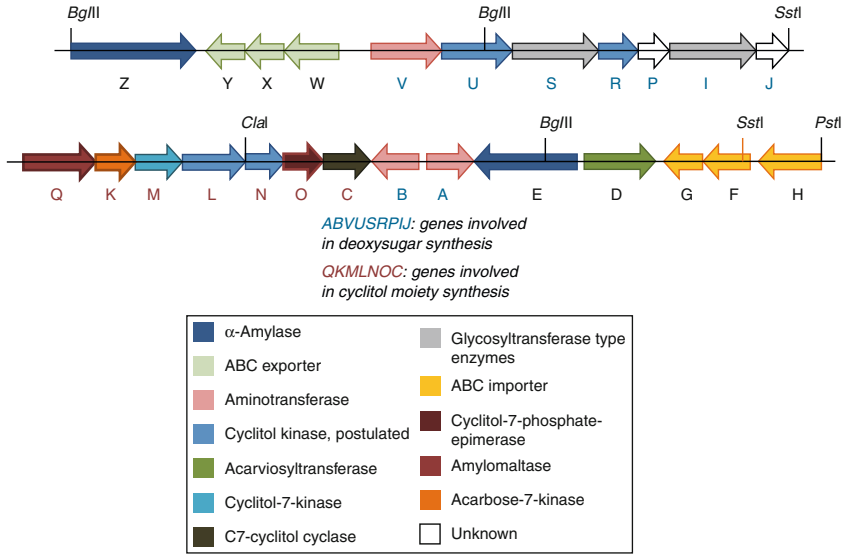

FIGURE 2.4 *Acb* gene cluster (Apeler *et al.*, 2001; Hemker *et al.*, 2001).

moiety is proposed to be synthesized from a galactoside which can be formed from D-galactose.

Table 2.1 lists the various digestive enzyme inhibitors and biguanides, along with their postulated names and function. These 25 genes have a very peculiar arrangement consisting of several transcription units, with three operons at the least. *AcbWXY* and *acbHFG* are two operons encoding three genes each. It is suggested that they are actually ABC-exporters and ABC-importers with *acbHFG* being membrane bound and extracytoplasmic enzymes, having highly conserved sequences to ABC-importers from *MsmEFG* of *Streptococcus mutans* (Wehmeier and Piepersberg, 2004). It is believed that *acbVUSRPIJQKMLNOC* forms a single transcription unit. The genes *acbKMLNOC* have been studied in detail and their functions are determined (Zhang *et al.*, 2002). More specifically, it is proposed that *acbC* (C7-cyclitol cyclase) is responsible for the synthesis of the 2-*epi*-5-*epi*-valiolone (Mahmud *et al.*, 1999). It was initially presumed that *acbK* (acarbose 7-kinase) is responsible for the phosphorylation of 2-*epi*-5-*epi*-valiolone, although in later experiments it was shown that *acbK* fails to phosphorylate 2-*epi*-5-*epi*-valiolone using an ATP-labeled phosphorylation assay. Instead, *acbM* showed positive results, suggesting that *acbM* was the first enzyme in the acarbose biosynthesis pathway resulting in the synthesis of 2-*epi*-5-*epi*-valiolone-7-phosphate. Further studies revealed that the next enzyme on the pathway was an epimerase encoded by *acbO*. The product of the enzymatic reaction of *acbO* was characterized

TABLE 2.1 Genes from *acb* cluster and their accession numbers

Gene	Enzyme	Accession number
acbA	dTDP-glucose synthase (i)	CAA77210
acbB	dTDP-4,6-dehydrogenase (i)	Q9ZAE8
acbC	C7-cyclitol cyclase (i)	CAA77208
acbD	Acarviosyltransferase (e)	CAJ81031
acbE	Acarbose resistant α-amylase (e)	CAJ81030
acbF	Carbohydrate ABC transporter (m)	CAJ81033
acbG	Carbohydrate ABC transporter (m)	CAJ81032
acbH	Carbohydrate ABC transporter(e–l)	CAJ81034
acbI	Glycosyl transferase (i)	CAJ81027
acbJ	Putative hydrolase (i)	CAJ81028
acbK	Acarbose-7-kinase (i)	CAD29481
acbL	Polyol dehydrogenase (i)	CAD29483
acbM	Cyclitol-7-kinase (i)	CAD29482
acbN	Oxidoreductase (i)	CAD29484
acbO	Cyclitol-7-phosphate-epimerase (i)	CAD29485
acbP	Unknown (i)	CAJ81026
acbQ	Amylomaltase (i)	CAJ81029
acbR	NDP-polyol synthase (i)	CAJ81025
acbS	Putative glycosyl transferase (i)	CAJ81024
acbU	Putative cyclitol kinase (i)	CAJ81023
acbV	Aminotransferase (i)	CAJ81022
acbW	ATP binding component of ABC exporter (i, m)	CAJ81021
acbX	ABC transporter (i, m)	CAJ81020
acbY	ABC exporter	CAJ81019
acbZ	α-Amylase (e)	CAJ81018

e, extracellular; i, intracellular (cytoplasmic); e–l, extracytoplasmic lipoprotein; m, membrane-integrated (Wehmeier and Piepersberg, 2004).

using mass spectrometry. *AcbO* functions independently without the need for cofactors or coenzymes indicating that it is a representative of a new class of epimerases (Zhang *et al.*, 2003a). *AcbN* and *acbL* showed distinct similarity to various members of oxidoreductase families such as zinc-dependent dehydrogenases and short chain alcohol dehydrogenases, respectively, and were shown to catalyze the formation of 1-*epi*-valienol-7-phosphate (Zhang *et al.*, 2002).

The cluster of *acbBAED* has been studied to some extent, with *acbD* having been expressed heterologously in *Streptomyces lividans* TK23, and

characterized. *AcbD*, which was initially postulated to be a glycosyltransferase, turned out to be acarviosyl transferase that modifies acarbose extracellularly (Hemker *et al.*, 2001). At the same time, *acbA* and *acbB* catalyze the first two reactions in the biosynthetic pathway for the formation of the deoxyhexose moiety (Liu and Thorson, 1994; Piepersberg, 1994).

The biosynthetic pathway from 2-*epi*-5-*epi*-valiolone and glucose-1-phosphate to acarbose is depicted in Fig. 2.5. The first precursor responsible for the cyclitol moiety of acarbose is 2-*epi*-5-*epi*-valiolone, which was affirmed by NMR studies from its incorporation into acarbose pathway in *Actinoplanes* sp. (Mahmud *et al.*, 1999). Its precursor is sedoheptulose 7-phosphate, which is derived from the pentose phosphate pathway (Mahmud, 2003). Its phosphorylation at C7 takes place by a postulated enzyme, cyclitol-7-kinase, encoded by *acbM* to formulate 2-*epi*-5-*epi*-valiolone-7-phosphate (Zhang *et al.*, 2002). Its epimerization by *acbO* results in the formation of 5-*epi*-valiolone-7-phosphate, which has been characterized by mass spectroscopic and NMR spectroscopic methods (Zhang *et al.*, 2003a). Further reduction of the C-1 keto group takes place by NADH-dependent dehydrogenase, *acbL*, giving the next intermediate in the biosynthetic pathway, 5-*epi*-valiolol-7-phosphate. Further steps involve postulated enzymes based on phylogenetic studies and reaction intermediates which are not fully characterized yet. The *acbN* protein (suggested oxidoreductase) could catalyze synthesis of the next intermediate, 1-*epi*-valienol-7-phosphate. A new kinase activity was characterized in *Actinoplanes*, which could phosphorylate 1-*epi*-valienol to 1-*epi*-valienol-7-phosphate, although this kinase activity could not be attributed to any gene from the *acb* cluster (Thomas, 2001; Zhang *et al.*, 2003b). The enzyme necessary for catalyzing the conversion of 1-*epi*-valienol-7-phosphate to 1-7-diphospho-1-*epi*-valienol by performing a phosphorylation at the C-1 position is not characterized. The next enzyme, however, has been characterized: *acbR* (Tatusov *et al.*, 2001), an ADP-glucose synthase-like protein that catalyzes nucleotidation at C-1 position of 1-7-diphospho-1-*epi*-valienol, a proposed precursor. This reaction completes the synthesis of cyclitol moiety of acarbose which involves the majority of proteins encoded by genes in the acbQKMLNOC operon (Wehmeier and Piepersberg, 2004).

Parallel to the formation of this cyclitol moiety of acarbose is the synthesis of the deoxysugar moiety, which starts with glucose-1-phosphate, activated by a nucleotidation step catalyzed by *acbA* (suggested dTDP-glucose synthase). The dTDP-D-glucose, thus formed, is further converted into dTDP-4-keto-6-deoxy-glucose by *acbB* (suggested dTDP-glucose-4-6-dehydratase) (Wehmeier and Piepersberg, 2004). The next reaction is catalyzed by *acbV*, an enzyme that belongs to the family of GabT-like aminotransferases, which is involved in primary metabolism (Piepersberg, 1997; Piepersberg and Distler, 1997; Piepersberg *et al.*, 2002). It is suggested that when *acbV* was heterologously expressed in *S. lividans 66*, it catalyzed the amination of

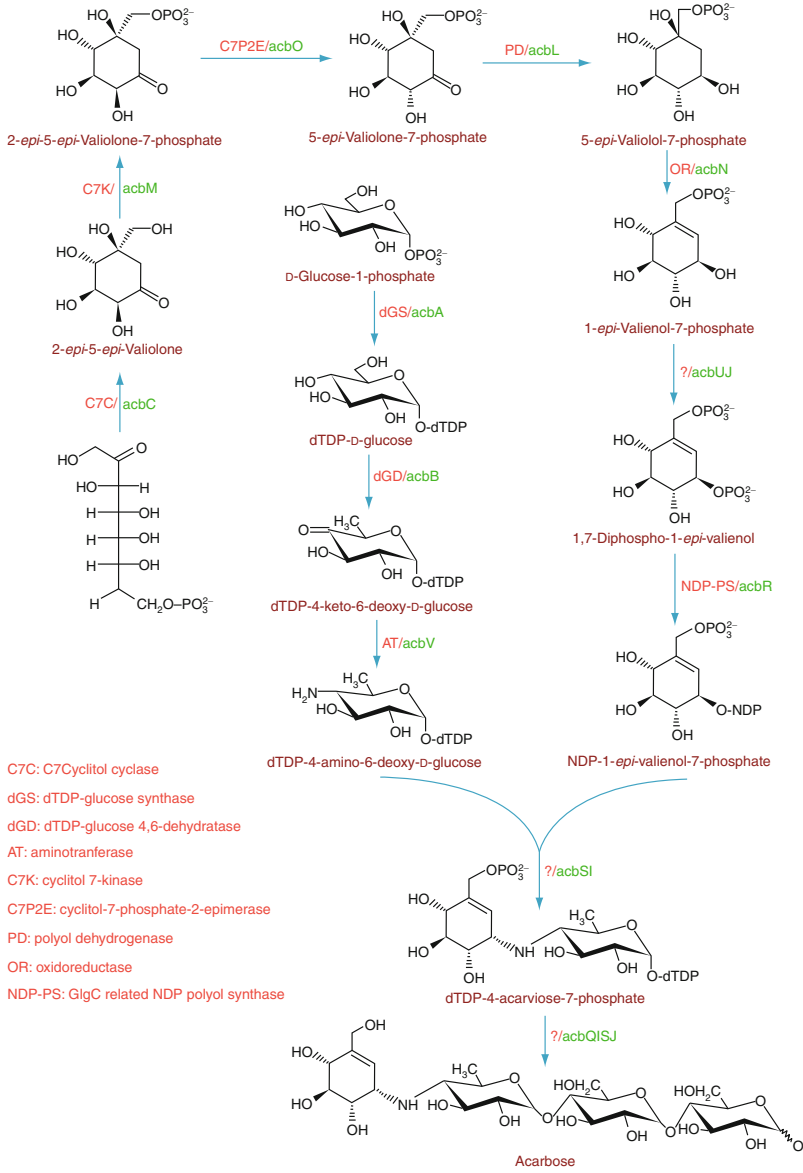

FIGURE 2.5 Biosynthesis pathway of acarbose (Mahmud *et al.*, 1999; Zhang *et al.*, 2002).

dTDP-4-keto-6-deoxy-D-glucose probably resulting in dTDP-4-amino-4,6-dideoxy-D-glucose (Piepersberg *et al.*, 2002). This aminotransferase reaction is crucial in acarbose biosynthesis, as this amino group nitrogen bridges the

valienamine moiety and the deoxysugar moiety. Another 12-step synthesis of dTDP-4-amino-4,6-dideoxy-D-glucose was suggested (Bowers *et al.*, 2002), wherein this moiety is proposed to be synthesized from a galactoside which can be formed from D-galactose.

AcbS and *acbI* are related to glycogen and sucrose synthases and they are thus speculated to catalyze the necessary glycosyltransferase-like reaction to formulate dTDP-acarviose-7-phosphate. This is achieved by a combined reaction between the cyclitol precursor NDP-1-*epi*-valienol-7-phosphate and deoxysugar precursor dTDP-4-amino-4,6-dideoxy-D-glucose, thus synthesizing a speculated precursor of acarbose. However, the end product may be acarbose-7-phosphate or some other compound instead of acarbose itself (Wehmeier and Piepersberg, 2004); it might need more than just one step to convert dTDP-acarviose-7-phosphate into acarbose. The biosynthetic pathway in Fig. 2.5 shows the postulated precursor and the postulated enzymes that catalyze its formation and its conversion to acarbose.

D. Effect on hyperglycemia

Various placebo-controlled dose comparison studies for the safety and efficacy of acarbose have been conducted and published, most of which demonstrated high efficiency of acarbose in correcting hyperglycemia. Comparison studies with other antidiabetic drugs indicate that acarbose can be used effectively as a monotherapy to reduce postprandial blood glucose levels or in combination with other drugs.

One such study checked the efficacy of acarbose as monotherapy, with metformin, with sulfonylureas, and with insulin on four different groups (50–200 mg twice daily (tid)) for 52 weeks (Chiasson *et al.*, 1994). Each group showed a remarkable decrease in glycosylated hemoglobin A (HbA_{1c} and HbA_1), with 0.9%, 0.8%, 0.9%, and 0.4% reduction, respectively, for each group against diet alone, only metformin, only sulfonylureas, and only insulin. Another study carried out indicates its enhanced antihyperglycemic effects when acarbose is applied in a combination therapy with metformin (Scheen *et al.*, 1993). The 24-week study for acarbose as monotherapy showed reduction in fasting blood glucose by 1.4 mM and postprandial glucose level by 2.2 mM and decreased HbA_{1c} by 1.1% as opposed to placebo. A comparison with glyburide (sulfonylureas) indicated similar decrease of 0.9% in HbA_{1c} on comparison with placebo (Hoffmann and Spengler, 1994). If acarbose is used as monotherapy in combination with adequate diet management, it has been found to decrease fasting glucose plasma level by 1 mmol/L and postprandial glucose levels by approximately 3 mmol/L. Postprandial insulin levels decreased by about 20–25%, while fasting insulin levels remained unchanged and HbA_{1c} values were decreased by 0.65 to 1.0% when compared with placebo (Coniff, 1991).

Recently, different comparative studies were carried out for different drugs for treatment of Type II diabetes, such as the Diabetes Prevention Program (DPP) in the United States, the Study TO Prevent Non-Insulin-Dependent diabetes mellitus (STOP-NIDDM) in various European countries and Canada, the Chinese Diabetes Prevention Study (CDPS), the Early Diabetes Intervention Trial (EDIT) in United Kingdom, and the Indian Diabetes Prevention Program (IDPP). Most of these studies are carried out in randomized, placebo-controlled and blind folded trials, for a prolonged period of 3 years to check the development of diabetes mellitus after treatments with drug or placebo in patients with IGT. The STOP-NIDDM study (Chiasson *et al.*, 2002) checked for delay in progress toward diabetes in patients having IGT, and their study showed reduction in risk of progression toward diabetes by 25% over 3.3 years. From a total of 1429 randomized patients (age $\sim$ 55 years, body-mass index (BMI) 31 kg/m^2), 714 were treated with 100 mg (tid) acarbose and 715 were treated with placebo. Sixty-one patients out of the total pool were later excluded from the study since they did not meet IGT criteria nor had postrandomization data. Out of 682 analyzed for acarbose, 32% developed diabetes mellitus, whereas out of 686 treated with placebo, 42% developed diabetes. Administration of acarbose also increased the probability of IGT reverting to normal glucose tolerance over time (Chiasson *et al.*, 2002). In the CDPS study (Yang *et al.*, 2001), 88 patients having BMI 25 kg/m^2 and IGT were subjected to treatment with acarbose or metformin, while 85 received conventional education (control group). In this study, 50 mg of acarbose (tid) was administered to the patients for 6 years (Scheen, 2007). Of the control patients 34.9% progressed to diabetes, whereas only 6% of those treated with acarbose progressed to diabetes. This implies an 87.8% reduction in risk as compared with 25% from the previous study. However, the EDIT study did not confirm this high reduction in the progress to diabetes; however, it confirms that administration of acarbose decreased the risk of IGT patients progressing to diabetes (Scheen, 2007).

When checked for efficacy as a combination therapy with sulfonylureas, the effect is additive. However, acarbose is less effective than tolbutamide when both treatments are given independently (Coniff *et al.*, 1995). The mechanisms of action of sulfonylureas and α-glucosidase inhibitors are different, which perhaps can explain why the treatment with these compounds as monotherapy has different efficacies. A total of 290 subjects having Type II diabetes and fasting glucose levels no less than 140 mg/dL were treated with 200 mg of acarbose and 250–1000 mg (tid) of tolbutamide either alone or in combination for 24 weeks. The reduction in postprandial plasma glucose levels were reported as 85 mg/dL for acarbose-plus-tolbutamide, 71 mg/dL for tolbutamide alone, 56 mg/dL for acarbose alone, and only 13 mg/dL for placebo (Coniff *et al.*, 1995) (Table 2.2).

TABLE 2.2 Clinial trials of acarbose in Type II diabetes

Study (reference)	Drug(s)	Dose of acarbose (mg tid)	Duration of study	*N*	Results
(Chiasson *et al.*, 1994)	A,A/M,A/S,A/I	50–200	52 weeks	354	HbA_{1c} decreased by 0.9%, 0.8%, 0.9%, 0.4% resp.
(Hoffmann and Spengler, 1994)	A, G	100	24 weeks	96	HbA_{1c} decreased by 1.0%, 0.9% resp.
STOP-TYPE II DIABETES (Chiasson *et al.*, 2002)	A	100	3.2 years	1368	RR = 0.75, $P = 0.0015$
EDIT (Holman *et al.*, 2003; Scheen, 2007)	A	50	6 years	631	RR = 0.81, $P = 0.81$
	M	500	6 years	631	RR = 0.81, $P = 0.94$
CDPS (Yang *et al.*, 2001)	A	50	3 years	261	RR = 0.12, $P = 0.00001$
(Coniff *et al.*, 1995)	A, T, A/T	200	24 weeks	290	HbA_{1c} decreased by 0.54%, 0.93%, 1.32% resp.

A, acarbose; M, metformin; S, sulfonylureas; I, insulin; G, glyburide; T, tolbutamide; RR, relative risk of developing diabetes versus placebo.

Acarbose is expected to be useful in treatment of insulin-dependent diabetes mellitus (IDDM) as well, but there has not been as much data on IDDM published as there is for Type II diabetes. A few studies indicate positive results, proving that acarbose helps smoothing out postprandial glycemic fluctuations and preventing both hyperglycemia and hypoglycemia in insulin-treated patients having IDDM (Balfour and McTavish, 1993; Lebovitz, 1992). Reduction in the plasma glucose levels (0.1–1.1%) and insulin requirements to 35% were reported (Balfour and McTavish, 1993). Two hundred and thirty-six patients with IDDM were treated in a randomized double-blind study with acarbose 150–600 mg/day or placebo for 24 weeks along with usual insulin requirements. Such a treatment reduced postprandial plasma glucose levels at roughly 3 mmol/L. The study also showed that insulin requirements decreased by 3.5 IU/day (Hollander and Coniff, 1991).

III. MIGLITOL

One of the widely used α-glucosidase inhibitors for treatment of Type II diabetes is miglitol ($C_8H_{17}NO_5$; IUPAC name (2*R*,3*R*,4*R*,5*S*)-1-(2-hydroxyethyl)-2-(hydroxymethyl)piperidine-3,4,5-triol; molecular weight 207.2). Miglitol is a second-generation α-glucosidase inhibitor derived from 1-deoxynojirimycin, which is yet another α-glucosidase inhibitor and is structurally similar to glucose (Fig. 2.1) (Tan, 1997). It is a white to pale yellow powder and is soluble in water (Campbell *et al.*, 2000). Miglitol was approved by the U.S. Food and Drug Administration (FDA) in 1996 as an additional therapy to diet alone therapy or diet plus sulfonylurea therapy in patients with Type II diabetes. Miglitol's story begins with the successful attempts for identifying new compounds with inhibitory properties, which initially resulted in the discovery of nojirimycin, deoxynojirimycin, and their derivatives from various *Bacillus* and *Streptomyces* strains (Schmidt *et al.*, 1979). During initial attempts, 1-deoxynojirimycin was successfully obtained (Schmidt *et al.*, 1979); however, its *N*-hydroxyethyl analog (miglitol) later proved to possess better inhibitory activities. It is currently being manufactured by Bayer AG under the trade name of Glyset® in USA and as Diastabol® in Europe. Miglitol is considered to be a good choice for the therapy of patients who have the relative risk of developing hypoglycemia, weight gain, or lactic acidosis (Campbell *et al.*, 2000). It is observed to have the same efficacy as acarbose at lesser dosages (50 and 100 mg tid). Miglitol therapy provides better reduction on fasting and postprandial plasma glucose levels in patients in comparison with sulfonylureas (Scott and Spencer, 2000), whereas voglibose, another α-glucosidase inhibitor, could achieve reduction only for postprandial glucose levels.

A. Mechanism of action and pharmacokinetics

The mechanism of action of miglitol is very similar to that of acarbose; it has strong binding affinity to digestive enzymes and, as a result, prevents these enzymes from binding to complex carbohydrates thereby delaying glucose absorption and resulting in reduction in postprandial plasma levels. The difference to note is that miglitol is a competitive inhibitor of digestive enzymes as a substitute for glucose, whereas acarbose functions as a substitute for the starch and oligosaccharides. Miglitol shows inhibitory action toward almost all the digestive enzymes present in the brush border of small intestine with the following ranking order: sucrase > glucoamylase > isomaltase > lactase > trehalase, and some inhibitory activity toward α-amylase (Lembcke *et al.*, 1985; Scott and Spencer, 2000).

Both acarbose and voglibose are not absorbed in the upper section of upper intestine. Miglitol, however, is almost completely absorbed in the small intestine (Scott and Spencer, 2000; Tan, 1997). The absorption of miglitol is dose dependent, with 25 mg of miglitol rapidly and completely absorbed. However, higher doses of up to 100 mg do not get fully absorbed, and 95% of miglitol is excreted out of the system via urine and feces almost unchanged. The amount excreted depends upon the systemic absorption, and therefore on the dose administered. With the lowest dose of 25 mg, almost 95% excretion is achieved, but with higher dosages this amount drops. The half-life of miglitol in healthy volunteers is 2–3 h for a less potent dose of 50 mg (Ahr *et al.*, 1997; Campbell *et al.*, 2000; Scott and Spencer, 2000).

B. Biosynthesis and large-scale production of miglitol

Several efforts were put into achieving large-scale production of miglitol. Unlike acarbose, large-scale production of miglitol involves a combination of biochemical and chemical syntheses.

As mentioned above, miglitol is an N-derivative of 1-deoxynojirimycin which is obtained from D-glucose as a starting material. The formation of miglitol from D-glucose is made possible by the ability of *Glucanobactor oxydans* to regio- and stereoselectively oxidize polyol substrates (Schedel, 2000). This conversion from glucose to miglitol is a simple three-step reaction using a highly selective enzyme, polyol dehydrogenase, which essentially rules out the necessity of any protection group chemistry. The first step carries out amination to obtain 1-amino-D-sorbitol through a reduction reaction. 1-Amino-D-sorbitol thus obtained is then oxidized at C5 by polyol dehydrogenase from *Glucanobactor oxydans.* Finally, ring closure is achieved by reduction (Deppenmeier *et al.*, 2002; Schedel, 2000) (Fig. 2.6).

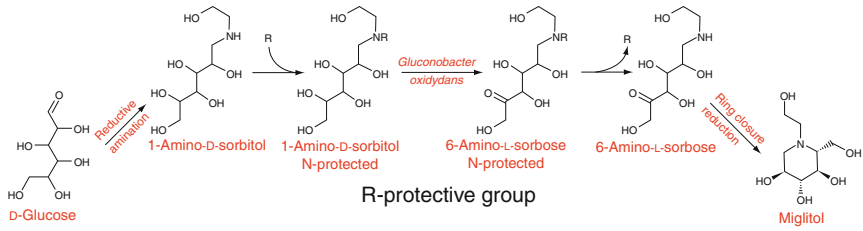

FIGURE 2.6 Combined approach of chemical and biotechnological synthesis of miglitol (Deppenmeier *et al.*, 2002; Schedel, 2000).

Miglitol requires 1-deoxynojirimycin as a precursor which can be obtained via three different routes: extraction from plants such as the mulberry tree, fermentation using various bacterial strains, and a complete chemical synthesis. Industrially feasible production of miglitol was, however, restricted by expensive purification steps or low yields. Hence, a new approach was adopted in which a combination of biochemical and chemical synthesis was employed (Schedel, 2000). In this approach, D-glucose is converted to 1-amino-D-sorbitol by reduction with suitable amines and hydrogen, with nickel as catalyst, and then further reaction of products with appropriate acid esters (Kinast and Schedel, 1979). The oxidation of 1-amino-D-sorbitol to 6-amino-L-sorbose is then carried out in a fermenter using *Gluconobacter oxydans* grown at temperatures between 20 and 45 °C, preferably at room temperature and maintaining the pH between 2.0 and 9.0. At this pH, 6-amino-L-sorbose is present in the medium as piperidinose, which is reduced to 1-desoxy-nojirimycin in the presence of inert solvents and by choosing the appropriate pH. After this, miglitol is obtained by first centrifuging the biomass followed by clarification using active charcoal. Next, separation of catalyst, evaporation of solvents, and isolation of any remaining salts in the medium is carried out (Kinast and Schedel, 1979). An important modification necessary in this process is the addition of protection groups before feeding 1-amino-D-sorbitol to the *G. oxydans* cultures and their subsequent removal before the ring-closure reaction. This is necessary since1-amino-D-sorbitol is readily oxidized by *G. oxydans* strains to form 3-hydroxy-2-hydroxymethyl-pyridine at near-neutral pH as a result of spontaneous ring closure (Schedel, 2000).

C. Effect on hyperglycemia

As mentioned earlier, miglitol was approved as a monotherapy or as a combination therapy with sulfonylureas in patients with Type II diabetes along with dietary control. Various double-blind, randomized studies for efficacy and safety of miglitol have been carried out on healthy volunteers as well as on patients with Type II diabetes. When studied as

monotherapy in patients for its efficacy and tolerability in comparison with sulfonylureas, it was observed that small doses of miglitol are not as effective as sulfonylureas. In a 1-year long, double-blind, randomized, placebo-controlled trial, 411 elderly patients (age 60 or more) were split into four groups wherein the first group received placebo, the second group received miglitol at 25 mg (tid), the third received 50 mg miglitol (tid), and the last received glyburide based on fasting glucose levels (once daily). After a year, HbA_{1c} levels were dropped by 0.49%, 0.4,%, and 0.92% for 25 mg miglitol, 50 mg miglitol, and glyburide groups, respectively versus placebo ($P < 0.05$–0.01 vs. placebo) (Johnston *et al.*, 1997). Similar results were obtained when 100 patients were treated with either glyburide or miglitol (47 and 49, respectively) for a total of 24 weeks, where the administration of drug was 50 mg (tid) for miglitol for the first 6 weeks which was then raised to 100 mg (tid) for 18 weeks while for glyburide the administered dose was 2.5 mg (tid) for 6 weeks raised to 5 mg (tid) for the rest of the study. After 24 weeks, HbA_{1c} was reduced from baseline by 0.78% for the miglitol group whereas it was reduced by 1.18% for glyburide, indicating it is more potent than miglitol in reducing plasma glucose levels. When compared for postprandial glucose reduction, miglitol was observed to achieve similar decrease as glyburide after breakfast; however, after lunch the effect was more pronounced for miglitol with 57.6 mg/dL ($P < 0.001$ vs. placebo) as compared to only 36 mg/dL for glyburide ($P < 0.001$ vs. placebo) (Pagano *et al.*, 1995).

Another multicenter, double-blind, randomized, and placebo-controlled study to determine the effect of miglitol treatment involved 192 patients who had been receiving sulfonylureas for at least 6 months prior to the trial and the results were recorded after 8, 14, and 20 weeks from the start of the study (Campbell *et al.*, 2000; Johnston *et al.*, 1994). After a placebo treatment for 6 weeks, the subjects were randomized into three groups receiving 50 mg miglitol (tid), 100 mg (tid) miglitol, or placebo. The resulting reduction in HbA_{1c} was significant ($P = 0.0001$) with 50 and 100 mg of miglitol treatment (0.49% and 0.41% decrease, respectively) as compared to placebo (treatment with sulfonylurea only), indicating an additive effect due to combinational therapy. Weight increase was observed by 0.13 kg in placebo, 0.55 kg with miglitol treatment of 50 mg, and 0.08 kg with 100 mg (NS) miglitol treatment (Johnston *et al.*, 1994). Similar rise in lowering HbA_{1c} was also observed in a study on patients receiving insulin therapy (Escobar-Jimenez *et al.*, 1995); it was also reported that requirement of insulin in such patients dropped (Dimitriadis *et al.*, 1991).

Miglitol has similar side effects as acarbose, such as diarrhea, flatulence, and abdominal pain (Campbell *et al.*, 2000; Johnston *et al.*, 1994; Scott and Spencer, 2000). All these side effects were dose dependent and were subdued on continued therapy and resolved completely upon stopping the treatment (Johnston *et al.*, 1994).

IV. VOGLIBOSE

Voglibose, whose IUPAC name is 5-(1,3-dihydroxypropan-2-ylamino)-1-(hydroxymethyl)cyclohexane-1,2,3,4-tetrol ($C_{10}H_{21}NO_7$), is mainly used as the antidiabetic drug in Asia and is sold under different trade names in various countries. In India, it is sold by Ranbaxy Labs under the trade name Volix®, whereas it is marketed under the name of Basen® in Japan. It is synthesized from valiolamine, which is isolated from fermentation broth of *Streptomyces hydroscopicus* subsp. *limoneus* (Matsuo *et al.*, 1992). Just like acarbose and miglitol, it falls in the category of α-glucosidase inhibitors and inhibits competitively and reversibly glucoamylase, sucrase, and isomaltase. While acarbose also weakly inhibits α-amylase, voglibose has no inhibitory action toward α-amylases (Goke *et al.*, 1995; Horii *et al.*, 1986). Various studies have proven that voglibose successfully reduces plasma glucose levels, insulin, and C peptide postprandially in a dose-dependent manner (Chen *et al.*, 2006; Goke *et al.*, 1995; Matsuo *et al.*, 1992).

A. Mechanism of action and pharmacokinetics

As observed in the case of acarbose, voglibose inhibits α-glucosidases in a reversible and competitive manner and delays the complex carbohydrate absorption resulting in decrease in hyperglycemia and hyperinsulinemia (Chen *et al.*, 2006; Vichayanrat *et al.*, 2002). Its structure is similar to oligosaccharides and other derivatives of starch and involves a valiolamine moiety connected to propanediol moiety with a nitrogen bridge which plays an important role in the drug's activity. Voglibose binds to the digestive enzymes and as a result they fail to break it down due to this nitrogen bridge. Its IC_{50} values toward porcine maltase and sucrase have been evaluated and reported as 1.5×10^{-2} and 4.6×10^{-3} μM, respectively (Chen *et al.*, 2006). Valienamine derivatives were observed to have lesser inhibition of porcine maltase and sucrase as compared to valiolamine derivatives. Although its chemical synthesis from glucose has been described (Chen *et al.*, 2006), its exact biosynthesis from valiolamine (obtained from *S. hydroscopicus* subsp. *limoneus*) is not completely understood.

B. Effect on hyperglycemia

Voglibose (AO-128) is not as widely studied as acarbose, the latter being the first representative α-glucosidase inhibitor. Despite that, several groups have studied its effects on postprandial glucose levels and on insulin and C-peptide content in patients with Type II diabetes. In general,

voglibose has been found to significantly decrease the rapid rise in postprandial glucose. One of the early studies on voglibose efficiency and its effects on digestive enzymes indicated up to 33-fold increased inhibition of semipurified porcine small intestine disacchridases than acarbose (Matsuo *et al.*, 1992). It reduced blood glucose levels after administration of maltose, sucrose, and starch but not upon administration of glucose, fructose, and lactose, something that is in accordance with its mechanism of action wherein it binds to enzymes which break down complex starch and disaccharides into simple sugars. It also showed successful reduction in plasma insulin and plasma glucose levels (Matsuo *et al.*, 1992). Although α-glucosidase inhibitors work based on the same mechanism of delaying carbohydrate absorption and break down into simple sugars, they have differences in their potency, probably due to differences in their structure and affinity to digestive enzymes. While comparing the efficacy and safety of acarbose and voglibose in 30 subjects, both were observed to decrease 1-h postprandial blood glucose levels, from 224.9 ± 42.8 to 206 ± 38.9 mg/dL for voglibose, whereas the decrease was 228.3 ± 37.4 to 186.6 ± 36.1 mg/dL for acarbose (Vichayanrat *et al.*, 2002). The quantity of the drug administered was different, with acarbose treatment being 100 mg (tid) whereas for voglibose it was 0.2 mg (tid). Abdominal discomfort and increased flatulence were observed in both therapies; however, the effects were more pronounced in acarbose therapy. Interestingly, while both therapies showed decrease in 1-h postprandial blood glucose levels and rise in insulin levels, only acarbose showed significant decrease in 2-h postprandial blood glucose levels (Vichayanrat *et al.*, 2002).

A recent double-blind study (Goke *et al.*, 1995) treated 72 healthy volunteers around 30 years of age and body mass of 75 kg with varying dosage of voglibose (0.5, 1.0, 2.0, or 5.0 mg) or placebo. At the end of 7 days, blood glucose levels were at 10 mg/dL for the most potent dose of voglibose. As for insulin, voglibose reduced the rise in its levels in a dose-dependent manner: the highest reduction of 75% as compared to placebo was achieved when 5 mg doses were administered to the patients. It was also found to reduce gastric inhibitory polypeptide (GIP) plasma concentrations up to 50%. Similar phenomena were observed in the case of acarbose administration (Folsch *et al.*, 1987); thus, it is suggested that glucose absorption is necessary for GIP secretion, the delay of which results in a decrease in GIP rise. At the same time, it increased incretin hormone glucagon-like peptide 1 (GLP-1) plasma concentrations in dose-dependent manner wherein a rise of 5 pmol/L was observed in the 5.0 mg dose on the 7th day (Goke *et al.*, 1995). In a study conducted in Japan for combination therapy of voglibose with a thiazolidinedione (pioglitazone), 31 patients were separated into two groups, of which 16 received 30 mg of thiazolidinedione and

0.9 mg voglibose treatment whereas the rest were administered only voglibose for 12 weeks. The results indicated increased reduction in the plasma glucose levels in patients on the combination therapy of both the drugs (Abe *et al.*, 2007).

V. ANTHOCYANINS

Various polyphenols such as flavonoids have demonstrated numerous health benefits, especially in the treatment of obesity and diabetes. It is interesting that natural compounds can be addressing the issue of obesity and diabetes in more than one way, such as digestive enzyme inhibition, induction of apoptosis in adipose tissue, etc. (Nelson-Dooley *et al.*, 2005). Anthocyanins, a subgroup of flavonoids, are water-soluble plant pigments responsible for the blue, purple, and red color of many plant tissues. In plants they provide some important functions such as UV protection, signaling, antimicrobial activities, etc. In the past two decades, they have received great attention worldwide due to their potential and proven health benefits in humans, such as anti-inflammatory, anticancer, antiobesity and antidiabetic properties (Yan *et al.*, 2008). They occur primarily as glycosides of their respective aglycon anthocyanidin chromophores (Prior and Wu, 2006). The sugar moiety is mainly attached at the 3-position on the C-ring or the 5, 7-positions on the A-ring. Glucose (glc), galactose (gal), arabinose (arab), rhamnose (rham), and xylose (xyl) are the most common sugars that are bonded to anthocyanidins in the form of mono-, di-, or trisacchrides except for the 3-deoxyanthocyanidins such as luteolinidin and apigeninidin in sorghum (Wu and Prior, 2005).

About 17 anthocyanidins, the aglycon forms of anthocyanins, are found in nature, whereas only 6 of them, cyanidin (Cy), delphinidin (Dp), petunidin (Pt), peonidin (Pn), pelargonidin (Pg), and malvidin (Mv), are ubiquitously distributed (Fig. 2.7). The differences in chemical structure of these six common anthocyanidins occur at the 3′ and 5′ positions of the B-ring. The sugar moieties may also be acylated by a range of aromatic or aliphatic acids. Over 600 naturally occurring anthocyanins are known to be present (Anderson, 2002) and they vary in (1) the number and position of hydroxyl and methoxyl groups on the basic anthocyanidin skeleton; (2) The identity, number, and positions at which the sugars are attached; and (3) The extent of sugar acylation and the identity of the acylating agent.

A. Anthocyanin metabolism

Anthocyanidin glycosides are hydrolyzed by the intestinal microflora within 20 min to 2 h after consumption, depending on the sugar moiety (Keppler and Humpf, 2005). Due to the high instability of the released

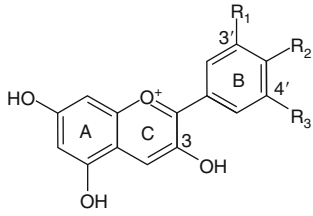

Anthocyanidin	R_1	R_2	R_3
Pelargonidin (Pg)	H	OH	H
Cyanidin (Cy)	OH	OH	H
Delphinidin (Dp)	OH	OH	OH
Peonidin (Pn)	OCH_3	OH	H
Petunidin (Pt)	OCH_3	OH	OH
Malvidin (Mv)	OCH_3	OH	OCH_3

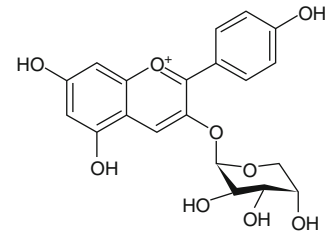

Pelargonidin 3-arabinoside (from strawberry)

FIGURE 2.7 Structure of anthocyanidins and anthocyanins.

anthocyanidin aglycones at neutral pH, primary phenolic degradation products are detected within 20 min of incubation. Further metabolism of the phenolic acids is accompanied by demethylation. Such anthocyanin metabolites, derived from anthocyanin metabolism, may be responsible for the observed antioxidant activities and other physiological effects *in vivo*. Moreover, anthocyanins have low bioavailability and therefore are unlikely to provide protection at the cellular level. For example, a large proportion of the ingested polyphenols taken from berries is not taken up in to the circulation but instead passes through the upper gastrointestinal tract (GIT) to the large intestine where polyphenols may be biotransformed or broken down by the indigenous microflora (McDougall and Stewart, 2005). Due to the complexity of phenolic composition, it is hard to determine the exact nature of the compounds that are actually generated from anthocyanins. Labeled anthocyanins are thus necessary to determine the degraded compounds that are generated from anthocyanins (Prior and Wu, 2006).

Biotransformation enzymes involved in the pathway may include UDP-glucuronosyl transferase, UDP-glucose dehydrogenase, or catechol-*O*-methyltransferase (COMT), which are located in the small intestine, liver, or kidney. Depending on the chemical structure, anthocyanins could exist mainly in their native forms or as metabolites in blood and urine, whereas most other flavonoids are generally recovered as metabolites (Prior and Wu, 2006). Glucuronidation has been demonstrated to be a major chemical modification of anthocyanins. However, the extent of glucuronidation is significantly affected by the type of aglycone, substitution pattern, and amount of anthocyanins consumed (Wu *et al.*, 2005).

Anthocyanins have shown significant antiobesity and antidiabetic effects. More specifically, anthocyanin-rich foods have been shown to lead to a 24% decrease in weight gain in mice and decreased lipid accumulation in the liver, including a significant decrease in liver triacylglycerol concentration (Prior and Wu, 2006). Moreover, it was shown that anthocyanins enhance adipocytokine secretion and upregulate adipocyte-specific gene expression through AMP activated protein kinase activation (Ghosh, 2005). Anthocyanins from Cornelian cherries (*Cornus mas*) such as Cy-3-glc, Dp-3-glc, Cy-3-gal, and Pg-3-gal stimulate insulin secretion from rodent pancreatic beta-cells. Pg-3-gal, and its aglycone, Pg, caused a 1.4-fold increase in insulin secretion. The rest of the anthocyanins tested had only marginal effects on insulin (Jayaprakasam *et al.*, 2005).

B. Novel production technique

The variety of their biological roles has drawn much attention to anthocyanins, something that necessitates the development of methodologies for their efficient production. Anthocyanins are most commonly extracted as mixtures from plants or plant waste. However, due to the low anthocyanin concentration *in planta,* abundant natural resources are required for large-scale production. To resolve this problem, certain plants have been genetically engineered by increasing the activity of anthocyanin biosynthetic enzymes. However, the existence of competing pathways in plants complicates the substantial increase of content of specific anthocyanin compounds (Liu *et al.*, 2002). For that reason, blocking of competing pathways had to be implemented in order to further increase its content (Yu *et al.*, 2003). Plant cultivation also depends heavily on environmental, seasonal, and geological conditions. Therefore, consistent quality and quantity of plant resources could present a rate-limiting step to large-scale production. In the downstream processing line, anthocyanin extraction and purification is also inefficient due to the contamination of numerous plant small molecules and the loss of products due to processing conditions (Wang and Murphy, 1996).

In addition to extraction from plants, anthocyanins have already been known to be produced by plant cell cultures like *Vitis hybrids, Haplopappus gracilis*, and *Daucus carota*. However, plant cell cultures are not always a straightforward approach for meeting market needs due to several problems involved with the fermentation process. For example, plant cells tend to form aggregates that influence anthocyanin culture productivity since cells within aggregates are not adequately exposed to lighting required to induce anthocyanin biosynthesis. For example, formation of phenylalanine ammonia lyase (PAL), a key enzyme in the biosynthetic pathway, is promoted primarily by UV, particularly those of the UV-B region (Wellmann, 1975). Other enzymes in the pathway, particularly

those of the anthocyanin biosynthetic branch, appear to be regulated in part by UV and in part by phytochrome-activating wavelengths (700–800 nm) (Meyer *et al.*, 2002). In that respect, irradiance becomes a limiting factor to productivity (Hall and Yeoman, 1986). Also, the average light dosage is reduced or insufficient within a dense cell culture since the cell wall composition selectively restricts certain wavelengths (Smith and Spomer, 1995).

As a result of some of the limitations mentioned with the current production methodologies, anthocyanins are becoming attractive targets for fermentation production from well-characterized microbial hosts such as *Escherichia coli* (Yan *et al.*, 2005). In general, flavonoid production in recombinant microorganisms is advantageous because the cloned pathway(s) are under microbial promoters and therefore the production is independent of light or other regulatory elements (such as the MYB transcription factors) required by plants. In addition, *E. coli* and *S. cerevisiae* cultures can achieve higher yields than plant cell cultures because of their better duplication times. In addition, no plant peroxidases are present in bacteria and yeast and therefore the ''browning effect'' problem is significantly reduced. Browning effect refers to the formation of a brown color in plant anthocyanin extracts as a result of a two-step process. First, anthocyanins are oxidized by plant polyphenol oxidases present in the plant extract. Second, the oxidized anthocyanins undergo condensation and form brown pigments, which are usually undesired by the food industry. A simplified extraction procedure is another advantage of using microbial production platforms over plant crops or cultures. Since anthocyanins are not naturally produced in microbial hosts, a much less complicated matrix of products is generated through the heterologous expression of pathways that lead to specific product targets. This minimizes the downstream processing required for purification of the target molecules.

Engineering microorganisms for the production of anthocyanins has been facilitated by the discovery of the core metabolic pathway leading to their production. This biosynthetic pathway begins with chalcones leading to flavanone, dihydroflavonol, anthocyanidin, and finally anthocyanin (Fig. 2.8). Recently, *E. coli* was engineered to produce anthocyanins (Yan *et al.*, 2005). To achieve this goal, the flavanone pathway was bypassed by supplemental feeding of flavanones into *E. coli* JM109 strain carrying a gene assembly which consisted of *M. domestica* F3H (flavanone 3′-hydroxylase), *A. andraeanum* DFR (dihydroflavonol 4-reductase), ANS (anthocyanin synthase) from *M. domestica*, and a PGT8 from *P. hybrida*. Upon heterologous expression of these genes in *E. coli* and feeding glucose supplemented cultures with the flavanones naringenin or eriodictyol, their corresponding anthocyanins pelargonidin 3-*O*-glucoside and cyanidin 3-*O*-glucoside were obtained in the

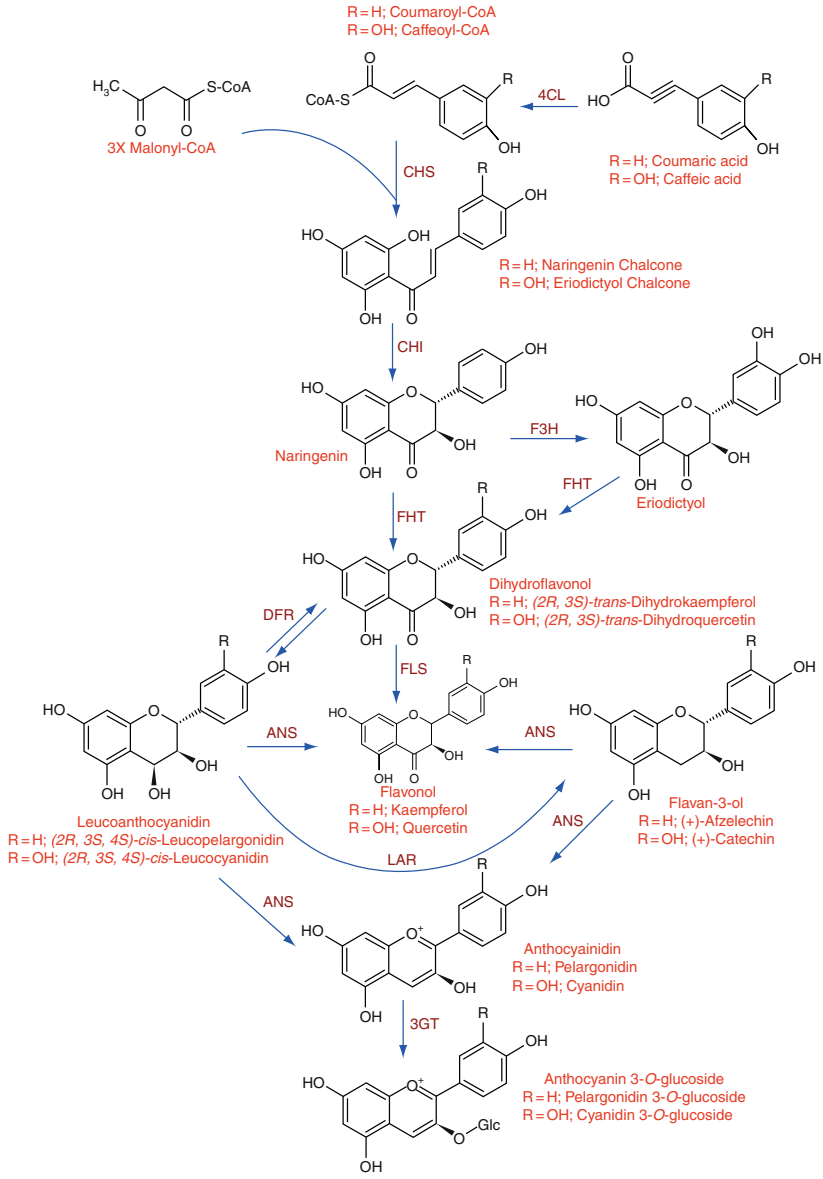

FIGURE 2.8 Biosynthesis of anthocyanins in *E. coli* (Yan *et al.*, 2008; Yan *et al.*, 2005).

culture and their biosynthesis confirmed by high-performance liquid chromatography (HPLC) and mass spectrometry (MS) analyses (Yan *et al.*, 2005). The product levels obtained from such system were low,

however, due to various systemic constraints. Some of the limitations in this production system were found to include the instability of the final anthocyanin molecules at normal pH, the intracellular availability of UDP-glucose, and the substrate specificity of ANS. Hence, several strategies were employed to overcome these barriers: (1) The culture medium pH was adjusted to pH 5.0 for enhanced stability of anthocyanins; (2) A translational fusion protein between ANS and 3GT (flavonoid 3-*O*-glucosyltransferase) was created in order to duplicate the possible multienzyme system in the plant cell; (3) The native *E. coli* metabolic network was manipulated by overexpressions and deletions in order to improve the intracellular UDP-glucose pool along with other cofactors necessary for ANS activity; (4) Catechin, rather than flavanones were employed as the precursor anthocyanin metabolites (Yan *et al.*, 2008). As a result of these optimization efforts, the volumetric production of pelargonidin 3-*O*-glucoside and cyanidin 3-*O*-glucoside was increased several fold. More specifically, the development of a two-step fermentation strategy in which first high biomass of *E. coli* was obtained in rich medium which was next transferred into minimal media at pH 5.0 during which period anthocyanins were produced resulted in a volumetric production of 38.9 mg/L of cyanidin 3-*O*-glucoside. Creation of the fusion protein 3GT-ANS boosted the production even further by 16% to approximately 45 mg/L. Combined implementation of coexpression of the two enzymes involved in the conversion of glucose 6 phosphate to UDP-glucose, deletion of UDP-glucose-consuming metabolic reactions, and fermentation media optimization resulted in a further increase in anthocyanin production to a final volumetric yield of approximately 75 mg/L (Yan *et al.*, 2008). Recently, the metabolism of *E. coli* was successfully manipulated toward the production of anthocyanins through the introduction of novel carbon assimilation pathways and the attenuation of several gene targets in order to increase the availability of UDP-glucose. With these genetic and metabolic engineering strategies, the recombinant production of anthocyanins has reached up to 113 mg/L (Leonard *et al.*, 2008).

C. Mechanism of action

Recent studies on classes of polyphenols such as anthocyanins and ellagitannins have shown that they have pathophysiological properties such as antioxidant and antihypertensive activities and have also demonstrated the inhibition of lipid oxidation (Matsui *et al.*, 2001a). More specifically, anthocyanins inhibit α-glucosidase activity and can reduce blood glucose levels after starch-rich meals. In general, polyphenolic extracts from a number of plants have been shown to be effective inhibitors of intestinal α-glucosidase/maltase activity (Matsui *et al.*, 2001b) with K_i values in the same range as other inhibitors such as the previously

described acarbose and voglibose (Toeller, 1994). From the various polyphenols, it has been shown that α-glucosidase activity *in vitro* is significantly inhibited by anthocyanin-rich extracts of blueberry and blackcurrant which contain a small proportion of acylated anthocyanins (McDougall *et al.*, 2005). The inhibitory effects of anthocyanins depend on their structure. Acylated anthocyanins are more potent α-glucosidase inhibitors than deacylated anthocyanins. Acylated anthocyanins from *Clitoria ternatea* flowers (Terahara *et al.*, 1996) and acylated anthocyanins from storage roots of purple sweet potato, *Ipomoea batatas* (Terahara *et al.*, 1996, 1999), have shown inhibitory effects on α-glucosidase activity thus lowering the glucose absorbtion. Three deacylated anthocyanins isolated from the red flowers of the morning glory, *Pharbitis nil* cv. Scarlett O'Hara (SOA), and the storage roots of the purple sweet potato, *I. batatas* cv. Ayamurasaki (YGM), with different aglycons of pelargonidin(Pg), cyanidin (Cy), and peonidin (Pn) have been shown experimentally to have a lower inhibitory effect than acylated extracts. Inhibitory activities of these deacylated anthocyanins are decreased by a factor of 1/70–1/90 compared to their acylated forms. The enhanced inhibition exhibited by acylated anthocyanins over their deacylated forms (Matsui *et al.*, 2001a) perhaps reflects the enhanced stability of the acylated anthocyanins at intestinal pH but such differences in effectiveness may not be particularly relevant when 200 mg of anthocyanins are available from a single portion of berries (Clifford, 2000). Ellagitannins also inhibit α-amylase activity and there is potential for synergistic effects on starch degradation after ingestion of berries such as raspberries and strawberries, which contain substantial amounts of ellagitannins and anthocyanins (McDougall and Stewart, 2005). Finally, anthocyanins have been shown to directly induce secretion of insulin from pancreatic cells in ex vivo assays (Jayaprakasam *et al.*, 2005), but this effect may be marginal *in vivo* because of the low serum bioavailability of anthocyanins. The mechanism of α-glucosidase inhibition action by anthocyanins is not fully understood but one can assume that the inhibition, like that of acarbose, is competitive and results from the structural similarity between the normal substrate maltose and the glucosyl groups β-linked to the anthocyanin which bind to the active site but are not hydrolyzed. Structure–activity relationships with respect to the aglycone and the attached sugars are still not well understood. Various other anthocyanin-rich plant extracts have been studied and they have shown different degree of α-glucosidase inhibition. Table 2.3 summarizes the different anthocyanin-rich plant extracts that have been tested for their potential therapeutic properties against Type II diabetes through inhibition of alpha-glucosidase. The order of α-glucosidase is SOA > BOC > YGM > ternatin, with SOA extract showing the strongest α-glucosidase inhibitory activity with an IC_{50} value of 0.22 mg/mL (Matsui *et al.*, 2001b) (Table 2.4).

TABLE 2.3 Anthocyanin extracts from various plants (Keppler and Humpf, 2005)

Scientific name	English name	Abbreviation
Clitoria ternatea L. flower	Butterfly pea	Ternatin
Ipomoea batatas L. root	Sweet potato	YGM
Brassica oleracea L. leaf	Cabbage	BOC
Paphanus sativus L. root	Radish	RPS
Dioscorea alata L. tuber	Yam	DOA
Pisum sativum L. pod	Pea	PSP
Sambucus nigra L. berry	Elderberry	SNB
Fatsia japonica L. berry skin	–	FJB
Rubas loganbaccus berry	Boysenberry	RLB
Pharbitis nil cv. Scarlett O′ Hara flower	Morning glory	SOA
Houttuynia cordata Thunb. Leaf	–	HCT
Zea mays L. seed coat	Corn	ZML

TABLE 2.4 α-Glucosidase inhibitions by two active anthocyanins extract (Matsui *et al.*, 2001b)

	IC_{50} (mg/mL)		
Extract	Free α-glucosidase	Immobilized α-glucosidase	α-Amylase
SOA	0.35	0.17	0.43
YGM	0.36	0.26	0.61
Green tea	0.23	0.22	–

These anthocyanin extracts have also been shown to inhibit both free and immobilized α-glucosidase. Among the extracts, SOA (IC_{50} = 0.35 mg/mL) and YGM (IC_{50} = 0.36 mg/mL) are sufficient α-glucosidase inhibitors, being comparable to green tea extract (IC_{50}= 0.23 mg/mL) (Table 2.4). In addition, these extracts were tested for their inhibitory potential against sucrase: none of them inhibited sucrase whereas green tea extract did inhibit sucrase activity (Matsui *et al.*, 2001b). α-glucosidase inhibitory activities of all the isolated anthocyanins are 5 times higher than that of the natural inhibitor, D-xylose (IC_{50}=11_{90} μM). Among them, SOA-4 possessed the most potent activity as shown by an IC_{50} value of 60 μM, and their inhibitory behavior is in the order of SOA-4 > SOA-6 > YGM-3 = YGM-6 (Table 2.5). The inhibitory effects when compared with therapeutic α-glucosidase inhibitors like Acarbose and Voglibose, is very less. But a daily intake of the extracts as food helps to keep a moderate plasma blood glucose control. Thus anthocyanins have a great potential as therapeutic drugs for diabetes.

TABLE 2.5 iAGH inhibitory activities of isolated acylated anthocyanins, D-Xylose and therapeutic drugs voglibose and acarbose

	IC_{50} value	
Compound	μM	mg/mL
SOA-4	60	0.081
SOA-6	107	0.128
YGM-3	193	0.239
YGM-6	200	0.245
D-Xylose	1190	0.1785 mg/mL
Voglibose	0.0055	0.0015×10^{-3}mg/mL
Acarbose	0.426	0.275×10^{-3}mg/mL

VI. PINE BARK EXTRACT

Pycnogenol is the patented trade name for the water extract of French maritime Pine bark (*Pinus pinaster)* extract that is rich in polyphenols (Markham and Porter, 1973), and it has recently been demonstrated to have various biological and health beneficial effects (Sanbongi *et al.*, 1997). Pycnogenol contains oligomeric proanthocyanidins as well as other bioflavonoids like catechin, epicatechin, phenolic fruit acids (such as ferulic acid and caffeic acid), and taxifolin. Procyanidins are oligometric catechins found at high concentrations in red wine, grapes, cocoa, cranberries, and apples.

Among others, pycnogenol has been reported to display antidiabetic effects (Liu *et al.*, 2004a). Supplementation with 100 mg Pycnogenol for 3 months significantly lowered blood glucose levels compared to placebo, and improved endothelial function was observed in patients with Type II diabetes. The glucose lowering effect was dose dependent and not accompanied by an increase in insulin secretion (Liu *et al.*, 2004b).

Among others, it is believed that the antidiabetic effect of Pycnogenol is due to its digestive enzyme inhibitory activity. The digestive enzyme inhibitory activity of Pycnogenol is comparable to that of green tea catechin extracts and to acarbose (Schafer and Hogger, 2007). Its IC_{50} (5.34 μg/mL) is about four times lower than that of green tea extract, which has an IC_{50} of 19.74 μg/mL. Acarbose had a 190 times lower ability to inhibit α-glucosidase than the pine bark extract (Table 2.6).

Experiments were carried out to determine which of the monomeric polyphenolic compounds in the extract fractions of Pycnogenol were responsible for the inhibitory activity toward α-glucosidase (Schafer and

TABLE 2.6 Comparison of inhibitory effects of pycnogenol (Schafer and Hogger, 2007)

Compound	IC_{50} (μg/mL)
Acarbose	1010 ± 210
(+) Catechin	52.14 ± 20.3
Pycnogenol	5.34 ± 0.91
Green tea extract	19.74 ± 1.8

Hogger, 2007). Only (+)-catechin and procyanidins were shown to inhibit α-glucosidase, whereas the other compounds such as ferulic acid, (–)-epicatechin, gallic acid, 4-hydroxybenzoic acid, caffeic acid, protocatechuic acid, sinapic acid, and (±) taxifolin did not demonstrate any inhibitory activity. The activity of Pycnogenol toward α-glucosidase increases with the degree of polymerization of procyanidins (Schafer and Hogger, 2007). In addition to alpha-glucosidase, pine bark extract has shown competitive inhibition against human salivary and porcine pancreas α-amylases as well (Kim *et al.*, 2005).

Pine bark extract is found to be very stable under thermal conditions and comparatively stable under acidic conditions. Thus, pine bark extract is easier to handle during processing or manufacturing steps and remains stable when exposed to the human digestive tract.

VII. OTHER EXTRACTS OF PLANT ORIGIN

As mentioned, various plant extracts harbor the promise of potential Type II diabetes treatment through different mechanisms, with inhibition of digestive enzymes being the most prominent. However, in most cases, the active substance(s) of many of these extracts have not been found. In addition, lots of information related to their therapeutic potential is anecdotal or indirect or still limited to animal studies. Broadly, we have classified plant extracts into two groups, one composed of plant extracts with known active compounds, and the other where the active compounds are unknown, although positive inhibitory effects on digestive enzymes have been reported. A number of such plants and their active component (when known) are provided in Table 2.7.

A. Known active compounds

Momordica charantia: *Momordica charantia* known as bittermelon or bittergourd belongs to the family of *Cucurbitaceae*. Cultivated fruits of *Momordica charantia* are widely used to treat diabetes in Asia and Australia.

TABLE 2.7 Traditional antidiabetic plants with active substance

Plants	Active part of plants	Active substance	Activity demonstrated in	References
Momordica Charantia	Fruits and seeds	Charantin, alkaloids	Alloxan-induced diabetic rats	Fernandes *et al.* (2007)
Phyllanthus Reticulatus	Leaves	Terpenoids glycosides	Aloxan-induced diabetic mice	Kumar *et al.* (2008)
Panax Ginseng	Roots, berry, leaves	Ginsenosides	Diabetic mice	Xie *et al.* (2005)
Zea mays (purple corn)	Kernel	Anthocyanins	Rats	Jones (2005)
Trigonella foenumgraecum	Seeds	Trigonelline (alkaloid)	Alloxan-induced diabetic mice	Vijayakumar *et al.* (2005)
Ipomoea batatas	Purple fleshed sweet potato	Acylated anthocyanins, caffeoylsophorose	Sprague Dawley Rats	Matsui *et al.* (2004), Suda *et al.* (2003)
Lens esculenta	Seeds	Condensed tannins (polyphenols)	*In vitro*	Quesada *et al.* (1996)
Theobroma cacao	Seeds	Condensed tannins (polyphenols)	*In vitro*	Quesada *et al.* (1996)
Cephalotaxus sinensis	Leaves	Epigenin, epigenin glycoside	Streptozotocin-induced diabetic rats	Li *et al.* (2007)
Feculae bombycis	Unknown	1-Deoxynojirimycin (DNJ)	Wistar rats	Zhu *et al.* (2005)

(*continued*)

TABLE 2.7 (*continued*)

Plants	Active part of plants	Active substance	Activity demonstrated in	References
Curcuma longa	Unknown	Natural curcumin, demethoxycurcumin	*In vitro*	Du *et al.* (2006)
Bauhinia forficate	Leaves	Kaempferitrin	Alloxan-induced diabetic rats	de Sousa *et al.* (2004)
Syzygium zeylanicum	Leaves	Polyphenols	*In vitro*	Mai *et al.* (2007)
Cleistocalyx operculatus	Leaves	Polyphenols	*In vitro*	Mai *et al.* (2007)
Careya arborea	Leaves	Polyphenols	*In vitro*	Mai *et al.* (2007)
Horsfieldia amygdalina	Leaves	Polyphenols	*In vitro*	Mai *et al.* (2007)
Aconitum carmichaeli	Root	Aconitan A (polysaccharide)	Diabetic mice	Konno *et al.* (1985a)
Allium cepa	Bulb	Alkyldisulfides	Diabetic rabbits	Augusti (1974)
Allium sativum	Bulb	Alkyldisulfides	Healty rabbits	Jain *et al.* (1973)
Blighia sapida	Fruit	Hypoglycins	IDDM and Type II diabetes patients	Bressler *et al.* (1969)
Catharanthus roseus	Leaf	Hypoglycins	IDDM and Type II diabetes patients	Bressler *et al.* (1969)
Cyamopsis tetragonolobus	Seed and pod	Alkaloids	Healthy rats	Farnsworth and Segelman (1971), Peters (1957)

Vaccinium myrtillus	Leaf	Neomyrtillin	Diabetic humans	Allen (1927)
Tecoma stans	Leaf	Saccharan C, characterized alkaloid	Diabetic mice, diabetic rabbit	Hammouda and Amer (1966), Hammouda and Khalafallah (1971)
Saccharum officinarum	Stalk	Quiquefolans	Diabetic mice	Takahashi *et al.* (1985)
Momordica foetida	Ariel	Uncharacterized glycosides and alkaloids	Type II diabetes patients	Olaniyi (1975)
Galega officinalis	Leaf	Guanidine	Diabetic mice	Hermann (1973)
Ficus bengalensis	Stem bark	Bengalenoside(glycoside)	Diabetic mice	Brahmachari and Augusti (1964)
Ephedra distachya	Aerial	Eleutherans	Diabetic mice	Konno *et al.* (1985b)
Ganoderma lucidum	Fruit body	Uncharacterized glycoside	Healthy rodents	Hikino *et al.* (1985)
Lupines termis	Seed	Quinolizidine alkaloids	Alloxan-induced diabetic mice	Mishkinsky *et al.* (1974)
Cinnamomum cassia	Bark of tree	Procyanidin type-A polymers	Clinical trials	Chase and McQueen (2007)

Despite their bitter taste, they are often included in regular diet due to their prophylactic properties. The fruit and its extract have been introduced in Europe as alternatives to conventional treatments for non-insulin-dependent diabetes mellitus. Charantin, a mixture of glycosides, mainly β-sitosterol-D-glucoside and stigmadine glucoside, is the active substance responsible for the fruit's hypoglycemic action (Fernandes *et al.*, 2007). It has been shown that the hypoglycemic effect is mediated through (1) suppression of the key hepatic gluconeogenic enzymes glucose-6-phosphatase and fructose-1,6-bisphosphatase, and (2) an accelerated rate of glucose metabolism through the pentose phosphate pathway (Jain *et al.*, 1973). Fifty milliliters of the aqueous extract of the plant reduced glucose concentration of diabetic patients by 20% within 1 h. The above results have been shown in healthy and alloxan-induced diabetic animals. Ethanolic extracts of *M. charantia* showed an antihyperglycemic as well as hypoglycemic effect in normal and streptozotocin (STZ) induced diabetic rats by decreasing blood sugar by 23% and 27%, respectively (Shibib *et al.*, 1993).

Allium sativum: Garlic, scientifically known as *Allium sativum*, is a perennial herb cultivated throughout India and is commonly used as a food ingredient. It has long been used as dietary supplement for traditional treatment of diabetes in Asia, Europe, and the Middle East. Concentrated plant extracts exerted a weak hypoglycemic effect in healthy and alloxan-induced diabetic animals and healthy humans. Fasting glucose levels were lowered and oral glucose tolerance was improved by 7–18% within 1–2 h after oral administration of aqueous and ethanolic extracts of garlic at doses of 10 g extract/kg body weight. This effect has been attributed to the volatile oils allyl propyl disulfide and diallyl disulfide oxide (Jain *et al.*, 1973). *S*-Allyl cystiene (SACS), precursor of allicin and garlic oil, is a sulfur-containing amino acid. It is isolated from garlic extract and pharmacokinetic studies show its rapid absorption in the gastrointestinal tract and high bioavailability after oral administration (Wagman and Nuss, 2001). Oral administration of SACS to alloxan-diabetic rats for 1 month ameliorated glucose intolerance and resulted in weight loss and depletion of liver glycogen in diabetic rats in comparison to glibenclamide and insulin-treated animals. SACS also stimulated *in vitro* insulin secretion from β cells isolated from rats (Jain *et al.*, 1973).

Panax Ginseng: Ginseng, often described as the ''king herb,'' holds an important position in traditional Oriental medicine in many countries. This highly valued plant is currently cultivated in China, Korea, Japan, Russia, the United States, and Canada. Of the several species of ginseng, the root of the Asian and American varieties (*Panax ginseng*) is a popular dietary supplement in the United States.

Historical records on traditional medicinal systems reveal that ginseng root was used to treat diabetes. Research on the effects of treatment with ginseng root on blood sugar levels started early last century. Between

1921 and 1932, Japanese scientists reported that ginseng root decreased baseline blood glucose and reduced hyperglycemia caused by adrenaline or high concentration glucose administration. Ginseng root has since been used to treat patients with diabetes. Results of *in vitro* studies, animal experiments, and clinical trials strongly support the claim that ginseng root possesses antidiabetic properties (Xie *et al.*, 2005). The root of the ginseng plant is constituted of organic (80–90%) and inorganic substances (approximately 10%) and consists of a number of active constituents, such as saponins or ginsenosides, carbohydrates (including polysaccharides), nitrogenous substances, amino acids, peptides, phytosterol, essential oils, organic acids, vitamins, and minerals. Of these, the extract fractions containing ginsenosides and polysaccharides have demonstrated hypoglycemic activity, with ginsenosides being the principal bioactive constituents of ginseng (Xie *et al.*, 2005). Ginsenoside content is in the order leaf > berry > root. Ginsenosides are classified as protopanaxatriol (Rg1, Rg2, Rg3, Re, and Rf) and protopanaxadiol (Rb1, Rb2, Rc, and Rd). Among these, ginsenoside Re has demonstrated significant antihyperglycemic effect as well as reduction of serum insulin levels in fed or fasting mice (Attele *et al.*, 2002). Ginsing berry extract exhibited significantly more potent antidiabetic effects than the root extract. The difference in ginsenoside Re content between root and berry extracts may account for the difference in their pharmacological effects. Ginseng might mediate its antidiabetic actions through a variety of mechanisms, including actions on the insulin-secreting pancreatic β-cells and the target tissues that take up glucose. Ginseng treatment increased insulin release from pancreatic β-cells, which is probably caused by increased β-cell stimulation and increased insulin synthesis. Furthermore, the effect of ginsenoside Re in reducing expression of enzymes involved in lipid metabolism could be beneficial in diabetes (Xie *et al.*, 2005).

Moreover, Asian ginseng root extracts administered to alloxan-treated diabetic mouse models decreased blood glucose levels significantly. Complex components in the carbohydrate fraction of ginseng root extract, including different panaxans A, B, C, D, E, panaxans I, J, K, L, and panaxans Q, R, S, T, U also demonstrated hypoglycemic properties in normal and alloxan-induced hyperglycemic mice. Similar to Asian ginseng, three constituents obtained from the water extracts of American ginseng root, viz. quinquefolans A, B, and C, displayed hypoglycemic actions in normal and hyperglycemic mice. Clinical trials have also reported antihyperglycemic activity when a single dose of 3 g American ginseng root was administered in both nondiabetic and Type II diabetic individuals.

Trigonella foenumgraecum (fenugreek): The seeds of *T. foenumgraecum* are widely recommended for patients with diabetes. More specifically, fenugreek seed extracts (FSE) have been shown to significantly improve

glucose homeostatis in alloxan-induced diabetic mice by effectively lowering blood glucose levels (Jain *et al.*, 1973; Vijayakumar *et al.*, 2005). The hypoglycemic activity has been attributed to an uncharacterized alkaloid termed trigonelline, although other possible hypoglycemic agents such as nicotinic acid have been isolated from the seeds (Bailey and Day, 1989).

Glucose uptake, facilitated by translocation of glucose transporters from an intracellular site to the plasma membrane, is the rate-limiting step in hyperglycemic conditions. FSE induces a rapid, dose-dependent stimulatory effect on cellular glucose uptake by activating cellular responses that lead to glucose transporter's translocation to the cell surface (Jain *et al.*, 1973). Moreover, a novel amino acid (4-hydroxyisoleucine) extracted and purified from fenugreek seeds has shown an increase in glucose-induced insulin release in both rats and humans (Grover *et al.*, 2002; Vijayakumar *et al.*, 2005).

Ipomoea batatas: This is a trialing herb cultivated for its succulent tuberous roots. Oral administration of *I. batatas* reduces hyperinsulinemia in Zucker fatty rats by 23%, 26%, 60%, and 50% after 3, 4, 6, and 8 weeks, respectively. In addition, inhibition of blood glucose level after glucose loading was observed after 7 weeks of treatment along with regranulation of pancreatic beta cells and reduction in insulin resistance (Kusano and Abe, 2000; Matsui *et al.*, 2004; Suda *et al.*, 2003). Hypolipidemic activity has also been described (Kusano and Abe, 2000). Acylated anthocyanins are the active substances isolated from *I. batatas* and are responsible for its hypoglycemic action.

Cinnamomum cassia (cinnamon): Cinnamon is a common spice that has recently gained attention as a possible treatment for diabetes. Historically, cinnamon has been used medicinally for loss of appetite and dyspeptic complaints. The two major types of cinnamon are from the bark of different but related trees (Chase and McQueen, 2007): (1) *Cinnamomum verum*, also known as *Cinnamomum zeylanicum*, is true cinnamon, (2) *C. cassia*, also known as *Cinnamomum aromaticum*, Chinese cinnamon, cassia cinnamon, and bastard cinnamon, is commonly used as a spice. This more easily available species is also the type used medicinally. Little is known about the mechanism of action and activities of cinnamon. *C. cassia* is thought to have more insulin-stimulating properties than true cinnamon (Verspohl *et al.*, 2005). The active compounds responsible for the insulin-like activity of cinnamon are believed to be procyanidin type-A polymers (Anderson *et al.*, 2004); these compounds have been shown to promote insulin receptor autophosphorylation, increasing insulin sensitivity (Anderson *et al.*, 2004; Imparl-Radosevich *et al.*, 1998). It has been shown that a quarter of a teaspoonful of cinnamon taken twice a day by patients with diabetes lowers blood sugar by an average of 18–29%, triglycerides by 23– 30%, LDL cholesterol by 7– 27%, and total cholesterol by 12–26% (Khan *et al.*, 2003).

Cinnamon may have the potential to become a common adjunct to diabetes treatment. Relative safety, low cost, and potential efficacy make cinnamon a viable option for patients interested in using more natural therapies.

B. Unknown active compounds

Agaricus bisporous (common edible mushroom): It is considered a useful dietary adjunct for diabetes in Europe, and a hypoglycemic effect has been shown in streptozocin (STZ) induced diabetic mice. More specifically, *A. bisporous* consumption improved insulin sensitivity in diabetic mice and a lectin from this mushroom stimulated insulin release by isolated islets of healthy rats (Swanston-Flatt *et al.*, 1989).

Aloe vera: It is a native of North Africa and is also cultivated in Turkey and drier parts of India. *Aloe* species have been commonly used for centuries as laxatives and for their anti-inflammatory and antitumor activities. Moreover *Aloe vera* extracts from leaf pulp and leaf gel have shown significant antidiabetic activity (Okyar *et al.*, 2001). Extracts of aloe gum effectively increased glucose tolerance in both normal and diabetic rats (Ghannam *et al.*, 1986). Chronic but not single administration of the exudate of the leaves of *Aloe barbadensis* (500 mg/kg PO) showed significant hypoglycemic effect in alloxan-diabetic mice. However, single as well as chronic administration of the bitter principle (5 mg/kg IP) showed significant hypoglycemic effect in the same model. The hypoglycemic effect of single dose of the bitter principle was extended over a period of 24 h with maximum hypoglycemia observed at 8 h, while chronic administration (exudate twice daily and the bitter principle once a day for 4 days) showed maximum reduction in plasma glucose level on the 5th day (Grover *et al.*, 2002). Hypoglycemic effect of aloe and its bitter principle is mediated through stimulation of synthesis and/or release of insulin from the β-cells of langerhans. Additionally, both *Aloe vera* and *Aloe gibberellins* (over a dose range of 2–100 mg/kg) inhibit inflammation in a dose-response manner and improve wound healing in STZ diabetic mice. The dried sap of the plant (half a teaspoonful daily for 4–14 weeks) has shown significant hypoglycemic effect both clinically as well as experimentally.

Sclerocarya birrea: Popularly known as a Cider tree, it is a South African medicinal plant. The stem bark, roots, and leaves of the plant have been reported to possess medicinal and other properties in addition to the nutritional values of the fruits and seeds of the plant. In southern and some other parts of Africa, the stem bark, roots, and leaves of *S. birrea* are used for the treatment of diabetes mellitus. The plant's aqueous extract like chlorpropamide (a sulfonylurea antidiabetic agent) produced significant reductions in the blood glucose levels of the fasted normal and fasted

STZ-treated diabetic rats. The hypoglycemic effects of *S. birrea* stem bark aqueous extract therefore appear to be mediated via a mechanism that is similar to that of chlorpropamide, a sulfonylurea antidiabetic drug (Ojewole, 2004). *S. birrea* has been widely reported to contain many chemical compounds, including coumarins, terpenoids, flavonoids, tannins, β-sitosterol, oils, organic acids, and inorganic substances. At present, the exact chemical constituents of the plant's stem bark aqueous extract that is specifically responsible for the antidiabetic activity of the plant remain speculative.

Tinospora cordifolia: It is found in Asia and is widely used in Ayurveda as tonic, vitalizer, and as a remedy for diabetes mellitus and metabolic disorders. Diabetic rats with mild (plasma sugar = 180 mg/dL), moderate (plasma sugar = 280 mg/dL), and severe (plasma sugar = 400 mg/dL) diabetes, respectively, showed maximum hypoglycemia after being administered the aqueous extract of *T. cordifolia* for 15 weeks. The functional status of the pancreatic β-cells influences the hypoglycemic effect, and a significant reduction in blood glucose, increase in body weight, total hemoglobin, and hepatic hexokinase in alloxanized diabetic rats is observed by its oral administration (Stanely *et al.*, 2000). Thus, the plant has a potential to be used as an antidiabetic drug, but further research is required in order to identify its active substance and the mechanism of action.

Eucalyptus globules: It is a lofty tree of about 90 m in height and is grown in various parts of India. Aqueous extract (0.5 gm/L) of eucalyptus increases peripheral glucose utilization in the mouse abdominal muscle and stepwise enhancement of insulin secretion from the clonal pancreatic β-cell line by 70–160% (Gray and Flatt, 1998). Administration of *E. globulus* leaves in the diet of normal rats (6.25%, w/w) for 12 days did not result in hypoglycemia. In addition, STZ administration to these pretreated rats did not produce hyperglycemia. Pretreated rats have also shown less polydypsia and body weight loss. (Swanston-Flatt *et al.*, 1989).

The various plants having antidiabetic properties but where the active components are yet unknown are summarized in Table 2.8.

VIII. METFORMIN

The history of diabetes mellitus is replete with many therapies, nearly all, including insulin, first given without any knowledge of a mechanism of action. In medieval times, a prescription of *Galega officinalis*, also known as Goat's rue, the French lilac, or Italian fitch, was given to cure diabetes mellitus. It has also been used as galactogogue in cows. The active ingredient in the French lilac that produced the lowering of blood glucose was shown to be galegine or isoamylene guanidine (Cusi and DeFronzo, 1998;

TABLE 2.8 Traditional antidiabetic plants with hypoglycemic effects

Plants	Active part of the plant	Activity demonstrated in	Reference
Sclerocarya birrea	Stem bark	Diabetic mice	Ojewole (2004)
Aconitum carmichaeli	Root	Streptozotocin-induced diabetic mice	Liou *et al.* (2006)
Pine bark	Bark	Rats	Kim *et al.* (2005)
Clitoria ternatea	Flower	*In vitro*	Matsui *et al.* (2001b)
Brassica oleracea	Leaf	*In vitro*	Matsui *et al.* (2001b)
Pisum sativum	Pod	*In vitro*	Matsui *et al.* (2001b)
Dioscorea alata	Tuber	*In vitro*	Matsui *et al.* (2001b)
Pharbitis nil cv.	Flower	*In vitro*	Matsui *et al.* (2001b)
Enicostemma littorale	Aqueous extract (whole plant)	Alloxan-induced diabetic mice	Maroo *et al.* (2002)
Commelina communis	Dried leaves, stem	Male ICR mice	Youn *et al.* (2004)
Potentilla fulgens	Tap roots	Alloxan-induced diabetic mice	Syiem *et al.* (2002)
Helichrysum graveolens	Capitulums	Streptozotocin-induced diabetic rat	Aslan *et al.* (2007)
Agaricus bisporas	Mushrooms	Streptozocin-induced diabetic rats	Swanston-Flatt *et al.* (1989)
Coriandrum sativum	Seeds	Streptozocin-induced diabetic mice	Sharaf *et al.* (1963)
Juniperus communis	Berries	Streptozocin-induced diabetic mice	Swanston-Flatt *et al.* (1990)

(*continued*)

TABLE 2.8 (*continued*)

Plants	Active part of the plant	Activity demonstrated in	Reference
Opuntia streptacantha	Stems	Type II diabetes patients, alloxan-induced diabetic rabbits	Ibanez-Camacho *et al.* (1983)
Tinospora cordifolia	Aqueous extract	Alloxan-induced diabetic rats	Swanston-Flatt *et al.* (1990)
Phaseolus vulgaris	Pods	Alloxan-induced diabetic rats	Sharaf *et al.* (1963)
Aloe vera	Ariel	Type II diabetes patients, alloxan-induced diabetic mice	Ghannam *et al.* (1986)
Coprinus comatus	Fruit body	Healthy rats and mice	Lelley (1983)
Eucalyptus globules	Leaf	Diabetic mice	Swanston-Flatt *et al.* (1990)
Salvia lavandulifolia	Flower	Diabetic rabbits	Jimenez *et al.* (1986)
Teucrium oliverianum	Aerial	Diabetic mice	Ajabnoor *et al.* (1984)
Lythrum salicaria	Aerial	Healthy rabbits	Torres and Suarez (1980)
Cuminum nigram	Seeds	Diabetic rabbits	Akhtar and Ali (1985)

Witters, 2001). The guanidine agent's hypoglycemic activity for lowering of blood glucose levels was demonstrated from the mistaken notion that the tetany of hypoparathyroidism was due to the production of increased guanidine following parathyroidectomy (Watanabe, 1918). Though guanidine and certain derivatives are too toxic for the treatment of diabetes mellitus, the biguanides (two linked guanidine rings) have proved useful and became commercially available for diabetes therapy in the 1950s.

Phenformin and buformin, both belonging to the biguanide class, were withdrawn from the pharmacopoeia in the early 1970s due to the emergence of frequent lactic acidosis and increased cardiac mortality. Metformin, a less lipophilic biguanide, proved safer and has been in use in Europe since the 1950s. The U.S. FDA approved the drug Metformin on December 30, 1994. It is indicated for the treatment of Type II diabetes as an adjunct to diet and exercise, either as a single oral agent or in combination with sulfonylureas, α-glucosidase inhibitors, or insulin. An extended-release (XR) formulation was approved in October 2000, and combination products containing metformin and glyburide, rosiglitazone, or glipizide have since been approved (Goodarzi and Bryer-Ash, 2005).

Metformin has been marketed under different trade names such as Glucophage®, Riomet®, Fortamet®, Glumetza,® and Diabex®. In the past few years, it has become the most popular anti diabetic drug in USA and is one of the two oral antidiabetics in the World Health Organization Model list of Essential Medicines. The chemical composition of metformin is *N*,*N*-dimethyl imido dicarbonimidic diamide ($C_4H_{11}N_5$). Due to its structure, metformin becomes polar and less soluble in lipids. The structure of metformin is shown in Fig. 2.1.

A. Mechanism of action

The blood-glucose-normalizing component of this drug is its biguanide structure; however, the exact mechanism of metformin's action is not completely understood. Its main blood-glucose-lowering activity appears to be primarily through suppression of hepatic glucose output (Einhorn *et al.*, 2000; Jones *et al.*, 2003). Metformin reduces gluconeogenesis by 0.6 mg/kg per min, in effect leading to a 75% reduction in hepatic glucose output.

Metformin does not induce hypoglycemia when used by nondiabetic patients (Karam *et al.*, 1975). It has little or no effect on gastrointestinal glucose absorption. Glucoregulatory actions of metformin occur at the liver to reduce glucose output and at the peripheral tissues to augment glucose uptake, chiefly in muscle (McIntyre *et al.*, 1991) although this has not been confirmed by all investigators (Fendri *et al.*, 1993). Clinical trials show that metformin monotherapy in patients with Type II diabetes mellitus reduces fasting plasma glucose by 3–4 mmol/L and hemoglobin

A1c (HbA_{1c}) by 1.5–2% while the failure to metformin therapy occurs with approximately the same frequency (about 5–10% per year) as with sulfonylureas (U.K. prospective diabetes study 16, 1995).

A variety of possible mechanisms elucidating metformin's inhibition of glucogenesis, which includes phosphorylation of the insulin receptor and insulin receptor substrate-2 have been proposed; inhibition of key enzymes like phosphoenolpyruvate carboxykinase, fructose-1,6-bisphosphatase, and glucose-6-phosphatase; and activation of pyruvate kinase (Gunton *et al.*, 2003). Moreover, depolarization of the hepatocyte membrane and inhibition of mitochondrial respiration by metformin have been speculated as other possible mechanisms (Lutz *et al.*, 2001; Detaille *et al.*, 2002). Recent studies performed in metformin-treated rats showed adenosine monophosphate activated protein kinase (AMPK) activation, accompanied by an inhibition of lipogenesis, and a modest stimulation of skeletal muscle glucose uptake (Gunton *et al.*, 2003). However, metformin does not lead to AMPK activation *in vitro*, indicating that it activates the kinase indirectly (Witters, 2001).

B. Pharmacokinetics and other effects

In addition to its actions on glucose metabolism, several other metabolic effects of metformin have been known, with beneficial effect on patients with typical Type II diabetic. Administration of metformin has resulted in either modest weight reduction or stability of weight, while patients taking sulfonylurea, thiazolidinedione (TZD), or insulin therapy have observed an increase in weight. A number of beneficial effects relating to the cardiovascular profile of the patients have been reported, which include lowering of total cholesterol, low-density lipoprotein (LDL) cholesterol, and triglycerides (DeFronzo and Goodman, 1995). An additional, possibly beneficial, effect of metformin supplementation is the improvement of endothelium-dependent vasodilation, reduction of fibrinogen levels, and increase activity of the fibrinolytic system. Reduced levels of C-reactive protein have also been associated with metformin therapy (Goodarzi and Bryer-Ash, 2005).

C. Adverse effects

The most frequently encountered adverse effects of metformin therapy are gastrointestinal in nature. Abdominal discomfort, anorexia, or diarrhea initially affect about one-fifth of patients. Fortunately, these effects are minimized when metformin is administered with meals and with gradual dosage titration, and generally necessitate discontinuation of the drug in less than 5% of patients (Goodarzi and Bryer-Ash, 2005; Krentz *et al.*, 1994). Other adverse effects are few, including a metallic taste, reduction in serum B12 levels, and cholestatic jaundice (Goodarzi

and Bryer-Ash, 2005). Moreover, hypoglycemia has been reported when metformin is used in combination therapy. Combination therapy of the α-glucosidase inhibitor acarbose and metformin causes a significant reduction in bioavailability and peak plasma levels of metformin, though the HbA_{1c} levels are improved (Scheen *et al.*, 1994).

Lactic acidosis is another adverse effect associated with biguanide treatment, which leads to respiratory distress and nonspecific abdominal pain. Action of biguanides on nonoxidative glucose metabolism results in accelerated conversion of pyruvate to both lactate and acetyl CoA, leading to the above effect. However, the incidence of lactic acidosis with metformin is very low and has been estimated at 1 case per 30,000 patient per year (Goodarzi and Bryer-Ash, 2005).

D. Metformin in combination therapy

In recent years, there has been a lot of focus ondeveloping new antidiabetic drugs in which metformin has been combined with other antidiabetic agents to give an overall improved effect in diabetic patients. Much data have been published regarding the combination therapy of metformin and there are drugs available in the market based on this therapy.

Metformin with sulfonylureas: Combination of metformin with sulfonylureas has been frequently used and does not generally result in weight gain (DeFronzo and Goodman, 1995). Conversely, sulfonylureas may be added when glycemic control is suboptimal with metformin alone. Most patients remain on maximal dosage of sulfonylurea when metformin is added or vice versa. Dosage titration should be gradual, because the tendency of sulfonylureas to cause hypoglycemia may resurface when metformin is added.

Metformin with Repaglinide: Combined metformin and repaglinide therapy exhibits enhanced glycemic control over monotherapy with metformin or repaglinide in subjects with poorly controlled Type II diabetes mellitus. Repaglinide plus metformin therapy showed greater reductions in HbA_{1c} and fasting glucose levels than observed in nateglinide plus metformin.

Metformin with Pioglitazone: Studies have been conducted where the combined effect of pioglitazone with metformin has been observed. Patients attained greater reduction in fasting plasma glucose and HbA_{1c} levels as well as greater improvements in triglycerides and HDL cholesterol (Einhorn *et al.*, 2000). The dosage given was 30 mg daily, which indicates a very useful combination therapy.

Metformin with Rosiglitazone: Combination of rosiglitazone and metformin has consistently shown improved glycemic control over metformin monotherapy along with better insulin sensitivity and β-cell function (Jones *et al.*, 2003). The adverse effects associated with combination therapy are low and comparable to the metformin monotherapy, thereby increasing its therapeutic importance (Table 2.9).

TABLE 2.9 Currently available formulations containing metformin

Formulation	Brand names	Available doses (mg)
Metformin	GLUCOPHAGE®	500, 850, 1000
Metformin XR	GLUCOPHAGE® XR	500, 750
Glyburide/metformin	GLUCOVANCE®	1.25/500, 2.5/500, 5/500
Glipizide/metformin	METAGLIP®	2.5/500, 5/500
Rosiglitazone/ metformin	AVADAMENT®	1/500, 2/500, 4/500, 2/1000, 4/1000

REFERENCES

Abe, M., *et al.* (2007). Combination therapy of pioglitazone with voglibose improves glycemic control safely and rapidly in Japanese type 2-diabetic patients on hemodialysis. *Clin. Nephrol.* **68**(5), 287–294.

Ahr, H. J., *et al.* (1989). Pharmacokinetics of acarbose. Part I: Absorption, concentration in plasma, metabolism and excretion after single administration of [14C]acarbose to rats, dogs and man. *Arzneimittelforschung* **39**(10), 1254–1260.

Ahr, H. J., *et al.* (1997). Pharmacokinetics of miglitol. Absorption, distribution, metabolism, and excretion following administration to rats, dogs, and man. *Arzneimittelforschung* **47**(6), 734–745.

Ajabnoor, M. A., *et al.* (1984). Anti-diabetic activity of Teucrium oliverianum. *Fitoterapia LV* **2,** 227.

Akhtar, M. S., and Ali, M. R. (1985). Study of hypoglycaemic activity of *Cuminum nigrum* seeds in normal and alloxan diabetic rabbits. *Planta Med.* **51**(2), 81–85.

Allen, F. (1927). Leaf extract: Physiologic and clinical properties in relation to carbohydrate metabolism. *JAMA* **89,** 1577–1581.

Anderson, O. M. (2002). Paper presented at the anthocyanin occurrences and analysis. Proceedings of the International Workshop on Anthocyanins: Research and Development of Anthocyanins, Adelaide, South Australia, pp. 17–19.

Anderson, R. A., *et al.* (2004). Isolation and characterization of polyphenol type-A polymers from cinnamon with insulin-like biological activity. *J. Agric. Food Chem.* **52**(1), 65–70.

Apeler, H., *et al.* (2001). Neue Enzyme in der Acarbose-Synthese und deren Verwendung. German Patent DEOS 10021667.

Aslan, M., *et al.* (2007). A study of antidiabetic and antioxidant effects of Helichrysum graveolens capitulums in streptozotocin-induced diabetic rats. *J. Med. Food* **10**(2), 396–400.

Attele, A. S., *et al.* (2002). Antidiabetic effects of Panax ginseng berry extract and the identification of an effective component. *Diabetes* **51**(6), 1851–1858.

Augusti, K. T. (1974). Effect of alloxan diabetes of allyl propyl disulphide obtained from onion. *Naturwissenschaften* **61**(4), 172–173.

Bailey, C. J., and Day, C. (1989). Traditional plant medicines as treatments for diabetes. *Diabetes Care* **12**(8), 553–564.

Balfour, J. A., and McTavish, D. (1993). Acarbose. An update of its pharmacology and therapeutic use in diabetes mellitus. *Drugs* **46**(6), 1025–1054.

Beunink, J., Schedel, M., and Steiner, U. (1997). Osmotically Controlled Fermentation Process for the Preparation of acarbose. German Patent DE 19637591 (US patent 6, 130, 072).

Bowers, S. G., Mahmud, T., and Floss, H. G. (2002). Biosynthetic studies on the alpha-glucosidase inhibitor acarbose: The chemical synthesis of dTDP-4-amino-4, 6-dideoxy-alpha-D-glucose. *Carbohydr. Res.* **337**(4), 297–304.

Brahmachari, H. D., and Augusti, K. T. (1964). Isolation of orally effective hypoglycemic compounds from Ficus bengalensis Linn. *Indian J. Physiol. Pharmacol.* **8,** 60–64.

Bressler, R., Corredor, C., and Brendel, K. (1969). Hypoglycin and hypoglycin-like compounds. *Pharmacol. Rev.* **21**(2), 105–130.

Campbell, L. K., Baker, D. E., and Campbell, R. K. (2000). Miglitol: Assessment of its role in the treatment of patients with diabetes mellitus. *Ann. Pharmacother.* **34**(11), 1291–1301.

Chase, C. K., and McQueen, C. E. (2007). Cinnamon in diabetes mellitus. *Am. J. Health Syst. Pharm.* **64**(10), 1033–1035.

Chen, X., Zheng, Y., and Shen, Y. (2006). Voglibose (Basen, AO-128), one of the most important alpha-glucosidase inhibitors. *Curr. Med. Chem.* **13**(1), 109–116.

Chiasson, J. L., *et al.* (1994). The efficacy of acarbose in the treatment of patients with non-insulin-dependent diabetes mellitus. A multicenter controlled clinical trial. *Ann. Intern. Med.* **121**(12), 928–935.

Chiasson, J. L., *et al.* (2002). Acarbose for prevention of type 2 diabetes mellitus: The STOP-NIDDM randomised trial. *Lancet* **359**(9323), 2072–2077.

Clifford, M. N. (2000). Anthocyanins—Nature, occurrence and dietary burden. *J. Sci. Food Agric.* **80**(7), 1063–1072.

Clissold, S. P., and Edwards, C. (1988). Acarbose. A preliminary review of its pharmacodynamic and pharmacokinetic properties, and therapeutic potential. *Drugs* **35**(3), 214–243.

Coniff, R. F. (1991). Results of US trials with acarbose in treatment of NIDDM. FDA application.

Coniff, R. F., *et al.* (1995). Multicenter, placebo-controlled trial comparing acarbose (BAY g 5421) with placebo, tolbutamide, and tolbutamide-plus-acarbose in non-insulin-dependent diabetes mellitus. *Am. J. Med.* **98**(5), 443–451.

Cusi, K., and DeFronzo, R. (1998). Metformin: A review of its metabolic effects. *Diabetes Rev.* **6**(2), 89–131.

de Sousa, E., *et al.* (2004). Hypoglycemic effect and antioxidant potential of kaempferol-3, 7-O-(alpha)-dirhamnoside from Bauhinia forficata leaves. *J. Nat. Prod.* **67**(5), 829–832.

DeFronzo, R. A., and Goodman, A. M. (1995). Efficacy of metformin in patients with non-insulin-dependent diabetes mellitus. The Multicenter Metformin Study Group. *N. Engl. J. Med.* **333**(9), 541–549.

Deppenmeier, U., Hoffmeister, M., and Prust, C. (2002). Biochemistry and biotechnological applications of Gluconobacter strains. *Appl. Microbiol. Biotechnol.* **60**(3), 233–242.

Detaille, D., *et al*. (2002). Obligatory role of membrane events in the regulatory effect of metformin on the respiratory chain function. *Biochem. Pharmacol.* **63**(7), 1259–1272.

Dimitriadis, G., *et al.* (1991). Effects of alpha-glucosidase inhibition on meal glucose tolerance and timing of insulin administration in patients with type I diabetes mellitus. *Diabetes Care* **14**(5), 393–398.

Donner, T. (2006). Tight control of hyperclycemia in type 2 diabetes mellitus. *Insulin* **1**(4), 166–172.

Du, Z. Y., *et al.* (2006). Alpha-glucosidase inhibition of natural curcuminoids and curcumin analogs. *Eur. J. Med. Chem.* **41**(2), 213–218.

Einhorn, D., *et al.* (2000). Pioglitazone hydrochloride in combination with metformin in the treatment of type 2 diabetes mellitus: A randomized, placebo-controlled study. The Pioglitazone 027 Study Group. *Clin. Ther.* **22**(12), 1395–1409.

Escobar-Jimenez, F., *et al.* (1995). Efficacy and tolerability of miglitol in the treatment of patients with non-insulin-dependent diabetes mellitus. *Curr. Ther. Res.* **56,** 258–268.

Farnsworth, N., and Segelman, A. (1971). Hypoglycemic plants. *Tile Till* **57,** 52–55.
Fendri, S., *et al.* (1993). Metformin effects on peripheral sensitivity to insulin in non diabetic obese subjects. *Diabete Metab.* **19**(2), 245–249.
Fernandes, N. P., *et al.* (2007). An experimental evaluation of the antidiabetic and antilipidemic properties of a standardized Momordica charantia fruit extract. *BMC Complement. Altern. Med.* **7,** 29.
Folsch, U. R., *et al.* (1987). The enteroinsular axis during treatment with glucosidase inhibitors. *Front. Horm. Res.* **16,** 197–205.
Frommer, W., Puls, W., and Schmidt, D. (1977a). Process for the Production of a Sacchrase Inhibitor. German Patent DE 2209834 (US patent 4, 019, 960).
Frommer, W., *et al.* (1977b). Amino Sugar Derivatives. German Patent DE 2347782 (US patent 4,062,950).
Ghannam, N., *et al.* (1986). The antidiabetic activity of aloes: Preliminary clinical and experimental observations. *Horm. Res.* **24**(4), 288–294.
Ghosh, D. (2005). Anthocyanins and anthocyanins-rich extracts in biology and medicine: Biochemical, cellular and medicinal properties. *Curr. Top. Nutraceutical Res.* **3**(2), 113–124.
Goke, B., *et al.* (1994). Intestinal effects of alpha-glucosidase inhibitors: Absorption of nutrients and enterohormonal changes. *Eur. J. Clin. Invest.* **24**(Suppl. 3), 25–30.
Goke, B., *et al.* (1995). Voglibose (AO-128) is an efficient alpha-glucosidase inhibitor and mobilizes the endogenous GLP-1 reserve. *Digestion* **56**(6), 493–501.
Goodarzi, M. O., and Bryer-Ash, M. (2005). Metformin revisited: Re-evaluation of its properties and role in the pharmacopoeia of modern antidiabetic agents. *Diabetes Obes. Metab.* **7**(6), 654–665.
Gray, A. M., and Flatt, P. R. (1998). Antihyperglycemic actions of Eucalyptus globulus (Eucalyptus) are associated with pancreatic and extra-pancreatic effects in mice. *J. Nutr.* **128**(12), 2319–2323.
Grover, J. K., Yadav, S., and Vats, V. (2002). Medicinal plants of India with anti-diabetic potential. *J. Ethnopharmacol.* **81**(1), 81–100.
Gunton, J. E., *et al.* (2003). Metformin rapidly increases insulin receptor activation in human liver and signals preferentially through insulin-receptor substrate-2. *J. Clin. Endocrinol. Metab.* **88**(3), 1323–1332.
Hall, R. D., and Yeoman, M. M. (1986). Temporal and spatial heterogeneity in the accumulation of anthocyanins in cell-cultures of catharanthus-roseus (L) Don, G. *J. Exp. Botany* **37**(174), 48–60.
Hammouda, Y., and Amer, M. S. (1966). Antidiabetic effect of tecomine and tecostanine. *J. Pharm. Sci.* **55**(12), 1452–1454.
Hammouda, Y., and Khalafallah, N. (1971). Stability of tecomine, the major antidiabetic factor of Tecoma stans (Juss.) f. bignoniaceae. *J. Pharm. Sci.* **60**(8), 1142–1145.
Hemker, M., *et al.* (2001). Identification, cloning, expression, and characterization of the extracellular acarbose-modifying glycosyltransferase, AcbD, from *Actinoplanes* sp. strain SE50. *J. Bacteriol.* **183**(15), 4484–4492.
Hermann, M. (1973). Herbs and Medicinal Flowers. Galahad, New York, NY.
Hikino, H., *et al.* (1985). Isolation and hypoglycemic activity of ganoderans A and B, glycans of ganoderma lucidum fruit bodies1. *Planta Med.* **51**(4), 339–340.
Hoffmann, J., and Spengler, M. (1994). Efficacy of 24-week monotherapy with acarbose, glibenclamide, or placebo in NIDDM patients. The Essen study. *Diabetes Care* **17**(6), 561–566.
Hollander, P., and Coniff, R. F. (1991). Two multicenter, double-blind, placebo-controlled studies of efficacy and safety of acarbose treatment of type I diabetes. *Diabetes* **40**(Suppl. 1), 307A.
Holman, R. R., *et al.* (2003). Six-years results from early diabetes intervention trail. *Diabet. Med.* **20** (Suppl. 2), S15 (Abstract).

Horii, S., *et al.* (1986). Synthesis and alpha-D-glucosidase inhibitory activity of N-substituted valiolamine derivatives as potential oral antidiabetic agents. *J. Med. Chem.* **29**(6), 1038–1046.

Ibanez-Camacho, R., Meckes-Lozoya, M., and Mellado-Campos, V. (1983). The hypoglucemic effect of Opuntia streptacantha studied in different animal experimental models. *J. Ethnopharmacol.* **7**(2), 175–181.

Imparl-Radosevich, J., *et al.* (1998). Regulation of PTP-1 and insulin receptor kinase by fractions from cinnamon: Implications for cinnamon regulation of insulin signalling. *Horm. Res.* **50**(3), 177–182.

Jain, R. C., Vyas, C. R., and Mahatma, O. P. (1973). Letter: Hypoglycaemic action of onion and garlic. *Lancet* **2**(7844), 1491.

Jayaprakasam, B., *et al.* (2005). Insulin secretion by bioactive anthocyanins and anthocyanidins present in fruits. *J. Agric. Food Chem.* **53**(1), 28–31.

Jimenez, J., *et al.* (1986). Hypoglycemic activity of Salvia lavandulifolia. *Planta Med.* **52**(4), 260–262.

Johnston, P. S., *et al.* (1994). Effects of the carbohydrase inhibitor miglitol in sulfonylurea-treated NIDDM patients. *Diabetes Care* **17**(1), 20–29.

Johnston, P. S., *et al.* (1997). Advantages of alpha-glucosidase inhibition as monotherapy in elderly type 2 diabetic patients. *J. Clin. Endocrinol. Metab.* **83**(5), 1515–1522.

Jones, K. (2005). The potential health benefits of purple corn. Herbalgram. *Am. Bot. Council* **65,** 46–49.

Jones, T. A., *et al.* (2003). Addition of rosiglitazone to metformin is most effective in obese, insulin-resistant patients with type 2 diabetes. *Diabetes Obes. Metab.* **5**(3), 163–170.

Karam, J. H., Matin, S. B., and Forsham, P. H. (1975). Antidiabetic drugs after the University Group Diabetes Program (UGDP). *Annu. Rev. Pharmacol.* **15,** 351–366.

Keppler, K., and Humpf, H. U. (2005). Metabolism of anthocyanins and their phenolic degradation products by the intestinal microflora. *Bioorg. Med. Chem.* **13**(17), 5195–5205.

Khan, A., *et al.* (2003). Cinnamon improves glucose and lipids of people with type 2 diabetes. *Diabetes Care* **26**(12), 3215–3218.

Kim, M. J., *et al.* (1999). Comparative study of the inhibition of alpha-glucosidase, alpha-amylase, and cyclomaltodextrin glucanosyltransferase by acarbose, isoacarbose, and acarviosine-glucose. *Arch. Biochem. Biophys.* **371**(2), 277–283.

Kim, Y. M., *et al.* (2005). Inhibitory effect of pine extract on alpha-glucosidase activity and postprandial hyperglycemia. *Nutrition* **21**(6), 756–761.

Kinast, G., and Schedel, M. (1979). Production of N-substituted derivatives of 1-desoxynojirimycin. US patent 4, 266, 025.

Konno, C., *et al.* (1985a). Isolation and hypoglycemic activity of aconitans A, B, C and D, glycans of Aconitum carmichaeli Roots1. *Planta Med.* **51**(2), 160–161.

Konno, C., Mizuno, T., and Hikino, H. (1985b). Isolation and hypoglycemic activity of ephedrans A, B, C, D and E, glycans of Ephedra distachya Herbs1. *Planta Med.* **51**(2), 162–163.

Krentz, A. J., and Bailey, C. J. (2005). Oral antidiabetic agents: Current role in type 2 diabetes mellitus. *Drugs* **65**(3), 385–411.

Krentz, A. J., Ferner, R. E., and Bailey, C. J. (1994). Comparative tolerability profiles of oral antidiabetic agents. *Drug Saf.* **11**(4), 223–241.

Kumar, S., *et al.* (2008). Antidiabetic potential of Phyllanthus reticulatus in alloxan-induced diabetic mice. *Fitoterapia* **79**(1), 21–23.

Kusano, S., and Abe, H. (2000). Antidiabetic activity of white skinned sweet potato (Ipomoea batatas L.) in obese Zucker fatty rats. *Biol. Pharm. Bull.* **23**(1), 23–26.

Lange, P., and Rauenbusch, E. (1986). Rauenbusch, Polymers for the Purification of Acarbose. German Patent DE 3439008 (US patent 4, 767, 850).

Lebovitz, H. (1992). Oral antidiabetic agents: The emergence of alpha-glucosidase inhibotors. *Drugs* **44**(Suppl. 3), 21–28.
Lebovitz, H. (2004). Oral antidiabetic agents: 2004. *Med. Clin. North Am.* **88,** 847–863.
Lelley, J. (1983). Investigations on the culture of the ink cap, C. coniurus (Mull ex Fr) Gray. *Mushroom J.* **129,** 14.
Lembcke, B., Folsch, U. R., and Creutzfeldt, W. (1985). Effect of 1-desoxynojirimycin derivatives on small intestinal disaccharidase activities and on active transport in vitro. *Digestion* **31**(2–3), 120–127.
Leonard, E., *et al.* (2008). Strain improvement of recombinant *Escherichia coli* for efficient production of plant flavonoids. *Mol. Pharm.* **5**(2), 257–265.
Li, W., *et al.* (2007). Antihyperglycemic effect of *Cephalotaxus sinensis* leaves and GLUT-4 translocation facilitating activity of its flavonoid constituents. *Biol. Pharm. Bull.* **30**(6), 1123–1129.
Liou, S. S., Liu, I. M., and Lai, M. C. (2006). The plasma glucose lowering action of Hei-Shug-Pian, the fire-processed product of the root of Aconitum (Aconitum carmichaeli), in streptozotocin-induced diabetic rats. *J. Ethnopharmacol.* **106**(2), 256–262.
Liu, H. W., and Thorson, J. S. (1994). Pathways and mechanisms in the biogenesis of novel deoxysugars by bacteria. *Annu. Rev. Microbiol.* **48,** 223–256.
Liu, C. J., *et al.* (2002). Bottlenecks for metabolic engineering of isoflavone glycoconjugates in Arabidopsis. *Proc. Natl. Acad. Sci. USA* **99**(22), 14578–14583.
Liu, X., *et al.* (2004a). Antidiabetic effect of Pycnogenol French maritime pine bark extract in patients with diabetes type II. *Life Sci.* **75**(21), 2505–2513.
Liu, X., *et al.* (2004b). Pycnogenol, French maritime pine bark extract, improves endothelial function of hypertensive patients. *Life Sci.* **74**(7), 855–862.
Lutz, T. A., *et al*. (2001). Depolarization of the liver cell membrane by metformin. *Biochim. Biophys. Acta* **1513**(2), 176–184.
Mahmud, T. (2003). The C7N aminocyclitol family of natural products. *Nat. Prod. Rep.* **20**(1), 137–166.
Mahmud, T., *et al.* (1999). Biosynthesis Studies on the alpha-Glucosidase Inhibitor Acarbose in *Actinoplanes* sp.: 2-epi-5-epi-Valiolone Is the Direct Precursor of the Valienamine Moeity. *J. Am. Chem. Soc.* **121**(30), 6973–6983.
Mai, T. T., *et al.* (2007). Alpha-glucosidase inhibitory and antioxidant activities of Vietnamese edible plants and their relationships with polyphenol contents. *J. Nutr. Sci. Vitaminol. (Tokyo)* **53**(3), 267–276.
Markham, K. R., and Porter, L. J. (1973). Extractives of Pinus radiata bark 1, phenolic compounts. *N. Z. J. Sci.* **56,** 751–761.
Maroo, J., *et al.* (2002). Glucose lowering effect of aqueous extract of Enicostemma littorale Blume in diabetes: A possible mechanism of action. *J. Ethnopharmacol.* **81**(3), 317–320.
Matsui, T., *et al.* (2001a). alpha-Glucosidase inhibitory action of natural acylated anthocyanins. 2. alpha-Glucosidase inhibition by isolated acylated anthocyanins. *J. Agric. Food Chem.* **49**(4), 1952–1956.
Matsui, T., *et al.* (2001b). alpha-Glucosidase inhibitory action of natural acylated anthocyanins. 1. Survey of natural pigments with potent inhibitory activity. *J. Agric. Food Chem.* **49**(4), 1948–1951.
Matsui, T., *et al.* (2004). Caffeoylsophorose, a new natural alpha-glucosidase inhibitor, from red vinegar by fermented purple-fleshed sweet potato. *Biosci. Biotechnol. Biochem.* **68**(11), 2239–2246.
Matsuo, T., Odaka, H., and Ikeda, H. (1992). Effect of an intestinal disaccharidase inhibitor (AO-128) on obesity and diabetes. *Am. J. Clin. Nutr.* **55**(1 Suppl), 314S–317S.
McDougall, G. J., and Stewart, D. (2005). The inhibitory effects of berry polyphenols on digestive enzymes. *Biofactors* **23**(4), 189–195.

McDougall, G. J., *et al.* (2005). Different polyphenolic components of soft fruits inhibit alpha-amylase and alpha-glucosidase. *J. Agric. Food Chem.* **53**(7), 2760–2766.

McIntyre, H. D., *et al.* (1991). Metformin increases insulin sensitivity and basal glucose clearance in type 2 (non-insulin dependent) diabetes mellitus. *Aust. N. Z. J. Med.* **21**(5), 714–719.

Meyer, J. E., Pepin, M. F., and Smith, M. A. L. (2002). Anthocyanin production from Vaccinium pahalae: Limitations of the physical micro environment. *J. Biotechnol.* **93**(1), 45–57.

Mishkinsky, J. S., *et al.* (1974). Hypoglycaemic effect of Trigonella foenum graecum and Lupinus termis (leguminosae) seeds and their major alkaloids in alloxan-diabetic and normal rats. *Arch. Int. Pharmacodyn. Ther.* **210**(1), 27–37.

Nelson-Dooley, C., *et al.* (2005). Novel treatments for obesity and osteoporosis: Targeting apoptotic pathways in adipocytes. *Curr. Med. Chem.* **12**(19), 2215–2225.

Ojewole, J. A. (2004). Evaluation of the analgesic, anti-inflammatory and anti-diabetic properties of Sclerocarya birrea (A. Rich.) Hochst. stem-bark aqueous extract in mice and rats. *Phytother. Res.* **18**(8), 601–608.

Okyar, A., *et al.* (2001). Effect of Aloe vera leaves on blood glucose level in type I and type II diabetic rat models. *Phytother Res.* **15**(2), 157–161.

Olaniyi, A. A. (1975). A neutral constituent of Momordica foetida. *Lloydia* **38**(4), 361–362.

Pagano, G., *et al.* (1995). Comparison of miglitol and glibenclamide in diet-treated type 2 diabetic patients. *Diabete Metab.* **21**(3), 162–167.

Peters, G. (1957). Ubersichten Insulin: Ersatzmittel Pflanzlichen Ursprungs (Review of insulin substitutes from vegetable resources). *Dtsch. Med. Wochenschr.* **82,** 320–322.

Piepersberg, W. (1994). Pathway engineering in secondary metabolite-producing actinomycetes. *Crit. Rev. Biotechnol.* **14**(3), 251–285.

Piepersberg, W. (1997). Molecular biology, biochemistry and fermentation of aminoglycoside antibiotics. *Biotechnol. Ind. Antibiot.* 81–163.

Piepersberg, W., and Distler, J. (1997). Aminoglycosides and sugar components in other secondary metabolites. *In* ''Biotechnology'' (H.-J. Rehm, G. Reed, A. Puhler and P. Stadler, Eds.), Products of secondary metabolism Vol. 7, pp. 397–488.

Piepersberg, W., *et al.* (2002). Recent Develoments in the biosynthesis and regulation of aminoglycosides. *In* ''Microbial Secondary Metabolites: Biosynthesis, Genetics and Regulation'' (F. Fierro and J. F. Martin, Eds.), pp. 1–26.

Prior, R. L., and Wu, X. (2006). Anthocyanins: Structural characteristics that result in unique metabolic patterns and biological activities. *Free Radic. Res.* **40**(10), 1014–1028.

Putter, J., *et al.* (1982). Pharmacokinetics of Acarbose. *In* ''Proceedings of First International Synopsium on Acarbose'' pp. 38–48.

Quesada, C., *et al.* (1996). Phenolic inhibitors of α-amylase and trypsin enzymes by extracts from pears, lentils, and cocoa. *J. Food Prot.* **59**(2), 185–192.

Rauenbusch, E. (1987). Highly Pure Acarbose. German Patent DE 3543999 (US patent 4, 904, 769).

Rauenbusch, E., and Schmidt, D. (1978). Process for Isolating Glucopyranose Compound from Culture Broths. German Patent DE 2719912 (US patent 4, 174, 439).

Sanbongi, C., Suzuki, N., and Sakane, T. (1997). Polyphenols in chocolate, which have antioxidant activity, modulate immune functions in humans in vitro. *Cell. Immunol.* **177**(2), 129–136.

Schafer, A., and Hogger, P. (2007). Oligomeric procyanidins of French maritime pine bark extract (Pycnogenol) effectively inhibit alpha-glucosidase. *Diabetes Res. Clin. Pract.* **77**(1), 41–46.

Schedel, M. (2000). Regioselective oxidation of aminosorbitol with Glucanobactor oxydans, a key reaction in the industrial synthesis of 1-deoxynojirimycin. *In* ''Biotechnology'' (D. R. Kelly, Ed.), Biotransformations II Vol. 8b, pp. 296–308.

Scheen, A. J. (2003). Is there a role for alpha-glucosidase inhibitors in the prevention of type 2 diabetes mellitus? *Drugs* **63**(10), 933–951.

Scheen, A. J. (2007). Antidiabetic agents in subjects with mild dysglycaemia: Prevention or early treatment of type 2 diabetes? *Diabetes Metab.* **33**(1), 3–12.

Scheen, A. J., *et al.* (1993). Reduction of metformin acute bioavailability by the alpha-glucosidase inhibitor acarbose in normal man. *Eur. J. Clin. Invest.* **23**(Suppl. 1).

Scheen, A. J., *et al*. (1994). Reduction of the acute bioavailability of metformin by the alpha-glucosidase inhibitor acarbose in normal man. *Eur. J. Clin. Invest.* Suppl **3,** 50–54.

Schmidt, D. D., *et al.* (1979). Glucosidase inhibitors from Bacilli. *Naturwissenschaften* **66**(11), 584–585.

Scott, L. J., and Spencer, C. M. (2000). Miglitol: A review of its therapeutic potential in type 2 diabetes mellitus. *Drugs* **59**(3), 521–549.

Sharaf, A. A., Hussein, A. M., and Mansour, M. Y. (1963). The anti-diabetic effect of some plants. *Planta Med.* **11,** 159–168.

Shibib, B. A., Khan, L. A., and Rahman, R. (1993). Hypoglycaemic activity of Coccinia indica and Momordica charantia in diabetic rats: Depression of the hepatic gluconeogenic enzymes glucose-6-phosphatase and fructose-1, 6-bisphosphatase and elevation of both liver and red-cell shunt enzyme glucose-6-phosphate dehydrogenase. *Biochem. J.* **292**(Pt 1), 267–270.

Smith, M. A. L., and Spomer, L. A. (1995). Vessels, gels, liquid media, and support systems. *In* ''Automation and Environmental Control in Plant Tissue Culture'' (J. Aitken-Christie, T. Kozai and M. A. L. Smith, Eds.), pp. 371–404. Kluwer Academic Publishers, Dordrecht, The Netherlands.

Stanely, P., Prince, M., and Menon, V. P. (2000). Hypoglycaemic and other related actions of Tinospora cordifolia roots in alloxan-induced diabetic rats. *J. Ethnopharmacol.* **70**(1), 9–15.

Suda, I., *et al.* (2003). Physiological functionality of purple-fleshed sweet potatoes containing anthocyanins and their utilization in foods. *JARQ* **37**(3), 167–173.

Swanston-Flatt, S. K., *et al.* (1989). Glycaemic effects of traditional European plant treatments for diabetes. Studies in normal and streptozotocin diabetic mice. *Diabetes Res.* **10**(2), 69–73.

Swanston-Flatt, S. K., *et al.* (1990). Traditional plant treatments for diabetes. Studies in normal and streptozotocin diabetic mice. *Diabetologia* **33**(8), 462–464.

Syiem, D., *et al.* (2002). Hypoglycemic effects of *Potentilla fulgens* L. in normal and alloxan-induced diabetic mice. *J. Ethnopharmacol.* **83**(1–2), 55–61.

Takahashi, M., Konno, C., and Hikino, H. (1985). Isolation and hypoglycemic activity of saccharans A, B, C, D, E and F, glycans of Saccharum officinarum Stalks1. *Planta Med.* **51**(3), 258–260.

Tan, M. (1997). Alpha-glucosidase inhibitors in the treatment of diabetes. *Curr. Opin. Endocrinol. Diabetes* **4**(1), 48–55.

Tatusov, R. L., *et al.* (2001). The COG database: New developments in phylogenetic classification of proteins from complete genomes. *Nucleic Acids Res.* **29**(1), 22–28.

Terahara, N., *et al.* (1996). Five new anthocyanins, ternatins A3, B4, B3, B2, and D2, from Clitoria ternatea flowers. *J. Nat. Prod.* **59**(2), 139–144.

Terahara, N., *et al.* (1999). Six diacylated anthocyanins from purple sweet potato, Ipomoea batatas cv Yamagawamurasaki. *Biosci. Biotechnol. Biochem.* **63,** 1420–1424.

Thomas, H. (2001). Acarbose Metabolismus in *Actinplanes* sp. query.

Toeller, M. (1994). alpha-Glucosidase inhibitors in diabetes: Efficacy in NIDDM subjects. *Eur. J. Clin. Invest.* **24**(Suppl. 3), 31–35.

Torres, I. C., and Suarez, J. C. (1980). A preliminary study of hypoglycemic activity of Lythrum salicaria. *J. Nat. Prod.* **43**(5), 559–563.

U.K. prospective diabetes study 16 (1995). Overview of 6 years' therapy of type II diabetes: A progressive disease. U.K. Prospective Diabetes Study Group. *Diabetes* **44**(11), 1249–1258.

Verspohl, E. J., Bauer, K., and Neddermann, E. (2005). Antidiabetic effect of *Cinnamomum cassia* and *Cinnamomum zeylanicum* in vivo and in vitro. *Phytother. Res.* **19**(3), 203–206.

Vichayanrat, A., *et al.* (2002). Efficacy and safety of voglibose in comparison with acarbose in type 2 diabetic patients. *Diabetes Res. Clin. Pract.* **55**(2), 99–103.
Vijayakumar, M. V., *et al.* (2005). The hypoglycaemic activity of fenugreek seed extract is mediated through the stimulation of an insulin signalling pathway. *Br. J. Pharmacol.* **146**(1), 41–48.
Wagman, A. S., and Nuss, J. M. (2001). Current therapies and emerging targets for the treatment of diabetes. *Curr. Pharm. Des.* **7**(6), 417–450.
Wang, H. J., and Murphy, P. A. (1996). Mass balance study of isoflavones during soybean processing. *J. Agric. Food Chem.* **44**(8), 2377–2383.
Watanabe, C. K. (1918). Studies in the metabolic changes induced by administration of guanidine bases. I. Influence of injected guanidine hydrochloride upon blood sugar content. *J. Biol. Chem.* **33,** 253–265.
Wehmeier, U. F. (2003). The biosynthesis and metabolism of acarbose in *Actinoplanes* sp. SE50/110: A progress report. *Biocatal. Biotransformation* **21,** 279–284.
Wehmeier, U. F., and Piepersberg, W. (2004). Biotechnology and molecular biology of the alpha-glucosidase inhibitor acarbose. *Appl. Microbiol. Biotechnol.* **63**(6), 613–625.
Wellmann, E. (1975). UV dose-dependent induction of enzymes related to flavonoid biosynthesis in cell-suspension cultures of parsley. *FEBS Lett.* **51**(1), 105–107.
Witters, L. A. (2001). The blooming of the French lilac. *J. Clin. Invest.* **108**(8), 1105–1107.
Wu, X., and Prior, R. L. (2005). Identification and characterization of anthocyanins by high-performance liquid chromatography-electrospray ionization-tandem mass spectrometry in common foods in the United States: Vegetables, nuts, and grains. *J. Agric. Food Chem.* **53**(8), 3101–3113.
Wu, X., *et al.* (2005). Aglycones and sugar moieties alter anthocyanin absorption and metabolism after berry consumption in weanling pigs. *J. Nutr.* **135**(10), 2417–2424.
Xie, J. T., McHendale, S., and Yuan, C. S. (2005). Ginseng and diabetes. *Am. J. Chin. Med.* **33**(3), 397–404.
Yan, Y., *et al.* (2005). Metabolic engineering of anthocyanin biosynthesis in *Escherichia coli*. *Appl. Environ. Microbiol.* **71**(7), 3617–3623.
Yan, Y. J., Li, Z., and Koffas, M. A. G. (2008). High-yield anthocyanin biosynthesis in engineered *Escherichia coli*. *Biotechnol. Bioeng.* **100**(1), 126–140.
Yang, W., Lin, L., and Qi, J. (2001). The preventing effect of acarbose and metformin on the IGT population from becoming diabetes mellitus: A 3 year multicentre prospective study. *Chin. J. Endocrinol. Metab.* **17,** 131–136.
Youn, J. Y., Park, H. Y., and Cho, K. H. (2004). Anti-hyperglycemic activity of *Commelina communis* L.: Inhibition of alpha-glucosidase. *Diabetes Res. Clin. Pract.* **66**(Suppl. 1), S149–S155.
Yu, O., *et al.* (2003). Metabolic engineering to increase isoflavone biosynthesis in soybean seed. *Phytochemistry* **63**(7), 753–763.
Zhang, C. S., *et al.* (2002). Biosynthesis of the C(7)-cyclitol moiety of acarbose in *Actinoplanes* species SE50/110. 7-O-phosphorylation of the initial cyclitol precursor leads to proposal of a new biosynthetic pathway. *J. Biol. Chem.* **277**(25), 22853–22862.
Zhang, C. S., *et al.* (2003a). The acarbose-biosynthetic enzyme AcbO from *Actinoplanes* sp. SE 50/110 is a 2-*epi*-5-*epi*-valiolone-7-phosphate 2-epimerase. *FEBS Lett.* **540**(1–3), 47–52.
Zhang, C. S., *et al.* (2003b). Identification of a 1-epi-valienol 7-kinase activity in the producer of acarbose, *Actinoplanes* sp. SE50/110. *FEBS Lett.* **540**(1–3), 53–57.
Zhu, G., *et al.* (2005). Analysis and bio activity detection of the α-glucosidase inhibitors in total alkaloids from Feculae bombycis. *Chin. Tradit. Herbal Drugs* **36,** 159–162.

CHAPTER 4

Biosynthesis of Peptide Signals in Gram-Positive Bacteria

Matthew Thoendel and **Alexander R. Horswill**[1]

Contents

Abstract

Gram-positive bacteria coordinate social behavior by sensing the extracellular level of peptide signals. These signals are biosynthesized through divergent pathways and some possess unusual functional chemistry as a result of posttranslational modifications.

Department of Microbiology, Roy J. and Lucille A. Carver College of Medicine, University of Iowa, Iowa City, Iowa, USA
[1] Corresponding author: E-mail address: alex-horswill@uiowa.edu

Advances in Applied Microbiology, Volume 71
ISSN 0065-2164, DOI: 10.1016/S0065-2164(10)71004-2

In this chapter, the biosynthetic pathways of *Bacillus* intracellular signaling peptides, *Enterococcus* pheromones, *Bacillus subtilis* competence pheromones, and cyclic peptide signals from *Staphylococcus* and other bacteria are covered. With the increasing prevalence of the cyclic peptide signals in diverse Gram-positive bacteria, a focus on this biosynthetic mechanism and variations on the theme are discussed. Due to the importance of peptide systems in pathogenesis, there is emerging interest in quorum-quenching approaches for therapeutic intervention. The quenching strategies that have successfully blocked signal biosynthesis are also covered. As peptide signaling systems continue to be discovered, there is a growing need to understand the details of these communication mechanisms. This information will provide insight on how Gram-positives coordinate cellular events and aid strategies to target these pathways for infection treatments.

I. INTRODUCTION

There is growing appreciation that bacteria are social creatures. Most representative organisms under investigation have evolved a system to coordinate regulatory events by communicating with neighbors using signaling molecules. This social behavior allows the bacterial population to invest energy in cellular processes only at the appropriate time, usually when a neighboring population has reached a critical mass or ''quorum'' for a specific response (Camilli and Bassler, 2006; Parsek and Greenberg, 2005; Waters and Bassler, 2005). Thus, this type of communication has been coined ''quorum-sensing'' for the cell density dependence of the regulatory events that ensue. For a pathogen, this coordinated activity can have benefits, allowing the invader to fly under the radar of an immune system until the opportune time to produce virulence factors and overwhelm host defenses. Similarly for symbiotic bacteria, communicating with neighbors allows bacteria to synchronize an important cellular response with the host that facilitates the cooperative lifestyle.

In general, the signaling molecules used for quorum-sensing in Gram-negative bacteria are predominantly small chemicals. The best known class of these signals is the acyl-homoserine lactones, although more divergent signal chemistry continues to be discovered. Many excellent reviews are available on the Gram-negative quorum-sensing mechanisms and the reader is referred to these articles for more information (Fuqua and Greenberg, 2002; Fuqua *et al.*, 2001). In contrast, Gram-positive bacteria prefer to communicate with signals that are based on short peptides. These peptide signals, sometimes called ''autoinducing peptides,'' can be secreted as unmodified structures or they can be the target of diverse posttranslational modifications (Fig. 4.1).

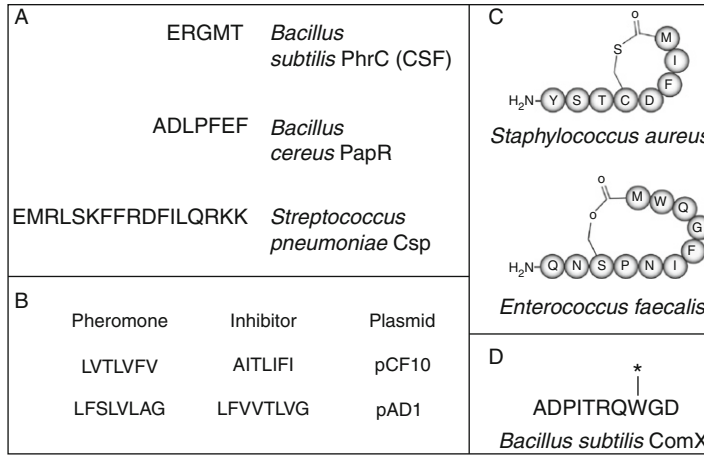

FIGURE 4.1 Examples of quorum-sensing signals produced by Gram-positive bacteria. (A) Unmodified linear peptide signals produced by *Bacillus* and *Streptococcus*. (B) *Enterococcus* plasmid pheromones and their corresponding inhibitors. (C) The cyclic autoinducing peptides produced by many Gram positives. (D) The ComX competence pheromone of *B. subtilis* 168. The tryptophan residue is farnesylated through an unusual posttranslational modification.

Among the Gram-positive peptide signals, there is a surprising amount of chemical variation. The simplest of these signals are the unmodified, linear peptides that are secreted by many Gram-positives. Some of the best known examples of this signal class are the *Bacillus* peptide signals, the competence peptide of *Streptococcus pneumoniae*, and the *Enterococcus* pheromones. An emerging class of peptide signals are the cyclic lactones and thiolactones produced by *Staphylococcus*, *Enterococcus*, and many other genera of Gram-positives. Finally, some peptide signals are the subject of more complex posttranslational modification, such as the *Bacillus subtilis* competence pheromones.

Among the peptide signals, there is surprising diversity and complexity within the biosynthetic pathways. For the Gram-negatives, acyl-homoserine lactones are freely permeable across membranes, making the production of these signals dependent on usually one enzyme and otherwise simplistic. However, the Gram-positive peptides are not permeable and thus are the subject of more complex biosynthesis and export mechanisms. Although the peptide signals are ribosomally generated, there is considerable diversity within the pathways to achieve the functional, extracellular end product. This area of research is constantly evolving as new details are being elucidated. At this time, three general mechanisms of biosynthesis and export have emerged and most of the peptide signals fall into one of these three groupings (Fig. 4.2). In this review, the three biosynthetic pathways of the

signaling peptides will be covered in detail. Although the *Enterococcus* pheromones mediate conjugation and not a typical quorum-sensing response, the unusual features of their biosynthetic pathway warrant attention and are covered herein. Due to the growing importance of the cyclic peptide systems, there is a focus on the paradigm biosynthetic pathways of the *Staphylococcus aureus* autoinducing peptides. Emerging information about quorum-quenching approaches and peptide signals from other Gram positives are also discussed.

II. *BACILLUS* INTRACELLULAR SIGNALING PEPTIDES

Peptide-mediated regulation is an important part of the spore-forming *Bacillus* lifestyle. Many critical cellular events, such as competence, spore formation, and virulence factor expression are all under the control of these intracellular acting regulatory peptides. Similar to the *Enterococcus* pheromones, *Bacillus* signaling peptides are exported out of the cell and then are reimported through an oligopeptide permease to perform an intracellular regulatory function (Fig. 4.2A). The active form of these

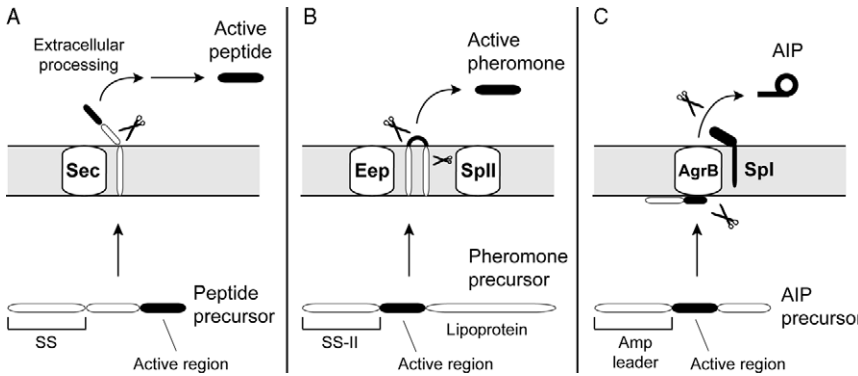

FIGURE 4.2 Comparison of peptide signal biosynthetic pathways in Gram positives. (A) The biosynthesis of intracellular acting peptides in *Bacillus*. The active region is usually on the C-terminus of the precursor peptide, and the leader is a standard signal sequence (SS). Following Sec secretion, the precursor is processed outside the cell by extracellular proteases. (B) The biosynthesis of *Enterococcus* pheromones. The precursor has a Type II signal sequence and a long lipoprotein C-terminal tail (not drawn to scale). Type II signal peptidase (SpII) removes the lipoprotein tail, and an integral membrane peptidase (Eep) removes the N-terminal leader (SS-II). In some cases, extracellular processing also occurs. (C) The biosynthesis of cyclic peptide signals. The precursor has an amphipathic leader and a charged C-terminal tail. The tail is removed by an AgrB-like membrane endopeptidase, and the leader is removed by Type I signal peptidase (SpI). AgrB is proposed to also catalyze the ring formation and export of the AIP signal.

peptides is a linear segment of unmodified amino acids, usually five to seven residues in length. The signaling peptides are chromosomally encoded and expressed as polypeptide precursors of about 40–45 amino acids. The precursors have an amino-terminal leader with a signal peptidase cleavage site, and the business end is located at the C-terminal region. For most of the regulatory peptides, the active form is the last five residues of the C-terminal region, but in some cases, such as PhrE of *B. subtilis*, the active form is located internally in the region.

A. *B. subtilis* CSF

Perhaps the best studied of the *Bacillus* intracellular acting signaling peptides is CSF (PhrC), named for its ability to stimulate competence and sporulation. CSF is a five-residue, unmodified peptide that is encoded in the *phrC* gene and is expressed as a 40-amino acid precursor. The active form of CSF is reimported through an oligopeptide permease and the peptide exerts its regulatory action inside the cell (Fig. 4.3). The CSF regulatory functions have been described in detail elsewhere and will not be covered here (Lazazzera, 2001; Lazazzera *et al.*, 1997). More recently, important details of the biosynthetic pathway leading to functional CSF peptide have been investigated. The N-terminal leader of the PhrC polypeptide precursor has all the features of a standard signal sequence, including a consensus AXA cleavage site for Type I signal peptidase. Surprisingly, attempts to demonstrate that signal peptidase is required for processing through genetic and biochemical approaches have not been successful (Stephenson *et al.*, 2003). The reason for the lack of processing is not clear. Signal peptidase is an essential enzyme and there are five encoded on the *B. subtilis* chromosome, making genetic analysis of this function challenging. Additionally, kinetic studies have demonstrated that signal peptidase enzymes process peptides inefficiently unless the substrate is presented in a manner more similar to actual secretion (Stein *et al.*, 2000).

Following export of the PhrC propeptide into the extracellular environment, the propeptide has to be processed into the active pentapeptide form of CSF. In recent studies by Lanigan-Gerdes *et al.* (2007), protease inhibitor profiling, localization studies, and regulatory tests demonstrated that the processing enzyme was an extracellular serine protease under sigma-H control. The subtilisin, Epr, and Vpr proteases meet these criteria and purified subtilisin and Vpr processed the propeptide into functional CSF signal. Further mutational analysis of the propeptide residues in the –1 to –5 location from the CSF cleavage site demonstrated that these residues are critical for extracellular processing (Lanigan-Gerdes *et al.*, 2008).

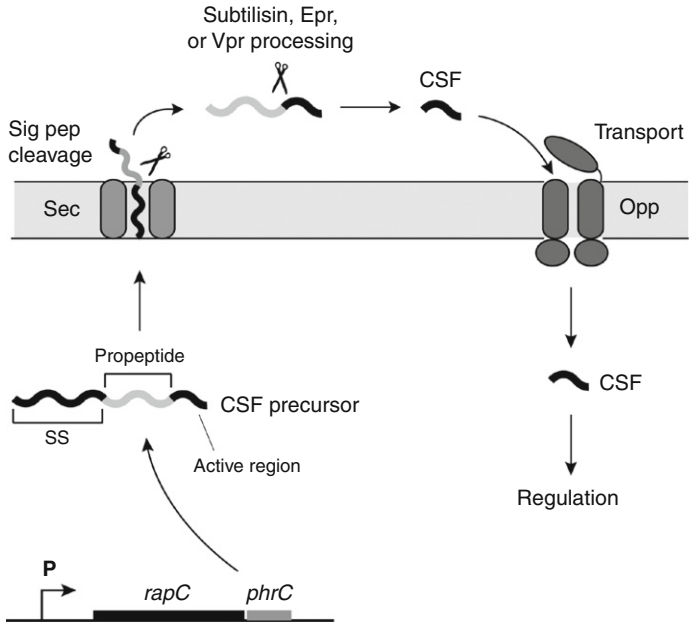

FIGURE 4.3 CSF biosynthesis in *B. subtilis*. The precursor of the CSF signal is ribosomally synthesized from the *phrC* gene. Following synthesis, the signal sequence directs the section through the Sec system, and Type I signal peptidase removes the leader. Outside the cell, the propeptide is processed to the active form of CSF through the cleavage activities of the extracelluar serine proteases subtilisin, Epr, and Vpr. Once active CSF is generated, the signal can be reimported through an oligopeptide permease (Opp), and CSF can exert its regulatory function inside the cell.

B. *Bacillus cereus* PapR

Additional examples of intracellular acting peptides among the *Bacillus* species continue to be discovered. Perhaps the most notable example is the PapR peptide from *B. cereus*. The functional form of PapR is a linear, unmodified heptapeptide that is derived from a 48-residue precursor (Bouillaut *et al.*, 2008). After import through an oligopeptide permease, PapR activates the PlcR global transcriptional regulator and induces virulence gene expression (Slamti and Lereclus, 2002). The biosynthetic pathway shows similarity to *B. subtilis* CSF and related Phr peptides. The PapR N-terminal leader looks like a signal sequence that facilitates Sec secretion, and following cleavage, a 27-residue propeptide is released into the extracellular environment. Synthetic versions of this propeptide activate gene expression, supporting the release of this sequence (Slamti and Lereclus, 2002). However, oligopeptide permeases prefer shorter peptide segments and, coupled with the known active form of PapR as

a heptapeptide, extracelluar processing is necessary to remove the leader on the propeptide. Recently, Pomerantsev and colleagues identified the NprB protease as having a role in processing the 27-residue propeptide into the active form of PapR (Pomerantsev *et al*., 2009). In support of this finding, exogenous addition of the propeptide cannot complement an *nprB* mutant, while the active form of PapR was functional. Interestingly, the *nprB* gene is flanking the *plcR-papR* region on the *B. cereus* chromosome, suggesting that this molecular arrangement may be informative for future identification of signaling peptides.

At this time, the CSF and PapR-like peptide signals appear limited to the species of *Bacillus*. Challenges have precluded the discovery of additional intracellular acting peptides of this class. For instance, the biosynthetic mechanism is performed entirely by housekeeping functions, such as the Sec system, signal peptidase, and a variety of extracellular proteases. None of these functions has unique qualities making the potential for bioinformatic discovery of new regulatory peptides difficult. Also, the target protein encoded next to the propeptide gene, such as the *plcR* gene flanking *papR*, is not conserved among the *Bacillus* peptide signals, limiting its utility as a mining tool. There have been proposals that mutations in the oligopeptide permease (Opp) could be a means for detecting functional, intracellular acting peptides, and Opp mutants have phenotypes in some Gram positives (Lazazzera, 2001). However, many Gram positives have two or more of these permease systems, making this approach to uncovering new peptides less straightforward.

III. *ENTEROCOCCUS* PHEROMONES

Another well-known peptide signaling system is the regulation of *Enterococcus faecalis* plasmid conjugation using pheromones. Like other Gram-positive peptide systems, this mechanism relies on the accumulation of a pheromone peptide that activates a response, in this case the assembly of the conjugation machinery to transfer a plasmid from a donor cell to a recipient. Unlike other peptide systems, the threshold peptide concentration cannot be reached when only a donor cell is around. Recipient cells without plasmid must be present for enough activating pheromone to be produced. This control is mediated by plasmid-encoded inhibitory peptides which resemble the activating pheromones but function to inhibit their activity. Additional cell-bound proteins decrease pheromone levels produced by donor strains (Buttaro *et al*., 2000; Hedberg *et al*., 1996), maintaining the tight regulatory control. This design prevents the energy-intensive assembly of the conjugative apparatus until a plasmid-free recipient cell is present. For more detailed information on

the regulation of this system, the reader is referred to comprehensive reviews (Chandler and Dunny, 2004; Dunny, 2007).

A number of studies have investigated the biosynthetic mechanism of the *E. faecalis* activating and inhibitory pheromones. Interestingly, the pheromones themselves are encoded within the N-terminal signal sequences of lipoproteins (Clewell *et al.*, 2000). The first step of pheromone synthesis occurs when these lipoproteins are transported across the membrane and cleaved by Type II signal peptidase (Fig. 4.2B). This enzyme cleaves at the N-terminal side of a cysteine residue in the leader to allow lipid modification at the cysteine side chain. The released peptide consists of the 12–16 N-terminal residues that correspond to the signal sequence and another seven- to eight-residue pheromone. For one pheromone precursor, cCF10p, the signal peptidase cleavage also leaves three residues on the C-terminal end of the final pheromone product, which are later removed by an unknown carboxy exopeptidase mechanism (Antiporta and Dunny, 2002).

The integral membrane protease, named Eep for *e*nhanced *e*xpression of *p*heromone, mediates the second cleavage in the pheromone precursor (An *et al.*, 1999). The second cut occurs at the N-terminal leader to release the peptide from the rest of the signal sequence. Eep belongs to a class of metalloproteases capable of carrying out regulated intramembrane proteolysis (RIP). These proteases cleave at transmembrane segments within the cell membrane and are conserved from bacteria to humans (Brown *et al.*, 2000). Studies using truncated pheromone peptides lacking the attached lipoprotein demonstrated that the signal sequences alone serve as substrates for Eep, suggesting that Eep cleavage occurs after signal peptidase II (Chandler and Dunny, 2008). This sequence of events coincides with other RIP systems in which intramembrane proteolysis follows an initial cleavage by another protease. Production of inhibitory peptides of the pheromone system occurs via a similar mechanism. These inhibitory peptides, which are encoded on the conjugatable plasmids, consist of only an N-terminal signal sequence and the active peptide region without the C-terminal lipoprotein domain (Clewell *et al.*, 2000). The inhibitory peptides are cleaved by Eep and released from the cell in a manner thought to be similar to the activating pheromones (An and Clewell, 2002).

IV. *S. AUREUS* AUTOINDUCING PEPTIDES

A. The *agr* system and AIP signal

The accessory gene regulator (*agr*) system serves as the quorum-sensing system in *S. aureus* and is a major regulator of virulence factor production. Activation of *agr* results in the upregulation of many genes, most notably

secreted virulence factors, while also downregulating production of many surface proteins (Novick and Geisinger, 2008). Not surprisingly, the *agr* locus has been demonstrated to be important for pathogenesis in numerous animal models of infection (Abdelnour *et al.*, 1993; Bubeck Wardenburg *et al.*, 2007a,b).

The *agr* locus consists of two divergent transcripts controlled by the P2 and P3 promoters. P2 drives transcription of a four-gene operon (*agrBDCA*) whose products are involved in the production (*agrBD*) and sensing (*agrCA*) of the quorum-sensing signal autoinducing peptide (AIP). P3 activates transcription of RNAIII, a 514-nucleotide regulatory RNA which acts as the effector molecule to upregulate and downregulate *agr*-controlled genes (Dunman *et al.*, 2001; Novick *et al.*, 1993). Extracellular AIP is detected by histidine kinase, AgrC, which is localized to the cell surface and acts in concert with AgrA to form a two-component sensory system. AIP binding activates AgrC to phosphorylate AgrA, and the activated AgrA proceeds to induce the P2 and P3 promoters (Koenig *et al.*, 2004), leading to autoinduction of the system and production of RNAIII effector. The mechanism of AIP sensing by AgrC and the *agr* regulatory effects is an active area of research and beyond the scope of this review, and the reader is referred elsewhere for more information (Lyon and Novick, 2004; Novick and Geisinger, 2008).

The AIP signal itself is a seven- to nine-residue peptide with the C-terminal five residues wrapped into an unusual cyclic thiolactone (Fig. 4.1C). In the ring structure, the cysteine side chain is directly linked to the carboxylic acid moiety on the C-terminal residue. Among Staphylococcal species, the cysteine residue is conserved except in *S. intermedius* where it is replaced with a serine, resulting in lactone ring formation (Ti *et al.*, 2005; Kalkum *et al.*, 2003). Not surprisingly, the cysteine (or serine in the case of *S. intermedius*) is essential for AIP biosynthesis (Thoendel and Horswill, 2009).

Among *S. aureus* stains, there are four classes of AIP signals that fall into three cross inhibitory groups (Jarraud *et al.*, 2000; Ji *et al.*, 1997). These signals all share the same five-residue thiolactone ring with a short N-terminal extension, but the actual amino acids in the signal are divergent. The inhibitory activity comes into play when two different *agr* types are in close proximity. The AIP of one strain, such as AIP Type I (AIP-I), will interfere with the function of AgrC on the opposing *S. aureus* cell by competing for the receptor. The inhibition is surprisingly effective with near-equal affinity for both activating and inhibiting receptors, and the mechanism has been coined ''*agr* interference'' (Ji *et al.*, 1997). Why *S. aureus* has evolved this mechanism is unknown, although fitness tests suggest that the producing strain has a competitive advantage (Fleming *et al.*, 2006). Exploiting this interference mechanism has been useful in quenching the *agr* response and blocking *S. aureus* infection (Wright *et al.*, 2005).

To simplify coverage of the biosynthetic pathway, hereafter only the Type I class of AIP molecule will be discussed unless otherwise stated.

B. AgrD and AgrB properties

The process of transforming the propeptide encoded by *agrD* into the functional AIP molecule is surprisingly complex. The propeptide has to be cleaved two times, cyclized to generate the thiolactone ring, and exported. Production of AIP begins with the synthesis of AgrD, the propeptide that is processed into the final, functional AIP signal. AgrD is a 46-amino acid peptide consisting of three distinct regions. The N-terminal leader forms an amphipathic helix, the middle segment encodes the final AIP sequence, while the C-terminal tail is highly charged and more conserved than the first two segments. Studies on the amphipathic helix domain have demonstrated that its role is to target the AgrD propeptide to the cell membrane (Zhang *et al.*, 2004). Removal of the N-terminal helix prevents association with the membrane, while swapping the native helix with a different amphipathic helix preserves the function of AgrD. It is important to stress that the N-terminal region is not a signal sequence, and replacing the region with a prototype Sec signal peptide blocked AIP production (Zhang *et al.*, 2004).

Continuing with AgrD, the middle segment consists of eight residues that make up the final AIP molecule, while the C-terminal domain is composed of 14 residues, many of which are negatively charged. The role of the C-terminal tail in AIP production remains to be fully determined and has been an active area of investigation. Experiments in our laboratory have demonstrated that the terminal four residues are dispensable, but the remaining 10 are essential for optimal AIP production (Thoendel and Horswill, 2009). Of note, glutamate 34 and leucine 41 play important roles in the tail's function, as replacing either of these residues prevents AgrD cleavage and AIP production. We have hypothesized that the C-terminal region interacts with AgrB, facilitating orientation of the peptide for cleavage.

AgrB is a 22-kDa integral membrane endopeptidase (Qiu *et al.*, 2005; Thoendel and Horswill, 2009). PhoA mapping studies indicate that the enzyme contains six transmembrane helices with the N and C-terminal ends located in the cytoplasm (Zhang *et al.*, 2002). One known role of AgrB is the removal of the AgrD C-terminal tail. Two residues, histidine 77 and cysteine 84, have been shown to be essential for AgrB peptidase activity, suggesting that AgrB acts as a cysteine endoprotease despite a lack of homology to known proteases (Qiu *et al.*, 2005). Both of the catalytic residues are predicted to be exposed to the cytoplasmic face (Zhang *et al.*, 2002), indicating that cleavage of the AgrD C-terminal domain occurs in the cytoplasm. To date there are no reports of a tertiary

or quaternary structure of AgrB, in large part due to the difficulty of overexpressing and purifying integral membrane proteins. Studies of this nature would be useful in examining the proposed role of AgrB as a possible transport protein for AIP secretion.

C. AIP biosynthetic mechanism

The detailed mechanism of how AgrD is processed into AIP remains an active area of investigation. Figure 4.4 provides a summary of a proposed model for the sequence of AgrD processing and how the AIP thiolactone structure might be formed (Thoendel and Horswill, 2009). Initially, the AgrD propeptide associates with the cytoplasmic membrane via its amphipathic N-terminal helix (Step 1). AgrB then interacts with AgrD and removes the C-terminal region of AgrD by carrying out a nucleophilic attack with the essential cysteine (C84) residue (Step 2). The nature of this initial interaction remains unclear; however, it is interesting to note that the cytoplasmic loop portions of AgrB contain numerous positively charge residues, while the C-terminal portion of AgrD is highly negatively charged, suggesting a potential charge–charge interaction. The cleavage reaction creates an intermediate in which the N-terminal leader and AIP regions of AgrD are covalently linked to the AgrB cysteine residue (C84) via a thioester bond. Following formation of this intermediate, the AgrD cysteine (C28) within the AIP region attacks the activated

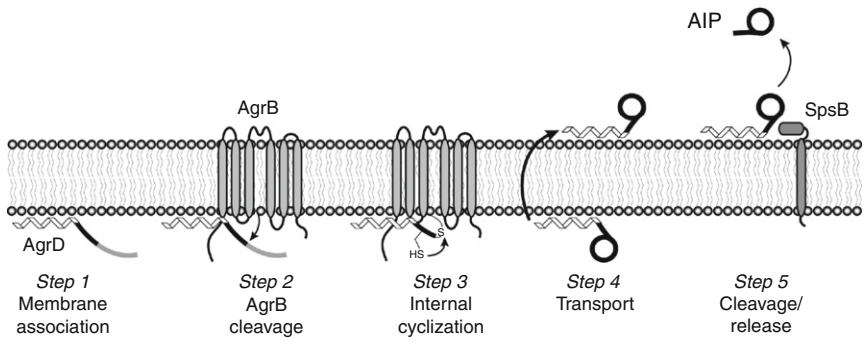

FIGURE 4.4 Schematic of AIP biosynthesis in *S. aureus*. Step 1: the AgrD N-terminal amphipathic helix associates with the cytoplasmic membrane. Step 2: the endopeptidase activity of AgrB removes the C-terminal tail of AgrD. Step 3: the remaining AgrD peptide fragment (N-terminal and AIP regions) is covalently bound to AgrB as a linked thioester at cysteine residue C84. Nucleophilic attack of the AgrD cysteine residue (C28) can displace the peptide and form the thiolactone ring through thioester exchange. Step 4: the N-terminal leader and thiolactone is transported to the outer face of the membrane. Step 5: Type I signal peptidase (SpsB) removes the leader and releases AIP into the extracellular environment. This figure was originally published in the *Journal of Biological Chemistry* (Thoendel and Horswill, 2009).

carbonyl to carry out thioester exchange, resulting in thiolactone ring formation between the cysteine side chain and the C-terminal carboxylic group of the peptide (Step 3). This thioester exchange could be spontaneously driven by structurally positioning the nucleophilic thiol near the labile thioester. After ring formation, the intermediate structure would be released from AgrB and must be moved to the outer face of the membrane (Step 4). It has been proposed that AgrB is capable of mediating this transport, though this remains to be experimentally demonstrated. Other possible mechanisms include the use of housekeeping export functions, cell lysis, or self-mediated membrane flipping as a means of reaching the outer face. AIP can be produced in *Escherichia coli* by providing only *agrB* and *agrD*, which indicates that alternative *Staphylococcus* transport proteins would have to be retained in *E. coli* (Thoendel and Horswill, 2009). In the final step of processing, the N-terminal helix of AgrD is removed to release AIP into the extracellular environment (Step 5). Type I signal peptidase (SpsB) has been shown to mediate this cleavage for *S. aureus* AIP-I production (Kavanaugh *et al.*, 2007), though it has yet to be shown that this mechanism is used by other *Staphylococcus* species.

Interestingly, AgrB-mediated processing of AgrD occurs in a species and *agr* group specific manner. In a study by Ji *et al.* (1997), AgrB proteins from *S. aureus agr* groups I, II, and III and *Staphylococcus lugdunensis* were coexpressed with AgrD peptides from each group and tested for AIP production. The Type I and III versions of AgrB were both able to produce type AIP-I or AIP-III; however, Type II AgrB was able to produce only AIP-II, and the same restriction was observed with *S. lugdenensis*. It is worth noting that that the *S. aureus* Type II *agr* system is the most divergent of the *agr* subtypes. AgrB and AgrD must have coevolved to maintain the specific interactions necessary for AgrD processing.

V. OTHER CYCLIC PEPTIDE SIGNALING SYSTEMS

Many Gram-positive species contain quorum-sensing systems that are analogous to the *agr* system of *S. aureus*. These systems possess similar production and sensory components as found in *agr*, and they also use cyclic peptides as their signaling cue. While two-component sensory components are ubiquitous in bacteria, the defining feature of these analogous peptide systems is the presence of AgrB-like proteins with sequence similarity to those found in *S. aureus*. In fact, the uniqueness of AgrB enables the use of this protein as a bioinformatics mining tool to uncover new peptide signaling systems in sequenced genomes (Wuster and Babu, 2008). Through a simple alignment search, it is apparent that many diverse genera of Gram positives, even noted pathogens, contain open reading frames that encode AgrB-like proteins. Whether or not these

diverse bacteria all have cyclic peptide systems remains to be determined, but the conserved nature of the system across many Gram positives is striking.

The AgrD-like propeptides also show strong conservation in their overall organization of three distinct regions, with the middle portion always encoding the final cyclic thiolactone or lactone. One key area of variability is the presence of divergently transcribed regulatory RNA near the signaling operons. Bioinformatic analysis suggests that the RNAIII-like molecule is limited to the *Staphylococcus* species (Wuster and Babu, 2008). In other bacteria, there seems to be a more primary role for the response regulator in controlling transcription of the target genes. Several examples of cyclic peptide systems from non-Staphylococci are outlined below.

A. *E. faecalis fsr* system

After the *S. aureus agr* system, the *fsr* system of *E. faecalis* is perhaps the second most intensively studied cyclic peptide sensory mechanism. The *fsr* system was originally identified by its proximity to the *gelE* gene encoding gelatinase. The locus consists of four genes, *fsrABDC*, whose products show significant homology to the *agr* genes in *S. aureus*. However, the molecular arrangement of the *fsr* locus is divergent from the *agr* system. In the *fsrABDC* operon, the first and last genes encode a two-component sensory pair, FsrA and FsrC, while the middle two genes encode factors involved in signal biosynthesis, FsrB and FsrD.

The signaling peptide produced is a cyclic lactone named the gelatinase biosynthesis-activating pheromone (GBAP). GBAP is an 11-residue peptide containing a nine-membered ring and a two-amino acid tail (Figure 4.1c). Originally the GBAP peptide was thought be produced as the C-terminal end of FsrB, from which the peptide precursor was cleaved and processed to make GBAP. While the FsrD propeptide is encoded in frame with FsrB, further studies revealed that a Shine–Dalgarno sequence and start codon are present within the 3′ end of the *fsrB* gene. Disruption of either of these elements dramatically reduced GBAP activity, while inserting a stop codon between *fsrB* and *fsrD* did not affect GBAP production (Nakayama *et al.*, 2006). Taken together, it is clear that FsrD is indeed translated independently of FsrB.

The FsrD propeptide shares the same three-domain structure of AgrD; however, the C-terminal portion of FsrD has an overall positive charge. Interestingly, many of the positively charged residues in a cytoplasmic loop of AgrB have been replaced with neutral or negatively charged residues in FsrB, again suggesting a possible interaction between the membrane peptidase cytoplasmic loop and the C-terminal portion of the signaling propeptide (Nakayama *et al.*, 2006). It is plausible that FsrD is

processed in a mechanism similar to the one proposed for AgrD in *S. aureus*, with the exception being that the serine of GBAP substitutes for the cysteine to form a lactone bond. Activation of *fsr* in *E. faecalis* results in upregulation of gelatinase and serine protease production (Qin *et al.*, 2000, 2001), both of which are encoded immediately downstream of the *fsr* operon. Other global transcriptional regulatory effects also occur following *fsr* activation (Bourgogne *et al.*, 2006). Importantly, the *fsr* locus is required for *E. faecalis* pathogenesis in models of mouse peritonitis, invertebrate infection (Sifri *et al.*, 2002), and rabbit endophthalmitis (Mylonakis *et al.*, 2002).

B. *Listeria monocytogenes agr* system

L. monocytogenes is a foodborne pathogen capable of causing parasitic infections in humans. A chromosomal locus with similarity to the *agrBDCA* operon was identified in a transposon mutagenesis screen and found to affect virulence in an intravenous mouse model (Autret *et al.*, 2003). Mutations in either *agrA* or *agrD* resulted in decreased biofilm formation (Rieu *et al.*, 2007), unlike the *S. aureus agr* system, where *agr* mutations increase biofilm formation (Boles and Horswill, 2008). The *L. monocytogenes agrD* mutant also displayed moderate attenuation in a mouse infection model (Riedel *et al.*, 2009). Although studies were performed showing the supernatants contain active signal (Riedel *et al.*, 2009), the autoinducing peptide has yet to be purified from these strains, leaving the exact structure of the final peptide unknown.

C. *Clostridium perfringens agr* system

C. perfringens is another human pathogen in which the *agr* system plays an important role in virulence gene regulation (Ohtani *et al.*, 2009). Strains lacking *agrBD* showed a significant reduction in the transcription of theta-, alpha-, and kappa-toxin genes. Unlike other *agr*-containing species, *C. perfringens* (and other *Clostridium* species) does not encode an AgrCA-like two-component sensory system next to the *agrBD* genes. The VirR/VirS system in *C. perfringens* has been demonstrated to be necessary for toxin gene activation in response to the quorum-sensing signal; however, further studies demonstrating direct activation of VirR/VirS by the AIP are needed to confirm that these proteins are filling the sensory role.

D. *Lactobacillus plantarum agr* system

L. plantarum is an example of a nonpathogenic, environmental isolate that contains an *agr*-like quorum-sensing system. *L. plantarum* is found in diverse environmental niches, such as plant material and fermented

food, and is often identified as part of the intestinal microflora. The *agr*-like system on the chromosome is called the *lamBDCA* operon and has a similar molecular arrangement with the biosynthetic machinery encoded before the two-component system (Sturme *et al.*, 2005). The *lam* regulatory system is important for adherence and biofilm development, in contrast to the *S. aureus agr* system. To structurally identify the *lam* signal, the *lamBD* genes were overexpressed and a peptide corresponding to a cyclized version of the sequence CVGIW was purified. Similar to the Staphylococcal AIPs, the five residues were joined as a thiolactone ring with the cysteine side chain linked to tryptophan carboxy terminus. However, this peptide is notable for its lack of N-terminal tail residues found in other AIP-like molecules. Whether this structure represents the full secreted peptide remains unclear given that exogenous addition of synthesized peptide was unable to induce *lam* operon expression. It is interesting to note that *L. plantarum* possesses dual two-component systems (*lamCA* and *lamKR*) capable of responding to the quorum-sensing signal, both of which regulate the same subset of genes (Fujii *et al.*, 2008).

VI. *B. SUBTILIS* COMPETENCE PHEROMONES

One of the most interesting biosynthetic mechanisms of the peptide signaling systems is the *B. subtilis* competence pheromones. These peptides are ribosomally synthesized from the *comX* gene, which encodes a 55-amino acid precursor of the pheromone in the *B. subtilis* 168 type strain (Magnuson *et al.*, 1994). The *comX* gene is part of a four-gene operon, *comQXPA*, and the overall molecular arrangement has similarity to the *S. aureus agr* locus (Bacon Schneider *et al.*, 2002; Ji *et al.*, 1995; Tortosa *et al.*, 2001). For the encoded functions, ComQ would be the AgrB counterpart and ComX is the signal precursor like AgrD, while ComA and ComP compromise a two-component regulatory system that detects the mature form of extracellular ComX pheromone.

The functional form of the pheromone in the 168 type strain is a 10-residue linear peptide derived from the C-terminal end of the ComX 55-residue precursor (Magnuson *et al.*, 1994). Perhaps the most intriguing aspect of the signal is the posttranslational modification on the tryptophan residue (Ansaldi *et al.*, 2002). The tryptophan is isoprenylated through an unusual addition of a farnesyl group to form a ring-like structure (Okada *et al.*, 2008). Depending on the *Bacillus* isolate, the exact sequence of the functional peptide pheromone and type of isoprenylation can vary. Other strains, such as *B. subtilis* RO-E-2, secrete an active pheromone that is comprised of only five residues with a tryptophan residue that is geranylated (Okada *et al.*, 2005, 2008).

For the biosynthetic pathway in *B. subtilis* 168, the *comX* and *comQ* genes are essential for pheromone production. Expression of *comX* and *comQ* in *E. coli* reconstitutes biosynthesis, suggesting that these encoded proteins are the only unique functions in *B. subtilis* required to produce the pheromone (Tortosa *et al.*, 2001). To date, only limited information about ComQ is available and there is no obvious homology to *S. aureus* AgrB. For this reason, we have not included this biosynthetic pathway in Fig. 4.2.

The ComQ protein is 299 residues in length and appears to have membrane spanning regions (Weinrauch *et al.*, 1991), although further analysis is necessary to confirm this prediction. Interestingly, the ComQ protein shows sequence similarity to isoprenyl phosphate synthases (Bacon Schneider *et al.*, 2002). Considering the homology to isoprenyl transfer enzymes, the known farnesylation of the pheromone, and *E. coli* reconstitution experiments, it seems likely that ComQ is the primary enzyme involved in processing the 55-residue precursor to the functional pheromone. Consistent with this proposal, mutations in a putative isoprenoid binding domain on ComQ blocked signal production (Bacon Schneider *et al.*, 2002), supporting the proposed isoprenyl transfer activity of the enzyme. However, the ComQ enzyme has not been biochemically characterized in further detail to elucidate the complex enzymatic mechanism. Based on available information, the precursor peptide has to be proteolytically cleaved, isoprenylated on a tryptophan, and secreted all through the action of ComQ. It is possible that some of these functions could be performed by house-keeping proteins, but they would have to be conserved in *E. coli* (Tortosa *et al.*, 2001). Further studies are necessary to unravel these complex questions about ComX pheromone biosynthesis.

VII. QUENCHING SIGNAL BIOSYNTHESIS

The requirement for bacterial communication in pathogenesis has raised considerable interest in quorum-quenching approaches (Fig. 4.5). The essential nature of communication mechanisms in *S. aureus* and *L. monocytogenes* infections highlights the value of this research direction (Bubeck Wardenburg *et al.*, 2007a,b; Riedel *et al.*, 2009). Currently, most of these approaches have targeted the signals themselves or the receptors, while attempts to block the biosynthesis of the signals have remained relatively unexplored. As the knowledge of these biosynthetic mechanisms grows, this remains a fertile area for future development of innovative approaches towards quorum-quenching.

Whether or not the biosynthetic apparatus in Gram-positive pathogens becomes an appealing target remains to be determined. The current target of choice for inhibitor development is the signal receptor, especially

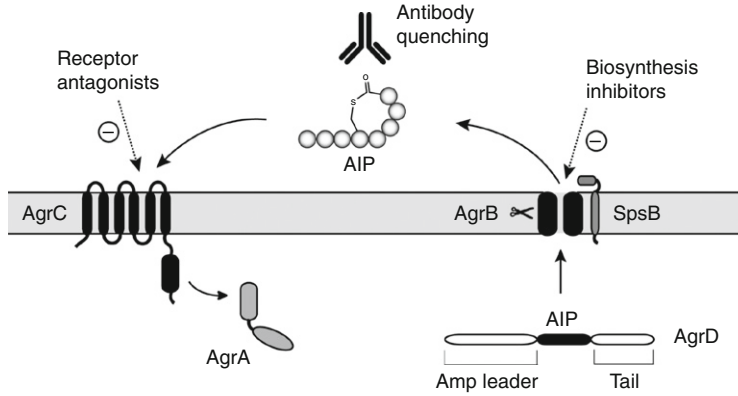

FIGURE 4.5 Strategies to quench peptide communication mechanisms. A schematic of the *S. aureus agr* system is shown as an example. A common approach for interrupting peptide quorum sensing is through receptor antagonists, and there are many examples of successful inhibitors that have been identified through synthesis and screening approaches. Recently, an antibody sequestering strategy against AIP was shown to be successful in quenching the *S. aureus agr* system *in vitro* and *in vivo*. For interrupting signal biosynthesis, several successful attempts have been reported, the most notable being against the *E. faecalis fsr* system.

for the cyclic-based signals. Antagonist discovery for the receptors is appealing due to their extracellular exposure and lack of outer membrane barriers, diversifying the functional chemistry that can be employed in inhibitor design (Chan *et al.*, 2004; George *et al.*, 2008; Lyon and Novick, 2004). The eventual challenge of this approach is the variation among signal receptor classes even within one species of bacterial pathogen. While efforts at identifying broad-spectrum inhibitors have been made (George *et al.*, 2008; Lyon *et al.*, 2000), there will always be challenges due to the inequality of antagonist activity across a particular pathogen subgroup. Thus, the receptor-based approach faces the ongoing difficulty of narrowness in application, which could limit the therapeutic potential.

As a counter to this problem, researchers have stepped back further in the quorum-sensing mechanism and focused on the peptide signals themselves (Fig. 4.5). The appeal of this strategy is that nature has already taken this approach and evolved multiple host defense mechanisms to either inactivate or sequester the signal. One successful therapeutic strategy has been the preparation of monoclonal antibodies to the *S. aureus* AIP Type IV signal (Park *et al.*, 2007). Normally in the host, the AIP signals are transient by design to facilitate the temporal response of the bacterial regulatory systems. To counter this challenge, synthetic mimics of the AIP were prepared, and mouse monoclonal antibody was generated from the hapten. The most effective antibody quenched the *agr* system response, and most importantly prevented acute infection in abscess models.

Stepping back even further in the pathway, there are several examples of small-molecule inhibition of cyclic peptide signal biosynthesis (Fig. 4.5). For *S. aureus*, linear peptide inhibitors of Type I signal peptidase were identified and found to reduce AIP-I production and quench *agr* function (Kavanaugh *et al*., 2007). Signal peptidase is an essential enzyme and also a promising antimicrobial target due to the extracellular location of the active site. In *E. faecalis*, screens of actinomyces extracts lead to the identification of siamycin I, a known lantibiotic, as a quencher of the *fsr* quorum-sensing system (Nakayama *et al*., 2007). Further investigation lead to the discovery that siamycin directly reduced the amount of GBAP signal produced. The inhibition was potent, functioning at submicromolar levels, but whether siamycin reduces GBAP levels through the inhibition of FsrB or another mode of action is not clear.

In one of the most impressive quorum-quencher reports, Nakayama *et al*. (2009) identified ambuic acid as a powerful inhibitor of cyclic peptide signal biosynthesis. Ambuic acid quenches the *fsr* quorum-sensing system in *E. faecalis* and reduces the amount of GBAP secreted. Importantly, ambuic acid found was found to directly inhibit FsrB proteolytic activity, suggesting that this membrane endopeptidase is the inhibitor target. Perhaps most notable, ambuic acid functions as a general quencher of cyclic peptide quorum-sensing across numerous Gram positives. Liquid chromatography-mass spectrometry (LC/MS) studies revealed that the production of *S. aureus* AIP-I and the *Listeria innocua* peptide signal (structure unknown) were inhibited following ambiuc acid treatment (Nakayama *et al*., 2009). Whether or not the compound targets the AgrB-type enzymes in *S. aureus* and *L. innocua* is not clear, but it seems likely based on the FsrB precedent from the *E. faecalis* studies. The broad-spectrum activity of ambuic acid highlights the value of inhibitor screening on the peptide signal biosynthetic machinery versus the divergent signal receptors. While this approach has promise for future inhibitor discovery, the lack of knowledge of AgrB/FsrB type enzymes is currently limiting screening or rational design efforts.

VIII. CONCLUSIONS

While tremendous effort has been placed on unraveling the complexities of Gram-negative quorum-sensing systems, the corresponding Gram-positive systems have not received the same research attention. This is somewhat surprising considering that the peptide systems are essential for pathogenesis in *S. aureus*, *E. faecalis*, and *L. monocytogenes*. Moreover, peptide communication mechanisms are conserved in environmental and commensal isolates, suggesting that an improved understanding of these regulatory systems has broad implications.

The aspect of peptide quorum sensing with the most unanswered questions is signal biosynthesis. As outlined in Fig. 4.2, there are three general pathways of biosynthesis that accommodate the known classes of signals. For some peptides, such as the intracellular acting *Bacillus* signals, the route of biosynthesis appears straightforward through a Sec secretion and extracellular processing mechanism. In contrast, for signals with posttranslational modifications (Fig. 4.1), essential enzymes in the biosynthetic pathways have been identified, but there is limited information on how these enzymes catalyze steps at a biochemical level. Perhaps more striking, almost nothing is known about how the processed signals are transported into the extracellular environment. Despite the limited information, quorum-quenching approaches are growing in popularity as a means of therapeutic intervention for treating infections. Further, evidence is emerging that interrupting signal biosynthesis may be attractive for quenching across diverse genera of pathogens. Considering the contrast between available knowledge and the rising interest in the targets, there is a growing need to fill the void and address the open questions. With the steady improvement in genetic and molecular approaches for investigating Gram positives, hopefully continued progress can be made on unraveling the mechanistic details of the peptide quorum-sensing systems.

ACKNOWLEDGMENTS

M. Thoendel was supported by NIH Training Grant No. T32 AI07511. Research in the laboratory of A. R. Horswill was supported by award AI078921 from the National Institute of Allergy and Infectious Diseases.

REFERENCES

Abdelnour, A., Arvidson, S., *et al.* (1993). The accessory gene regulator (*agr*) controls *Staphylococcus aureus* virulence in a murine arthritis model. *Infect. Immun.* **61**(9), 3879–3885.

An, F. Y., and Clewell, D. B. (2002). Identification of the cAD1 sex pheromone precursor in *Enterococcus faecalis*. *J. Bacteriol.* **184**(7), 1880–1887.

An, F. Y., Sulavik, M. C., *et al.* (1999). Identification and characterization of a determinant (eep) on the *Enterococcus faecalis* chromosome that is involved in production of the peptide sex pheromone cAD1. *J. Bacteriol.* **181**(19), 5915–5921.

Ansaldi, M., Marolt, D., *et al.* (2002). Specific activation of the Bacillus quorum-sensing systems by isoprenylated pheromone variants. *Mol. Microbiol.* **44**(6), 1561–1573.

Antiporta, M. H., and Dunny, G. M. (2002). ccfA, the genetic determinant for the cCF10 peptide pheromone in *Enterococcus faecalis* OG1RF. *J. Bacteriol.* **184**(4), 1155–1162.

Autret, N., Raynaud, C., *et al.* (2003). Identification of the agr locus of *Listeria monocytogenes*: Role in bacterial virulence. *Infect. Immun.* **71**(8), 4463–4471.

Bacon Schneider, K., Palmer, T. M., *et al.* (2002). Characterization of comQ and comX, two genes required for production of ComX pheromone in *Bacillus subtilis*. *J. Bacteriol.* **184**(2), 410–419.

Boles, B. R., and Horswill, A. R. (2008). *agr*-Mediated dispersal of *Staphylococcus aureus* biofilms. *PLoS Pathogens* **4**(4), e1000053.

Bouillaut, L., Perchat, S., *et al.* (2008). Molecular basis for group-specific activation of the virulence regulator PlcR by PapR heptapeptides. *Nucleic Acids Res.* **36**(11), 3791–3801.

Bourgogne, A., Hilsenbeck, S. G., *et al.* (2006). Comparison of OG1RF and an isogenic *fsrB* deletion mutant by transcriptional analysis: The Fsr system of *Enterococcus faecalis* is more than the activator of gelatinase and serine protease. *J. Bacteriol.* **188**(8), 2875–2884.

Brown, M. S., Ye, J., *et al.* (2000). Regulated intramembrane proteolysis: A control mechanism conserved from bacteria to humans. *Cell* **100**(4), 391–398.

Bubeck Wardenburg, J., Bae, T., *et al.* (2007a). Poring over pores: Alpha-hemolysin and Panton-Valentine leukocidin in *Staphylococcus aureus* pneumonia. *Nat. Med.* **13**(12), 1405–1406.

Bubeck Wardenburg, J., Patel, R. J., *et al.* (2007b). Surface proteins and exotoxins are required for the pathogenesis of *Staphylococcus aureus* pneumonia. *Infect. Immun.* **75**(2), 1040–1044.

Buttaro, B. A., Antiporta, M. H., *et al.* (2000). Cell-associated pheromone peptide (cCF10) production and pheromone inhibition in *Enterococcus faecalis*. *J. Bacteriol.* **182**(17), 4926–4933.

Camilli, A., and Bassler, B. L. (2006). Bacterial small-molecule signaling pathways. *Science* **311**(5764), 1113–1116.

Chan, W. C., Coyle, B. J., *et al.* (2004). Virulence regulation and quorum sensing in staphylococcal infections: Competitive AgrC antagonists as quorum sensing inhibitors. *J. Med. Chem.* **47**(19), 4633–4641.

Chandler, J. R., and Dunny, G. M. (2004). Enterococcal peptide sex pheromones: Synthesis and control of biological activity. *Peptides* **25**(9), 1377–1388.

Chandler, J. R., and Dunny, G. M. (2008). Characterization of the sequence specificity determinants required for processing and control of sex pheromone by the intramembrane protease Eep and the plasmid-encoded protein PrgY. *J. Bacteriol.* **190**(4), 1172–1183.

Clewell, D. B., An, F. Y., *et al.* (2000). Enterococcal sex pheromone precursors are part of signal sequences for surface lipoproteins. *Mol. Microbiol.* **35**(1), 246–247.

Dunman, P. M., Murphy, E., *et al.* (2001). Transcription profiling-based identification of *Staphylococcus aureus* genes regulated by the *agr* and/or *sarA* loci. *J. Bacteriol.* **183**(24), 7341–7353.

Dunny, G. M. (2007). The peptide pheromone-inducible conjugation system of *Enterococcus faecalis* plasmid pCF10: Cell-cell signalling, gene transfer, complexity and evolution. *Philos. Trans. R. Soc. Lond. B Biol. Sci.* **362**(1483), 1185–1193.

Fleming, V., Feil, E., *et al.* (2006). Agr interference between clinical *Staphylococcus aureus* strains in an insect model of virulence. *J. Bacteriol.* **188**(21), 7686–7688.

Fujii, T., Ingham, C., *et al.* (2008). Two homologous Agr-like quorum-sensing systems cooperatively control adherence, cell morphology, and cell viability properties in Lactobacillus plantarum WCFS1. *J. Bacteriol.* **190**(23), 7655–7665.

Fuqua, C., and Greenberg, E. P. (2002). Listening in on bacteria: Acyl-homoserine lactone signalling. *Nat. Rev. Mol. Cell Biol.* **3**(9), 685–695.

Fuqua, C., Parsek, M. R., *et al.* (2001). Regulation of gene expression by cell-to-cell communication: Acyl-homoserine lactone quorum sensing. *Annu. Rev. Genet.* **35,** 439–468.

George, E. A., Novick, R. P., *et al.* (2008). Cyclic peptide inhibitors of staphylococcal virulence prepared by Fmoc-based thiolactone peptide synthesis. *J. Am. Chem. Soc.* **130**(14), 4914–4924.

Hedberg, P. J., Leonard, B. A., *et al.* (1996). Identification and characterization of the genes of *Enterococcus faecalis* plasmid pCF10 involved in replication and in negative control of pheromone-inducible conjugation. *Plasmid* **35**(1), 46–57.

Jarraud, S., Lyon, G. J., *et al.* (2000). Exfoliatin-producing strains define a fourth agr specificity group in *Staphylococcus aureus*. *J. Bacteriol.* **182**(22), 6517–6522.

Ji, G., Beavis, R. C., *et al.* (1995). Cell density control of staphylococcal virulence mediated by an octapeptide pheromone. *Proc. Natl. Acad. Sci. USA* **92**(26), 12055–12059.
Ji, G., Beavis, R., *et al.* (1997). Bacterial interference caused by autoinducing peptide variants. *Science* **276**(5321), 2027–2030.
Ji, G., Pei, W., *et al.* (2005). *Staphylococcus intermedius* produces a functional agr autoinducing peptide containing a cyclic lactone. *J. Bacteriol.* **187**(9), 3139–3150.
Kalkum, M., Lyon, G. J., *et al.* (2003). Detection of secreted peptides by using hypothesis-driven multistage mass spectrometry. *Proc. Natl. Acad. Sci. USA* **100**(5), 2795–2800.
Kavanaugh, J. S., Thoendel, M., *et al.* (2007). A role for Type I signal peptidase in *Staphylococcus aureus* quorum-sensing. *Mol. Microbiol.* **65,** 780–798.
Koenig, R. L., Ray, J. L., *et al.* (2004). *Staphylococcus aureus* AgrA binding to the RNAIII-agr regulatory region. *J. Bacteriol.* **186**(22), 7549–7555.
Lanigan-Gerdes, S., Dooley, A. N., *et al.* (2007). Identification of subtilisin, Epr and Vpr as enzymes that produce CSF, an extracellular signalling peptide of *Bacillus subtilis*. *Mol. Microbiol.* **65**(5), 1321–1333.
Lanigan-Gerdes, S., Briceno, G., *et al.* (2008). Identification of residues important for cleavage of the extracellular signaling peptide CSF of *Bacillus subtilis* from its precursor protein. *J. Bacteriol.* **190**(20), 6668–6675.
Lazazzera, B. A. (2001). The intracellular function of extracellular signaling peptides. *Peptides* **22**(10), 1519–1527.
Lazazzera, B. A., Solomon, J. M., *et al.* (1997). An exported peptide functions intracellularly to contribute to cell density signaling in *B. subtilis*. *Cell* **89**(6), 917–925.
Lyon, G. J., and Novick, R. P. (2004). Peptide signaling in *Staphylococcus aureus* and other Gram-positive bacteria. *Peptides* **25**(9), 1389–1403.
Lyon, G. J., Mayville, P., *et al.* (2000). Rational design of a global inhibitor of the virulence response in *Staphylococcus aureus*, based in part on localization of the site of inhibition to the receptor-histidine kinase, AgrC. *Proc. Natl. Acad. Sci. USA* **97**(24), 13330–13335.
Magnuson, R., Solomon, J., *et al.* (1994). Biochemical and genetic characterization of a competence pheromone from *B. subtilis*. *Cell* **77**(2), 207–216.
Mylonakis, E., Engelbert, M., *et al.* (2002). The *Enterococcus faecalis* fsrB gene, a key component of the fsr quorum-sensing system, is associated with virulence in the rabbit endophthalmitis model. *Infect. Immun.* **70**(8), 4678–4681.
Nakayama, J., Chen, S., *et al.* (2006). Revised model for *Enterococcus faecalis* fsr quorum-sensing system: The small open reading frame fsrD encodes the gelatinase biosynthesis-activating pheromone propeptide corresponding to staphylococcal agrd. *J. Bacteriol.* **188**(23), 8321–8326.
Nakayama, J., Tanaka, E., *et al.* (2007). Siamycin attenuates fsr quorum sensing mediated by a gelatinase biosynthesis-activating pheromone in *Enterococcus faecalis*. *J. Bacteriol.* **189**(4), 1358–1365.
Nakayama, J., Uemura, Y., *et al.* (2009). Ambuic acid inhibits the biosynthesis of cyclic peptide quormones in Gram-positive bacteria. *Antimicrob. Agents Chemother.* **53**(2), 580–586.
Novick, R. P., and Geisinger, E. (2008). Quorum sensing in staphylococci. *Annu. Rev. Genet.* **42,** 541–564.
Novick, R. P., Ross, H. F., *et al.* (1993). Synthesis of staphylococcal virulence factors is controlled by a regulatory RNA molecule. *EMBO J.* **12**(10), 3967–3975.
Ohtani, K., Yuan, Y., *et al.* (2009). Virulence gene regulation by the agr system in Clostridium perfringens. *J. Bacteriol.* **191**(12), 3919–3927.
Okada, M., Sato, I., *et al.* (2005). Structure of the *Bacillus subtilis* quorum-sensing peptide pheromone ComX. *Nat. Chem. Biol.* **1**(1), 23–24.
Okada, M., Yamaguchi, H., *et al.* (2008). Chemical structure of posttranslational modification with a farnesyl group on tryptophan. *Biosci. Biotechnol. Biochem.* **72**(3), 914–918.

Park, J., Jagasia, R., *et al.* (2007). Infection control by antibody disruption of bacterial quorum sensing signaling. *Chem. Biol.* **14**(10), 1119–1127.

Parsek, M. R., and Greenberg, E. P. (2005). Sociomicrobiology: The connections between quorum sensing and biofilms. *Trends Microbiol.* **13**(1), 27–33.

Pomerantsev, A. P., Pomerantseva, O. M., *et al.* (2009). PapR peptide maturation: Role of the NprB protease in Bacillus cereus 569 PlcR/PapR global gene regulation. *FEMS Immunol. Med. Microbiol.* **55**(3), 361–377.

Qin, X., Singh, K. V., *et al.* (2000). Effects of *Enterococcus faecalis* fsr genes on production of gelatinase and a serine protease and virulence. *Infect. Immun.* **68**(5), 2579–2586.

Qin, X., Singh, K. V., *et al.* (2001). Characterization of fsr, a regulator controlling expression of gelatinase and serine protease in *Enterococcus faecalis* OG1RF. *J. Bacteriol.* **183**(11), 3372–3382.

Qiu, R., Pei, W., *et al.* (2005). Identification of the putative staphylococcal AgrB catalytic residues involving the proteolytic cleavage of AgrD to generate autoinducing peptide. *J. Biol. Chem.* **280**(17), 16695–16704.

Riedel, C. U., Monk, I. R., *et al.* (2009). AgrD-dependent quorum sensing affects biofilm formation, invasion, virulence and global gene expression profiles in *Listeria monocytogenes*. *Mol. Microbiol.* **71**(5), 1177–1189.

Rieu, A., Weidmann, S., *et al.* (2007). Agr system of *Listeria monocytogenes* EGD-e: Role in adherence and differential expression pattern. *Appl. Environ. Microbiol.* **73**(19), 6125–6133.

Sifri, C. D., Mylonakis, E., *et al.* (2002). Virulence effect of *Enterococcus faecalis* protease genes and the quorum-sensing locus fsr in *Caenorhabditis elegans* and mice. *Infect. Immun.* **70**(10), 5647–5650.

Slamti, L., and Lereclus, D. (2002). A cell-cell signaling peptide activates the PlcR virulence regulon in bacteria of the *Bacillus cereus* group. *EMBO J.* **21**(17), 4550–4559.

Stein, R. L., Barbosa, M. D., *et al.* (2000). Kinetic and mechanistic studies of signal peptidase I from *Escherichia coli*. *Biochemistry* **39**(27), 7973–7983.

Stephenson, S., Mueller, C., *et al.* (2003). Molecular analysis of Phr peptide processing in *Bacillus subtilis*. *J. Bacteriol.* **185**(16), 4861–4871.

Sturme, M. H., Nakayama, J., *et al.* (2005). An *agr*-like two-component regulatory system in *Lactobacillus plantarum* is involved in production of a novel cyclic peptide and regulation of adherence. *J. Bacteriol.* **187**(15), 5224–5235.

Thoendel, M., and Horswill, A. R. (2009). Identification of *Staphylococcus aureus* AgrD residues required for autoinducing peptide biosynthesis. *J. Biol. Chem.* **284**(33), 21828–21838.

Tortosa, P., Logsdon, L., *et al.* (2001). Specificity and genetic polymorphism of the Bacillus competence quorum-sensing system. *J. Bacteriol.* **183**(2), 451–460.

Waters, C. M., and Bassler, B. L. (2005). Quorum sensing: Cell-to-cell communication in bacteria. *Annu. Rev. Cell Dev. Biol.* **21,** 319–346.

Weinrauch, Y., Msadek, T., *et al.* (1991). Sequence and properties of comQ, a new competence regulatory gene of *Bacillus subtilis*. *J. Bacteriol.* **173**(18), 5685–5693.

Wright, J. S., 3rd, Jin, R., *et al.* (2005). Transient interference with staphylococcal quorum sensing blocks abscess formation. *Proc. Natl. Acad. Sci. USA* **102**(5), 1691–1696.

Wuster, A., and Babu, M. M. (2008). Conservation and evolutionary dynamics of the agr cell-to-cell communication system across firmicutes. *J. Bacteriol.* **190**(2), 743–746.

Zhang, L., Gray, L., *et al.* (2002). Transmembrane topology of AgrB, the protein involved in the post-translational modification of AgrD in *Staphylococcus aureus*. *J. Biol. Chem.* **277**(38), 34736–34742.

Zhang, L., Lin, J., *et al.* (2004). Membrane anchoring of the AgrD N-terminal amphipathic region is required for its processing to produce a quorum-sensing pheromone in *Staphylococcus aureus*. *J. Biol. Chem.* **279**(19), 19448–19456.

CHAPTER 5

Cell Immobilization for Production of Lactic Acid: Biofilms Do It Naturally

Suzanne F. Dagher,[*] Alicia L. Ragout,[†] Faustino Siñeriz,[†,‡] and José M. Bruno-Bárcena[*,§,1]

Contents

[*] Department of Microbiology, North Carolina State University, Raleigh, North Carolina, USA
[†] PROIMI, Universidad Nacional de Tucumán, Belgrano y Pje, Caseros, SM Tucumán, Argentina
[‡] Cátedra de Microbiología Superior, Fac. Bioq. Qca. y Fcia, Universidad Nacional de Tucumán, Belgrano y Pje, Caseros, SM Tucumán, Argentina
[§] Golden Leaf Bio-manufacturing Training and Education Center, North Carolina State University, Raleigh, North Carolina, USA
[1] Corresponding author: Department of Microbiology and Bio-manufacturing Training and Education Center (BTEC), 4510 Gardner Hall, Campus Box 7615, Raleigh, North Carolina, USA; e-mail address: jbbarcen@ncsu.edu

Advances in Applied Microbiology, Volume 71
ISSN 0065-2164, DOI: 10.1016/S0065-2164(10)71005-4

Abstract

Interest in natural cell immobilization or biofilms for lactic acid fermentation has developed considerably over the last few decades. Many studies report the benefits associated with biofilms as industrial methods for food production and for wastewater treatment, since the formation represents a protective means of microbial growth offering survival advantages to cells in toxic environments. The formation of biofilms is a natural process in which microbial cells adsorb to a support without chemicals or polymers that entrap the cells and is dependent on the reactor environment, microorganism, and characteristics of the support. These unique characteristics enable biofilms to cause chronic infections, disease, food spoilage, and devastating effects as in microbial corrosion. Their distinct resistance to toxicity, high biomass potential, and improved stability over cells in suspension make biofilms a good tool for improving the industrial economics of biological lactic acid production. Lactic acid bacteria and specific filamentous fungi are the main sources of biological lactic acid. Over the past two decades, studies have focused on improving the lactic acid volumetric productivity through reactor design development, new support materials, and improvements in microbial production strains. To illustrate the operational designs applied to the natural immobilization of lactic acid producing microorganisms, this chapter presents the results of a search for optimum parameters and how they are affected by the physical, chemical, and biological variables of the process. We will place particular emphasis upon the relationship between lactic acid productivity attained by various types of reactors, supports, media formulations, and lactic acid producing microorganisms.

I. INTRODUCTION

The first mention of biocomplexity in the form of a biofilm was in the dental plaque and visualized at the onset of microbiology by Leeuwenhoeck (1683) following the development of the first microscope. He described

them as different forms of ''animalculi'' adhering to his teeth. Biofilms are a complex society of interacting microbiological communities that attach to various materials at the solid–liquid interface (Branda *et al.*, 2005; Davey and O'toole, 2000). Remarkably, biofilms can have enhanced resistance to solvents and toxins when compared to their suspension counterparts (Anderson and O'toole, 2008; Hall-Stoodley *et al.*, 2004; O'Toole *et al.*, 2000). This distinction is observed when pathogenic microbes forming microbial biofilms exhibit enhanced resistance to antimicrobial agents and cause chronic infections and persistent disease (Brady *et al.*, 2008; Bryers, 2008; Costerton *et al.*, 1999; Fux *et al.*, 2005; Hall-Stoodley *et al.*, 2004; O'Toole *et al.*, 2000; Spormann, 2008). Biofilms commonly cause food spoilage (Kubota *et al.*, 2008), devastating corrosion that can wear away or block water pipes, and common problems associated with surfaces exposed to water, such as growth on ship hulls causing drag (Little and Wagner, 1997; Spormann, 2008). One of the latest developments in biofilm formation has taken place in the production of probiotics with increased resistance to environmental stress, such as more resilient *Bifidobacterium* or *Lactobacillus*. Factors encountered by these organisms during production and consumption also include adaptation to conditions encountered in the gastrointestinal ecosystem. Therefore, biofilm formed on the surface of food particles leads to the development of cultures with improved capacity to survive and function during production and passage through unfavorable conditions within the digestive tract (Cinquin *et al.*, 2004; Lacroix and Yildirim, 2007; Macfarlane *et al.*, 1997; Probert and Gibson, 2002).

Apart from their natural environments, where biofilms are widely distributed, they have found an application in biotechnology as an immobilization method. Today, natural immobilization as an industrial application is widely used for the treatment of wastewater, desulfurization of gas, and food production (Kornaros and Lyberatos, 2006; Lazarova *et al.*, 2000; Linko and Linko, 1984; Majumder and Gupta, 2003; Nicolella *et al.*, 2000), as well as for converting agriculturally derived materials into alcohols and organic acids such as acetic acid, ethanol, and butanol (Crueger and Crueger, 1990; Demirci *et al.*, 1997; El-Mansi and Ward, 2007; Ho *et al.*, 1997; Qureshi *et al.*, 2004, 2005; Wang and Chen, 2009).

Biofilm as a technology applied to production allows high cell density processes, improves cell stability, enables continuous operation, and reduces downstream processing needed to separate product from cells. From an industrial standpoint, cell immobilization is becoming one of the most useful methods for increasing catalyst concentration in bioreactors and, as a result, the rate of product generation. Biofilm-based processes also present economic and environmental advantages such as the reduction in waste and side products and the low cost of immobilization materials. While operating immobilized cell reactors, the biological catalyst is kept fixed in a natural or artificial matrix and substrates and

products continuously flow in the mobile phase. The production rates can be accelerated by increasing cell density in the bioreactor or through a lengthy process of selection and development of hyperproductive cells (Davidson *et al.*, 1995; Demirci and Pometo, 1992).

As shown in the following lines, immobilized cells exhibit protective features against toxic substances and other adverse conditions, in addition to an increase in plasmid stability and increased metabolic activity with respect to their suspension cell planktonic counterparts (Anderson and O'toole, 2008; Cassidy *et al.*, 1996; Groboillot *et al.*, 1994). A number of studies have also exploited biofilm processes without cellular degeneration or contamination over several months, strengthening biofilm's potential as a feasible industrial application (Cho *et al.*, 1996; Hekmat *et al.*, 2007; Lewis and Yang, 1992; Qureshi *et al.*, 2005; Xia *et al.*, 2005). Problems with biofilm-based processes have included excessive biomass growth and cell shedding. Nutrient limitations and flow rate adjustments have been used to control cell growth while maintaining an active productive state. Technical improvements incorporate enhanced reactor designs and supports that can sustain controlled biofilm formation and growth (Bruno-Bárcena, 1997; Bruno-Bárcena *et al.*, 2001; Huang *et al.*, 1998; Qureshi *et al.*, 2005). Ultimately, development of new strains through recombinant technology and/or screening with the aim of finding microbial strains suitable for long-term production are viable options for solving the above-mentioned problems. This review examines lactic acid production using biofilm reactors. Special emphasis is placed on reactor design, support type, microorganism employed, nutrient source, and long-term stability. The overall aim is to present a viable technology suitable for biological lactic acid production.

II. BIOFILM FORMATION

When cells come in contact with wet surfaces, they show an adherent phenotype which results in colonization of the surface, for example, cells growing in suspension tend to adhere to the wall of the container or to any solid support immersed in the liquid. If the material is porous, there is an increase in the surface area available for cells to bind to the external and internal surface structures. This type of cellular dynamic is known as immobilized cells naturally attached to a surface, or biofilm growth. Cell attachment is a critical step in the multilayered process of biofilm generation. By attaching to organic and/or inorganic materials, cell growth results in microcolonies on their surfaces and, ultimately, mature biofilms are formed. An important factor throughout biofilm formation is the production of polymers that allows many individual adherent cells (sessile cells) to bond together, providing structure to the microcolonies

during formation and growth. To trigger this process it is postulated that cells can produce and sense molecules, allowing the whole population to initiate a concerted action once a critical concentration (corresponding to a particular population density) of the molecule has been reached, a phenomenon known as quorum-sensing. AI-2 is suggested to be a universal bacterial signaling molecule synthesized by the LuxS, which forms an integral part of the activated methyl cycle. Moreover, previous reports have shown that the well-documented probiotic strain *Lactobacillus rhamnosus* GG, a human isolate, produces AI-2-like molecules (Lebeer *et al.*, 2007). In fact, many potentially probiotic bacteria such as *Bifidobacterium* and *Lactobacillus* strains possess a *luxS* homologue (Altermann *et al.*, 2005; Azcarate-Peril *et al.*, 2008; Buck *et al.*, 2009) and can produce AI-2. The role of *luxS* in the adhesion of *L. acidophilus* and *L. rhamnosus* GG to surfaces has been investigated. The same genomic organization of the *luxS* gene has been found in *L. acidophilus*, *L. casei*, and *L. gasseri* (Buck *et al.*, 2009; Rodionov *et al.*, 2004)

Functional biofilm formation and growth generally involve the following series of events:

- *Absorption to surfaces*. The ability of microorganisms to adsorb to exposed surfaces is dependent on the characteristics of the support, the microorganism, and the environment. Rough surface textures and electrostatic forces on the surface (Van der Waals forces as well as ionic and hydrogen bonds), have been suggested to promote cell settlement and biofilm growth (Goller and Romeo, 2008). Cell adhesion is also dependent on the physiological state of the microorganism, mass transport phenomena, and response to chemical concentration gradients such as motile attachment using flagella or chemotaxis (Annachhatre and Bhamidimarri, 1992; Gjaltema *et al.*, 1994; Hekmat *et al.*, 2007; Li *et al.*, 2007; Pedraza *et al.*, 2009; Ragout *et al.*, 1996). The hydrodynamic conditions of the medium can also favor adherence to the surface by minimizing cell shearing. Many microorganisms react to excessive turbulence and shearing forces by inducing a global genetic response that causes a complete modification of cell surface components including flagella, fimbriae, pili, capsule, and other cell-wall polysaccharides (Lawrence *et al.*, 1995).
- *Polysaccharide production*. Once the cells are in contact with the surface and the conditions are adequate, biofilm formation is further strengthened by cell growth and synthesis of extracellular polymeric substances (EPS) which can consist of special combinations of polysaccharides, proteins, carbohydrates, DNA, and lipids, depending on the microorganisms and environmental conditions (Karatan and Watnick, 2009; Steinberger and Holden, 2004; Sutherland, 2001). The polysaccharide will eventually build bridges between cells providing a type of support

that can overcome electrostatic repulsion allowing negatively charged cells to adhere to both positively and negatively charged surfaces (Little and Wagner, 1997).

- *Biofilm maturing process*. As maturation progresses, the heterogeneous distribution of cells and the diffusion limitations within the organization form a differentiated biofilm with unique characteristics that affect cell physiology and fermentation activities (Stewart and Franklin, 2008; Werner *et al.*, 2004; Xu *et al.*, 1998). Biofilm populations often contain cells resistant to toxic compounds and specialized in aerobic or anaerobic growth, fixation to surfaces, and food scavenging, as well as cells that synthesize protective films. The specific subpopulations have been suggested to form channels used for substrate delivery, waste removal, and product delivery. This architecture of circulatory channels within the biofilm is strongly dependent on its structure and the hydrodynamic conditions (sheer forces) applied (Beyenal and Lewandowski, 2001; Costerton *et al.*, 1995; De Beer and Stoodley, 1995; De Beer *et al.*, 1994; O'Toole *et al.*, 2000).
- *Planktonic cell dispersal*. Following maturation, planktonic cells detach and/or disperse from the mature biofilms. Factors such as nutrient availability and cell density have been suggested to trigger biofilm dispersal (Spormann, 2008; Stoodley *et al.*, 2002). Detachment of planktonic cells is often seen as a mechanism of dispersion to colonize new surfaces (Costerton *et al.*, 1999; Hall-Stoodley *et al.*, 2004; Stoodley *et al.*, 2002). These mechanisms have been suggested to be quorum-sensing-regulated swarming phenotypes, or flagella-driven movement of differentiated swarmer cells (hyperflagellated, elongated, multinucleated) by which bacteria can spread as biofilm over surfaces (Daniels *et al.*, 2004). Studies with immobilized reactors working in two-stage systems have shown that the phenomena of physical detachment may also be due in great measure to shear forces that can separate pieces of biofilm in the flow. The detached pieces are in fact capable of efficient colonization on new surfaces (Bruno-Bárcena *et al.*, 1999).

III. APPLICATION OF BIOFILMS TO LACTIC ACID PRODUCTION

Lactic acid (2-hydroxypropanoic acid) is a chiral molecule with two optical enantiomers, L(+) and D(–), widely used by the pharmaceutical, plastics, food, and cosmetic industries (VickRoy, 1985). Lactic acid is either produced by chemical synthesis or microbial fermentation. To meet the growing demand for lactic acid, a number of different strategies have been pursued to improve productivity, accelerate

production rates, and reduce cost. Lactic acid production rates have been improved through increased cell density, use of systems such as multiple fiber reactors (Vick Roy *et al.*, 1982), cell recycling (Ohleyer *et al.*, 1985; Vick Roy *et al.*, 1983), cell entrapment in polymers such as κ-carrageenate or calcium alginate (Audet *et al.*, 1988; Boyaval and Goulet, 1988; Guoqiang *et al.*, 1991; Salter and Kell, 1991; Smidsrod and Skjakbraek, 1990), strain development (Demirci and Pometo, 1992), as well as cell immobilization on activated inert supports (Avnir *et al.*, 2006; Guoqiang *et al.*, 1992; Senthuran *et al.*, 1997). Others have analyzed the influence of support characteristics (Demirci *et al.*, 1993a,b; Gonçalves *et al.*, 1992) and also used strains with the ability to form biofilms to generate lactic acid (Bruno-Bárcena *et al.*, 1999; Demirci and Pometo, 1995; Krischke *et al.*, 1991).

Although there is abundant literature on lactic acid production by immobilized cells, most report poor productivity or low final metabolite concentrations (Norton and Vuillemard, 1994). Generally, production will depend on many parameters that influence the dynamics of the bioprocess including characteristics of the microorganism, reactor configurations, carbon source, nitrogen source, support type, and quantity and health of the immobilized biomass. Moreover, a major challenge continues to be the lactic acid inhibition of cell growth during production and accumulation (Friedman and Gaden, 1970).

IV. HOST ORGANISMS

The lactic acid bacteria group includes more than 125 species and subspecies (http://www.bacterio.cict.fr/). While a number of organisms capable of forming biofilms have been tested for metabolite production, homofermentive *L. rhamnosus* and *L. casei* have been well studied and are currently the most widely used species for lactic acid production. Since the description of a chemostat selection method to obtain an adhesive phenotype from an originally nonadherent strain of *Sreptococcus salivarius* subsp. *thermophilus* CRL 412 (Ragout *et al.*, 1996), only a small number of strains able to form biofilms have been tested for production: *L. rhamnosus* (RS 93), capable of forming biofilms, derived from *L. rhamnosus* DSM 20021 (Ragout *et al.*, 1995) and *L. casei* ADNOX95 (Culture collection of PROIMI, Tucumán, Argentina) an offspring of *L. casei* subsp. *casei* CRL 686 (Centro de Referencia para Lactobacilos, Tucumán, Argentina) (Bruno-Bárcena, 1997). Other biofilm formers were also recently reported for *Lactobacillus delbrueckii* NCIM 2365 on polyurethane foam (Rangaswamy and Ramakrishna, 2008) and *Lactobacillus casei* subsp. *rhamnosus* (ATCC 11443) (Table 5.1).

TABLE 5.1 Biofilm-forming strains used for production of lactic acid

Strain	Reference
Lactobacillus casei subsp. *casei* (DSM 20244)	Krischke *et al.* (1991)
Lactobacillus delbrueckii NRRL B445 renamed *L. rhamnosus*	Gonçalves *et al.* (1992)
Lactobacillus helveticus (ATCC 15009)	Silva and Yang (1995)
Lactobacillus rhamnosus RS 93	Ragout *et al.* (1995)
Streptococcus salivarius subsp. *thermophilus* CRL 412	Ragout *et al.* (1996)
Lactobacillus casei (ADNOX95)	Bruno-Bárcena *et al.* (1998, 1999)
Lactobacillus casei (ATCC 393)	Daraktchiev *et al.* (1997)
Lactobacillus casei subsp. *rhamnosus* (ATTC11443)	Ho *et al.* (1997), Cotton *et al.* (2001), Velazquez *et al.* (2001), Demirci *et al.* (2003)
Lactobacillus delbrueckii (NCIM 2365)	Rangaswamy and Ramakrishna (2008)

A. Optical purity of the product

Lactic acid bacteria strains usually generate a racemic mixture of L(+) and D(−) isomers of lactic acid. However, it is common to find organisms that are able to produce each isomer independently (Garvie, 1980). Microbial production has the advantage of being able to use strain selection to obtain an optically pure product, whereas synthetic production always results in a racemic mixture of lactic acid. The production of L(+)-lactate isomer is of significant importance to mammals since it is the only form that can be assimilated. Thus, optically pure L(+) lactic acid is the preferred and recommended choice for food industries (FAO/WHO, 1974). Optically pure L(+)-lactate is also required in the biomedical industry (Lipinsky, 1981; Tsai and Moon, 1998) and for manufacturing polymers such as polylactic acid (PLA) degradable plastics (Rincones *et al.*, 2009).

Since 1919 (Orla-Jensen, 1919), the type of isomer and its racemic proportion in the fermented broth have been used as a taxonomic characteristic. Current methods of lactate detection allow the quantification of millimolar amounts of each isomer previously impossible to detect (Gawehn and Bergmeyer, 1974). As a result of this improved detection method, species formerly assigned as producers of only one isomer have been recataloged. Some relevant cases have been *L. casei* ssp., previously

considered to exclusively produce L(+) lactate, and *L. delbrueckii* ssp. *bulgaricus* cataloged as a D(–) lactate exclusive producer (Dellaglio and Torriani, 1985; Ragout *et al.*, 1989).

It is well established that the biochemistry behind the generation of each lactate isomer from pyruvate requires the action of stereospecific enzymes called NAD-dependent lactate dehydrogenases (nLDHs EC 1.1.1.27 and EC 1.1.1.28). L(+) nLDHs are highly homologous proteins in amino acid sequence, diverse in size and behavior, and the allosteric group requires the action of additional molecules such as fructose 1, 6 diphosphate and Mn^{+2} to modulate its function. D(–) nLDHs are enzymes with diverse evolutionary origins. They are more closely related to the family of D-isocaproate dehydrogenases with high levels homology that indicate recent evolutionary divergence (Bhowmik and Steele, 1994; Delcour *et al.*, 1993; Taguchi and Ohta, 1999). D(–) nLDHs enzymes do not catalyze the oxidation of pyruvate *in vivo*; hence, cells also possess a different group of stereospecific enzymes named NAD-independent lactate dehydrogenases (iLDHs). However, in the lactic acid bacteria group iLDHs are not active when lactate is being actively generated. The last family of enzymes that can affect the L(+) and D(–) racemic ratio are the lactate racemases, though these enzymes are not frequently found in lactic acid bacteria (Garvie, 1980).

It has been suggested that the ratio of isomers generated by *L. delbrueckii* ssp. *bulgaricus* may be a function of nutrient availability and influenced by the initial concentration of carbon and energy source (Ragout *et al.*, 1989). This possible nutrient–isomer connection was later tested by evaluating the consequence of initial glucose concentration on isomer proportion from *L. casei* CRL686 (Bruno-Bárcena, 1997) (Fig. 5.1). The linearly of the plot clearly indicated that the isomer proportion was independent of the initial glucose concentration. These results suggest the isomer ratio may be organism-specific and differences in response to glucose limitations may require significant product profile studies before being placed in production. Speculation has also focused on whether the duration of production influences the behavior of the microorganism in a manner that favors creation of one lactate isomer over the other (Bruno-Bárcena, 1997). This was the case for artificially immobilized *L. rhamnosus*, where the proportion of L(+)-lactate could be correlated to the cells' age (Hjörleifsdottir *et al.*, 1990), and in two-stage chemostat, *L. helveticus* fermentation time and growth rate varied the fraction of L(+)-lactate from 55% to 70% (Aeschlimann *et al.*, 1990). The fraction of the L(+) isomer also increased with the dilution rate in continuous processes with cell recycling (Aeschlimann and Vonstockar, 1991). In contrast, the product and biomass yields remained constant and the ratio of L(+)- and D(–)-lactate isomers were not affected by the dilution rate or production time using continuous culture in chemostat operations with *L. coryniformis* and

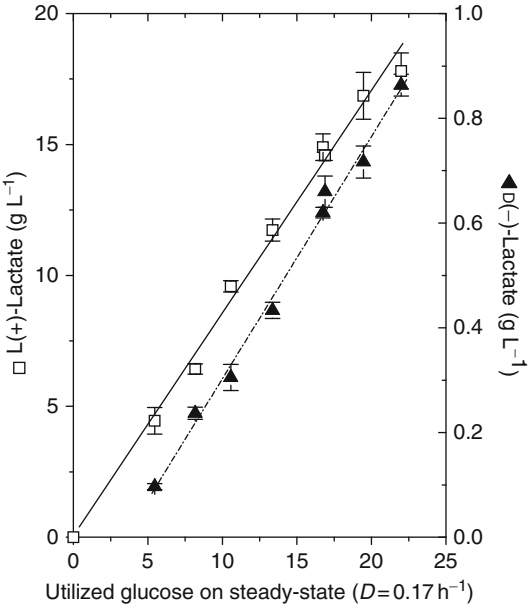

FIGURE 5.1 Lactic acid isomer concentrations generated by *Lactobacillus casei* CRL 686 during steady-state fermentation (D = 0.17 h^{-1}) at 37 °C in BFRS medium as a function of the glucose concentration.

L. casei (González-Vara *et al.*, 1996). However, the percentage of the D(–) fraction almost linearly increased from 4% to 18% during the long, 8-day stationary phase in a batch process of *Lactobacillus case* ssp. *rhamnosus* (Hjörleifsdottir *et al.*, 1990). Therefore, the isomer ratio attained will be strain-specific and must be taken into consideration for the production process. Clearly, young cells produce more L(+)-lactate then older ones, and consistently high L(+)-lactate production can be correlated with elevated growth rate. Production values evaluated as OP% = 100 × {L(+) − D(−)}/{L(+) + D(−)} presented later in this review reveal that biofilm age (with natural adhered cells) does not appear to influence the final optical purity. However, batch cultures of cells in suspension and artificially immobilized cells will eventually show the symptoms of age caused by nutrient depletion or confined growth. One of the most beneficial steps for increasing total product output is related to the ability to prolong the duration of the process. This has been demonstrated with extended production cycles from regenerated natural adherent biomass that provides a constant stream of new cells and also counteracts the variable physiology of isomer production observed in conventional processes.

V. CELL IMMOBILIZATION

Cell attachment has been explored with a variety of support materials including wood chips (Krischke *et al.*, 1991), porous bricks and cotton cloth (Gonçalves *et al.*, 1992), glass and ceramics (Guoqiang *et al.*, 1992), foam (Dong *et al.*, 1996), and plastic composite supports (PCS) (Demirci and Pometo, 1995; Demirci *et al.*, 1993a,b; Guoqiang *et al.*, 1992; Ho *et al.*, 1997; Velazquez *et al.*, 2001). A number of supports have also been evaluated for biofilm formation for lactic acid production (Demirci *et al.*, 1993b). Cell immobilization has not been limited to chemical cross-linking and polymer entrapment; for example, when used in conjunction with natural biofilm former strains, those strains can entrap non-natural biofilm formers. Among different strains tested as helpers for entrapment good results were obtained using *Pseudomonas fragi*, *Streptomyces viridosporus*, and *Thermoactinomyces vulgaris* (Demirci *et al.*, 1993a).

Other common supports have included polyurethane foams (PUFs) (Rangaswamy and Ramakrishna, 2008). Testing support materials for biofilm reactors have benefited lactic acid production methods: increasing lactic acid production rates, minimizing lag phase, rising tolerance to high glucose concentrations, reducing requirement for micronutrients, increasing cell density (Demirci *et al.*, 2003; Velazquez *et al.*, 2001), and reducing the toxic effects from solvent leakage (Demirci *et al.*, 2003). Characteristics of some common supports are displayed in Table 5.2.

A. Cell immobilization by entrapment and attachment

The cell immobilization method selected can influence cell physiology, metabolism, and distribution of cells in the matrix, resulting in variable outcomes. If cell immobilization is accomplished by entrapment or cross-linking to a support, there is generally good initial performance, but the cells decrease in viability and productivity over time and must be replaced (Guoqiang *et al.*, 1991, 1992). Furthermore, covalent binding to a support has the major disadvantages of high cost and low yield due to exposure of the cells to toxic reagents or severe reaction conditions (Tanka and Kawamoto, 1999). Cell entrapment with calcium alginate or k-carrageenan beads have been used to increase cell density; nonetheless, industrial applications are not feasible because of bead disintegration, slow leakage of cells during lengthy continuous operation, and mass transfer limitations (Audet *et al.*, 1988; Boyaval and Goulet, 1988). Shrinkage and reduced strength of the entrapment during lactic acid fermentation has been attributed to the displacement of Ca^{+2} ions by lactate ions in alginate beads (Roy *et al.*, 1987).

TABLE 5.2 Characteristics of supports used for microorganism's immobilization

Supports	Form	Material	Average pore diameter (μm)	Porosity (%)	Density (g cm^{-3})	Reference
Poraver®[a]	Beads	Recycled glass	<200	49	0.225	Bruno-Bárcena (1997), Bruno-Bárcena *et al.* (1999), Gonçalves *et al.* (1992), Ragout *et al.* (1995)
	Beads	Sintered glass	60–300	55–60	2.4	Krischke *et al.* (1991), Gonçalves *et al.* (1992)
Rings	Raschig	Sintered glass	60–100	60		Gonçalves *et al.* (1992)
Bi86	Irregular particles	Ceramic	22	70	3.21	Gonçalves *et al.* (1992)
Plastic carbon support (PCS)	Disk	Polypropilene and organic[b]				Cotton *et al.* (2001), Demirci *et al.* (2003), Ho *et al.* (1997), Velazquez *et al.* (2001)
Polyurethane	Foam		Not reticulated	91		Bruno-Bárcena (1997)
Cotton fibers			Not reticulated			Silva and Yang (1995)

[a] Dennert Shaumglass GmbH, 8439 Postbauer-Heng, Gewerbebiet Ost, FRG.
[b] 50% (w/w) polypropylene, 35% (w/w) ground soybean hulls, 5% (w/w) yeast extract, 5% (w/w) soybean flour, and 5% (w/w) bovine albumin.

B. Natural cell attachment

Cell adhesion and adsorption is common in natural systems, though strains and species differ in their ability to adhere to surfaces. Adsorption through electrostatic interaction to solid supports can be achieved by treating either the microbial cells or the support matrix with cations (Thonart *et al.*, 1982). Also, adsorption on inert supports allows bacteria to form biofilms, although the properties of the attachment surface do impact biofilm formation. For example, rough surfaces can enhance biofilm formation because of increased surface area for cells to attach and decreased shear forces near the surface. Shear forces will also be low within pores of porous material, providing a protective environment for cells to attach and grow. Hydrophobicity and ionic charge of the surface material also increase biofilm formation. Numerous studies using continuous processes and diverse cellular supports have focused on increasing adhesion properties of the support matrix. Such adhesive properties can also be varied to create a more functional three-dimensional structure for greater ability to control cell concentration and the mass-transfer properties in the reactor. One method used for increasing biofilm reactor productivity is to increase the support attachment surface area by growing biofilms on porous support materials or plastic composite supports. An earlier report studied a PCS packed-bed biofilm reactor for lactic acid production from rich media and polypropylene chips blended with various agricultural materials as support for biofilms with pure and mixed cultures (Demirci and Pometo, 1995). It was theorized that the agricultural material blended in the with polypropylene forming the PCS probably stimulated biofilm formation on the support surface by serving as a carbon and/or nitrogen source, increasing adsorption of the microorganism to the surface or creating a favorable surface energy.

C. Free and adhered biomass

Since the complex biology of biofilm formation tends to vary among organisms, of greatest concern is the possibility of cell attachment fluctuations due to the dynamic nature of biofilms. For this reason, long-term studies must be carried out with each particular strain to evaluate its benefit to the process. Estimates of free and adhered biomass should be evaluated at the end of assays. Table 5.3 shows that the percentages of free cells with respect to total cell number in Poraver®- and polyurethane-filled reactors for strains RS93 and ADNOX95 performed at two dilution rates. The values for Poraver-filled reactors were 5.8% for strain RS93 at $D = 0.3\ h^{-1}$ and 3.18% at $D = 0.55\ h^{-1}$. For strain ADNOX95, the values were 4.87% at $D = 0.3\ h^{-1}$ and 3.36% at $D = 0.5\ h^{-1}$. In the case of the polyurethane-filled reactors, the percentages were 2.29% at $D = 0.3\ h^{-1}$

TABLE 5.3 Biomass values for planktonic and sessile cells in two up-flow packed-bed reactors inoculated with two biofilm forming-*Lactobacillus* strains

	Planktonic cells (g l^{-1})		Sessile cells (g l^{-1})
Strain	$D = 0.3\ h^{-1}$	$D = 0.55\ h^{-1}$	Final
Reactor filled with Poraver®			
RS93	4.0	2.2	69.1
ADNOX95	4.2	2.9	86.2
Reactor filled with polyurethane foam			
RS93	4.0	2.9	174
ADNOX95	4.9	3.3	174

Values are the means of at least two independent determinations. Free biomass was measured by dry weight determination: Cells were centrifuged at 5000 × g for 10 min, washed with distilled water, and dried at 105 °C. The immobilized biomass was determined by weight differences of a measured volume of the matrix dried at 105 and 550 °C.

and 1.66% at $D = 0.55\ h^{-1}$ for strain RS93; in the case of strain ADNOX95, the percentages were 2.81% at $D = 0.3\ h^{-1}$ and 1.9% at $D = 0.5\ h^{-1}$. Adhered biomass in polyurethane-filled reactors was 174 g l^{-1} for both strains and there were no significant differences between the two strains in the case of Poraver®-filled reactors. Poraver® beads and polyurethane foam supports showed adsorption after 7 days of incubation and continued to improve with time, indicated by the decrease in the percentage of free cells, even with decreasing feed rates. Cell adhesion to both supports was very high (as shown by the sessile/planktonic ratio), indicating that the production kinetics of the system was primarily controlled by the sessile cells in both packed reactors. It is important to consider that, due to the substantial structural differences between the supports, the performance of the cells attached to Poraver® was substantially enhanced compared to those attached to polyurethane foam. The same behavior in specific productivity reduction could be obtained by decreasing the Poraver® bead size, which resulted in higher biomass accumulation. Therefore, very small bead sizes (<200 μm) can become a double-edged sword (Gonçalves *et al.*, 1992). The reason for this phenomenon is that at a given dilution rate the velocity of media or ascensional velocity increases as the bead size decreases due to the reduced active volume or the space between the biomass-covered beads. This increase in velocity can result in preferential flow paths, higher biomass sheering, lower assimilation of nutrients and, consequently, lower volumetric product formation.

VI. CULTIVATION MEDIA

Nutrient availability in the culture medium can obviously affect the specific growth rate and impact biofilm formation, thereby altering substrate conversion and productivity (Aeschlimann and von Stockar, 1990). Homolactic bacteria are demanding in terms of their nutritional requirements; consequently, a great number of the lactic acid fermentation processes have been conducted with nutrient-rich media which favor biofilm generation. The high cost of rich media is of particular concern for moving lactic acid production to industrial levels when considering downstream processing and production separations. In order to reduce downstream processing to a minimum, the preferred compound choice should be feedstock low in nitrogen, low effluent cell mass production, and negligible amounts of residual substrate or other biological products (Córdoba *et al.*, 1999; Raya-Tonetti *et al.*, 1999; Senthuran *et al.*, 2004). Nitrogen sources used in lactic acid fermentation include steep liquor, malt sprout extract, casein hydrolysate, whey permeates, and yeast extract. The most common effective media supplement has traditionally been yeast extract; however, yeast extract is expensive and, when its concentration exceeds 1% in the medium, the optical purity of lactic acid in the fermented broth can be reduced by the D(–)-lactic acid inherently found in yeast extract (Bruno-Bárcena *et al.*, 1998, 1999). Previous studies in chemostat carried out for media optimization showed that *L. casei* subsp. *casei* CRL 686 could result in the same biomass yields in medium BRFS as in MRS (Bruno-Bárcena *et al.*, 1998). Growth of the strain RS93 was compared in BRFS and MRS media using the R3 reactor design, (Fig. 5.2) filled with Poraver® beads. Maximal productivity values were comparable to those obtained by Ragout *et al.* (1995), 8.7 and 14.9 $g\,l^{-1}h^{-1}$, using GS medium (Guoqiang *et al.*, 1992) (Fig. 5.3). Similar tendencies were observed in volumetric productivity with both culture media at similar dilution rates, demonstrating that both media are suitable for growth and production of biofilms. The simplicity of medium BFRS makes it more than adequate for downstream processing (Córdoba *et al.*, 1999; Raya-Tonetti *et al.*, 1999), and its low cost makes BFRS medium more cost effective for the continuous production of lactic acid.

Another feedstock for lactic acid production of particular interest is whey, a byproduct from cheese production. Lactose (4–5%) is the major component of whey solids in addition to minerals, proteins, and water-soluble vitamins (Marwaha and Kennedy, 1988; Tuli *et al.*, 1985). Whey permeate, along with added supplements, can provide the complex nutrients demanded by *L. casei* (Table 5.2). However, *L. casei* cells in batch fermentation are unable to utilize untreated or unsupplemented whey,

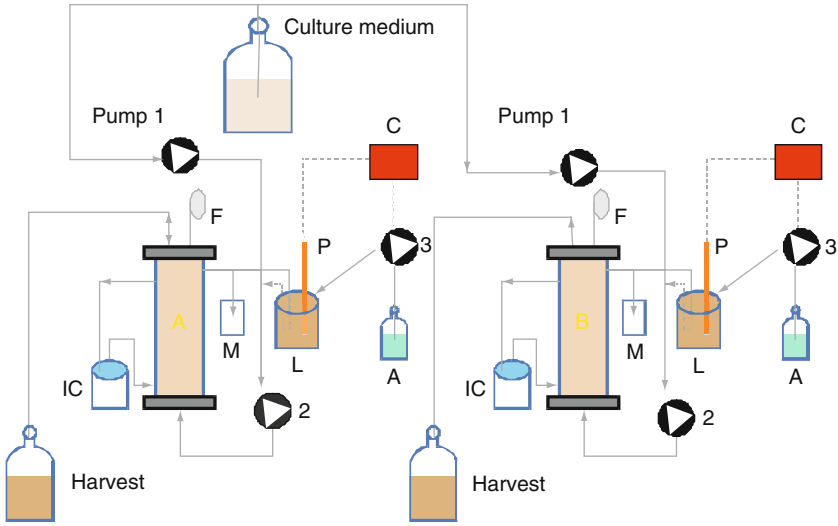

FIGURE 5.2 Schematic diagram of two up-flow packed-bed reactors (R3). A, alkali; 1, feed pump for complete medium; 2, recycling pump; 3, alkali pump; C, pH controller; F, air filter; IC, heat exchanger; L, external pH controller device; M, sampling port; R, reactor; P, pH electrode.

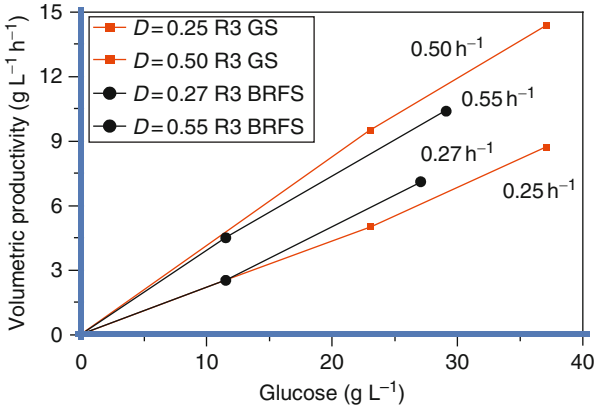

FIGURE 5.3 Volumetric productivities as a function of glucose concentration of *L. rhamnosus* RS93, at two dilution rates in different culture media using Poraver® as support and (R3) reactor design. In each case, the reactors were inoculated with 6% (v/v) of an overnight culture.

leading to poor productivity and incomplete sugar utilization. Alternatively, whey hydrolysates can serve as an inexpensive nitrogen base and carbon source. Nevertheless, pretreatment of whey with protease or supplementation contributes to the overall cost of lactic acid production and is not desirable for large-scale industrial processes. Lactic acid fermentation in unsupplemented whey medium has been reported for lactic acid bacteria. *L. helveticus* immobilized to a continuous fibrous bed reactor resulted in productivity of 5 g l^{-1} h^{-1} with total lactose conversion in unsupplemented acid whey; productivity was further improved by supplementing with yeast extract, indicating that substrate utilization was incomplete (Krischke *et al.*, 1991; Senthuran *et al.*, 1997; Silva and Yang, 1995). Media components were also used to investigate the performance of immobilized *L. rhamnosus* on a sintered glass support in a continuous recycle tubular reactor at different substrate concentrations. The observed volumetric productivity increased when the substrate concentration was raised from 50 to 100 g l^{-1} while complete conversion occurred only when 50 g l^{-1} of glucose or very low dilution rates (>0.1 h^{-1}) were used (Gonçalves *et al.*, 1992). Bear in mind that industrial processes require high substrate conversion rates because unused carbon sources such as glucose can complicate extraction and final purification of lactic acid.

VII. BIOFILM APPARATUS AND OPERATION

The popularity of lactic acid production over the past two decades has led to the development of a number of different reactor configurations designed especially to improve volumetric productivity. Reactor productivity is directly correlated with the reaction rate, which can be improved by increasing cell biomass to a point where volumetric productivity remains positively correlated to high substrate utilization. In this context, high cell concentrations are achieved by adsorption to supports naturally, without chemicals or artificial entrapment. Biofilm reactors allow continuous fermentation by providing a faster flow of fresh media to the cells, eliminating nutrient limitations, and increasing cell surface/volume ratios. Compared to conventional free cell systems, biofilm reactors show improved productivity, simplify separation of cells from products, and operate at high dilution rates without cell washout. Likewise, biofilm reactors are extremely adequate for microaerophilic or anaerobic processes though there is a loss in stability in processes where gas generation occurs. Important parameters considered in reactor designs have been volumetric productivity, cell attachment, and biofilm stability. The media compositions, cell adsorption supports, and microorganisms have been important components in studying new reactor designs.

A number of biofilm reactor configurations have been tested for lactic acid production including batch reactors (BRs), continuous-stirred tank rectors (CSTRs), fluidized-bed reactors (FBRs), and packed-bed reactors (PBRs).

Batch biofilm reactors are not rationally used for industrial fermentation procedures since nutrients are provided by emptying and refilling the reactor rather than by continuous flow, increasing downtime and reducing productivity. However, batch reactors have been used to quickly evaluate new conditions before moving to other reactor designs. The performances of repeated batch fermentations were evaluated with and without polypropylene composite supports (PCS) consisting of polypropylene, soybean hulls, soybean flour, yeast extract, dried bovine albumin, and mineral salts. In repeated immobilized batch cultures, PCS were shown to perform better for L-lactic acid production than polypropylene alone. In those experiments, cultures of *Streptomyces viridosporus* T7A ATCC 39115 formed a biofilm that was utilized to entrap *Lactobacillus casei* subsp. *rhamnosus* ATCC 11443 (Demirci and Pometo, 1995). Suspended culture and repeated fed-batch cultures with PCS biofilm were used to evaluate control of yeast contamination with nystatin (Velazquez *et al.*, 2001). Chemical mutagenesis was used to develop enhanced strains of *Lactobacillus* with faster growth rates and higher product yields in various media modifications in batch fermentations and continuous fermentations (Demirci and Pometo, 1992).

CSTRs attempt to achieve perfect mixing of the reactor contents with more efficient control of the temperature and pH than in high-density systems. Unlike the PBR, the support cannot be packed into the bioreactor; however, fibrous types of bed supports can be used for adsorption of cells. This system is well suited for reactions in which substrate inhibition is problematic and stable productivity is crucial. Examples of continuous biofilm reactors used to study lactic acid production include the evaluation of PCS tubes to improve the growth of *L. casei* (Cotton *et al.*, 2001). This type of reactor was used with PCS tubes fixed to the agitator shaft to favor biofilm generation, whereas the biofilm thickness on the PCS tubes was controlled by the agitation speed. More recently, two reactor systems composed of a stirred-tank bioreactor coupled to a packed-bed biofilm column operating in continuous mode were used to develop a functional biofilm of *L. delbrueckii* (Rangaswamy and Ramakrishna, 2008).

The *PBR* is most commonly used for lactic acid fermentation. The support can be readily packed into a column and the feed can be moved across the bed of adhered cells. The substrates are usually fed from the bottom and the product is collected from the top of the reactor. The R3 reactor has been evaluated for long-term activity and enhanced tolerance to toxins and these characteristics were used to evaluate the production of lactic acid and performance using foam glass beads (Poraver®) and

polyurethane foam (Fig. 5.2). This type of reactor design has low contamination potential, operational simplicity, and low cost. Examples of PBRs include the two-stage, two-stream immobilized upflow PBR system used to obtain high productivity and high lactic acid concentrations. This operational system keeps production costs down by using a simplified medium while maintaining overall yeast extract concentration at 5 g l^{-1} (Bruno-Bárcena *et al.*, 1999).

In *FBRs* the biofilm surrounding the adsorbent particles are kept in motion by a continuous flow of the substrate, offering good solid–fluid mixing with minimal pressure drops. Biofilm surrounding the adsorbent particles also allows long operation times compared to PBRs and CSTRs. Unlike PBRs, the media is recycled and less biofilm formation and blockage is observed. The use of FBRs allows the testing and use of feed without pretreatment. For example, FBRs and CSTRs were used to evaluate culture media consisting of whey permeate and various supplements, which enabled exponential growth of *L. casei* (Krischke *et al.*, 1991).

A. Comparison between productivities of *L. rhamnosus* cells immobilized through natural adhesion to different supports in an identical reactor design

Figure 5.2 provides an example of reactor configurations applied to biofilm lactic acid production processes in the form of two immobilized PBRs operated in parallel (R3 reactor). As an example of operational similarity, lactic acid production by natural biofilm systems using strains from different origins have been summarized in Table 5.4. The parallel reactors A and B shown in Fig. 5.2 were inoculated with *L. casei* RS93 and *L. casei* ADNOX95, respectively. Those homofermentative adherent variants were previously obtained from *L. casei* subsp. *casei* CRL 686 and *L. rhamnosus* DSM 20021, respectively. Reactors were run in parallel for each strain and support type used. The recirculation rate was adjusted to a 50:1 ratio to ensure that pH levels are maintained and nutrient gradients do not develop inside the reactors. The dilution rate was increased stepwise to test different steady states. After a month of operation at the highest rate, the initial dilution rate was reset to check the system's stability. This series of assays analyzed the ability of the strains to adhere to a support and to produce lactic acid (considering kinetic and yield parameters) (Table 5.1). For reactors filled with Poraver®, the results showed that glucose conversions ranged from 61.1% to 100% in the reactor inoculated with strain RS93 and between 85% and 96.8% when using strain ADNOX95. Similar yields were obtained with both strains. Strains RS93 and ADNOX95 showed similar productivity results though strain ADNOX95 presented a slightly higher value (11.9 g $l^{-1}h^{-1}$ for $D = 0.55$ h^{-1}) associated with a higher conversion rate. At the highest

TABLE 5.4 Continuous fermentation at 42 °C using BFRS medium with two adhesive *Lactobacillus* strains in different supports

Strains	*L. rhamnosus* RS93				*L. casei* ADNOX95			
Dilution rate (h^{-1})	$Y_{p/s}$[a] (%)	Glucose used (%)	Productivity ($g\ l^{-1}h^{-1}$)	OP (%)	$Y_{p/s}$ (%)	Glucose used (%)	Productivity ($g\ l^{-1}\ h^{-1}$)	OP (%)
Poraver®								
0.30	91.4	95.3	7.1	85	91.9	95.4	8.3	88
0.36	87.0	100	8.3	86	85.5	96.8	7.8	82
0.40	100	63.2	8.1	86	100	72.2	8.1	83
0.48	86.0	77.9	10.3	86	100	88.3	10.7	89
0.55	83.0	61.1	10.4	87	88.0	85.0	11.9	88
0.70	89.7	31.9	7.4	86	98.0	37.3	8.4	86
Polyurethane-foam								
0.30	96.4	74.2	7.7	91	97.1	84	7.1	88
0.36	79.9	91.8	9.1	93	81.1	81.2	8.9	91
0.40	96.7	71.4	9.2	91	97.9	87.8	11.3	91
0.48	100.0	48.6	8.3	84	80.0	44.2	4.7	87
0.55	98.0	46.3	7.7	85	94.1	41	5.1	89

[a] Yield as lactic acid ($g\ l^{-1}$) per used glucose ($g\ l^{-1}$).

dilution rate ($D = 0.70\ h^{-1}$) tested, both strains showed reduced glucose consumption and lactic acid production. On the other hand, strain ADNOX95 showed more efficient glucose conversion at $D = 0.55\ h^{-1}$, though no significant differences were found in productivity. The results for reactors filled with polyurethane foam are shown in Table 5.4. Maximal productivity values were obtained at $D = 0.40\ h^{-1}$, 9.2 g $l^{-1}h^{-1}$ for strain RS93 and 11.3 g $l^{-1}h^{-1}$ for strain ADNOX95. Strain ADNOX95 was also more efficient at converting glucose than with RS93. However, at a dilution rate of 0.55 h^{-1} glucose consumption and productivity decreased significantly, with final product yields in the range of 94–98%. The polyurethane support accumulated more biomass (174 g l^{-1} active volume) than Poraver®, though the Poraver®-filled reactor resulted in increased productivity (11.9 g l^{-1} h^{-1}) using 27 g l^{-1} initial glucose concentration. Biofilms that adhered to polyurethane and Poraver® supports proved to be very effective and suitable for lactic acid production. Among the two strains tested, Poraver® performed better than polyurethane in its effectiveness for the production of lactic acid.

B. Comparison between productivities of *L. rhamnosus* cells immobilized with polyethyleneimine (PEI) or by natural adhesion in different reactor designs

In the R3 reactor shown in Fig. 5.2, the medium flows through the bottom of the reactor and goes out through the top with continuous recirculation at a constant ascensional velocity (1.5 cm min^{-1}). This design permits the elimination of the planktonic biomass, and the generated shear eliminates weakly adhered biomass fragments. A steady state between the adhered self-proliferating microorganisms and the pieces of biofilm that break off due to shear and continuous recycling of the medium inside the reactor is generated. This balance allows management of recycling rate, residence time, and optimal addition of nutrients for easier and more practical control of the process. The R3 biofilm reactor with Poraver® is designed to increase cell density, productivity, and yield for continuous lactic acid fermentations over long periods. These bioreactors can be employed to economically produce lactic acid and can be operated for months or even years, reducing tear-down and reassembly costs. The geometry of Poraver® achieves spatial control over biofilm development by naturally controlling biofilm thickness in addition to an established positive effect on cell density, production rates, and yields.

With the purpose of illustrating the relationship between different reactor designs filled with Poraver®, the volumetric productivity with respect to initial concentration of glucose in each assay was analyzed. The results obtained by Guoqiang *et al*. (1992) using *L. rhamnosus* DSM 20021 immobilized with PEI are compared with those obtained by

Ragout *et al*. (1995) using the adhesive offspring strain *L. rhamnosus* RS93 growing in identical culture media (Fig. 5.4). The productivity of the strain immobilized with PEI reached 2 g l^{-1} h^{-1} at a dilution rate of 0.25 h^{-1}, with an initial glucose concentration of 30 g l^{-1}, and at $D = 0.5$ h^{-1} the productivity reached 3.3 g l^{-1} h^{-1} at the same sugar concentration.

The adhesive variant RS93 grown in a PBR (R2), differing from R3 by holding a larger recirculation circuit, exhibits productivities with a direct relationship to the initial glucose concentration at the different dilution rates assayed (Fig. 5.4). Operating the R3 with a smaller recirculation circuit (Fig. 5.2) showed better performance than R2, and productivities were even larger under the same conditions (14.9 g l^{-1} h^{-1}, $D = 0.5$ h^{-1} and 37 g l^{-1} initial glucose) (Bruno-Bárcena, 1997). These results demonstrate that the reactor using the biofilm-forming strain shows enhanced performance over systems using chemically induced adhesion, given that productivity values are larger at the same initial glucose concentration. The results also indicate that minimizing recirculation volumes allows for more efficient cell biotransformation supposedly by increasing the cells' contact time with media components.

VIII. LACTIC ACID VOLUMETRIC PRODUCTIVITY VERSUS CONCENTRATION

Compared with completely mixed systems where homogeneous substrate concentration could be assumed, in immobilized cell reactors the substrate concentration on the biofilm surface is not identical to the concentration in the mobile phase, and consequently mass transfer events

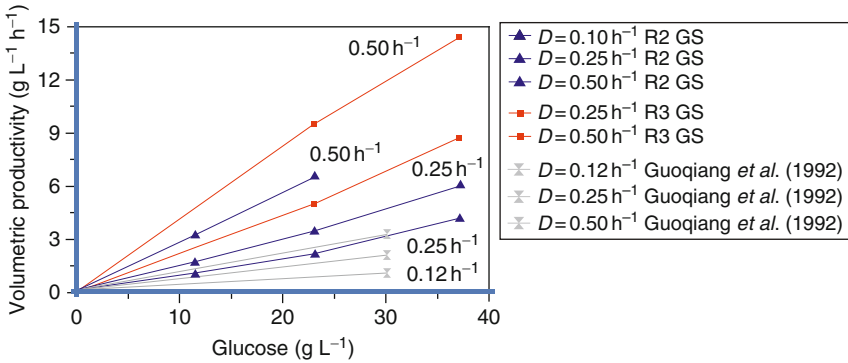

FIGURE 5.4 Productivities obtained by different authors with different reactor designs and methods of immobilization using a microorganism of the same origin and identical culture medium.

can occur on the biofilm surface even if the general environmental conditions in liquid phase may not be favorable. Compared to a fully agitated reactor, the biomass is denser in the biofilm where distance is minimal facilitating accelerated conversion rates. In the differentiated biofilm, with naturally adhered cells, there is continuous replacement of biomass allowing for constant regeneration of the biofilm along the operating time, resulting in long periods of stable performance. Regeneration is achieved by operating the system in such a way that optimal mixing of the inflow feed (new and recirculation currents) is ensured, thus allowing for real steady-state values of product yield accompanied of high substrate conversions and high product concentration. Kinetic and yield parameters for lactic acid production by different operational systems have been summarized in Table 5.5.

Productivity is often used to correlate or compare lactic acid production between diverse processes. Achieving high lactic acid concentrations inversely affects productivity, since product and substrate inhibition simultaneously act to drive the production values downward. Therefore, as lactic acid builds up in the broth, the rate of carbon utilization is reduced which forces a proportional reduction in the dilution rates in order to maintain high volumetric concentrations (Bruno-Bárcena *et al.*, 1999; Senthuran *et al.*, 2004).

Dilution rates in continuous systems can also influence the adherence of a microorganism, consequently altering productivity and yields. Higher dilution rates and increased agitation have resulted in increased suspended EPS, while production rates increased, and percent yields can be adversely affected in FBRs (Krischke *et al.*, 1991) and PCS continuous reactors (Cotton *et al.*, 2001). The effectiveness of using PCS tubes has been tested in continuous lactic acid fermentation where biofilm thickness is controlled by agitation. The production rate, yield, and cell density of a reactor with PCS tubes was compared to those a reactor with polypropylene tubes at increasing dilution rates. At a dilution rate of 0.4 h^{-1} the PCS tube biofilm reactor demonstrated productivity of 5.08 and 8.95 g l^{-1} h^{-1} with yields of 68.89% and 70.7%, while the polypropylene control reactor showed productivity of 5.75 g l^{-1} h^{-1} and 69.55% yield. At double the dilution rate, productivity of the PCS biofilm reactor increased slightly to 9.88 g $l^{-1}h^{-1}$; however, percentage yields dropped to 52.38% and 58.61% (Cotton *et al.*, 2001). Other studies have also noticed that high productivity appears to be coupled to incomplete use of substrate leading to lower conversion and decreased yields. Reduced yields were reported for higher dilution rates when continuous fermentations in stirred-tank and FBRs with sintered glass beads were compared. In the stirred reactor, 100% substrate conversion at 0.22 h^{-1} dilution rate could be obtained. At 0.4 h^{-1} dilution rate in the FBR, productivity of 10 g l^{-1} h^{-1} with 93% yield could be obtained, while further increasing the dilution rate to

TABLE 5.5 Comparison between different systems used for lactic acid production as function medium enrichment coefficients

System	Nitrogen source	Sugar	Sugar utilization (%)	Lactic acid ($g\ l^{-1}$)	Lactic acid productivity ($g\ l^{-1}\ h^{-1}$)	Productivity/ nitrogen source[a]	Organism	Reference
Batch								
Repeated batch Biofilm reactors	Y extract, 10 $g\ l^{-1}$	Glucose 80 $g\ l^{-1}$	89	55	0.75	0.075	*Streptomices viridospurus L. casei*	Demirci and Pometo (1995)
Immobilized alginate (batch)	Y extract, 10 $g\ l^{-1}$	Glucose 30 $g\ l^{-1}$	99.2	25	1.60	0.160	*L. casei*	Guoqiang *et al.* (1991)
Continuous								
Chemostat	Y extract, 5 $g\ l^{-1}$; whey retenate 50 $g\ l^{-1}$	Lactose 40 $g\ l^{-1}$	100	33	5.5 ($D = 0.22\ h^{-1}$)	0.100	*L. casei*	Krischke *et al.* (1991)
Chemostat	Y extract, 30 $g\ l^{-1}$	Glucose 40 $g\ l^{-1}$	70	29	14.43 ($D = 0.467\ h^{-1}$)	0.481	*L. casei*	González-Vara *et al.* (1996)
Single chemostat	Y extract, 10 $g\ l^{-1}$	Glucose 22 $g\ l^{-1}$	100	18.6	3.2 ($D = 0.17\ h^{-1}$)	0.320	*L. casei*	Bruno-Bárcena *et al.* (1999)
Single chemostat	Y extract, 10 $g\ l^{-1}$; whey permeate 60 $g\ l^{-1}$	Lactose 45 $g\ l^{-1}$[b]	51[b]	20.6[b]	8.27 ($D = 0.4\ h^{-1}$)	0.118	*L. helveticus*	Aeschlimann *et al.* (1990)

Two chemostats	Overall Y extract 5 g l^{-1}	Glucose 71 g l^{-1}	100	48.5	2.42 (D = 0.06 h^{-1})[c]	0.480	*L. casei*	Bruno-Bárcena *et al.* (1999)
Two chemostats	Y extract 10 g l^{-1}; whey permeate 60 g l^{-1}	Lactose 45 g l^{-1}[b]	59[b]	18.2[b]	7.64 (D = 0.42 h^{-1})	0.109	*L. helveticus*	Aeschlimann *et al.* (1990)
Fluidized bed	Y extract 5 g l^{-1}; whey retenate 50 g l^{-1}	Lactose 40 g l^{-1}	50	13	13.5 (D = 1.0 h^{-1})	0.245	*L. casei*	Krischke *et al.* (1991)
Immobilized stirred tank	Y extract 10 g l^{-1}	Glucose 30 g l^{-1}	99.2[b]	[b]28	5.2 (D = 0.18 h^{-1})	0.520	*L. casei*	Guoqiang *et al.* (1992)
Packed bed	Y extract 10 g l^{-1}	Glucose 12 g l^{-1}	90[b]	9.5[b]	1.17 (D = 0.11 h^{-1})[c]	0.120	*L. casei*	Guoqiang *et al.* (1992)
Single packed bed	Y extract 10 g l^{-1}	Glucose 26 g l^{-1}	96.8	22	7.8 (D = 0.36 h^{-1})	0.780	*L. casei*	Bruno-Bárcena *et al.* (1999)
Two packed beds	Overall Y extract 5 g l^{-1}	Glucose 92 g l^{-1} Glucose 95 g l^{-1}	89.5 58.7	57.6 37.4	5.76 (D = 0.15 h^{-1})[c] 9.72 (D = 0.40 h^{-1})	1.150 1.940	*L. casei*	Bruno-Bárcena *et al.* (1999)
Packed bed	Y extract, 15 g l^{-1}	Glucose 100 g l^{-1}	75[b]	51.4[b]	20.1 (D = 0.39 h^{-1})	1.300	*L. delbrueckii*	Gonçalves *et al.* (1992)

(*continued*)

TABLE 5.5 (*continued*)

System	Nitrogen source	Sugar	Sugar utilization (%)	Lactic acid (g l^{-1})	Lactic acid productivity (g l^{-1} h^{-1})	Productivity/ nitrogen source[a]	Organism	Reference
Repeated batch Biofilm reactor	Y extract 8 g l^{-1} plus PCS	Glucose 100 g l^{-1}		60	4.26	0.540[d]	*L. casei*	Ho *et al.* (1997)
Repeated fed batch fermentation	Y extract 7 g l^{-1} plus PCS	Glucose 80 g l^{-1}		146	4.2	0.600[d]	*L. casei.*	Velazquez *et al.* (2001)
Continuous stirred tank bioreactor	Y extract 5 g l^{-1} plus PCS	Glucose 40 g l^{-1}	70.7	12.34	8.95 ($D = 0.4$ h^{-1})	N/D[d]	*L. casei*	Cotton *et al.* (2001)
Continuous fibrous bed immobilized cell bioreactor system	Acid whey plus PCS Not reported	Lactose 86.2 g l^{-1}	76	50.8	4.8	N/D[d]	*L. helveticus*	Silva and Yang (1995)
Stirred-tank reactor coupled to a packed-bed biofilm column	Not reported	Molasses (10% sugar)	90–95	60	5 ($D = 0.0833$ h^{-1})	N/D[d]	*L. delbrueckii*	Rangaswamy and Ramakrishna (2008)

[a] Medium enrichment coefficients (MEC). Calculated utilizing nitrogenous source evaluated from data of methodology in reference cited.
[b] Values obtained from published results.
[c] Values of productivity corresponding to the highest sugar conversion.
[d] Total nitrogen source not reported.

1.0 h^{-1} produced higher productivity of 13.5 g l^{-1} h^{-1}, the yield dropped to 50% (Krischke *et al.*, 1991).

A satisfactory agreement between dilution rates and experimental productivity predictions must be demonstrated since high concentrations of lactic acid could be achieved only with high sugar conversion at the expense of reducing lactic acid volumetric productivity. Higher dilution rates can result in changes in the carbon flow in *Lactobacillus*. Moreover, maintenance of the glycolytic activity in non-growing, immobilized cells can lead to increases in lactic acid concentration and reduction in the amount of nitrogen source needed, generating lower amounts of impurities than single-state process and lowering the quantity of cell mass for disposal. Immobilization supports for microbial cells have been tested to reduce or eliminate inhibition caused by high concentrations of substrate or product and also enhance productivity. PCS-containing biofilm reactors have shown minimal lag phase, increased cell tolerance to high glucose concentration, increased cell density, reduced requirement for micronutrients, and higher lactic acid production rates (Ho *et al.*, 1997; Velazquez *et al.*, 2001). The performance of PCS was characterized in suspended-cell bioreactors and repeated fed-batch biofilm lactic acid fermentations containing *L. casei* in the presence and absence of the antibiotic nystatin for controlling yeast contamination while optimizing yeast extract and glucose concentrations. Fed-batch reactors containing PCS supports demonstrated productivity of 2.45 g l^{-1} h^{-1}; however, lactic acid productivities and glucose consumption rate decreased with each glucose pulse (Velazquez *et al.*, 2001). The reduction in lactic acid productivity following each glucose pulse was thought to be caused by a dilution of the yeast extract concentration, by addition of ammonium hydroxide to control pH, or by increased lactic acid concentration (Gonçalves *et al.*, 1991; Velazquez *et al.*, 2001). Otherwise, repeated fed-batch fermentation containing PCS operated more efficiently than suspended-cell bioreactors by requiring less yeast extract to produce up to 146 g l^{-1} of lactic acid with 7 g of yeast extract (Velazquez *et al.*, 2001). Ho *et al.*, 1997 studied lactic acid production from three bioreactors containing PCS and compared the data to those in a bioreactor with suspended cells as a control. They found PCS bioreactors shortened the lag time up to sixfold, increased productivity from 2.78 g l^{-1} h^{-1} in the control to 3.26 g l^{-1} h^{-1} in the PCS bioreactors, and required reduced complex nutrient addition by lowering yeast extract in the medium and increasing starting glucose concentration. However, inhibition of substrate utilization by high starting glucose concentrations was observed, as also reported by Gonçalves *et al.* (1992). Results for typical lactic acid percentage yield for *L. casei* are between 70% and 72% (Cotton *et al.*, 2001; Ho *et al.*, 1997). Yields below 69% are thought to represent a physiological shift to overproduction of EPS and a reduction in lactic acid production (Cotton *et al.*, 2001; Ho *et al.*, 1997).

The values shown in Table 5.5 allow comparisons between datasets from lactic acid production processes under optimal conditions between reports in the literature, highlighting the uppermost lactate (g l^{-1}) producing condition within each study.

A. How much will cells pay for a good nitrogen source?

Theoretically, adding more yeast extract should increase biomass leading to higher volumetric lactic acid produced. However, yeast extract is a high-priced commodity and is major factor in costly lactic acid fermentations. Since yeast extract is a major expenditure, an unbiased method for comparing the efficiency of lactic acid production for diverse bioreactor operating conditions was accomplished by calculating productivity from a given amount of nitrogen source (productivity/gram nitrogen source), designated as medium enrichment coefficient (MEC) (Table 5.5). Scanning the lactic acid concentration and MEC values, it is clear that the naturally immobilized systems yielded lactic acid concentrations that parallel with productivity values when the results are analyzed in terms of the amount nitrogen source added. The amount of nitrogen source supplied for two-stage systems, chemostat, and PBRs is accompanied by substantially high substrate consumption and lactate concentration, and comparable with the high concentration values reported. However, many of the continuous fermentations with very high reported productivities were usually accomplished by adding high amounts yeast extract, reducing the benefits by escalating fermentation costs. Naturally immobilized PBRs and CSTRs produced the highest MEC values, while covalently immobilized or entrapped cells produced low MEC values and are comparable to batch and chemostat processes. Early kinetic studies on lactose utilization in acidogenic biofilms suggested that immobilization changes the physiological properties of the microorganisms resulting in decreased substrate utilization compared to free cells. This decrease in substrate utilization may be due to decreased cell surface area for substrate consumption and considerable internal mass transfer resistance inside the biofilm in addition to differences in apparent substrate affinity of the adsorbed cells (Jeffrey and Paul, 1986; Yu and Pinder, 1993).

Biofilm bioreactor designs that minimize diffusion limitations and inhibition by substrate, thereby improving productivity in reduced nitrogen media components, have been implemented (R3 design reactor Fig. 5.2) (Bruno-Bárcena, 1997; Bruno-Bárcena *et al.*, 1999) and tested in a two-stage, two-stream immobilized up-flow Poraver® PBRs with two mixed feed stock streams. The design predictions were in good agreement with the data reported. The results suggest that yeast extract concentrations can be maintained at low levels while still achieving high productivity and high lactic acid concentrations with no significant amount of

free cells, as compared to productivity obtained from nonadherent free cells. By using reactors operating in cascade for the two-stage, two-stream immobilized up-flow PBR, the overall nitrogen source can be reduced and simple medium recipes could be still simplified even further reducing downstream processing costs by the reduction in impurities.

IX. CONCLUSIONS

The advantages of microbial production of lactic acid over chemical synthesis from petroleum-based products are utilization of renewable carbon sources and the ability to mainly produce the L- or D-isomer of lactic acid. To make fermentation cost-competitive with chemical synthesis, improvements have been made that decrease production costs while increasing lactic acid productivity and product concentration. Production rates have been enhanced by increasing cell densities using various supports and advancing natural biofilm adsorption by strain development in addition to augmenting existing bioreactor designs.

Conventional artificial methods for cell immobilization involved cross-linking or entrapment within polymers. However, these artificial immobilization methods require additional intricate preparation steps, lack a universally applicable technology, limited mass transfer through the immobilization matrix, and reduced viability of the entrapped organism. Natural immobilization offers the best possibility for continuous fermentation that significantly increases product output and thus reduces cost when compared to artificial cell immobilization systems. Biofilms naturally adapt to their own matrix and show long-term viability as well as enhanced tolerance to toxins, allowing for continuous processing. Product inhibition continues to be a bottleneck in lactic acid fermentation processes, and has been addressed with bioreactor design modifications such as cell recycling thereby increasing productivity. Future modifications may also include developments in product removal in conjunction with the fermentation process. Consequently, industrial demand for technologies ensuring microbial stability remains strong, since high cell survival rather than constant replenishment continues to be economically important.

A comparison between reactor designs, organisms, and support matrices employed during the past two decades was presented. Numerous studies using continuous processes and various cellular supports with the aim of increasing cell concentration in the reactor have been researched. Ultimately, understanding the relationships between the support, strain, and productivity will allow for a more systematic tailoring of the process. It is clear that increases in cell density vastly improve reactor volumetric productivity, and further improvements should focus on

increasing specific cell productivity. As a final point, we would like to highlight that the use of naturally adherent strains in an adequate reactor design resulted in the highest efficiency reported, reinforcing the era that first began by examining longer operational times and high cell densities through constant biomass regeneration of naturally adherent microorganisms.

ACKNOWLEDGMENTS

This work was made possible by the generous support from the N.C. State University College of Agriculture and Life Sciences Agriculture Research Service, UNESCO, Consejo Nacional de Investigaciones Científicas y Técnicas (Argentina), and Agencia Española de Cooperación Internacional (AECI), Spain.

REFERENCES

Aeschlimann, A., and von Stockar, U. (1990). The effect of yeast extract supplementation on the production of lactic acid from whey permeate by *Lactobacillus helveticus*. *Appl. Microbiol. Biotechnol.* **32,** 398–402.

Aeschlimann, A., and Vonstockar, U. (1991). Continuous production of lactic acid from whey permeate by *Lactobacillus helveticus* in a cell recycle reactor. *Enzyme Microb. Technol.* **13,** 811–816.

Aeschlimann, A., Di Stasi, l., and von Stockar, U. (1990). Continuous production of lactic acid from whey permeate by *Lactobacillus helveticus* in two chemostats in series. *Enzyme Microb. Technol.* **12,** 926–932.

Altermann, E., Russell, W. M., Azcarate-Peril, M. A., Barrangou, R., Buck, B. L., McAuliffe, O., Souther, N., Dobson, A., Duong, T., Callanan, M., Lick, S., Hamrick, A., *et al.*, (2005). Complete genome sequence of the probiotic lactic acid bacterium *Lactobacillus acidophilus* NCFM. *Proc. Natl. Acad. Sci. USA* **102,** 3906–3912.

Anderson, G. G., and O'toole, G. A. (2008). Innate and induced resistance mechanisms of bacterial biofilms. *Curr. Top. Microbiol. Immunol.* **322,** 85–105.

Annachhatre, A. P., and Bhamidimarri, S. M. (1992). Microbial attachment and growth in fixed-film reactors: Process startup considerations. *Biotechnol. Adv.* **10,** 69–91.

Audet, P., Paquin, C., and Lacroix, C. (1988). Immobilized growing lactic acid bacteria with k-carrageenan—locust bean gum gel. *Appl. Microbiol. Biotechnol.* **29,** 11–18.

Avnir, D., Coradin, T., Lev, O., and Livage, J. (2006). Recent bio-applications of sol-gel materials. *J. Materials Chem.* **16,** 1013–1030.

Azcarate-Peril, M. A., Altermann, E., Goh, Y. J., Tallon, R., Sanozky-Dawes, R. B., Pfeiler, E. A., O'Flaherty, S., Buck, B. L., Dobson, A., Duong, T., Miller, M. J., Barrangou, R., and Klaenhammer, T. R. (2008). Analysis of the genome sequence of *Lactobacillus gasseri* ATCC 33323 reveals the molecular basis of an autochthonous intestinal organism. *Appl. Environ. Microbiol.* **74,** 4610–4625.

Beyenal, H., and Lewandowski, Z. (2001). Mass-transport dynamics, activity, and structure of sulfate-reducing biofilms. *AIChE J.* **47,** 1689–1697.

Bhowmik, T., and Steele, J. L. (1994). Cloning, characterization and insertional inactivation of the *Lactobacillus helveticus* D(−) lactate dehydrogenase gene. *Appl. Microbiol. Biotechnol.* **41,** 432–439.

Boyaval, P., and Goulet, J. (1988). Optimal conditions for production of lactic acid from cheese whey permeate by Ca-alginate-entrapped *Lactobacillus helveticus*. *Enzyme Microb. Technol.* **10,** 725–728.

Brady, R. A., Leid, J. G., Calhoun, J. H., Costerton, J. W., and Shirtliff, M. E. (2008). Osteomyelitis and the role of biofilms in chronic infection. *FEMS Immunol. Med. Microbiol.* **52,** 13–22.

Branda, S. S., Vik, S., Friedman, L., and Kolter, R. (2005). Biofilms: The matrix revisited. *Trends Microbiol.* **13,** 20–26.

Bruno-Bárcena, J. M. (1997). Production of L(+) lactic acid by selected lactic acid bacteria. Facultad de Ciencias Naturales e Instituto Miguel Lillo, Universidad Nacional de Tucuman, Argentina.

Bruno-Bárcena, J. M., Ragout, A., and Siñeriz, F. (1998). Microbial physiology applied to process optimisation: Lactic acid bacteria. *In* ''Advances in Bioprocess Engineering II'' (E. Galindo and O. T. Ramirez, Eds.), pp. 97–110. Kluwer Academic Publishers, Netherlands.

Bruno-Bárcena, J. M., Ragout, A., Córdoba, P., and Siñeriz, F. (1999). Continuous production of L(+)-lactic acid by *Lactobacillus casei* in two-stage systems. *Appl. Microbiol. Biotechnol.* **51,** 316–324.

Bruno-Bárcena, J. M., Ragout, A. L., Cordoba, P. R., and Siñeriz, F. (2001). Reactor configuration for fermentation in immobilized continuous system. *In* ''Food Microbiology Protocols'' (J. F. T. Spencer and A. L. Ragout de Spencer, Eds.), Humana press, Totowa, NJ.

Bryers, J. D. (2008). Medical biofilms. *Biotechnol. Bioeng.* **100,** 1–18.

Buck, B. L., Azcarate-Peril, M. A., and Klaenhammer, T. R. (2009). Role of autoinducer-2 on the adhesion ability of *Lactobacillus acidophilus*. *J. Appl. Microbiol.* **107,** 269–279.

Cassidy, M. B., Lee, H., and Trevors, J. T. (1996). Environmental applications of immobilized microbial cells: A review. *J. Ind. Microbiol.* **16,** 79–101.

Cho, H. Y., Yousef, A. E., and Yang, S. T. (1996). Continuous production of pediocin by immobilized *Pediococcus acidilactici* P02 in a packed-bed bioreactor. *Appl. Microbiol. Biotechnol.* **45,** 589–594.

Cinquin, C., Le Blay, G., Fliss, I., and Lacroix, C. (2004). Immobilization of infant fecal microbiota and utilization in an *in vitro* colonic fermentation model. *Microb. Ecol.* **48,** 128–138.

Córdoba, P., Raya-Tonetti, G., Siñeriz, F., and Perotti, N. (1999). Purification of lactic acid from fermentation using a resin in a fluidized bed reactor. *Latin Am. Appl. Res.* **29,** 31–34.

Costerton, J. W., Lewandowski, Z., Caldwell, D. E., Korber, D. R., and Lappin-Scott, H. M. (1995). Microbial biofilms. *Annu. Rev. Microbiol.* **49,** 711–745.

Costerton, J. W., Stewart, P. S., and Greenberg, E. P. (1999). Bacterial biofilms: A common cause of persistent infections. *Science* **284,** 1318–1322.

Cotton, J. C., Pometto, A. L., III, and Gvozdenovic-Jeremic, J. (2001). Continuous lactic acid fermentation using a plastic composite support biofilm reactor. *Appl. Microbiol. Biotechnol.* **57,** 626–630.

Crueger, W., and Crueger, A. (1990). Acetic acids. *In* ''Biotechnology: A Textbook of Industrial Microbiology'' (T. D. Brock, Ed.), pp. 134–147. Science Tech.

Daniels, R., Vanderleyden, J., and Michiels, J. (2004). Quorum sensing and swarming migration in bacteria. *FEMS Microbiol. Rev.* **28,** 261–289.

Daraktchiev, R., Beschkov, V., Kolev, N., and Aleksandrova, T. (1997). Bioreactor with a semi-fixed packing: Anaerobic lactose to lactic acid fermentation. *Bioprocess Eng.* **16,** 115–117.

Davey, M. E., and O'toole, G. A. (2000). Microbial biofilms: From ecology to molecular genetics. *Microbiol. Mol. Biol. Rev.* **64,** 847–867.

Davidson, B. E., Llanos, R. M., Cancilla, M. R., Redman, N. C., and Hillier, A. J. (1995). Current research on the genetics of lactic acid production in lactic acid bacteria. *Int. Dairy J.* **5,** 763–784.

De Beer, D., and Stoodley, P. (1995). Relation between the structure of an aerobic biofilm and transport phenomena. *Water Sci. Technol.* **32,** 11–18.

De Beer, D., Stoodley, P., Roe, F., and Lewandowski, Z. (1994). Effects of biofilm structures on oxygen distribution and mass transport. *Biotechnol. Bioeng.* **43,** 1131–1138.

Delcour, J., Bernard, N., Garmyn, D., Ferain, T., and Hols, P. (1993). Génetique moléculaire des lactate-déshydrogénases des bactéries lactiques. *Lait* **73,** 127–131.

Dellaglio, F., and Torriani, S. (1985). Production of DL lactic acid by an atypic strain of *Lactobacillus bulgaricus*. *Microbiol. Aliments Nutr.* **3,** 87–90.

Demirci, A., and Pometo, Al, III (1992). Enhanced production of D(−)-lactic acid by mutants of *Lactobacillus delbrueckii* ATCC 9649. *J. Ind. Microbiol.* **11,** 23–28.

Demirci, A., and Pometo, Al., III (1995). Repeated-batch fermentation in biofilm reactors with plastic-composite supports for lactic acid production. *Appl. Microbiol. Biotechnol.* **43,** 585–589.

Demirci, A., Pometo, Al, III, and Johnson, K. E. (1993a). Lactic acid production in a mixed-culture biofilm reactor. *Appl. Environ. Microbiol.* **59,** 203–207.

Demirci, A., Pometto, A. L., and Johnson, K. E. (1993b). Evaluation of biofilm reactor solid support for mixed culture lactic acid production. *Appl. Microbiol. Biotechnol.* **38,** 728–733.

Demirci, A., Pometto, A. L., III, and Ho, K. L. (1997). Ethanol production by *Saccharomyces cerevisiae* in biofilm reactors. *J. Ind. Microbiol. Biotechnol.* **19,** 299–304.

Demirci, A., Cotton, J. C., Pometto, A. L., III, Harkins, K. R., and Hinz, P. N. (2003). Resistance of *Lactobacillus casei* in plastic-composite-support biofilm reactors during liquid membrane extraction and optimization of the lactic acid extraction system. *Biotechnol. Bioeng.* **83,** 749–759.

Dong, X. Y., Bai, S., and Sun, Y. (1996). Production of L(+)-lactic acid with *Rhizopus oryzae* immobilized in polyurethane foam cubes. *Biotechnol. Lett.* **18,** 225–228.

El-Mansi, E. M. T., and Ward, F. B. (2007). Microbiology of industrial fermentation. *In* ''Fermentation, Microbiology and Biotechnology'' (E. M. T. El-Mansi, Ed.), pp. 11–46. Taylor and Francis.

FAO/WHO (1974). Evaluation toxicologique de certains additifs alimentaires. Examens des principes generaux et des normes. Dix-septieme rapport, -du Comite Mixte F.A.O./O.M.S. d´Experts des Additifs Alimentaires. Food and Agriculture Organization of the United Nations/ World Health Organization.

Friedman, M. R., and Gaden, E. L., Jr. (1970). Growth and acid production by *Lactobacillus* (L.) *delbrueckii* in a dialysis culture system. *Biotechnol. Bioeng.* **XII,** 961–974.

Fux, C. A., Costerton, J. W., Stewart, P. S., and Stoodley, P. (2005). Survival strategies of infectious biofilms. *Trends Microbiol.* **13,** 34–40.

Garvie, E. I. (1980). Bacterial lactate dehydrogenases. *Microbiol. Rev.* **44,** 106–139.

Gawehn, K., and Bergmeyer, H. U. (1974). D-Lactate. *In* ''Methods of Enzymatic Analysis'' (H. U. Bergmeyer, Ed.), pp. 1492–1495. Academic Press, New York.

Gjaltema, A., Arts, P. A., van Loosdrecht, M. C., Kuenen, J. G., and Heijnen, J. J. (1994). Heterogeneity of biofilms in rotating annular reactors: Occurrence, structure, and consequences. *Biotechnol. Bioeng.* **44,** 194–204.

Goller, C. C., and Romeo, T. (2008). Environmental influences on biofilm development. *Curr. Top. Microbiol. Immunol.* **322,** 37–66.

Gonçalves, L. M. D., Xavier, A. M. R. B., Almeida, J. S., and Carrondo, M. J. T. (1991). Concomitant substrate and product inhibition kinetics in lactic acid production. *Enzyme Microb. Technol.* **13,** 314–319.

Gonçalves, L. M. D., Barreto, M. T. O., Xavier, A. M. R. B., Carrondo, M. J. T., and Klein, J. (1992). Inert supports for lactic acid fermentation a technological assessment. *Appl. Microbiol. Biotechnol.* **38,** 305–311.

González-Vara, A., Pinelli, D., Rossi, M., Fajner, D., Magelli, F., and Matteuzzi, D. (1996). Production of L(+) and D(−) lactic acid isomers by *Lactobacillus casei* subsp. *casei* DSM 20011 and *Lactobacillus coryniformis* subsp. *torquens* DSM 20004 in continuous fermentation. *J. Ferment. Bioeng.* **81,** 548–552.

Groboillot, A., Boadi, D. K., Poncelet, D., and Neufeld, R. J. (1994). Immobilization of cells for application in the food industry. *Crit. Rev. Biotechnol.* **14,** 75–107.

Guoqiang, D., Kaul, R., and Mattiasson, B. (1991). Evaluation of alginate-immobilized *Lactobacillus casei* for lactate production. *Appl. Microbiol. Biotechnol.* **36,** 309–314.

Guoqiang, D., Kaul, R., and Mattiasson, B. (1992). Immobilization of *Lactobacillus casei* cells to ceramic material pretreated with polyethylenimine. *Appl. Microbiol. Biotechnol.* **37,** 305–310.

Hall-Stoodley, L., Costerton, J. W., and Stoodley, P. (2004). Bacterial biofilms: From the natural environment to infectious diseases. *Nat. Rev. Microbiol.* **2,** 95–108.

Hekmat, D., Bauer, R., and Neff, V. (2007). Optimization of the microbial synthesis of dihydroxyacetone in a semi-continuous repeated-fed-batch process by in situ immobilization of *Gluconobacter oxydans*. *Process Biochem.* **42,** 71–76.

Hjörleifsdottir, S., Seevaratnam, S., Holst, O., and Mattiasson, B. (1990). Effects of complete cell recycling on product formation by *Lactobacillus case* ssp. *rhamnosus* in continuous cultures. *Curr. Microbiol.* **20,** 287–292.

Ho, K. G., Pometto, A. I., Hinz, P. N., and Demirci, A. (1997). Nutrient leaching and end product accumulation in plastic composite supports for L-(+)-lactic acid biofilm fermentation. *Appl. Environ. Microbiol.* **63,** 2524–2532.

Huang, Y. L., Mann, K., Novak, J. M., and Yang, S. T. (1998). Acetic acid production from fructose by *Clostridium formicoaceticum* immobilized in a fibrous-Bed bioreactor. *Biotechnol. Prog.* **14,** 800–806.

Jeffrey, W. H., and Paul, J. H. (1986). Activity of an attached and free-living *Vibrio* sp. as measured by thymidine incorporation, p-iodonitrotetrazolium reduction, and ATP/DNA ratios. *Appl. Environ. Microbiol.* **51,** 150–156.

Karatan, E., and Watnick, P. (2009). Signals, regulatory networks, and materials that build and break bacterial biofilms. *Microbiol. Mol. Biol. Rev.* **73,** 310–347.

Kornaros, M., and Lyberatos, G. (2006). Biological treatment of wastewaters from a dye manufacturing company using a trickling filter. *J. Hazard. Mater.* **136,** 95–102.

Krischke, W., Schröder, M., and Trösch, W. (1991). Continuous poduction of L-lactic acid from whey permeate by immobilized *Lactobacillus casei* subsp. *casei*. *Appl. Microbiol. Biotechnol.* **34,** 573–578.

Kubota, H., Senda, S., Nomura, N., Tokuda, H., and Uchiyama, H. (2008). Biofilm formation by lactic acid bacteria and resistance to environmental stress. *J. Biosci. Bioeng.* **106,** 381–386.

Lacroix, C., and Yildirim, S. (2007). Fermentation technologies for the production of probiotics with high viability and functionality. *Curr. Opin. Biotechnol.* **18,** 176–183.

Lawrence, J. R., Korber, D. R., Wolfaardt, G. M., and Caldwell, D. E. (1995). Behavioral strategies of surface-colonizing bacteria. *In* ''Advances in Microbial Ecology'' (J. Gwynfryn Jones, Ed.), pp. 1–75. Plenum Press, New York.

Lazarova, V., Perera, J., Bowen, M., and Sheilds, P. (2000). Application of aerated biofilters for production of high quality water for industrial reuse in West Basin. *Water Sci. Technol.* **41,** 417–424.

Lebeer, S., De Keersmaecker, S. C. J., Verhoeven, T. L. A., Fadda, A. A., Marchal, K., and Vanderleyden, J. (2007). Functional analysis of luxS in the probiotic strain *Lactobacillus rhamnosus* GG reveals a central metabolic role important for growth and Biofilm formation. *J. Bacteriol.* **189,** 860–871.

Leewenhoeck, A. (1683). An abstract of a Letter from Mr. Anthony Leewenhoeck at Delft, Dated Sep. 17. 1683. Containing some microscopical observations, about animals in the serf of the teeth, the substance call'd worms in the nose, the cuticula consisting of scales. *Philosophical Transactions* **14,** 568–574.

Lewis, V. P., and Yang, S. T. (1992). Continuous propionic acid fermentation by immobilized *Propionibacterium acidipropionici*in a novel packed-bed bioreactor. *Biotechnol. Bioeng.* **40,** 465–474.

Li, X. Z., Hauer, B., and Rosche, B. (2007). Single-species microbial biofilm screening for industrial applications. *Appl. Microbiol. Biotechnol.* **76,** 1255–1262.

Linko, P., and Linko, Y. Y. (1984). Industrial applications of immobilized cells. *Crit. Rev. Biotechnol.* **1,** 289–338.

Lipinsky, E. S. (1981). Chemicals form biomass: Petrochemical substitution options. *Science* **212,** 1465–1471.

Little, B. J., and Wagner, P. A. (1997). Spatial relationships between bacteria and mineral surfaces. *In* ''Geomicrobiology: Interactions between microbes and minerals'' (J. F. Banfield and K. H. Nealson, Eds.), pp. 125–167. Mineralogical Society of America, Washington, DC.

Macfarlane, S., McBain, A. J., and Macfarlane, G. T. (1997). Consequences of biofilm and sessile growth in the large intestine. *Adv. Dent. Res.* **11,** 59–68.

Majumder, P. S., and Gupta, S. K. (2003). Hybrid reactor for priority pollutant nitrobenzene removal. *Water Res.* **37,** 4331–4336.

Marwaha, S. S., and Kennedy, J. F. (1988). Whey—Pollution problem and potential utilization. *Int. J. Food Sci. Technol.* **23,** 323–336.

Nicolella, C., van Loosdrecht, M. C., and Heijnen, J. J. (2000). Wastewater treatment with particulate biofilm reactors. *J. Biotechnol.* **80,** 1–33.

Norton, S., and Vuillemard, J. C. (1994). Food bioconversions and metabolite production using immobilized cell technology. *Crit. Rev. Biotechnol.* **14,** 193–224.

Ohleyer, E., Wilke, Ch.R., and Blanch, H. W. (1985). Continuous production of lactic acid from glucose and lactose in a cell-recycle reactor. *Appl. Biochem. Biotechnol.* **11,** 457–463.

Orla-Jensen, S. (1919). The lactic acid bacteria, Andr. Fred. Host and Son, KGL. Hof-Boghandel Ejnar Munksgaard, Copenhagen.

O'Toole, G., Kaplan, H. B., and Kolter, R. (2000). Biofilm formation as microbial development. *Annu. Rev. Microbiol.* **54,** 49–79.

Pedraza, R. O., Motok, J., Salazar, S. M., Ragout, A., Mentel, M. I., Tortora, M. L., Guerrero-Molina, M. F., Winik, B. C., and Díaz-Ricci, J. C. (2009). Growth-promotion of strawberry plants inoculated with *Azospirillum brasilense*. *World J. Microbiol. Biotechnol.* 10.1007/s11274-009-0169-110.

Probert, H. M., and Gibson, G. R. (2002). Bacterial biofilms in the human gastrointestinal tract. *Curr. Issues Intest. Microbiol.* **3,** 23–27.

Qureshi, N., Karcher, P., Cotta, M., and Blaschek, H. P. (2004). High-productivity continuous biofilm reactor for butanol production: Effect of acetate, butyrate, and corn steep liquor on bioreactor performance. *Appl. Biochem. Biotechnol.* **113–116,** 713–721.

Qureshi, N., Annous, B. A., Ezeji, T. C., Karcher, P., and Maddox, I. S. (2005). Biofilm reactors for industrial bioconversion processes: Employing potential of enhanced reaction rates. *Microb. Cell Fact.* **4,** 24.

Ragout, A., PescedeRuizHolgado, A., Oliver, G., and Siñeriz, F. (1989). Presence of an L(+)-lactate dehydrogenase in cells of *Lactobacillus delbrueckii* ssp. *Biochemie* 36–42.

Ragout, A., Cordoba, P., Bruno-Bárcena, J. M., Siñeriz, F., Kaul, R., and Mattiasson, B. (1995). Lactic acid fermentation by *Lactobacillus casei* RS 93 grown on inert supports in up-flow reactors. (R. M. Buitelaar, H. S. Wessels, C. Bucke and J. Tramper, Eds.), Proceedings of the International Symposium of Immobilized Cell Basics and Applications.

Ragout, A., Siñeriz, F., Kaul, R., Guoqiang, D., and Mattiasson, B. (1996). Selection of an adhesive pehnotype of *Streptococcus salivarius* subsp. *thermophilus* for use in fixed-bed reactors. *Appl. Microbiol. Biotechnol.* **46,** 126–131.

Rangaswamy, V., and Ramakrishna, S. V. (2008). Lactic acid production by *Lactobacillus delbrueckii* in a dual reactor system using packed bed biofilm reactor. *Lett. Appl. Microbiol.* **46,** 661–666.

Raya-Tonetti, G., Cordoba, P., Bruno-Barcena, J., Sineriz, F., and Perotti, N. (1999). Fluidized bed ion exchange for improving purification of lactic acid from fermentation. *Biotechnol. Tech.* **13,** 201–205.

Rincones, J., Zeidler, A. F., Grassi, M. C. B., Carazzolle, M. F., and Pereira, G. A. G. (2009). The golden bridge for nature: The new biology applied to bioplastics. *Polymer Rev.* **49,** 85–106.

Rodionov, D. A., Vitreschak, A. G., Mironov, A. A., and Gelfand, M. S. (2004). Comparative genomics of the methionine metabolism in Gram-positive bacteria: A variety of regulatory systems. *Nucleic Acid Res.* **32,** 3340–3353.

Roy, D., Goulet, J., and Leduy, A. (1987). Continuous production of lactic acid from whey permeate by free and calcium alginate entrapped *Lactobacillus helveticus*. *J. Dairy Sci.* **70,** 506–513.

Salter, G. J., and Kell, D. B. (1991). New materials and technology for cell immobilization. *Curr. Opin. Biotechnol.* **2,** 385–389.

Senthuran, A., Senthuran, V., Mattiasson, B., and Kaul, R. (1997). Lactic acid fermentation in a recycle batch reactor using immobilied *Lactobacillus casei*. *Biotechnol. Bioeng.* **55,** 841–853.

Senthuran, A., Senthuran, V., Hatti-Kaul, R., and Mattiasson, B. (2004). Lactate production in an integrated process configuration: Reducing cell adsorption by shielding of adsorbent. *Appl. Microbiol. Biotechnol.* **65,** 658–663.

Silva, E. M., and Yang, S. T. (1995). Kinetics and stability of a fibrous bed bioreactor for continuous production of lactic acid from unsupplemented acid whey. *J. Biotechnol.* **41,** 59–70.

Smidsrod, O., and Skjakbraek, G. (1990). Alginate as immobilization matrix for cells. *Trends Biotechnol.* **8,** 71–78.

Spormann, A. M. (2008). Physiology of microbes in biofilms. *Curr. Top. Microbiol. Immunol.* **322,** 17–36.

Steinberger, R. E., and Holden, P. A. (2004). Macromolecular composition of unsaturated *Pseudomonas aeruginosa* biofilms with time and carbon source. *Biofilms* **1,** 37–47.

Stewart, P. S., and Franklin, M. J. (2008). Physiological heterogeneity in biofilms. *Nat. Rev. Microbiol.* **6,** 199–210.

Stoodley, P., Cargo, R., Rupp, C. J., Wilson, S., and Klapper, I. (2002). Biofilm material properties as related to shear-induced deformation and detachment phenomena. *J. Ind. Microbiol. Biotechnol.* **29,** 361–367.

Sutherland, I. (2001). Biofilm exopolysaccharides: A strong and sticky framework. *Microbiology* **147,** 3–9.

Taguchi, H., and Ohta, T. (1999). D-Lactate dehydrogenase is a member of the D-isomer-specific 2-hydroxyacid dehydrogenase family. *J. Biol. Chem.* **266,** 12588–12594.

Tanka, A., and Kawamoto, T. (1999). Cell and Enzyme Immobilization. American Society for Microbiology, Washington: 94.

Thonart, P., Custinne, M., and Paquot, M. (1982). Zeta potential of yeast-cells—Application in cell immobilization. *Enzyme Microb. Technol.* **4,** 191–194.

Tsai, S. P., and Moon, S. H. (1998). An integrated bioconversion process for production of L-lactic acid from starchy potato feedstocks. *Appl. Biochem. Biotechnol.* **70–2,** 417–428.

Tuli, A., Sethi, R. P., Khanna, P. K., Marwaha, S. S., and Kennedy, J. F. (1985). Lactic acid production from whey permeate by immobilized *Lactobacillus casei*. *Enzyme Microb. Technol.* **7,** 164–168.

Velazquez, A. C., Pometto, A. L., III, Ho, K. L., and Demirci, A. (2001). Evaluation of plastic-composite supports in repeated fed-batch biofilm lactic acid fermentation by *Lactobacillus casei*. *Appl. Microbiol. Biotechnol.* **55,** 434–441.

Vick Roy, T. B., Blanch, H. W., and Wilke, Ch.R. (1982). Lactic acid production by *Lactobacillus delbreuckii* in a hollow fiber fermenter. *Biotechnol. Lett.* **4,** 483–488.

Vick Roy, T. B., Mandel, D. K., Dea, D. K., Blanch, H. W., and Wilke, Ch.R. (1983). The application of cell recycle to continuous fermentative lactic acid production. *Biotechnol. Lett.* **5,** 665–670.

VickRoy, T. B. (1985). Lactic acid. *In* ''Comprehensive Biotechnology'' (M. Moo Young, Ed.), pp. 761–775. Pergamon Press, Oxford.

Wang, Z. W., and Chen, S. (2009). Potential of biofilm-based biofuel production. *Appl. Microbiol. Biotechnol.* **83,** 1–18.

Werner, E., Roe, F., Bugnicourt, A., Franklin, M. J., Heydorn, A., Molin, S., Pitts, B., and Stewart, P. S. (2004). Stratified growth in *Pseudomonas aeruginosa* biofilms. *Appl. Environ. Microbiol.* **70,** 6188–6196.

Xia, L., Chung, Y. K., Yang, S. T., and Yousef, A. E. (2005). Continuous nisin production in laboratory media and whey permeate by immobilized *Lactococcus lactis*. *Process Biochem.* **40,** 13–24.

Xu, K. D., Stewart, P. S., Xia, F., Huang, C. T., and McFeters, G. A. (1998). Spatial physiological heterogeneity in *Pseudomonas aeruginosa* biofilm is determined by oxygen availability. *Appl. Environ. Microbiol.* **64,** 4035–4039.

Yu, J., and Pinder, K. L. (1993). Intrinsic fermentation kinetics of lactose in acidogenic biofilms. *Biotechnol. Bioeng.* **41,** 479–488.

CHAPTER 6

Microbial Fingerprinting using Matrix-Assisted Laser Desorption Ionization Time-Of-Flight Mass Spectrometry (MALDI-TOF MS): Applications and Challenges

R. Giebel,[*] C. Worden,[*] S. M. Rust,[†] G. T. Kleinheinz,[*] M. Robbins,[‡] and T. R. Sandrin[†,1]

Contents

[*] Department of Biology and Microbiology, University of Wisconsin Oshkosh, Halsey Science Center, Oshkosh, Wisconsin, USA
[†] Division of Mathematical and Natural Sciences, Arizona State University, Phoenix, Arizona, USA
[‡] Department of Chemistry, The University of Tennessee, Knoxville, Tennessee, USA
[1] Corresponding author: Division of Mathematical and Natural Sciences, Arizona State University, Phoenix, Arizona, USA; e-mail address: Todd.Sandrin@asu.edu

Advances in Applied Microbiology, Volume 71
ISSN 0065-2164, DOI: 10.1016/S0065-2164(10)71006-6

Abstract

Recent threats posed by pathogenic microorganisms in food, recreational waters, and as agents of bioterror have underscored the need for the development of more rapid, accurate, and cost-effective methods of microbial characterization and identification. This chapter focuses on the use of matrix-assisted laser desorption ionization time-of-flight mass spectrometry (MALDI-TOF MS) to rapidly characterize and identify microorganisms through generation of characteristic fingerprints of intact cells. While most efforts have focused on bacteria, this technology has also been applied to fungi and viruses. Results of most studies suggest that MALDI-TOF MS can be used to rapidly and accurately characterize microorganisms. A variety of quantitative approaches have been employed in the analysis of MALDI-TOF MS fingerprints of microorganisms. The reproducibility of fingerprints of intact cells remains a primary concern and limitation associated with this approach. Protocols and instrumentation used have varied considerably and likely account for much of the variability in reproducibility reported. Key first steps to overcoming this limitation will be the development of standard approaches to quantifying reproducibility and the development of standard protocols for sample preparation and analysis.

I. INTRODUCTION

A. Need for a rapid and accurate tool to identify microorganisms

A number of events can result in human exposure to pathogenic microorganisms, microbial toxins, or even microbiological weapons. These events can be local, such as fecal contamination of recreational waters, which can expose people coming in contact with contaminated water to viruses (e.g., rotavirus, enteroviruses, and norovirus), protozoans (e.g., *Giardia* and *Cryptosporidium*), and bacteria (e.g., *Campylobacter*, *Salmonella*, *Shigella*, and *Vibrio cholerae*) (Geldreich, 1996; Kleinheinz *et al.*, 2003). These events can also occur on a large scale, such as contamination of food (e.g., the contamination of spinach with *Escherichia coli* in 2006), or threats of bioterrorism (e.g., the discovery of letters containing *Bacillus anthracis* spores that were delivered through the U.S. Mail in 2001).

No matter how large the threat to public safety, there is a need in each of these events to rapidly identify the microorganisms as well as the source of those microorganisms to reduce public health risks.

A variety of phenotypic (e.g., antibiotic resistance testing) and genotypic (e.g., ribotyping, pulsed-field gel electrophoresis (PFGE), repetitive sequence-based polymerase chain reaction (e.g., rep-PCR), 16S rDNA analysis) methods have been used to identify and fingerprint bacteria. Although these methods offer a relatively high rate of correct classification, there are drawbacks to these tools. First, for proper identification of unknown bacteria, particularly when using some genotypic tools, it is necessary to create a large database or library of isolates from known sources from varying geographic regions and times (Meays *et al.*, 2004; Stewart *et al.*, 2003). Also, both genetic and phenotypic tools can be costly to perform, are labor intensive, involve complex methods, and require days to complete (Meays *et al.*, 2004). The limitations of these methods underscore the need for the development of a more rapid, simple, and cost-effective method for bacterial source tracking (BST), particularly when public safety becomes an issue.

B. Characteristics of an ideal method

An ideal identification method should possess a number of characteristics. First, the method should be accurate. For many currently utilized phenotypic and genotypic methods, rates of correct classification of bacterial isolates according to their respective environmental sources have been relatively high. Average rates of correct source assignment using antibiotic sensitivity testing have ranged from 62% to 98%, depending on how bacterial isolates were classified (Hagedorn *et al.*, 1999; Harwood *et al.*, 2000; Parveen *et al.*, 1997; Wiggins, 1996; Wiggins *et al.*, 1999). Using ribotyping to identify bacterial isolates has allowed for correct identification rates ranging from 49% to 97% (Carson *et al.*, 2001; Parveen *et al.*, 1997). Studies utilizing rep-PCR for BST have shown conflicting data. Dombek *et al.* (2000) and Carson *et al.* (2003) have reported rates of correct classification by source ranging from 78% to 100%, but Holloway (2001) reported no significant grouping of either *E. coli* or *Enterococcus faecalis* isolates by source.

An ideal method of characterizing microbes should be rapid. Many methods for bacterial fingerprinting and identification are time intensive, often requiring days to complete (Meays *et al.*, 2004), because of the need to isolate, culture, and process bacterial samples using the desired method (e.g., antibiotic resistance testing, ribotyping, PCR). During severe threats to public safety and health, a method that would require only hours or minutes to complete may be required to mitigate significant harm to public health.

Finally, an ideal method of identifying microorganisms should be inexpensive, since utilization of a method for public health and safety applications would likely require large numbers of microorganisms to be identified. Currently utilized methods, especially genotypic methods, often require the use of expensive reagents, equipment, and data analysis software. Another factor that increases the expense of utilizing certain methods for identification of microorganisms is the cost of labor since many of these methods are time intensive.

C. Matrix-assisted laser desorption ionization time-of-flight mass spectrometry (MALDI-TOF MS)

1. Overview of technology

One tool that may have potential as a rapid, cost-effective, and simple method for microbial fingerprinting is mass spectrometry-based microbial fingerprinting. Mass spectrometry has been used for decades in chemistry, but it was not until 1975, in a pioneering study by Anhalt and Fenselau (1975), that its use in the general application of characterizing bacteria was proposed. In their study, Anhalt and Fenselau (1975) used pyrolysis, in which heat breaks a sample into smaller molecules, combined with mass spectrometry to analyze phospholipids and ubiquinones extracted from lyophilized bacteria. Using this approach, they observed that extracts from bacteria of not only different genera but also of different species produced unique mass spectra. Following this study, others explored the use of a variety of other mass spectrometry techniques, such as fast-atom bombardment and electrospray ionization (Ruelle *et al.*, 2004).

The use of MALDI-TOF MS was first proposed by Karas *et al.* (1987). The general concept behind MALDI-TOF MS is fairly simple: when ions of different mass and charge are exposed to an applied electric field and allowed to travel down a region of given length, they will travel that length in a time period that is dependent upon their mass and charge (Lennon, 1997). A sample is mixed with a matrix, which results in the crystallization of the sample within the matrix. The sample/matrix mixture is loaded into the mass spectrometer, where it is bombarded with a UV laser (Fig. 6.1). The matrix absorbs energy from the laser and the sample becomes vaporized, releasing ions of various sizes. The ions pass through accelerating grids and travel down a flight tube, with smaller ions travelling faster than larger ions. When the ions reach the end of the flight tube they strike a detector. The time of flight required to strike the detector is used to calculate the masses of the ions. The information gathered following the ions hitting the detector is used to create a mass spectrum (Fig. 6.2), which conveys not only the masses (m) and charges (z) of the ions, but also the number of ions of a particular size that struck the

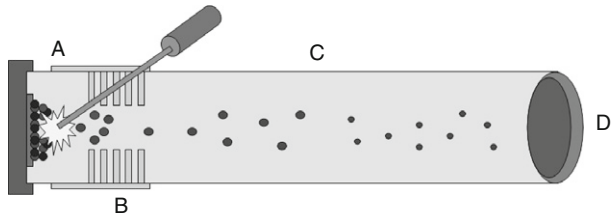

FIGURE 6.1 Schematic of MALDI-TOF MS. The sample/matrix mixture is irradiated with a UV laser (A). The matrix absorbs energy from the UV laser, causing the sample to become vaporized, forming ions. The ions pass through acceleration grids (B). The ions travel down a flight tube, with smaller ions travelling faster than larger ions (C). Once the ions reach the end of the flight tube, the ions strike a detector (D), which allows calculation of the masses of the ions based upon the time they take to travel the length of the flight tube.

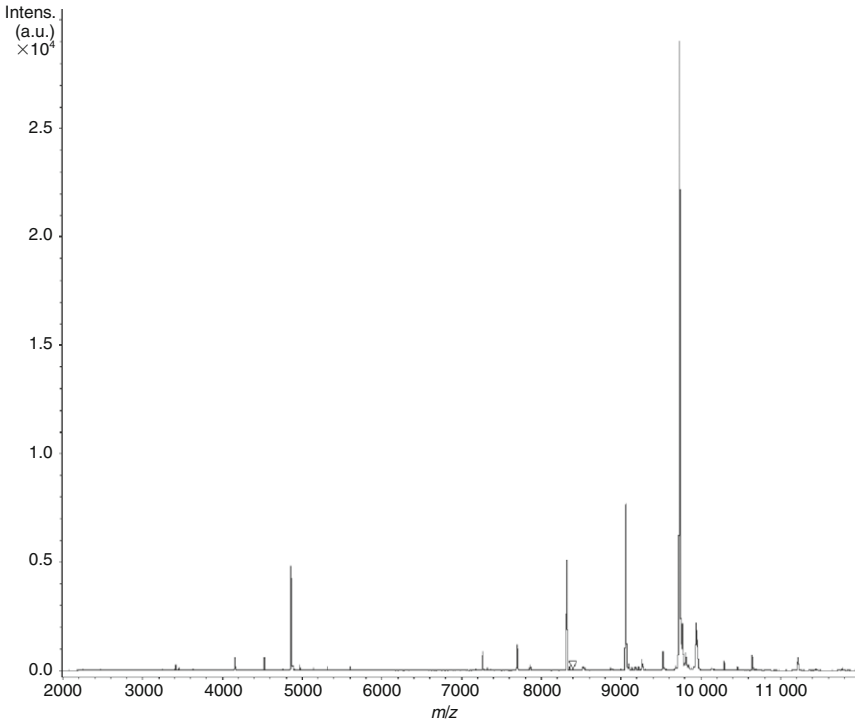

FIGURE 6.2 Information gathered when ions strike the detector is used to create a mass spectrum. The mass/charge (*m*/*z*) of the ions corresponds to the size and charge of the ions hitting the detector. The intensity corresponds to the number of particles of a particular *m*/*z* that struck the detector.

detector (intensity). Mass spectra typically report m/z values on the x-axis, and MALDI typically produces singly charged ($z = 1$) ions.

2. Overview of application

Two general approaches have been employed when using MALDI-TOF MS to characterize microorganisms: (1) fingerprinting of intact microorganisms and (2) bioinformatics-enabled approaches. In the first approach, intact cells are used to generate unique spectra (i.e., a ''fingerprint'') that can be compared with previously collected fingerprints. In many cases, these fingerprints are compared with previously assembled (and, in some cases, commercially available) libraries. This approach is relatively simple, because it is possible to use minimally processed intact cells. In general, an isolated microorganism is cultured on an agar-based medium or in liquid broth. Intact cells of the microorganism are then mixed with a matrix solution and placed onto a sample plate. Once dry, the sample is analyzed via MALDI-TOF MS. Spectra contain peaks (typically ranging from 0 to 20 kDa) that constitute a fingerprint. Peaks have been reported to represent biological molecules, including proteins, that reside in or on the outer surface of the microorganism, although some peaks may represent biological molecules of intracellular or cytoplasmic origin (Conway *et al.*, 2001; Dalluge, 2000; Evason *et al.*, 2001). The appearance of these unique proteins has been ascribed to the expression of genomic differences in bacteria at the genus, species, and strain level (Alberts *et al.*, 1994; Wang *et al.*, 1998).

In the second approach, masses associated with an unknown microorganism may be identified by comparison with masses of proteins in protein databases (Demirev *et al.*, 1999). Once a mass has been identified with statistical confidence, the identity of the microorganism can be inferred readily. More advanced mass spectrometry-based technologies (e.g., tandem MS-MS) can be used to more effectively identify proteins by fragmenting masses within the mass spectrometer (i.e., a top-down approach) (e.g., Fagerquist *et al.*, 2009). Alternatively, microbial proteins can be fragmented enzymatically (often using trypsin) prior to mass spectrometric analysis (i.e., a bottom-up approach) (e.g., Pribil and Fenselau, 2005).

While the bioinformatics approach does not require libraries of fingerprints and may be more reproducible than use of fingerprints of intact microorganisms, it requires that microorganisms of interest have at least partially sequenced genomes. While an ever-increasing number of microbial genome sequences are available, many environments contain microbial inhabitants without sequenced genomes. Thus, the utility of the bioinformatics approach may be limited in many settings. In addition, effective within-mass spectrometer fragmentation requires mass spectrometers with expensive MS-MS capabilities. This review focuses on the use of the fingerprinting of intact microorganisms for microbial

characterization via MALDI-TOF MS. An excellent review of use of additional mass spectrometry-based technologies and the bioinformatics approach to microbial characterization is available (Demirev and Fenselau, 2008a).

II. APPLICATIONS

MALDI-TOF MS has been used to characterize a wide variety of microorganisms, including bacteria, fungi, and viruses (Table 6.1). The majority of applications have been developed for bacteria.

A. Bacteria

One of the first studies to utilize MALDI-TOF MS to differentiate microorganisms relied upon extraction of water-soluble proteins (Cain *et al.*, 1994). The approach allowed differentiation of several Gram-negative and Gram-positive bacteria. While this method of analysis was useful, more rapid methods of sample preparation were later used. Holland *et al.* (1996) proposed the use of intact bacterial cells for analysis rather than bacterial extracts. In this study, bacterial colonies were removed from agar plates, mixed with a matrix solution, and placed directly onto the MALDI sample plate/target. Using mass spectra gathered from intact bacterial cells, Holland *et al.* (1996) were able not only to identify strains of *Enterobacter cloacae*, *Proteus mirabilis*, *Shigella flexneri*, *E. coli*, and *Serratia marcescens* but also to differentiate between three different species of *Pseudomonas*.

Shortly after Holland *et al.* (1996) reported success in identifying bacteria using mass spectra gathered from intact cells, Claydon *et al.* (1996), as well as Krishnamurthy and Ross (1996), published findings regarding analysis of intact bacterial cells. Both studies showed that this rapid technique allowed the acquisition of mass spectra containing peaks unique to individual species and strains of both Gram-negative and Gram-positive bacteria. The studies by Holland *et al.* (1996) in conjunction with those by Claydon *et al.* (1996) and Krishnamurthy and Ross (1996) were important to the future development of techniques to analyze intact bacterial cells using MALDI-TOF MS. Not only did these studies show that analysis of intact cells was sufficient to differentiate between different species and strains of bacteria, but they also demonstrated that preparation of intact cells offered a simpler and more rapid sample preparation method in comparison to the analysis of bacterial extracts. Indeed, the vast majority of the recent myriad applications developed for identification and characterization of bacteria described subsequently in this review have relied upon analysis of intact cells.

TABLE 6.1 An overview of applications of MALDI-TOF MS to characterize bacterial, fungal, and viral microorganisms

Microorganism	Sample preparation	Matrices	Instrument	Mass ranges (Da)	Algorithm/software for identification	Reference
Bacteria						
Arthrobacter spp.	Intact cells, 0.5 mg/mL lysozyme for 30 min or 70% ethanol at 100 °C for 10 min	CHCA, DHB and SA	Bruker Reflex III	2000–20,000	Applied Maths Bionumerics 3.5 software	Vargha *et al.* (2006)
Bacillus spp.	Intact cells	FA	PerSeptive Voyager-DE RP	2000–14,000	PNNL peak extraction algorithm	Wahl *et al.* (2002)
Bacillus spp.	Intact cells	FA	Bruker Reflex II	3000–25,000	Sequest & Mascot peptide mass fingerprinting tool and NCBI database	Dickinson *et al.* (2004)
Bacillus spp.	Intact cells/spores, 80% TFA inactivation for 30 min	CHCA	Bruker Autoflex	2000–20,000	Bruker Compass 1.1 software	Lasch *et al.* (2008)
Bacillus anthracis	0.1% SDS, 0.1 mM BME treatments and sonication for 10 min	CHCA and SA	Vestec 2000	2000–16,000	NR	Krishnamurthy *et al.* (1996)
Bacillus anthracis	Intact cells, trypsin digestion, or lysozyme treatment	CHCA and CMBT	Micromass UK MALDI	1000–20,000	Microbelynx software	Liu *et al.* (2007)
Bacillus subtilis	Intact cells	CHCA, MCA and SA	Kratos Kompact MALDI IV	4000–10,000	Sequence Retrieval System module in the SwissProt/ TrEMBL database	Demirev *et al.* (1999)

Brucella melitensis	0.1% SDS, 0.1 mM BME treatments and sonication for 10 min	CHCA and SA	Vestec 2000	2000–16,000	NR	Krishnamurthy *et al.* (1996)
Burkholderia spp.	Intact cells	CHCA	Applied Biosystems 4700 Proteomics Analyzer	2000–22,000	Applied Maths BioNumerics 4.5 & Applied Biosystems Data Explorer software	Vanlaere *et al.* (2008)
Burkholderia cepacia	Intact cells, trypsin digestion, or lysozyme treatment	CHCA and CMBT	Micromass UK MALDI	1000–20,000	Microbelynx software	Liu *et al.* (2007)
Campylobacter spp.	1 min bead beating	FA	Bruker Reflex II	5000–15,000	BACMASS software	Mandrell *et al.* (2005)
Citrobacter freundii	Intact cells	CHCA	Kratos Kompact MALDI III	500–2200	NR	Claydon *et al.* (1996)
Coxiella burnetii	Intact cells treated with gamma radiation	CHCA	Applied Biosystems 4700 Proteomics Analyzer	1000–6000	Applied Biosystems Data Explorer software	Pierce *et al.* (2007)
Enterobacter cloacae	Trypsin digestion	CHCA	Shimadzu Scientific Axima CFR Plus	800–2000	Mascot peptide mass fingerprinting tool and NCBI database	Pribil and Fenselau (2005)
Enterococcus spp.	0.05 mg/mL lysozyme treatment	SA	Bruker Reflex IV	1000–10,000	Bruker FlexAnalysis & Applied Maths GelComparII software	Giebel *et al.* (2008)

(*continued*)

TABLE 6.1 (*continued*)

Microorganism	Sample preparation	Matrices	Instrument	Mass ranges (Da)	Algorithm/software for identification	Reference
Erwinia herbicola	Trypsin digestion	CHCA	Shimadzu Scientific Axima CFR Plus	800–2000	Mascot peptide mass fingerprinting tool and NCBI database	Pribil and Fenselau (2005)
Escherichia spp.	Intact cells	CHCA	Applied Biosystems Voyager DE PRO	2500–15,000	Applied Biosystems Voyager Data Explorer software	Mazzeo *et al.* (2006)
Escherichia coli	Intact cells	CHCA	Kratos Kompact MALDI III	500–2200	NR	Claydon *et al.* (1996)
Escherichia coli	Intact cells	CHCA, MCA, and SA	Kratos Kompact MALDI IV	4000–10,000	Sequence Retrieval System module in the SwissProt/ TrEMBL database	Demirev *et al.* (1999)
Escherichia coli	Intact cells	FA	PerSeptive Voyager-DE RP	2000–14,000	PNNL peak extraction algorithm	Wahl *et al.* (2002)
Escherichia coli	Trypsin digestion	CHCA	Shimadzu Scientific Axima CFR Plus	800– 2000	Mascot peptide mass fingerprinting tool and NCBI database	Pribil and Fenselau (2005)
Escherichia coli	Intact cells, trypsin digestion or lysozyme treatment	CHCA and CMBT	Micromass UK MALDI	1000–20,000	Microbelynx software	Liu *et al.* (2007)
Escherichia coli	Intact cells	SA	Bruker Reflex IV	2000– 11,000	Bruker FlexAnalysis & Bio-Rad Diversity Database software	Siegrist *et al.* (2007)

Escherichia coli	Intact cells	CHCA	Bruker Ultraflex	1800–9000	Bruker ClinProTools software	Hsieh *et al.* (2008)
Francisella tularensis	0.1% SDS, 0.1 mM BME treatments, sonication for 10 min	CHCA and SA	Vestec 2000	2000–16,000	NR	Krishnamurthy *et al.* (1996)
Haemophilus spp.	Water/acetonitrile (2:1) treatment for 1 min	SA	PerSeptive Voyager-DE	5000–20,000	NR	Haag *et al.* (1998)
Helicobacter pylori	*n*-Octyl-β-D-glucopyranoside treatment	CHCA, FA, and SA	Bruker Reflex	4000–40,000	NR	Nilsson (1999)
Klebsiella aerogenes	Intact cells	CHCA	Kratos Kompact MALDI III	500–2200	NR	Claydon *et al.* (1996)
Klebsiella pneumoniae	Intact cells	CHCA	Bruker Ultraflex	1800–9000	Bruker ClinProTools software	Hsieh *et al.* (2008)
Listeria spp.	Intact cells	CHCA	Applied Biosystems Voyager DE PRO	2500–15,000	Applied Biosystems Voyager Data Explorer software	Mazzeo *et al.* (2006)
Listeria spp.	Intact cells	CHCA and FA	Bruker Microflex LT	2000–20,000	Bruker FlexAnalysis & BioTyper software	Barbuddhe *et al.* (2008)
Mycobacterium spp.	Intact cells	CHCA	Micromass UK MALDI	500–10,000	Microbelynx software	Pignone *et al.* (2006)
Mycobacterium smegmatis	Intact cells	CHCA	Kratos Kompact MALDI III	500–2200	NR	Claydon *et al.* (1996)
Pseudomonas spp.	Intact cells	FA	PerSeptive Voyager-DE RP	2000–14,000	PNNL peak extraction algorithm	Wahl *et al.* (2002)

(*continued*)

TABLE 6.1 (*continued*)

Microorganism	Sample preparation	Matrices	Instrument	Mass ranges (Da)	Algorithm/software for identification	Reference
Pseudomonas spp.	Intact cells	CHCA	Applied Biosystems Voyager DE PRO	2500–15,000	Applied Biosystems Voyager Data Explorer software	Mazzeo *et al.* (2006)
Pseudomonas aeruginosa	Intact cells	CHCA	Bruker Ultraflex	1800–9000	Bruker ClinProTools software	Hsieh *et al.* (2008)
Salmonella spp.	Intact cells	CHCA	Applied Biosystems Voyager DE PRO	2500–15,000	Applied Biosystems Voyager Data Explorer software	Mazzeo *et al.* (2006)
Salmonella spp.	Intact cells	SA	Bruker Ultraflex II	2000–11,000	Anagnostec SARAMIS software	Dieckmann *et al.* (2008)
Salmonella enterica	Intact cells	CHCA	Bruker Ultraflex	1800–9000	Bruker ClinProTools software	Hsieh *et al.* (2008)
Salmonella typhimurium	Trypsin digestion	CHCA	Shimadzu Scientific Axima CFR Plus	800–2000	Mascot peptide mass fingerprinting tool and NCBI database	Pribil and Fenselau (2005)
Serratia marcescens	Intact cells	FA	PerSeptive Voyager-DE RP	2000–14,000	PNNL peak extraction algorithm	Wahl *et al.* (2002)
Staphylococcus spp.	Intact cells	CHCA	Kratos Kompact MALDI III	500–2200	NR	Claydon *et al.* (1996)
Staphylococcus spp.	Intact cells	DHB	Bruker Autoflex	1000–11,000	Bruker flex control software	Carbonnelle *et al.* (2007)

Staphylococcus aureus	Intact cells	CHCA and CMBT	Micromass UK MALDI	500–3500	Microbelynx software	Du *et al*. (2002)
Staphylococcus aureus	Intact cells	CMBT	Kratos Kompact MALDI II	1–100,000	In-house cluster analysis software	Jackson *et al*. (2005)
Staphylococcus aureus	Intact cells, trypsin digestion or lysozyme treatment	CHCA and CMBT	Micromass UK MALDI	1000–20,000	Microbelynx software	Liu *et al*. (2007)
Staphylococcus aureus	Intact cells	CHCA	Bruker Ultraflex	1800–9000	Bruker ClinProTools software	Hsieh *et al*. (2008)
Streptococcus sp.	Intact cells	CHCA	Bruker Ultraflex	1800–9000	Bruker ClinProTools software	Hsieh *et al*. (2008)
Yersinia spp.	Intact cells	CHCA	Applied Biosystems Voyager DE PRO	2500–15,000	Applied Biosystems Voyager Data Explorer software	Mazzeo *et al*. (2006)
Yersinia spp.	Intact cells/spores, 80% TFA inactivation for 30 min	CHCA	Bruker Autoflex	2000–20,000	Bruker Compass 1.1 software	Lasch *et al*. (2008)
Yersinia pestis	0.1% SDS, 0.1 mM BME treatments and sonication for 10 min	CHCA and SA	Vestec 2000	2000–16,000	NR	Krishnamurthy *et al*. (1996)
Yersinia pestis	Intact cells, trypsin digestion or lysozyme treatment	CHCA and CMBT	Micromass UK MALDI	1000–20,000	Microbelynx software	Liu *et al*. (2007)

(*continued*)

TABLE 6.1 (*continued*)

Microorganism	Sample preparation	Matrices	Instrument	Mass ranges (Da)	Algorithm/software for identification	Reference
Fungi						
Aspergillus spp.	Intact spores	CHCA, DHCA, and SA	PerSeptive Voyager	4000–20,000	NR	Li *et al.* (2000)
Aspergillus spp.	3 × 1 min bead beating cycles	CHCA	Bio-Rad Ciphergen PBS-IIC	5000–20,000	Bio-Rad Biomarker Wizard software	Hettick *et al.* (2008b)
Aspergillus niger	Intact cells/spores or 50% nitric acid treatment for 45 min	FA and SA	PerSeptive Voyager-DE RP	2000–18,000	NR	Valentine *et al.* (2002)
Brachiola algerae	Intact spores or bead beating	CHCA and SA	Applied Biosystems Voyager DE-STR	2000–8000	ABI Voyager Data Explorer software	Moura *et al.* (2003)
Candida spp.	70% formic acid treatment for 2 min	CHCA	Bruker Microflex LT & Biflex III	2000–20,000	Bruker FlexAnalysis & BioTyper software	Marklein *et al.* (2009)
Candida albicans	25% formic acid treatment for 5 min	SA	Kratos MALDI TOF IV	4000–20,000	Sequence Retrieval System module in the SwissProt/ TrEMBL	Amiri-Eliasi and Fenselau (2001)
Cryptococcus neoformans	70% formic acid treatment for 2 min	CHCA	Bruker Microflex LT & Biflex III	2000–20,000	Bruker FlexAnalysis & BioTyper software	Marklein *et al.* (2009)
Encephalitozoon spp.	Intact spores or bead beating	CHCA and SA	Applied Biosystems Voyager DE-STR	2000–8000	ABI Voyager Data Explorer software	Moura *et al.* (2003)

Epidermophyton floccosum	25% formic acid treatment for 5 min	SA	Kratos MALDI TOF IV	4000–20,000	Sequence Retrieval System module in the SwissProt/ TrEMBL	Amiri-Eliasi and Fenselau (2001)
Fusarium spp.	Intact spores	SA, FA, DHB, THAP, and CHCA	Kratos AXIMA-TOF & AXIMA-CFR$^+$	4000–15,000	NR	Kemptner *et al.* (2009)
Penicillium spp.	Intact spores	CMBT, DHB, HABA, and SA	Fisons Instruments TofSpec	2000–13,000	NR	Welham *et al.* (2000)
Penicillium spp.	Intact spores	DHB and SA	Bruker Biflex III	2000–8000	NR	Chen and Chen (2005)
Penicillium spp.	3 × 1 min bead beating cycles	CHCA	Bio-Rad Ciphergen PBS-IIC	5000 – 20,000	Bio-Rad Biomarker Wizard software	Hettick *et al.* (2008a)
Phanerochaete chrysosporium	Intact cells/spores or 50% nitric acid treatment for 45 min	FA and SA	PerSeptive Voyager-DE RP	2000–18,000	NR	Valentine *et al.* (2002)
Rhizopus oryzae	Intact cells/spores or 50% nitric acid treatment for 45 min	FA and SA	PerSeptive Voyager-DE RP	2000–18,000	NR	Valentine *et al.* (2002)
Saccharomyces cerevisiae	25% formic acid treatment for 5 min	SA	Kratos MALDI TOF IV	4000–20,000	Sequence Retrieval System module in the SwissProt/ TrEMBL	Amiri-Eliasi and Fenselau (2001)
Saccharomyces cerevisiae	70% formic acid treatment for 2 min	CHCA	Bruker Microflex LT & Biflex III	2000–20,000	Bruker FlexAnalysis & BioTyper software	Marklein *et al.* (2009)

(*continued*)

TABLE 6.1 (*continued*)

Microorganism	Sample preparation	Matrices	Instrument	Mass ranges (Da)	Algorithm/software for identification	Reference
Scytalidium dimidiatum	Intact spores	CMBT, DHB, HABA, and SA	Fisons Instruments TofSpec	2000–13,000	NR	Welham *et al.* (2000)
Trichoderma reesei	Intact cells/spores or 50% nitric acid treatment for 45 min	FA and SA	PerSeptive Voyager-DE RP	2000–18,000	NR	Valentine *et al.* (2002)
Trichophyton rubrum	Intact spores	CMBT, DHB, HABA, and SA	Fisons Instruments TofSpec	2000–13,000	NR	Welham *et al.* (2000)
Viruses						
Avian influenza viruses	Amplification of viral HA gene	HPA	Bruker Ultraflex I	1500–9000	NR	Michael *et al.* (2009)
Hepatitis B virus (HBV)	Amplification of RT gene	Sequenom SpectroCLEAN resin	Bruker Compact MALDI	5000–8500	Sequenom Typer Analyzer application software NR	Luan *et al.* (2009)
Hepatitis C virus (HCV)	Amplified 5′ untranslated region of HCV genome	HPA	Bruker Reflex IV	1000–10,000		Ilina *et al.* (2005)

Newcastle disease virus	2% SDS, 10 mM dithiothreitol, and AspN protease treatments	CHCA and DHAP	Bruker Reflex	1000–12,000	FAST software routine in Bruker XTOF	Lopaticki *et al.* (1998)
Norovirus	Trypsin digestion	SA	Applied Biosystems Voyager DE-STR	700–5000	Mascot peptide mass fingerprinting tool and NCBI database	Colquhoun *et al.* (2006)
Sindbis virus	0.5% *n*-Octyl glucoside and 0.5% TFA treatment	SA	Kratos Kompact MALDI IV	20,000–70,000	NR	Kim *et al.* (2001)
Sindbis virus	Trypsin digestion	CHCA	Kratos Kompact MALDI IV	1000–4000	ExPASy PeptideMass software	Yao *et al.* (2002)

Abbreviations: BME, β-mercaptoethanol; CHCA, α-cyano-4-hydroxycinnamic acid; CMBT, 5-chloro-2-mercaptobenzothiozole; DHAP, 2,6-dihydroxyacetophenone; DHB, 2,5-dihydroxybenzoic acid; DHCA, 3,4-dihydroxycinnamic acid; FA, ferulic acid; HABA, [2-(4-hydroxyphenylazo)]benzoic acid; HPA, 3-hydroxypicolinic acid; MCA, 4-methoxycinnamic acid; SA, sinapinic acid; TFA, trifluoroacetic acid; THAP, 2,4,6-trihydroxyacetophenone.

B. Fungi

Although the majority of MALDI-TOF MS applications have focused on bacteria, an increasing number of studies have utilized MALDI-TOF MS to characterize fungi. The identification of fungal groups is still largely based on examination of morphological characteristics at the micro- and macroscopic levels (Hettick *et al.*, 2008b). One of the first studies that utilized MALDI to characterize fungi was performed by Welham *et al.* (2000). Various species of *Penicillium*, as well as *Scytalidum dimidiatum* and *Trichophyton rubrum* were characterized in this study.

As with bacterial applications, both cell extracts and intact cells have been analyzed. Amiri-Eliasi and Fenselau (2001) used formic acid to lyse the cell walls of *Saccharomyces cerevisiae* before analyzing the extracts. Hettick *et al.* (2008a) analyzed extracts of 12 *Penicillium* species by bead-beating conidia and hyphae. Both groups were able to differentiate between 12 species of each genus, and a biomarker at *m/z* 13,900 common to all of the *Penicillium* species was reported. Chen and Chen (2005) successfully identified six *Penicillium* strains using intact fungal spores. Hettick *et al.* (2008b) performed a study observing the extracts from 12 species of *Aspergillus* and 5 strains of *A. flavus*. All 12 species were correctly identified with 100% accuracy, but identification of the specific strains was only 95% accurate. Li *et al.* (2000) utilized intact spores to characterize different species of *Aspergillus*, including toxigenic species (i.e., *A. flavus*) and non-toxigenic species (i.e., *A. oryzae*).

Valentine *et al.* (2002) and Moura *et al.* (2003) utilized MALDI-TOF MS to characterize both fungal extracts and intact cells. Moura *et al.* (2003) correctly identified four types of microsporidia that affect humans using both fungal spores and extracts. Valentine *et al.* (2002) identified *Aspergillus niger*, *Rhizopus oryzae*, *Trichoderma reesei*, and *Phanerochaete chrysosporium* using either intact spores and hyphae or extracts. Intact cells, sonicated cells, and cells treated with acid yielded similar spectra.

Another fungal application of MALDI has been the accurate and timely identification of infectious fungi. Kemptner *et al.* (2009) characterized five *Fusarium* species, some of which produce a mycotoxin and are involved in significant crop losses and contamination of food. Marklein *et al.* (2009) used MALDI for the rapid identification of clinical yeast isolates, including *Candida*, *Cryptococcus*, *Saccharomyces*, *Trichosporon*, *Geotrichum*, *Pichia*, and *Blastoschizomyces* spp. with 92.5 % accuracy. These fungi initiate infections in immune-compromised hosts; therefore, rapid and accurate identification is necessary for treating the fungus with a species-specific antifungal.

C. Viruses

MALDI-TOF MS is less commonly used for identifying viruses and their associated proteins because the standard for viral testing is gene sequencing; however, MALDI has proved to be a more rapid method of

identification. Most studies focusing on characterization of viruses via MALDI have dealt with the detection of pathogens (Colquhoun *et al*., 2006; Ilina *et al*., 2005; Lopaticki *et al*., 1998; Luan *et al*., 2009; Michael *et al*., 2009; Parker *et al*., 1996). Instead of targeting entire viruses for MALDI analyses, a specific protein of interest is usually selected. The most abundant protein in most viruses is the capsid protein, which constitutes most of the viral coat. Colquhoun *et al*. (2006) used MALDI to target the capsid protein of a norovirus, which is the leading cause of gastroenteritis.

Other studies have focused on examining less abundant viral proteins with MALDI, such as fusion proteins (Lopaticki *et al*., 1998; Parker *et al*., 1996) or glycoproteins in enveloped viruses (Kim *et al*., 2001). Lopaticki *et al*. (1998) identified different variants of the fusion protein for the Newcastle disease virus. Different variations in the fusion protein affected virulence because some fusion proteins were not capable of binding to host cells. Parker *et al*. (1996) examined cells infected with HIV for the presence of the viral fusion protein. In order to identify a viral biomarker, Kim *et al*. (2001) studied viral glycoproteins in the envelope of the Sindbis virus, which is a model virus in the same family as the eastern and western equine encephalomyelitis viruses.

Another application of MALDI to viruses has involved determination of the molecular weight of specific restriction fragments from complementary DNA (Ilina *et al*., 2005; Luan *et al*., 2009; Michael *et al*., 2009). Luan *et al*. (2009) amplified a region of the reverse transcriptase gene of the hepatitis B virus. MALDI was used to detect various mutations within this region of the gene, and 60 variants of the virus were identified. Ilina *et al*. (2005) performed a similar study investigating variations in the 5′ untranslated region of the hepatitis C viral genome. This technique has also been used for a host of other viruses, including the avian influenza virus (H5N1). Michael *et al*. (2009) observed restriction fragments from the genome to determine point mutations that may indicate strains with more or less pathogenicity.

D. Current applications

The speed at which analyses can be performed using MALDI-TOF MS has important applications in areas such as bioterrorism, food safety, and environmental testing (Demirev and Fenselau, 2008a,b; Mazzeo *et al*., 2006; Meays *et al*., 2004). The increase in use of MALDI for identifying and characterizing microorganisms and their peptides has also led to the development of new software for relevant data analysis.

1. Biodefense

Within the past decade, it has become increasingly important to develop new methods for the rapid and accurate characterization of newly or re-emerging and bioengineered microorganisms. These microorganisms,

including bacteria (e.g., *Bacillus anthracis*, *Yersinia pestis*, and *Francisella tularensis*) and viruses (e.g., small pox and hemorrhagic fever viruses), have the potential to be used as weapons of bioterrorism. MALDI-TOF MS can be used for early determination of the causative microorganism and rapid identification of the exposed population (Scholl *et al.*, 1999). Mass spectra of intact cells of a number of biological threats, such as data from mass spectra for a number of biological threats, such as pathogenic species of *Bacillus*, *Pseudomonas*, *Staphylococcus*, and *Yersinia*, have already been added to various databases (Wahl *et al.*, 2002).

Bacillus anthracis spores represent an ideal weapon of bioterrorism because they are extremely persistent in the environment (Demirev and Fenselau, 2008a,b). Therefore, many studies have compared *B. anthracis* and nonpathogenic *Bacillus* spp. (i.e., *B. cereus*, *B. subtilis*, and *B. thuringiensis*) using MALDI (Elhanany *et al.*, 2001; Krishnamurthy *et al.*, 1996). Elhanany *et al.* (2001) reported four biomarkers unique to *B. anthracis*.

The prevalence of methicillin-resistant *Staphylococcus aureus* (MRSA) and other antibiotic-resistant bacteria is also increasing. Jackson *et al.* (2005), Carbonnelle *et al.* (2007), and Hsieh *et al.* (2008) have all utilized MALDI to identify species and strains of *Staphylococcus*. Carbonnelle *et al.* (2007) correctly identified 95% of 293 unknown clinical strains of *Staphylococcus* spp.

Other bioterrorism threats include *Coxiella burnetii* (the causative agent of Q fever) and *Francisella tularensis* (the causative agent of tularemia). Pierce *et al.* (2007) used MALDI to correctly identify five strain classes of *C. burnetii*. MALDI has been shown to be an ideal choice for identifying *F. tularensis* extracts because the organism is difficult to culture. The remarkable sensitivity of MALDI has proven to be an invaluable asset in detecting low concentrations of *F. tularensis*. For example, Jiang *et al.* (2007) detected *F. tularensis* peptides at the attomolar level.

One problem with identifying putative bioterrorism agents in the lab is that intact cells are hazardous to human health and must be analyzed in biosafety level 3 or 4 labs. Lasch *et al.* (2008) found that one possible solution included treating *B. anthracis* spores or *Y. pestis* vegetative cells with 80% trifluoroacetic acid (TFA) for 30 min. This treatment inactivated the bacteria while retaining much of the information content for MALDI.

2. Food microbiology

Rapid and accurate identification of foodborne pathogens (e.g., *Campylobacter* spp., *E. coli* O157:H7, *Listeria monocytogenes*, *Salmonella* spp., and *Shigella flexneri*) is essential for providing therapeutic management of their associated illnesses (Barbuddhe *et al.*, 2008; Dieckmann *et al.*, 2008; Holland *et al.*, 2000; Mandrell *et al.*, 2005; Ochoa and Harrington, 2005). MALDI-TOF MS has been applied to distinguish between pathogenic and nonpathogenic contaminants in foods. For example, Mazzeo *et al.* (2006) correctly identified 24 different bacterial species that were well-known

food contaminants and were able to distinguish between the pathogenic *E. coli* O157:H7 and the nonpathogenic *E. coli* ATCC 25922. *E. coli* O157:H7 has been known to contaminate a number of foods, especially ground beef (Holland *et al.*, 2000; Ochoa and Harrington, 2005). Ochoa and Harrington (2005) were also able to successfully discriminate between pathogenic and nonpathogenic forms of *E. coli*.

Other serious foodborne illnesses are caused by *Salmonella*, *Campylobacter* spp., and *Listeria monocytogenes*. Dieckmann *et al.* (2008) identified 126 strains of *Salmonella* spp. in chicken, turkey, swine, and cattle. Mandrell *et al.* (2005) characterized 75 strains of *Campylobacter* spp. from human, poultry, swine, dogs, and cats. Barbuddhe *et al.* (2008) used MALDI to correctly identify 146 strains of *Listeria* spp. in meat, poultry, dairy, and vegetables.

3. Recreational waters

Recreational waters can harbor many pathogens, including bacteria (e.g., *Campylobacter*, *E. coli* O157:H7, *Salmonella*, and *Vibrio cholerae*), protozoans (e.g., *Cryptosporidium* and *Giardia*), and viruses (e.g., enteroviruses, hepatitis viruses, and norovirus) (Colquhoun *et al.*, 2006; Gostin *et al.*, 2000; Sharma *et al.*, 2003). The source of these pathogens is often contamination from nearby wildlife, livestock, human fecal material, sewage, polluted surface water, or storm water runoff (Geldreich, 1996; Meays *et al.*, 2004). The source of the pollution must be determined to reduce the potential health risks posed by these pathogens. The pathogens also need to be detected in a timely fashion to accurately assess the need for swimming beach closures and fishing restrictions in these recreational waters, which can produce substantial economic losses (Rabinovici *et al.*, 2004).

Identifying the source and concentrations of microbial indicator organisms (i.e., *E. coli* and *Enterococcus* spp.) is necessary for preparing mitigation strategies and for assessing human health risks. The source can also provide insight into which other pathogenic organisms may be present in recreational waters (U.S. EPA, 2000). Siegrist *et al.* (2007) utilized MALDI-TOF MS to discriminate between closely related environmental strains of *E. coli* from mammalian and avian sources. Environmental isolates from fecal samples were more accurately assigned to their specific source group when using MALDI than when using other techniques that are more time consuming and labor intensive; however, reproducibility was lower using MALDI. Giebel *et al.* (2008) performed a similar study to characterize environmental isolates of *Enterococcus* spp. using MALDI. Although indicator organisms may be useful for providing insight into the level of contamination in recreational waters, they cannot predict the presence of all pathogens. Therefore, it is necessary to develop new techniques for direct pathogen monitoring (Savichtcheva and Okabe, 2006).

4. Data analysis

Several algorithms have been proposed to facilitate the matching of mass spectra from unknown sources with spectra from reference libraries. The multivariate linear least-squares regression algorithm is one method for finding the best match from a reference library for both the *m/z* and intensity values (Fenselau and Demirev, 2001).

A variety of commercial software packages have been developed to process raw MALDI spectra and to compare these spectra to those in reference libraries. Two such packages are MALDI BioTyper (Bruker Daltonik GmbH, Germany) and SARAMIS (Spectral Archiving and Microbial Identification System, AnagnosTec GmbH, Germany). Both software packages allow users to process raw data (i.e., perform smoothing, normalization, baseline subtraction) and to compare the processed data to a built-in reference library (Barbuddhe *et al.*, 2008; Erhard *et al.*, 2008).

One feature of some of this software is the ability to create a superspectrum for a particular strain by combining individual spectra obtained under different experimental conditions (Barbuddhe *et al.*, 2008; Dieckmann *et al.*, 2008; Erhard *et al.*, 2008; Mellmann *et al.*, 2008). The BioTyper reference library contains superspectra for over 3200 reference strains (Nagy *et al.*, 2009). Mellmann *et al.* (2008) and Barbuddhe *et al.* (2008) used BioTyper software to add superspectra for newly investigated bacteria to the reference database by combining 20 peak lists from each strain. Comparisons between spectra of unknown strains and the new superspectra allowed 85.9% accurate identification, regardless of the MALDI instrument or experimental conditions (Mellmann *et al.*, 2008). Nagy *et al.* (2009) obtained a higher accuracy rate by correctly identifying 97.5% of 277 clinical isolates from the *Bacteroides* genus. Seng *et al.* (2009) used BioTyper to identify 1660 bacterial isolates with 95.4% accuracy.

The SARAMIS database contains over 62,000 spectra from over 1160 species, most of which are pathogens. With this software, mass spectra from unknown organisms are compared with the database using a point system with peaks being weighed according to specificity. For example, Erhard *et al.* (2008) were able to correctly identify every *Trichophyton* strain studied using SARAMIS, regardless of host origin or pathology.

III. CHALLENGES

A. Reproducibility

A primary concern regarding characterization of intact microorganisms using MALDI-TOF MS is reproducibility (Lay, 2001). Mass spectra depict the presence of biomolecules, such as proteins, present in microorganisms.

The question of reproducibility stems from the fact that microorganisms express different proteins under different environmental conditions (e.g., Ellwood and Tempest, 1972); so experimental factors such as growth media, culture age, and sample preparation may have effects on the ability to gather reproducible mass spectra. In particular, several studies have investigated reproducibility within individual labs (i.e., intra-laboratory reproducibility) and across multiple labs (i.e., inter-laboratory reproducibility).

1. Intra-laboratory

Many studies have investigated levels of intra-laboratory reproducibility, in which mass spectra are gathered at different times using the same mass spectrometer. Generally, high levels of reproducibility have been reported. For example, studies by Arnold *et al.* (1999), Bernardo *et al.* (2002), and Smole *et al.* (2002), noted that when mass spectra were gathered over a number of days, or in the case of Bernardo *et al.* (2002), months, peaks were consistently observed in mass spectra for a variety of bacteria. Other studies have reported levels of reproducibility of 75% or higher (Saenz *et al.*, 1999; Walker *et al.*, 2002). In each of these studies, focus was placed on the presence or absence of particular peaks. Intensities of the characteristic peaks varied.

2. Inter-laboratory

Perhaps not surprisingly, inter-laboratory reproducibility appears lower than intra-laboratory reproducibility. Some studies comparing mass spectra gathered at different locations have shown promising results. For example, Wang *et al.* (1998) reported that most of the peaks associated with *Bacillus thuringiensis* were observed in mass spectra gathered in two separate laboratories when the same experimental protocols were followed. Similarly, Walker *et al.* (2002) reported that more than 60% of peaks observed for *Staphylococcus aureus* were present in mass spectra gathered at separate laboratories. In contrast, a study by Wunschel *et al.* (2005) investigated the reproducibility of mass spectra gathered using three different mass spectrometers at different locations. Of all the peaks reported for *E. coli* at each laboratory, only 23% of the peaks were observed in the mass spectra gathered at all three laboratories, but when mass spectra gathered from one mass spectrometer were analyzed in the other laboratories, 70% of the mass spectra were correctly identified as originating from *E. coli*. Wunschel *et al.* (2005) attributed the low levels of reproducibility to the fact that each of the different mass spectrometers used in the study had different capabilities and levels of mass accuracy. Indeed, this is an important finding, considering the diversity of mass spectrometers used to fingerprint microorganisms (Table 6.1).

B. Effects of culture conditions

1. Media

The choice of growth media may affect reproducibility of mass spectra. Studies conducted by Walker *et al.* (2002), Valentine *et al.* (2005), and Ruelle *et al.* (2004) reported differences in mass spectra obtained from bacteria grown on different growth media. Walker *et al.* (2002) noted that when bacteria were grown on selective agar, the mass spectra contained fewer peaks, particularly in the 500–1000 *m/z* range, in comparison to the more rich media used in the study. In contrast, Vargha *et al.* (2006), Conway *et al.* (2001), and Bernardo *et al.* (2002), reported that mass spectra obtained from bacteria grown on different media were quite similar, even when comparisons were conducted that examined cultures grown on agar plates versus broth. For example, Conway *et al.* (2001) noted that *E. coli* grown in two different broths yielded spectra with 80% similarity. Also, when the same cultures were grown in broth and on agar plates, the mass spectra were similar enough to correctly identify them as coming from *E. coli*.

Reports of differences in mass spectra when cultures are grown on different types of media are not surprising. Each type of media provides bacteria with different nutrients, and depending on nutrient needs, bacteria express different proteins (Ellwood and Tempest, 1972; Valentine *et al.*, 2005). In addition, dependent upon the content of the media, different media will produce different background peaks if present in the sample being analyzed (Lay, 2000). Although it would be desirable to have a standard medium to use for growth of bacterial cultures for MALDI-TOF MS analysis, it would be highly unlikely due to the fact that certain bacteria need certain growth conditions, often requiring the use of specialized media. According to Lay (2000), this underscores the importance of developing a method of bacterial analysis using MALDI-TOF MS that would allow for the acquisition of similar mass spectra regardless of the type of growth medium used.

2. Age

Culture age is also a factor that has been shown to affect MALDI mass spectra gathered from intact microorganisms. Several studies have examined how mass spectra change throughout different growth phases of bacteria (e.g., Arnold *et al.*, 1999; Conway *et al.*, 2001; Ruelle *et al.*, 2004; Vargha *et al.*, 2006). Conway *et al.* (2001) reported that bacterial samples analyzed following 1.5, 3.0, 6.0, and 16.0 h of growth yielded spectra that were 65% or greater in similarity. Unlike the study by Conway *et al.* (2001), the majority of studies have suggested that culture age has a pronounced effect on mass spectra. Vargha *et al.* (2006) found that although characteristic intense peaks were present throughout the growth cycles of *Arthrobacter*, *E. coli*, and *Pseudomonas*, unique spectra were

associated with cultures of the same microorganisms analyzed at different times. Ruelle *et al.* (2004) reported that mass spectra of bacteria produced similar peaks following 24 and 48 h of incubation, but peaks present in the 48-h mass spectra had higher intensities. Following analysis after 72 h of incubation, peaks present in the 24- and 48-h spectra disappeared (Ruelle *et al.*, 2004). Arnold *et al.* (1999) examined changes in mass spectra of *E. coli* K-12 when sampled at various times from 6 to 84 h of growth and pointed out several trends. In general, the number of peaks increased with culture age up to approximately the 28th h of culture growth, and the intensities of the peaks varied with culture age. During the early stages of growth, there were fewer peaks in the 0–8 kDa mass range, and certain peaks were consistently observed, but then disappeared as growth continued. It was also noted that there were a number of peaks that were not observed until later in growth. Arnold *et al.* (1999) attributed these changes to the cell adapting to changing growth conditions, such as nutrient depletion and buildup of waste products.

C. Effects of technical variability

1. Matrix

Another factor that can affect the mass spectra gathered from bacterial samples is the type of matrix used. Matrices commonly used for MALDI-TOF MS analysis of microorganisms include sinapinic acid, α-cyano-4-hydroxycinnamic acid (CHCA), 3,5-dimethoxy-4-hydroxycinnamic acid, ferulic acid, 2-(4-hydroxyphenylazo)benzoic acid (HABA), and 2,5-dihydroxybenzoate (DHB). Selection of the proper matrix is important, because different matrices allow analysis of varying types of biomolecules (Fenselau and Demirev, 2001). Sinapinic acid, CHCA, and ferulic acid have been shown to be useful for the detection of proteins (Vaidyanathan *et al.*, 2002; Kussmann *et al.*, 1997; Williams *et al.*, 2003; Fenselau and Demirev, 2001), while matrices such as DHB work well for the detection of glycopeptides and glycoproteins (Kussmann *et al.*, 1997).

Matrix selection not only affects the types of biomolecules that can be detected but can also play a role in the size and, to some extent, the intensities of the peaks of biomolecules detected. CHCA is commonly used for the detection of lower mass ions but, depending on the solvent used, is capable of allowing for detection of ions above 10 kDa (Williams *et al.*, 2003; Ruelle *et al.*, 2004). DHB is also useful for the detection of lower mass ions (Hathout *et al.*, 2000). Ferulic acid can be used for the detection of high-mass ions, but this matrix often produces peaks with lower intensities (Ruelle *et al.*, 2004). With regard to detecting higher mass ions, sinapinic acid has been shown to be one of the more useful matrices (Conway *et al.*, 2001; Vargha *et al.*, 2006).

The matrix has been shown to have significant effects on mass spectrometry of microorganisms (e.g., Kemptner *et al.*, 2009). In their work to develop a universal method of sample preparation for MALDI-TOF MS-enabled fingerprinting of microorganisms, Liu *et al.* (2007) reported that CHCA was particularly effective in providing high-quality and reproducible spectra of a limited, but diverse, set of microorganisms including *Y. pestis*, *E. coli*, *Burkholderia cepacia*, *B. anthracis*, and *S. aureus*. While the quality and reproducibility of the spectra were not quantified, the authors' efforts represent an important step towards standardizing important procedures.

2. Sample preparation and data acquisition

In addition to examining effects of matrix on the quality and reproducibility of spectra, Liu *et al.* (2007) also examined the effect of matrix solvent composition, sample preparation method, sample deposition method, and sample quantity on spectrum quality and reproducibility. The authors noted effects of each of these parameters and proposed a universal sample preparation method. With regard to sample preparation, the authors found no enhancement to spectra by treating samples with enzymes (trypsin and lysozyme). In contrast, Giebel *et al*. (2008) reported that treating samples with lysozyme enhanced spectra (increased signal-to-noise ratio associated with the most intense peaks in spectra). Liu *et al.* (2007) reported a universal method that consisted of analyzing 4–5 mg of bacteria grown on agar plates and washed with 0.1% TFA. After washing, the cells were resuspended in chloroform/methanol (1:1), vortexed, centrifuged, and resuspended in 0.1%TFA. In terms of application of the sample to the MALDI target plate, the authors concluded that the dried droplet approach was the most effective. This approach involves applying the sample to the target plate, allowing the sample to dry, and overlaying the sample with the matrix (CHCA in acetonitrile/methanol/water (1:1:1) with 0.1% formic acid and 0.01 M 18-crown-6). A rigorous, quantitative examination of the utility of this ''universal'' approach to a larger, more diverse set of microorganisms has not been performed.

While several aspects of the process of MALDI-enabled microbial fingerprinting have been examined, several remain unexplored. For example, methods of MALDI data acquisition have varied considerably. A few studies have examined the effects of this variation. Indeed, Wunschel *et al*. (2005) report that use of different instruments affects reproducibility; however, even with the use of a single instrument, methods of data collection vary. Acquisition of MALDI-TOF mass spectra typically involves the operator analyzing several locations on a spot of sample. Generally, spectra are considered of high quality if peaks have significant intensity and signal-to-noise (S/N) ratio. Most software that facilitates operation of MALDI-TOF mass spectrometers is capable of

performing automated data acquisition in which the operator merely provides criteria (e.g., peak S/N ratio, minimum peak intensity, etc.) by which the software determines whether the automatically acquired spectra are of adequate quality. The universal application of these criteria would seem to enhance the reliability, reproducibility, and objectivity of the method. Indeed, we have observed in our laboratory that automating the acquisition of spectra of intact cells of *E. coli* increases reproducibility from 86% to 98% (M. Robbins *et al*., unpublished data). Spectra of intact cells acquired in an automated fashion tend to exhibit fewer peaks than spectra acquired in a manual mode; however, these peaks tend to be more reproducible. For example, among five replicate spectra of a culture of a single strain of *E. coli*, manual data acquisition yielded spectra with 52% of the total number of peaks in all spectra appearing in only a single replicate spectrum. In contrast, automated data acquisition yielded spectra with only 29% of the peaks appearing in single replicate spectrum (Fig. 6.3). Whether the reduction in peak number that accompanies automated data acquisition compromises the discriminatory power of the method has not been investigated.

3. Assessing method reproducibility

Maximizing method reproducibility is critical to any approach for rapid and accurate microbial characterization. Unfortunately, no standard methods of evaluating reproducibility of MALDI-based methods of microbial fingerprinting have been proposed. Many evaluations of reproducibility have been largely qualitative and comparative. Moving toward more quantitative approaches, some (e.g., Liu *et al*., 2007) report numbers of peaks that appear in replicate spectra of a single microorganism. Others have calculated and reported similarity coefficients of replicate spectra (e.g., Giebel *et al*., 2008; Siegrist *et al*., 2007). Several similarity coefficients can be used for this purpose. Some account for peak presence/absence only (e.g., the Dice similarity coefficient), while others account for peak intensity (e.g., cosine and Pearson product–moment correlation coefficients).

The choice of similarity coefficient not only affects the reported reproducibility but also the discriminatory power of the method. Giebel *et al*. (2008) reported that use of the Pearson product–moment correlation coefficient facilitated more accurate classification of environmental isolates of *Enterococcus* sp. than use of the Dice similarity coefficient. Similarly, in our work with environmental isolates of *E. coli*, the Pearson coefficient allowed a greater proportion of isolates to be correctly classified with respect to their environmental source (e.g., from human, bovine, avian, etc. sources) than the Dice similarity coefficient. Specifically, use of the Pearson correlation coefficient facilitated a 28% increase in the rate of correct classification of *E. coli* isolates from six environmental sources (Robbins *et al*., 2007). Similarly, in our recent work with a larger number

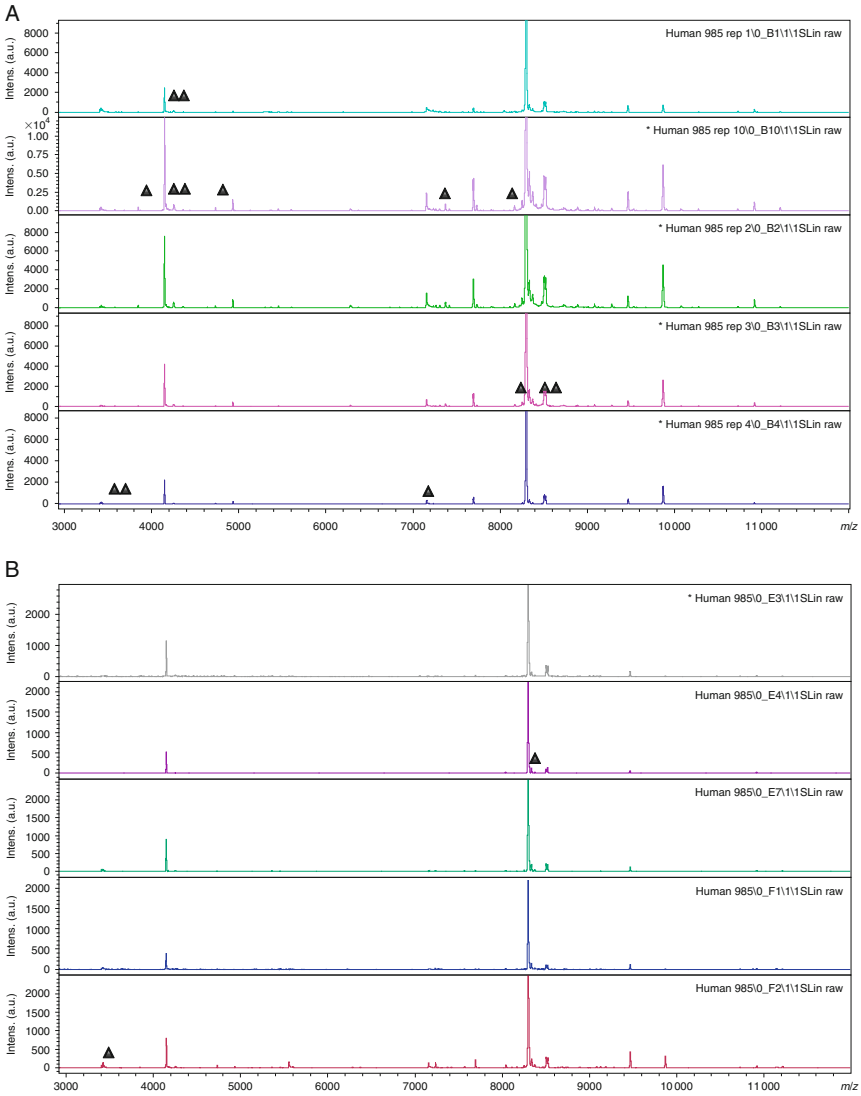

FIGURE 6.3 MALDI-TOF mass spectra of five replicates of a single isolate of *Escherichia coli* acquired using manual (A) and automated (B) approaches. A single operator obtained spectra manually, while a software (FlexControl; Bruker Daltonics; Billerica, MA) was used to acquire spectra in an automated fashion. Triangles represent peaks that appeared in only a single replicate spectrum and reduced reproducibility.

(263) of *E. coli* isolates, the Pearson coefficient facilitated closer grouping of isolates from the same sources than the Dice similarity coefficient (Fig. 6.4).

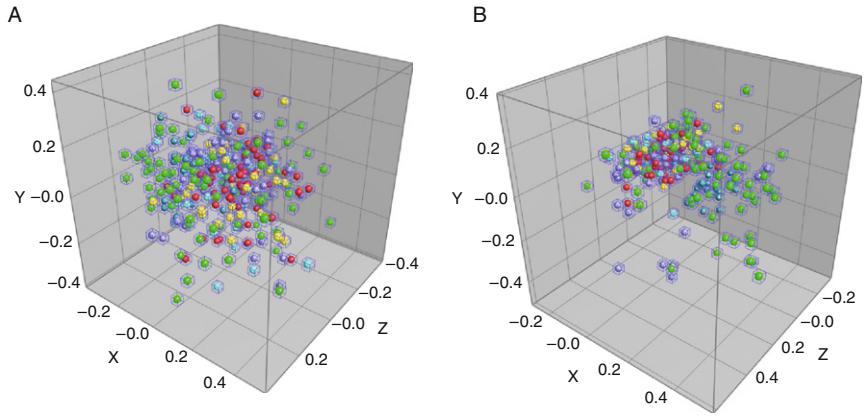

FIGURE 6.4 Multidimensional scaling (MDS) analysis of MALDI-TOF MS-based fingerprints of intact cells of 263 environmental isolates of *Escherichia coli*. Dice (A) and Pearson (B) similarity coefficients were used to determine similarity prior to MDS. Note closer grouping of isolates from same sources in MDS constructed using the Pearson similarity coefficient. Different sources (human, bovine, gull, goose, and canine) are represented by points with different colors (available online)/shades of gray (print).

IV. SUMMARY

MALDI-TOF MS clearly offers promise as a rapid, accurate, and versatile tool to characterize microorganisms. Further refinement of the approach, however, is warranted. As noted previously (e.g., Demirev and Fenselau, 2008a), the reproducibility of MALDI mass spectra of intact cells varies considerably. In many cases, reproducibility has not been rigorously and quantitatively examined. Neither standard methods of assessing reproducibility nor common threshold criteria of quality spectra have been established. Variable methods of sample preparation and data acquisition likely account for many of the differences reported in the reproducibility and accuracy of the method. Thus, the development of standard sample preparation, data acquisition, and data analysis approaches is warranted. Development of a single standard protocol for all microorganisms may not be practical, considering the distinct structures and architectures characteristic of the diverse members of the microbial universe (i.e., viruses, Gram-positive and Gram-negative bacteria, spore-forming and non-spore-forming bacteria, and fungi). Given this diversity, development of standard methods for taxonomically similar microorganisms may represent a critical first step towards standardization of use of MALDI to characterize microorganisms.

Bioinformatics-based approaches to characterizing microorganisms via MALDI are not as limited by issues of reproducibility. Unfortunately,

these approaches require databases of proteins that are not yet available for most novel and many environmental microorganisms. In addition, these approaches are most effective when used with a mass spectrometer with tandem MS-MS capabilities (e.g., MALDI-TOF-TOF). Bioinformatics-based strategies will likely become more prevalent and integrated into intact cell analysis via MALDI as more microbial genomes are sequenced and as MALDI-TOF-TOF mass spectrometers become more affordable and common in the microbiology laboratory.

ACKNOWLEDGMENTS

Original data from the corresponding author's lab and presented in this review are based upon work supported by the National Science Foundation under Grant Nos. 0452825 and 0321545. Any opinions, findings, conclusions, or recommendations expressed in this material are those of the author(s) and do not necessarily reflect the views of the National Science Foundation.

REFERENCES

Alberts, B., Bray, D., Lewis, J., Raff, M., Roberts, K., and Watson, J. D. (1994). Molecular Biology of the Cell. Garland Publishing Inc., New York.

Amiri-Eliasi, B., and Fenselau, C. (2001). Characterization of protein biomarkers desorbed by MALDI from whole fungal cells. *Anal. Chem.* **73,** 5228–5231.

Anhalt, J. P., and Fenselau, C. (1975). Identification of bacteria using mass spectrometry. *Anal. Chem.* **47,** 219–225.

Arnold, R. J., Karty, J. A., Ellington, A. D., and Reilly, J. P. (1999). Monitoring the growth of a bacteria culture by MALDI-MS of whole cells. *Anal. Chem.* **71,** 1990–1996.

Barbuddhe, S. B., Maier, T., Schwarz, G., Kostrzewa, M., Hof, H., Domann, E., Chakraborty, T., and Hain, T. (2008). Rapid identification and typing of listeria species by matrix-assisted laser desorption ionization-time of flight mass spectrometry. *Appl. Environ. Microbiol.* **74,** 5402–5407.

Bernardo, K., Pignatari, A. C. C., Macht, M., Krut, O., Seifert, H., Fleer, S., Hunger, F., and Kronke, M. (2002). Identification and discrimination of *Staphylococcus aureus* strains using matrix-assisted laser desorption/ionization time-of-flight mass spectrometry. *Proteomics* **2,** 747–753.

Cain, T. C., Lubman, D. M., and Weber, W. J., Jr. (1994). Differentiation of bacteria using protein profiles from matrix-assisted laser desorption/ionization time-of-flight mass spectrometry. *Rapid Commun. Mass Spectrom.* **8,** 1026–1030.

Carbonnelle, E., Beretti, J., Cottyn, S., Quesne, G., Berche, P., Nassif, X., and Ferroni, A. (2007). Rapid identification of *Staphylococci* isolated in clinical microbiology laboratories by matrix-assisted laser desorption ionization-time of flight mass spectrometry. *J. Clin. Microbiol.* **45,** 2156–2161.

Carson, C. A., Shear, B. L., Ellersieck, M. R., and Asfaw, W. (2001). Identification of fecal *Eshcerichia coli* from humans and animals by ribotyping. *Appl. Environ. Microbiol.* **67,** 1503–1507.

Carson, C. A., Shear, B. L., Ellersieck, M. R., and Schnell, J. D. (2003). Comparison of ribotyping and repetive exxtragenic palindromic-PCR for identification of fecal *Escherichia coli* from humans and animals. *Appl. Environ. Microbiol.* **69,** 1836–1839.

Chen, H., and Chen, Y. (2005). Characterization of intact *Penicillium* spores by matrix-assisted laser desorption/ionization mass spectrometry. *Rapid Commun. Mass Spectrom.* **19,** 3564–3568.

Claydon, M. A., Davey, S. N., Edwards-Jones, V., and Gordon, D. B. (1996). The rapid identification of intact microorganisms using mass spectrometry. *Nat. Biotechnol.* **14,** 1584–1586.

Colquhoun, D. R., Schwab, K. J., Cole, R. N., and Halden, R. U. (2006). Detection of norovirus capsid protein in authentic standards and in stool extracts by matrix-assisted laser desorption ionization and nanospray mass spectrometry. *Appl. Environ. Microbiol.* **72,** 2749–2755.

Conway, G. C., Smole, S. C., Sarracino, D. A., Arbeit, R. D., and Leopold, P. E. (2001). Phyloproteomics: Species identification of *Enterobacteriaceae* using matrix-assisted laser desorption/ionization time-of-flight mass spectrometry. *J. Mol. Microbiol. Biotechnol.* **3,** 103–112.

Dalluge, J. J. (2000). Mass spectrometry for direct determiniation of proteins in cells: Applications in biotechnology and microbiology. *Fresenius J. Anal. Chem.* **366,** 701–711.

Demirev, P., and Fenselau, C. (2008a). Mass spectrometry for rapid characterization of microorganisms. *Annu. Rev. Anal. Chem.* **1,** 71–93.

Demirev, P. A., and Fenselau, C. (2008b). Mass spectrometry in biodefense. *J. Mass Spectrom.* **43,** 1441–1457.

Demirev, P., Ho, Y., Ryzhov, V., and Fenselau, C. (1999). Microorganism identification by mass spectrometry and protein database searches. *Anal. Chem.* **71,** 2732–2738.

Dickinson, D. N., La Duc, M. T., Haskins, W. E., Gornushkin, I., Winefordner, J. D., Powell, D. H., and Venkateswaran, K. (2004). Species differentiation of a diverse suite of *Bacillus* spores by mass spectrometry-based protein profiling. *Appl. Environ. Microbiol.* **70,** 475–482.

Dieckmann, R., Helmuth, R., Erhard, M., and Malorny, B. (2008). Rapid classification and identification of salmonellae at the species and subspecies levels by whole-cell matrix-assisted laser desorption ionization-time of flight mass spectrometry. *Appl. Environ. Microbiol.* **74,** 7767–7778.

Dombek, P. E., Johnson, L. K., Zimmerley, S. T., and Sadowsky, M. J. (2000). Use of repetitive DNA sequences and the PCR to differentiate *Escherichia coli* isolates from human and animal sources. *Appl. Environ. Microbiol.* **66,** 2572–2577.

Du, Z., Yang, R., Guo, Z., Song, Y., and Wang, J. (2002). Identification of *Staphylococcus aureus* and determination of its methicillin resistance by matrix-assisted laser desorption/ionization time-of-flight mass spectrometry. *Anal. Chem.* **74,** 5487–5491.

Elhanany, E., Barak, R., Fisher, M., Kobiler, D., and Altboum, Z. (2001). Detection of specific *Bacillus anthracis* spore biomarkers by matrix-assisted laser desorption/ionization time-of-flight mass spectrometry. *Rapid Commun. Mass Spectrom.* **15,** 2110–2116.

Ellwood, D. C., and Tempest, D. W. (1972). Effects of environment on bacterial cell wall content and composition. *Adv. Microb. Physiol.* **7,** 83–117.

U.S. Environmental Protection Agency (2000). Improved enumeration methods for therecreational water quality indicators: Enterococci and *Escherichia coli*. Office of Science and Technology, Washington, DC.

Erhard, M., Hipler, U., Burmester, A., Brakhage, A. A., and Wöstemeyer, J. (2008). Identification of dermatophyte species causing onychomycosis and tinea pedis by MALDI-TOF mass spectrometry. *Exp. Dermatol.* **17,** 356–361.

Evason, D. J., Claydon, M. A., and Gordon, D. B. (2001). Exploring the limits of bacterial identification by intact cell-mass spectrometry. *J. Am. Soc. Mass Spectrom.* **12,** 49–54.

Fagerquist, C., Garbus, B., Williams, K., Bates, A., Boyle, S., and Harden, L. (2009). Web-based software for rapid top-down proteomic identification of protein biomarkers, with implications for bacterial identification. *Appl. Environ. Microbiol.* **75,** 4341–4353.

Fenselau, C., and Demirev, P. A. (2001). Characterization of intact microorganisms by MALDI mass spectrometry. *Mass Spectrom. Rev.* **20,** 157–171.

Geldreich, E. E. (1996). Pathogenic agents in freshwater resources. *Hydrol. Process.* **10,** 315–333.

Giebel, R. A., Fredenberg, W., and Sandrin, T. R. (2008). Characterization of environmental isolates of *Enterococcus* spp. by matrix-assisted laser desorption/ionization time-of-flight mass spectrometry. *Water Res.* **42,** 931–940.

Gostin, L. O., Lazzarini, Z., Neslund, V. S., and Osterholm, M. T. (2000). Water quality laws and waterborne diseases: *Cryptosporidium* and other emerging pathogens. *Am. J. Public Health* **90,** 847–853.

Haag, A. M., Taylor, S. N., Johnston, K. H., and Cole, R. B. (1998). Rapid identification and speciation of *Haemophilus* bacteria by matrix-assisted laser desorption/ionization time-of-flight mass spectrometry. *J. Mass Spectrom.* **33,** 750–756.

Hagedorn, C. S., Robinson, S. L., Filtz, J. R., Grubbs, S. M., Angier, T. A., and Reneau, R. B., Jr. (1999). Determining sources of fecal pollution in rural Virginia watershed with antibiotic resistance patterns in fecal streptococci. *Appl. Environ. Microbiol.* **65,** 5522–5531.

Harwood, V. J., Whitlock, J., and Withington, V. (2000). Classification of antibiotic resistance patterns of indicator bacteria by discriminant analysis: Use in predicting the source of fecal contamination in subtropical waters. *Appl. Environ. Microbiol.* **66,** 3698–3704.

Hathout, Y., Ryzhov, V., Demirev, P., and Fenselau, C. (2000). Kurstakins: A new class of lipopeptides isolated from *Bacillus thruingiensis*. *J. Nat. Prod.* **63,** 1492–1496.

Hettick, J. M., Green, B. J., Buskirk, A. D., Kashon, M. L., Slaven, J. E., Janotka, E., Blachere, F. M., Schmechel, D., and Beezhold, D. H. (2008a). Discrimination of *Penicillium* isolates by matrix-assisted laser desorption/ionization time-of-flight mass spectrometry fingerprinting. *Rapid Commun. Mass Spectrom.* **22,** 2555–2560.

Hettick, J. M., Green, B. J., Buskirk, A. D., Kashon, M. L., Slaven, J. E., Janotka, E., Blachere, F. M., Schmechel, D., and Beezhold, D. H. (2008b). Discrimination of *Aspergillus* isolates at the species and strain level by matrix-assisted laser desorption/ionization time-of-flight mass spectrometry fingerprinting. *Anal. Biochem.* **380,** 276–281.

Holland, R. D., Wilkes, J. G., Rafii, F., Sutherland, J. B., Persons, C. C., Voorhees, K. J., and Lay, J. O. (1996). Rapid identification of intact whole bacteria based on spectral patterns using matrix-assisted laser desorption/ionization with time-of-flight mass spectrometry. *Rapid Commun. Mass Spectrom.* **10,** 1227–1232.

Holland, R. D., Rafii, F., Heinze, T. M., Sutherland, J. B., Voorhees, K. J., and Lay, J. O. (2000). Matrix-assisted laser desorption/ionization time-of-flight mass spectrometric detection of bacterial biomarker proteins isolated from contaminated water, lettuce and cotton cloth. *Rapid Commun. Mass Spectrom.* **14,** 911–917.

Holloway, P. (2001). Tracing the source of *E. coli* fecal contamination of water using rep-PCR. Manitoba Livestock Manure Management Initiative (MLMMI). Final Report 00-02-08. http://www.manure.mb.ca/projects/pdfs/00-02-08.pdf.

Hsieh, S., Tseng, C., Lee, Y., Kuo, A., Sun, C., Lin, Y., and Chen, J. (2008). Highly efficient classification and identification of human pathogenic bacteria by MALDI-TOF MS. *Mol. Cell Proteomics* **7,** 448–456.

Ilina, E. N., Malakhova, M. V., Generozov, E. V., Nikolaev, E. N., and Govorun, V. M. (2005). Matrix-assisted laser desorption ionization-time of flight (mass spectrometry) for hepatitis C virus genotyping. *J. Clin. Microbiol.* **43,** 2810–2815.

Jackson, K. A., Edwards-Jones, V., Sutton, C. W., and Fox, A. J. (2005). Optimisation of intact cell MALDI method for fingerprinting of methicillin-resistant *Staphylococcus aureus*. *J. Microbiol. Methods* **62,** 273–284.

Jiang, J., Parker, C. E., Fuller, J. R., Kawula, T. H., and Borchers, C. H. (2007). An immunoaffinity tandem mass spectrometry (iMALDI) assay for detection of *Francisella tularensis*. *Anal. Chim. Acta* **605,** 70–79.

Karas, M., Bachmann, D., Bahr, U., and Hillenkamp, F. (1987). Matrix-assisted ultraviolet laser desorption of non-volatile compounds. *Int. J. Mass Spectrom. Ion Process.* **78,** 53–68.

Kemptner, J., Marchetti-Deschmann, M., Mach, R., Druzhinina, I. S., Kubicek, C. P., and Allmaier, G. (2009). Evaluation of matrix-assisted laser desorption/ionization (MALDI) preparation techniques for surface characterization of intact *Fusarium* spores by MALDI linear time-of-flight mass spectrometry. *Rapid Commun. Mass Spectrom.* **23,** 877–884.

Kim, Y. J., Freas, A., and Fenselau, C. (2001). Analysis of viral glycoproteins by MALDI-TOF mass spectrometry. *Anal. Chem.* **73,** 1544–1548.

Kleinheinz, G. T., McDermott, C. M., and Sampson, R. W. (2003). Recreational water: microbial contamination and human health. *In* ''Wisconsin's waters: A confluence of 16 Perspectives'' (C. Meine, Ed.) *Trans. Wisconsin Acad. Sci.* **90,** 75–86.

Krishnamurthy, T., and Ross, P. L. (1996). Rapid identification of bacteria by direct matrix-assisted laser desorption/ionization mass spectrometric analysis of whole cells. *Rapid Commun. Mass Spectrom.* **10,** 1992–1996.

Krishnamurthy, T., Ross, P. L., and Rajamani, U. (1996). Detection of pathogenic and non-pathogenic bacteria by matrix-assisted laser desorption/ionization time-of-flight mass spectrometry. *Rapid Commun. Mass Spectrom.* **10,** 883–888.

Kussmann, M., Nordhoff, E., Rabbek-Nielsen, H., Haebel, S., Rossel-Larsen, M., Jakobsen, L., Gobom, J., Mirgorodskaya, E., Kroll-Kristensen, A., Palm, L., and Roepstorff, P. (1997). Matrix-assisted laser desorption/ionization mass spectrometry sample preparation techniques designed for various peptide and protein analysis. *J. Mass Spectrom.* **32,** 593–601.

Lasch, P., Nattermann, H., Erhard, M., Stämmler, M., Grunow, R., Bannert, N., Appel, B., and Naumann, D. (2008). MALDI-TOF mass spectrometry compatible inactivation method for highly pathogenic microbial cells and spores. *Anal. Chem.* **80,** 2026–2034.

Lay, J. O. (2000). MALDI-TOF mass spectrometry and bacterial taxonomy. *Trends Anal. Chem.* **19,** 507–515.

Lay, J. O. (2001). MALDI-TOF mass spectrometry of bacteria. *Mass Spectrom. Rev.* **20,** 172–194.

Lennon, J. J. (1997). Matrix assisted laser desorption ionization time-of-flight mass spectrometry. *ABRF News.* **8**(2), http://www.abrf.org/ABRFNews/1997/June1997/jun97lennon.html.

Li, T. Y., Liu, B. H., and Chen, Y. C. (2000). Characterization of *Aspergillus* spores by matrix-assisted laser desorption/ionization time-of-flight mass spectrometry. *Rapid Commun. Mass Spectrom.* **14,** 2393–2400.

Liu, H., Du, Z., Wang, J., and Yang, R. (2007). Universal sample preparation method for characterization of bacteria by matrix-assisted laser desorption ionization-time of flight mass spectrometry. *Appl. Environ. Microbiol.* **73,** 1899–1907.

Lopaticki, S., Morrow, C. J., and Gorman, J. J. (1998). Characterization of pathotype-specific epitopes of newcastle disease virus fusion glycoproteins by matrix-assisted laser desorption/ionization time-of-flight mass spectrometry and post-source decay sequencing. *J. Mass Spectrom.* **33,** 950–960.

Luan, J., Yuan, J., Li, X., Jin, S., Yu, L., Liao, M., Zhang, H., Xu, C., He, Q., Wen, B., Zhong, X., Chen, X., *et al.* (2009). Multiplex detection of 60 hepatitis B virus variants by MALDI-TOF mass spectrometry. *Clin. Chem.* **55,** 1503–1509.

Mandrell, R. E., Harden, L. A., Bates, A., Miller, W. G., Haddon, W. F., and Fagerquist, C. K. (2005). Speciation of *Campylobacter coli*, *C. jejuni*, *C. helveticus*, *C. lari*, *C. sputorum*, and *C. upsaliensis* by matrix-assisted laser desorption ionization-time of flight mass spectrometry. *Appl. Environ. Microbiol.* **71,** 6292–6307.

Marklein, G., Josten, M., Klanke, U., Müller, E., Horré, R., Maier, T., Wenzel, T., Kostrzewa, M., Bierbaum, G., Hoerauf, A., and Sahl, H. (2009). Matrix-assisted laser desorption ionization-time of flight mass spectrometry for fast and reliable identification of clinical yeast isolates. *J. Clin. Microbiol.* **47,** 2912–2917.

Mazzeo, M. F., Sorrentino, A., Gaita, M., Cacace, G., Di Stasio, M., Facchiano, A., Comi, G., Malorni, A., and Siciliano, R. A. (2006). Matrix-assisted laser desorption ionization-time of flight mass spectrometry for the discrimination of food-borne microorganisms. *Appl. Environ. Microbiol.* **72,** 1180–1189.

Meays, C. L., Broersma, K., Nordin, R., and Mazumder, A. (2004). Source tracking fecal bacteria in water: A critical review of current methods. *J. Environ. Manage.* **73,** 71–79.

Mellmann, A., Cloud, J., Maier, T., Keckevoet, U., Ramminger, I., Iwen, P., Dunn, J., Hall, G., Wilson, D., Lasala, P., Kostrzewa, M., and Harmsen, D. (2008). Evaluation of matrix-assisted laser desorption ionization-time-of-flight mass spectrometry in comparison to 16S rRNA gene sequencing for species identification of nonfermenting bacteria. *J. Clin. Microbiol.* **46,** 1946–1954.

Michael, K., Harder, T. C., Mettenleiter, T. C., and Karger, A. (2009). Diagnosis and strain differentiation of avian influenza viruses by restriction fragment mass analysis. *J. Virol. Methods* **158,** 63–69.

Moura, H., Ospina, M., Woolfitt, A. R., Barr, J. R., and Visvesvara, G. S. (2003). Analysis of four human microsporidian isolates by MALDI-TOF mass spectrometry. *J. Eukaryot. Microbiol.* **50,** 156–163.

Nagy, E., Maier, T., Urban, E., Terhes, G., and Kostrzewa, M. (2009). Species identification of clinical isolates of *Bacteroides* by matrix-assisted laser-desorption/ionization time-of-flight mass spectrometry. *Clin. Microbiol. Infect.*

Nilsson, C. L. (1999). Fingerprinting of *Helicobacter pylori* strains by matrix-assisted laser desorption/ionization mass spectrometric analysis. *Rapid Commun. Mass Spectrom.* **13,** 1067–1071.

Ochoa, M. L., and Harrington, P. B. (2005). Immunomagnetic isolation of enterohemorrhagic *Escherichia coli* O157:H7 from ground beef and identification by matrix-assisted laser desorption/ionization time-of-flight mass spectrometry and database searches. *Anal. Chem.* **77,** 5258–5267.

Parker, C. E., Papac, D. I., and Tomer, K. B. (1996). Monitoring cleavage of fusion proteins by matrix-assisted laser desorption ionization/mass spectrometry: Recombinant HIV-1IIIB p26. *Anal. Biochem.* **239,** 25–34.

Parveen, S., Murphree, R. L., Edmiston, L., Kaspar, C. W., Portier, K. M., and Tamplin, M. L. (1997). Association of multiple-antibiotic-resistance profiles with point and nonpoint sources of *Escherichia coli* in Apalachicola Bay. *Appl. Environ. Microbiol.* **63,** 2607–2612.

Pierce, C. Y., Barr, J. R., Woolfitt, A. R., Moura, H., Shaw, E. I., Thompson, H. A., Massung, R. F., and Fernandez, F. M. (2007). Strain and phase identification of the U.S. category B agent *Coxiella burnetii* by matrix assisted laser desorption/ionization time-of-flight mass spectrometry and multivariate pattern recognition. *Anal. Chim. Acta* **583,** 23–31.

Pignone, M., Greth, K. M., Cooper, J., Emerson, D., and Tang, J. (2006). Identification of mycobacteria by matrix-assisted laser desorption ionization-time-of-flight mass spectrometry. *J. Clin. Microbiol.* **44,** 1963–1970.

Pribil, P., and Fenselau, C. (2005). Characterization of *Enterobacteria* using MALDI-TOF mass spectrometry. *Anal. Chem.* **77,** 6092–6095.

Rabinovici, S. J. M., Bernknopf, R. L., Wein, A. M., Coursey, D. L., and Whitman, R. L. (2004). Economic and health risk trade-offs of swim closures at a Lake Michigan beach. *Environ. Sci. Technol.* **38,** 2737–2745.

Robbins, M., Giebel, R., Sandrin, T., and Kleinheinz, G. T. (2007). Matrix Assisted Laser Desorption/Ionization Time-of-Flight Mass Spectroscopy (MALDI-TOF-MS) Analysis of Sunset Park *Escherichia coli* isolates. Great Lakes Beach Association/State of the Lake Annual Meeting, November 3–5, Traverse City, MI.

Ruelle, V., Moualij, B., Zorzi, W., Ledent, P., and De Pauw, E. (2004). Rapid identification of environmental bacterial strains by matrix-assisted laser desorption/ionization time-of-flight mass spectrometry. *Rapid Commun. Mass Spectrom.* **18,** 2013–2019.

Saenz, A. J., Petersen, C. E., Valentine, N. B., Gantt, S. L., Jarman, K. H., Kingsley, M. T., and Wahl, K. (1999). Reproducibility of matrix-assited laser desorption/ionization time-of-flight mass spectrometry for replicate bacterial culture analysis. *Rapid Commun. Mass Spectrom.* **13,** 1580–1585.

Savichtcheva, O., and Okabe, S. (2006). Alternative indicators of fecal pollution: Relations with pathogens and conventional indicators, current methodologies for direct pathogen monitoring and future application perspectives. *Water Res.* **40,** 2463–2476.

Scholl, P. F., Leonardo, M. A., Rule, A. M., Carlson, M. A., Antoine, M. D., and Buckley, T. J. (1999). The development of matrix-assisted laser desorption/ionization time-of-flight mass spectrometry for the detection of biological warfare agent aerosols. *John Hopkins APL0020Tech. Dig.* **20,** 343–351.

Seng, P., Drancourt, M., Gouriet, F., La Scola, B., Fournier, P., Rolain, J. M., and Raoult, D. (2009). Ongoing revolution in bacteriology: Routine identification of bacteria by matrix-assisted laser desorption ionization time-of-flight mass spectrometry. *Clin. Infect. Dis.* **49,** 543–551.

Sharma, S., Sachdeva, P., and Virdi, J. S. (2003). Emerging water-borne pathogens. *Appl. Microbiol. Biotechnol.* **61,** 424–428.

Siegrist, T. J., Anderson, P. D., Huen, W. H., Kleinheinz, G. T., McDermott, C. M., and Sandrin, T. R. (2007). Discrimination and characterization of environmental strains of *Escherichia coli* by matrix-assisted laser desorption/ionization time-of-flight mass spectrometry (MALDI-TOF-MS). *J. Microbiol. Methods* **68,** 554–562.

Smole, S. C., King, L. A., Leopold, P. E., and Arbeit, R. D. (2002). Sample preparation of gram-positive bacteria for identification by matrix assisted laser desorption/ionization time-of-flight. *J. Microbiol. Methods* **48,** 107–115.

Stewart, J. R., Ellender, R. D., Gooch, J. A., Jiang, S., Myoda, S. P., and Weisberg, S. B. (2003). Recommendations for microbial source tracking: Lessons from a methods comparison study. *J. Water Health* **1,** 225–231.

Vaidyanathan, S., Winder, C. L., Wade, S. C., Kell, D. B., and Goodacre, R. (2002). Sample prepatation in matrix-assisted laser desorption/ionization mass spectrometry of whole bacterial cells and the detection of high mass (>20 kDa) proteins. *Rapid Commun. Mass Spectrom.* **16,** 1276–1286.

Valentine, N. B., Wahl, J. H., Kingsley, M. T., and Wahl, K. L. (2002). Direct surface analysis of fungal species by matrix-assisted laser desorption/ionization mass spectrometry. *Rapid Commun. Mass Spectrom.* **16,** 1352–1357.

Valentine, N., Wunschel, S., Wunschel, D., Petersen, C., and Wahl, K. (2005). Effect of culture conditions on microorganism identification by matrix-assisted laser desorption ionization mass spectrometry. *Appl. Environ. Microbiol.* **71,** 58–64.

Vanlaere, E., Sergeant, K., Dawyndt, P., Kallow, W., Erhard, M., Sutton, H., Dare, D., Devreese, B., Samyn, B., and Vandamme, P. (2008). Matrix-assisted laser desorption ionization-time-of-flight mass spectrometry of intact cells allows rapid identification of *Burkholderia cepacia* complex. *J. Microbiol. Methods* **75,** 279–286.

Vargha, M., Takats, Z., Konopka, A., and Nakatsu, C. H. (2006). Optimization of MALDI-TOF MS for strain level differentiation of *Arthrobacter* isolates. *J. Microbiol. Methods* **66,** 399–409.

Wahl, K. L., Wunschel, S. C., Jarman, K. H., Valentine, N. B., Petersen, C. E., Kingsley, M. T., Zartolas, K. A., and Saenz, A. J. (2002). Analysis of microbial mixtures by matrix-assisted laser desorption/ionization time-of-flight mass spectrometry. *Anal. Chem.* **74,** 6191–6199.

Walker, J., Fox, A. J., Edwards-Jones, V., and Gordon, D. B. (2002). Intact cell mass spectrometry (ICMS) used to type methicillin-resistant *Staphylococcus aureus*: Media effects and inter-laboratory reproducibility. *J. Microbiol. Methods* **48,** 117–126.

Wang, Z., Russon, L., Li, L., Roser, D. C., and Long, S. R. (1998). Investigation of spectral reproducibility in direct analysis of bacteria proteins by matrix-assisted laser desorption/ionization time-of-flight mass spectrometry. *Rapid Commun. Mass Spectrom.* **12,** 456–464.

Welham, K. J., Domin, M. A., Johnson, K., Jones, L., and Ashton, D. S. (2000). Characterization of fungal spores by laser desorption/ionization time-of-flight mass spectrometry. *Rapid Commun. Mass Spectrom.* **14,** 307–310.

Wiggins, B. A. (1996). Discriminant analysis of antibiotic reisistance patterns in fecal streptococci, a method to differentiate human and animal sources of fecal pollution in natural waters. *Appl. Environ. Microbiol.* **62,** 3997–4002.

Wiggins, B. A., Andrews, R. W., Conway, R. A., Corr, C. L., Dobratz, E. J., Dougherty, D. P., Eppard, J. R., Knupp, S. R., Limjoco, M. C., Mettenburg, J. M., Rinehardt, J. M., Sonsino, J., *et al.* (1999). Use of antibiotic resistance analysis to identify nonpoint sources of fecal pollution. *Appl. Environ. Microbiol.* **65,** 3483–3486.

Williams, T. L., Andrzejewski, D., Lay, J. O., Jr., and Musser, S. M. (2003). Experiemental factors affecting the quality and reproducibility of MALDI TOF mass spectra obtained from whole bacterial cells. *J. Am. Soc. Mass Spectrom.* **14,** 342–351.

Wunschel, S. C., Jarman, K. H., Petersen, C. E., Valentine, N. B., Wahl, K. L., Schauki, D., Jackman, J., Nelson, C. P., and White, V. E. (2005). Bacterial analysis by MALDI-TOF mass spectrometry: An inter-laboratory comparison. *J. Am. Soc. Mass Spectrom.* **16,** 456–462.

Yao, Z., Demirev, P. A., and Fenselau, C. (2002). Mass spectrometry-based proteolytic mapping for rapid virus identification. *Anal. Chem.* **74,** 2529–2534.

INDEX

CONTENTS OF PREVIOUS VOLUMES

Volume 40

Volume 41

Volume 42

Volume 43

Volume 44

Volume 45

Volume 46

Volume 47

Volume 48

Volume 49

Volume 50

Volume 51

Volume 52

Volume 53

Volume 54

Volume 55

Volume 56

Volume 57

Volume 58

Volume 59

Volume 60

Volume 61

Volume 62

Volume 63

Volume 64

Volume 65

Volume 66

Volume 67

Volume 68

Volume 69

Volume 70